

# **CROSS-COUPLING OF AMIDES BY N-C BOND ACTIVATION**

By

GUANGRONG MENG

A dissertation submitted to the

Graduate School–Newark

Rutgers, The State University of New Jersey

In partial fulfillment of the requirements

For the degree of

Doctor of Philosophy

Graduate Program in Chemistry

Written under the direction of

Professor Michal Szostak

And approved by

---

---

---

---

Newark, New Jersey

October, 2019

©[2019]

GUANGRONG MENG

ALL RIGHTS RESERVED

## ABSTRACT OF THE DISSERTATION

### CROSS-COUPLING of AMIDES by N–C BOND ACTIVATION

By

GUANGRONG MENG

Dissertation Director:

Professor Michal Szostak

The amide bond is one the most important functional motifs in chemistry and biology. However, despite the central role of amides as ubiquitous pharmacophores in medicinal chemistry, but also as bench-stable intermediates in organic synthesis, transition-metal-catalyzed transformations of amides by N–C bond activation have been unexplored. The major reason is that high activation energy is required for the N–C(O) bond scission due to  $n_N \rightarrow \pi^*_{C=O}$  conjugation (amide bond resonance of 15-20 kcal/mol in planar amides, ca. 40% double bond character). In 2015, we introduced a new generic mode of activation of amide bonds by geometric distortion, whereby metal insertion into an inert amide bond can proceed only if the classic Pauling's amide bond resonance has been disrupted. With

this new concept put forward, we successfully developed several new types of twisted amides and metal-catalyzed transformations during my Ph.D. research.

The focus of this thesis is on three parts: (1) the use of amides as acyl electrophiles in metal-catalyzed Suzuki cross-coupling reactions; (2) the use of amides as aryl electrophiles in metal-catalyzed cross-coupling reactions, including palladium-catalyzed Heck reaction and rhodium-catalyzed C–H bond functionalization; (3) the development of new type of amides as acyl electrophiles with the use of new Pd-NHC catalyst systems. These studies have demonstrated the potential of amides as acyl- and aryl-electrophiles in catalytic cross-coupling chemistry by activation of the typically inert amide N–C(O) bond.

## **Acknowledgements**

At the beginning, I would say thanks to my supervisor Prof. Michal Szostak for all the support and encouragement he gave me in past five years. On the academic level, Dr. Szostak taught me how to conduct scientific research and how to publish the results. On a personal level, Dr. Szostak inspired me by his love to research and provided me invaluable advice on my future career.

I would like to thank Prof. Huixin He, Prof. John Sheridan and Prof. Mahesh Lakshman for taking time to serve as my committee member and for their helpful advice on my research. I would also like to thank Prof. Phil Huskey and Prof. Roger Lalancette for their interest of my research and help on X-ray studies.

The help from Dr. Lazaros Kakalis on NMR and the help from Dr. Roman Brukh on GC-MS and HRMS are sincerely appreciated.

My thanks also go to all my lab members for their kind help, and especially I would like to thank my best friends-Shicheng Shi, Qun Zhao and Peng Lei who bring me great convenience on my life and research.

My deepest appreciation belongs to my family for their patience and understanding in all my research time. They helped me in whatever way they could during this challenging five years. I love you all dearly.

Last but not the least, I wish to thank my wife for being the ever-supporting rock in my life. I dedicate this thesis to her.

## Table of Contents

<b>Abstract of the Dissertation</b>	ii
<b>Acknowledgements</b>	iv
<b>Table of Contents</b>	v
<b>List of Figures</b>	xi
<b>List of Tables</b>	xvi
<b>Chapter 1</b> Introduction	1
1.1 Amides as potential substrates in metal-catalyzed cross-coupling reactions	1
1.2 The inert character of amide bonds	3
1.3 Amide bond ground state distortion	4
1.4 Acyl cross-coupling and decarbonylative cross-coupling of amides	6
1.5 N-Heterocyclic carbene (NHC) ligands in amide bond activation	8
1.6 Brief summary of the work in this thesis	11
Reference	14
<b>Chapter 2</b> Acyl Cross-Coupling of Amides by N–C Bond Activation	18
2.1 Pd-catalyzed acyl cross-coupling of amides	18
2.1.1 Research background	18

2.1.2 Reaction discovery	21
2.1.3 Reaction optimization	24
2.1.4 Substrate scope	32
2.1.5 Mechanistic studies	36
2.1.6 Conclusion	43
2.1.7 Experimental section	44
References	60
2.2 Cooperative strategy for amide bond activation-acyl coupling	64
2.2.1 Research background	64
2.2.2 Reaction discovery	66
2.2.3 Reaction optimization	68
2.2.4 Substrate scope	70
2.2.5 Mechanistic studies	75
2.2.6 Conclusion	77
2.2.7 Experimental section	78
References	87
2.3 Reversible twisting of primary amides	92

2.3.1 Research background	92
2.3.2 Synthesis and proof of structure	95
2.3.3 Chemical reactivity	99
2.3.4 Conclusion	105
2.3.5 Experimental section	106
References	118
<b>Chapter 3 Decarbonylative Cross-Coupling of Amides</b>	124
3.1 Pd-catalyzed Heck cross-coupling of amides via N–C cleavage	124
3.1.1 Research background	124
3.1.2 Reaction discovery	126
3.1.3 Reaction optimization	128
3.1.4 Substrate scope	131
3.1.5 Mechanistic studies	135
3.1.6 Conclusion	138
3.1.7 Experimental section	139
References	151
3.2 Rh-catalyzed C–H bond activation via N–C cleavage	156



3.2.1 Research background	156
3.2.2 Reaction discovery	157
3.2.3 Reaction optimization	160
3.2.4 Substrate scope	163
3.2.5 Mechanistic studies	166
3.2.6 Conclusions	171
3.2.7 Experimental section	171
References	184
3.3 Cooperative strategy for double amide N–C(O) activation/aryl C–H activation	189
3.3.1 Research background	189
3.3.2 Reaction discovery	190
3.3.3 Reaction optimization	193
3.3.4 Substrate scope	196
3.3.5 Mechanistic studies	199
3.3.6 Conclusion	200
3.3.7 Experimental section	201
Reference	211

<b>Chapter 4</b> Amides as New Acyl Precursors Enabled by NHC Catalyst Systems	216
4.1 N-Acylpyrroles and pyrazoles: planar electronically-activated amides	216
4.1.1 Research background	216
4.1.2 Reaction discovery	217
4.1.3 Reaction optimization	219
4.1.4 Substrate scope	220
4.1.5 Mechanistic studies	223
4.1.6 Conclusion	225
4.1.7 Experimental section	225
References	234
4.2 N-Methylamino pyrimidyl amides (MAPA): planar electronically-activated amides	238
4.2.1 Research background	238
4.2.2 Reaction optimization	241
4.2.3 Substrate scope	243
4.2.4 Mechanistic studies	246
4.2.5 Conclusion	247

4.2.6 Experimental section	248
References	254
4.3 B-Alkyl cross-coupling of amides	257
4.3.1 Research background	257
4.3.2 Optimization studies	260
4.3.3 Substrate scope	262
4.3.4 Conclusion	265
4.3.5 Experimental section	265
References	270
<b>Chapter 5 Conclusion</b>	274

## List of Figures

<b>Figure 1.1</b> The broad utility of amide bonds	1
<b>Figure 1.2</b> General classes of acyl electrophiles	2
<b>Figure 1.3</b> General classes of aryl electrophiles	3
<b>Figure 1.4</b> Planar amides: amide bond resonance	4
<b>Figure 1.5</b> New strategies for activation of amide N-C bonds	4
<b>Figure 1.6</b> Selected examples of bridged lactams	5
<b>Figure 1.7</b> Metal-catalyzed acyl and aryl cross-coupling of amides	7
<b>Figure 1.8</b> Mechanism of metal-catalyzed acyl cross-coupling of amides	7
<b>Figure 1.9</b> Mechanism of metal catalyzed aryl cross-coupling of amides	8
<b>Figure 1.10</b> General structure of NHC-metal precatalysts	9
<b>Figure 1.11</b> NHC precatalysts employed in amide activation	10
<b>Figure 1.12</b> General mechanism of Pd-NHC-catalyzed cross-couplings	12
<b>Figure 2.1.1</b> (a) General strategies for nucleophilic addition to amides. (b) the first general Pd-catalyzed addition of boronic acid to amides	19
<b>Figure 2.1.2</b> Representative gram scale synthesis of the ketone product	20
<b>Figure 2.1.3</b> Boronic acid scope	33

<b>Figure 2.1.4</b> Additional substrate scope	34
<b>Figure 2.1.5</b> Scope of amides	35
<b>Figure 2.1.6</b> Mechanistic studies	37
<b>Figure 2.1.7</b> ESI studies	38
<b>Figure 2.1.8</b> Effects of substituents on aryl amide	39
<b>Figure 2.1.9</b> Effects of substituents on boronic acid	40
<b>Figure 2.1.10</b> Proposed catalytic cycle	42
<b>Figure 2.2.1</b> (a) Amide cross-coupling by N–C bond activation. (b) Suzuki-Miyaura cross-coupling of amides: previous work and this study	64
<b>Figure 2.2.2</b> Proposed mechanism for site-selective N,N-di-activation and cross-coupling of amides by cooperative catalysis	66
<b>Figure 2.2.3</b> Suzuki-Miyaur cross-coupling of amides: scope of boronic acids	72
<b>Figure 2.2.4</b> Suzuki-Miyaura cross-coupling of amides: scope of amides	73
<b>Figure 2.2.5</b> Cross-coupling of pharmaceuticals	74
<b>Figure 2.2.6</b> Large scale cross-coupling	75
<b>Figure 2.3.1</b> (a) Examples of highly distorted amides in cyclic frameworks (b) Amide distortion by peripheral coordination (c-d) Reversible	

twisting of acyclic primary amides by ground-state N–C(O) bond	
destabilization	93
<b>Figure 2.3.2</b> One-step synthesis of twisted amides	95
<b>Figure 2.3.3</b> Crystal structures of amides <b>2.3.2a-2.3.2e</b> :	98
<b>Figure 2.3.4</b> N–C(O) Cleavage reactivity of amide <b>2.3.2c</b>	100
<b>Figure 2.3.5</b> Thermal and acid-mediated deconstruction of <b>2.3.2c</b>	104
<b>Figure 2.3.6</b> Stability of amides <b>2.3.2c</b> in aqueous solutions	105
<b>Figure 2.3.7</b> ORTEP structure of <b>2.3.2a</b>	110
<b>Figure 2.3.8</b> ORTEP structure of <b>2.3.2b</b>	111
<b>Figure 2.3.9</b> ORTEP structure of <b>2.3.2c</b>	112
<b>Figure 2.3.10</b> ORTEP structure of <b>2.3.2d</b>	113
<b>Figure 2.3.11</b> ORTEP structure of <b>2.3.2e</b>	114
<b>Figure 3.1.1</b> The first Heck reaction of amides via ground-state distortion	125
<b>Figure 3.1.2</b> Gram scale reaction	127
<b>Figure 3.1.3</b> Scope of amides	133
<b>Figure 3.1.4</b> Large scale application	134
<b>Figure 3.2.1</b> Transformation of amides	157

<b>Figure 3.2.2</b> Screening of amides	158
<b>Figure 3.2.3</b> Scope of amides	163
<b>Figure 3.2.4</b> Heterocycle scope	165
<b>Figure 3.2.5</b> Proposed mechanism	170
<b>Figure 3.3.1</b> Decarbonylative cross-coupling of amides	190
<b>Figure 3.3.2</b> Proposed mechanism	191
<b>Figure 3.3.3</b> Scope of amides	195
<b>Figure 3.3.4</b> Heterocycle scope	196
<b>Figure 3.3.5</b> Sequential cross-coupling/C–H activation	198
<b>Figure 3.3.6</b> C–H activation with acyclic secondary amides	199
<b>Figure 3.3.7</b> Mechanistic studies	200
<b>Figure 4.1.1</b> Studies on activation of planar amide bonds	217
<b>Figure 4.1.2</b> Boronic acid scope	220
<b>Figure 4.1.3</b> Scope of amides	221
<b>Figure 4.1.4</b> Cross-coupling of N-acylpyrazole	222
<b>Figure 4.1.5</b> Cross-coupling of a twisted N-acyl-2,5-dimethylpyrrole	222
<b>Figure 4.1.6</b> Access to acyl-metals directly from primary amides	223

<b>Figure 4.1.7</b> Competition reactions	224
<b>Figure 4.2.1</b> (a) Activation of amides and derivatives. (b) Coupling of MAPA amides enabled by selective $n_N \rightarrow \pi_{Ar}$ delocalization	238
<b>Figure 4.2.2</b> Boronic acid scope	243
<b>Figure 4.2.3</b> Scope of amides	244
<b>Figure 4.2.4</b> Cross-coupling of MAPA amides using Pd-PEPPSI-IPr	245
<b>Figure 4.2.5</b> Synthesis of MAPA amides from 1° or 2° amides	245
<b>Figure 4.2.6</b> Effect of the activating group	246
<b>Figure 4.2.7</b> X-ray structure of MAPA amide <b>4.2.1b</b>	247
<b>Figure 4.3.1</b> Pd/NHC-catalyzed B-alkyl Suzuki coupling of amides	257
<b>Figure 4.3.2</b> Structures of palladium-NHC precatalysts	260
<b>Figure 4.3.3</b> Sequential alkyl/aryl cross-coupling of primary amides	262



## List of Tables

<b>Table 2.1.1</b>	Optimization of the amide bond geometry	22
<b>Table 2.1.2</b>	Effect of ligands on Suzuki-Miyaura cross-coupling of amides	25
<b>Table 2.1.3</b>	General optimization of Suzuki-Miyaura cross-coupling of amides	27
<b>Table 2.1.4</b>	Effect of catalysts on Suzuki-Miyaura cross-coupling of amides	29
<b>Table 2.1.5</b>	Effect of bases on Suzuki-Miyaura cross-coupling of amides	30
<b>Table 2.1.6</b>	Effect of solvents on Suzuki-Miyaura cross-coupling of amides	31
<b>Table 2.1.7</b>	Effect of concentration on Suzuki-Miyaura cross-coupling of amides	31
<b>Table 2.1.8</b>	Effect of catalyst/ligand stoichiometry on cross-coupling of amides	32
<b>Table 2.1.9</b>	Effect of base/boronic acid stoichiometry on the reaction rate	40
<b>Table 2.1.10</b>	Determination of TON	41
<b>Table 2.2.1</b>	Optimization of the reaction conditions	70
<b>Table 2.2.2</b>	Selectivity study in the Pd-catalyzed Suzuki-Miyaura cross-coupling of N,N-Boc <sub>2</sub> -amides	76
<b>Table 2.2.3</b>	Selectivity study in the Pd-catalyzed Suzuki-Miyaura cross-coupling of N,N-Boc <sub>2</sub> -amides	77
<b>Table 2.3.1</b>	Summary of structural parameters for the X-ray structures of	

<b>2.3.2a-2.3.2e</b> and reference benzamide	96
<b>Table 2.3.2</b> Summary of additional bond lengths (Å) and angles (deg) for the X-ray structures of <b>2.3.2a-2.3.2e</b>	97
<b>Table 2.3.3</b> Comparison of stability of amide <b>2.3.2c</b> under aqueous and acidic conditions	101
<b>Table 2.3.4</b> Comparison of stability of amide <b>2.3.2c</b> in different solvents	102
<b>Table 2.3.5</b> Crystal data and structure refinement summaries for <b>2.3.2a-2.3.2c</b>	108
<b>Table 2.3.6</b> Crystal data and structure refinement summaries for <b>2.3.2d</b> and <b>2.3.2e</b>	109
<b>Table 3.1.1</b> Optimization of twisted amides	128
<b>Table 3.1.2</b> General optimization studies	130
<b>Table 3.1.3</b> Optimization of ligands	130
<b>Table 3.1.4</b> Optimization of solvents	131
<b>Table 3.1.5</b> Optimization of temperature	131
<b>Table 3.1.6</b> Scope of olefins	134
<b>Table 3.1.7</b> Selectivity studies – amides: electronics	135
<b>Table 3.1.8</b> Selectivity studies – sterics	136
<b>Table 3.1.9</b> Additional selectivity studies	137

<b>Table 3.1.10</b> Selectivity studies – olefins	137
<b>Table 3.1.11</b> Determination of TON	138
<b>Table 3.2.1</b> General mechanism	161
<b>Table 3.2.2</b> Determination of TON	166
<b>Table 3.2.3</b> Selectivity studies: electronics	167
<b>Table 3.2.4</b> Additional selectivity studies	168
<b>Table 3.2.5</b> Selectivity studies: sterics	169
<b>Table 3.2.6</b> Selectivity studies: directing groups	169
<b>Table 3.3.1</b> Optimization of the reaction conditions	193
<b>Table 4.1.1</b> General optimization	219
<b>Table 4.2.1</b> General optimization	241
<b>Table 4.3.1</b> General optimization	259
<b>Table 4.3.2</b> Substrate scope	264

## Chapter 1

### Introduction

Parts of this section were adapted with permission from the article “Cross-Coupling of Amides by N–C Bond Activation” (*Synlett* **2016**, 27, 2530). Copyright ©2016, Thieme Gruppe.

#### 1.1 Amides as potential substrates in metal-catalyzed cross-coupling reactions

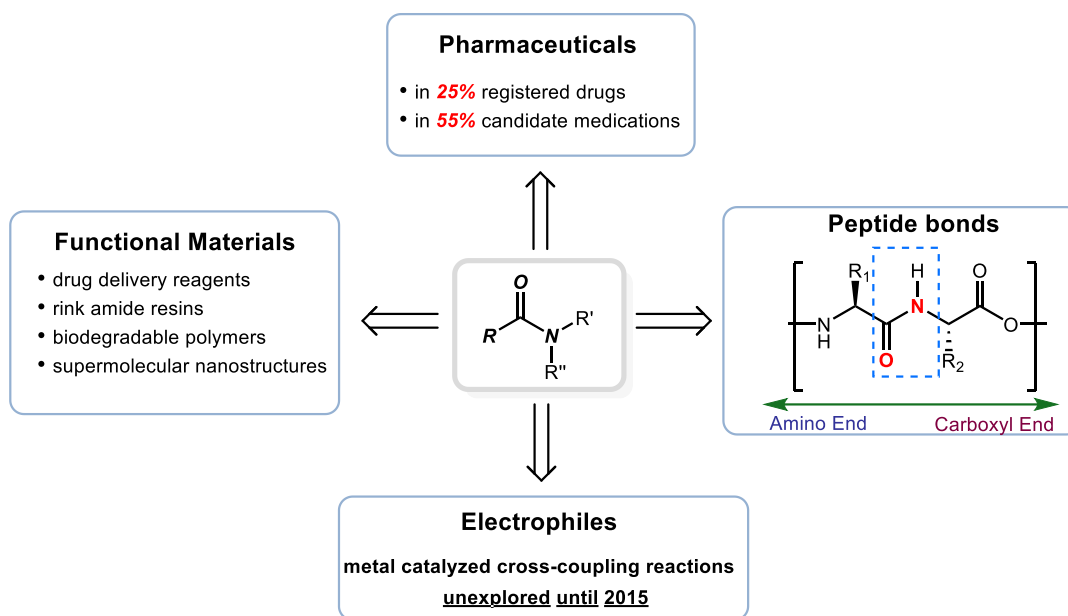


**Figure 1.1** The broad utility of amide bonds.

The amide bond is arguably the most important structural motif in organic synthesis, biology, medicinal chemistry and polymer science.<sup>1,2</sup> The unique importance of amide bonds is that they are the essential motifs in peptides and proteins (Figure 1.1). Furthermore, amides feature as prevalent pharmacophores in small molecule

pharmaceuticals.<sup>3</sup> It is estimated that the amide functional group is presented in 55% of candidate medications, while approximately 25% of all registered pharmaceuticals contain amides. A recent survey estimates that reactions involving amide bonds are among the most commonly performed processes by industrial organic chemists.<sup>4</sup> Amide structures are widely incorporated into the synthesis of a variety of useful polymers, supermolecular nanostructures and functional materials.<sup>5,6</sup> Moreover, amides serve as versatile, cheap and bench-stable intermediates in organic synthesis that are often derived from a different pool of precursors than carboxylic acids and halides.<sup>7-9</sup>

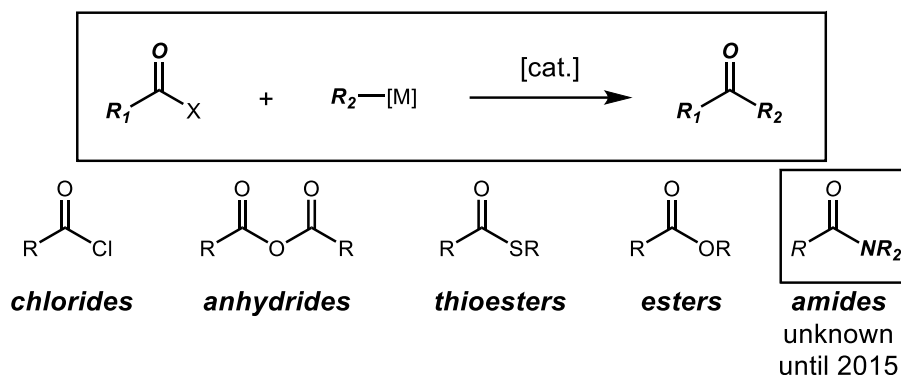


**Figure 1.2** General classes of acyl electrophiles.

However, despite the central role of amides as ubiquitous pharmacophores in medicinal chemistry, but also as bench-stable intermediates in organic synthesis and monomers in peptides and proteins, transition-metal-catalyzed transformations of amides by N–C bond activation had remained unexplored until 2015. As a comparison, other carboxylic acid derivatives, such as anhydrides, acyl halides and esters, have been widely used as acyl electrophiles<sup>10-13</sup> (Figure 1.2) or even as the more challenging aryl electrophiles (Figure 1.3) in metal-catalyzed cross-coupling reactions.<sup>14-17</sup>

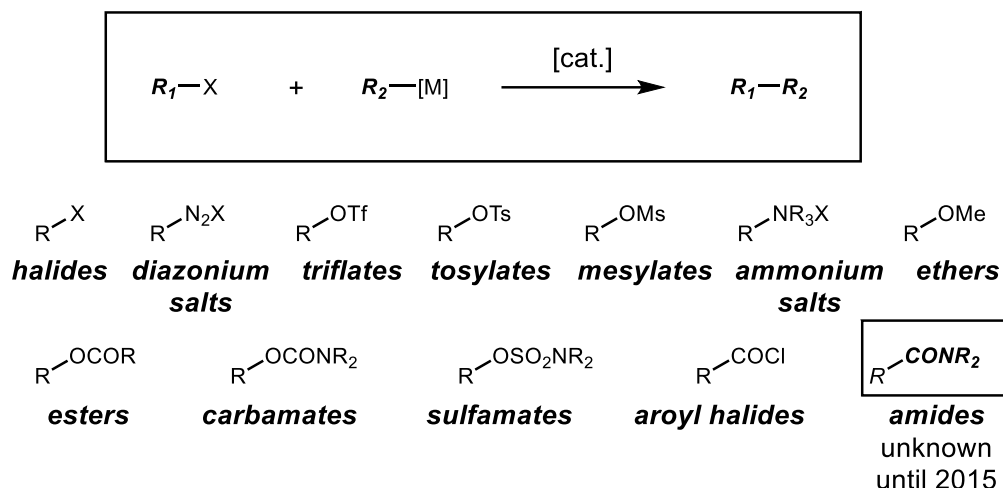


**Figure 1.3** General classes of aryl electrophiles.

## 1.2 The inert character of amide bonds

The major challenge in transition-metal-catalyzed transformations of amides by N–C cleavage is the high activation energy required for the N–C(O) bond scission due to  $n_N$  to  $\pi^*_{C=O}$  conjugation as well as low propensity of amines to act as the leaving group.<sup>18</sup> Classic studies by Pauling demonstrated that planar amide bonds contain approximately 40% double-bond character as a consequence of resonance (Figure 1.4), which represents a classic textbook effect in organic chemistry that has been used to explain properties of amides in biological and chemical contexts. The rotation energy of planar amides is as high as 15–20 kcal/mol due to the amide resonance. Amide delocalization is critical for the structure of proteins, but it also makes direct metal insertion into the N–C amide bond extremely difficult.

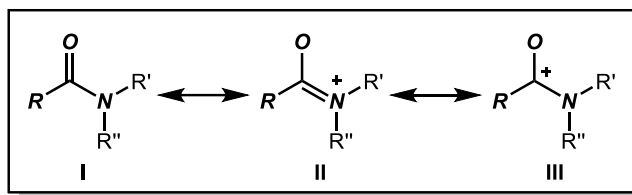


**Figure 1.4.** Planar amides: amide bond resonance.

### 1.3 Amide bond ground state distortion

In 2015, we reported a new generic mode of activation of amide bonds by geometric distortion, whereby metal insertion into an inert amide bond (amide bond resonance of 15-20 kcal/mol in planar amides, ca. 40% double bond character) can proceed only if the classic Pauling's amide bond resonance has been disrupted (Figure 1.5).<sup>19,20</sup>

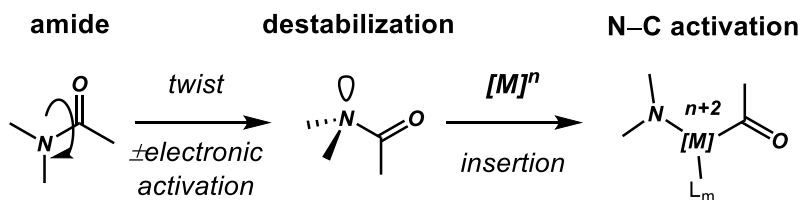


**Figure 1.5** New strategies for activation of amide N-C bonds via ground-state destabilization.

In consideration of the amide bond planarity<sup>18</sup> and our own expertise in the area,<sup>21</sup> we recognized that low valent metal insertion into effectively ‘double bonds’ in planar amides to afford versatile acyl-metal intermediates represents an unlikely scenario.<sup>22</sup> Furthermore, we recognized that for an amide bond activation mode to be generally useful, the method must be mild, selective, and employ bench-stable, readily accessible

reagents. In addition, it would be highly desirable if the rate of metal insertion could be controlled by both substrate and catalyst system, which could potential lead to a powerful cross-coupling selectivity by the judicious choice of reaction parameters and coupling partners.<sup>23</sup>

***Bridged lactams as models for disrupting amidic resonance***

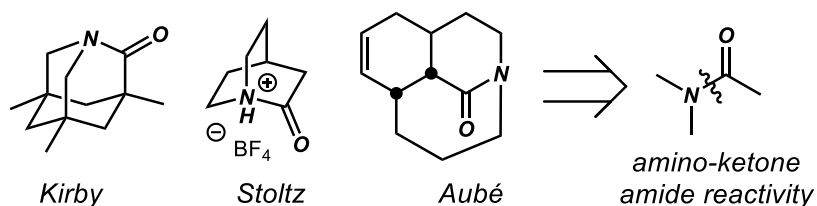


**Figure 1.6** Selected examples of bridged lactams.

The work of Kirby, Stoltz, Aubé and others on twisted amides was significant in realizing the concept.<sup>24-26</sup> These researchers showed that amide distortion in conformationally restricted cyclic lactams can be applied as a controlling feature to alter amidic resonance (Figure 1.6). Accordingly, we hypothesized that in amides in which amidic resonance is disfavored by steric or electronic reasons,<sup>27</sup> metal insertion into the N–CO bond should be feasible. On the basis of literature precedents<sup>28-31</sup> and our own studies on the N-/O-protonation aptitude of bridgehead bicyclic lactams,<sup>32,33</sup> we considered that in amides in which the additive Winkler-Dunitz distortion parameter ( $\Sigma\tau+\chi_N$ ) is close to 50°, metal insertion should be thermodynamically favourable under mild, synthetically useful reaction conditions. As such, amide bond distortion of approximately  $(\Sigma\tau+\chi_N) = 50^\circ$  (transient or permanent) would be required to effect low-valent metal insertion into the



N–C bond. A strong caveat of this model is that it seemingly contradicts the classic Pauling's amide bond resonance, which assumes co-planarity of typical acyclic amides.

However, the emergence of bridged twisted lactams and the increased understanding of the structure-reactivity relationship of non-planar amide bonds realized in the last decade brought about the possibility of effecting synthetically-useful distortion in simple acyclic amides. Indeed, literature reports described various examples of electronically- and sterically-distorted amides. However, most crucial to the amide bond N–C cross-coupling was the massively underestimated fact that steric- and electronic activation of the amide bond in simple, generally-accessible acyclic amides is relatively straightforward to achieve. All examples of amides undergoing the N–C bond cross-coupling feature markedly non-planar amide bonds. The ability to promote previously elusive transformations of amides via generic transition metal catalyzed activation modes represents a new powerful amide bond disconnection in organic synthesis with great relevance to biology, medicinal chemistry, polymers and materials science.

#### **1.4 Acyl cross-coupling and decarbonylative cross-coupling of amides**

Cross-coupling reactions are extremely powerful tool for chemists to synthesize simple or complex molecules by atom-economic and efficient routes. The tremendous importance of cross-couplings has been recognized by the 2010 Nobel Prize in Chemistry awarded to Prof. Suzuki, Prof. Heck and Prof. Negishi for their contribution in palladium-catalyzed cross-coupling reactions. More specifically in the present context, the cross-couplings of carboxylic acid derivatives by acyl or decarbonylative pathways to build carbon-carbon

bonds are among the most powerful transformations in organic synthesis (Figure 1.7).

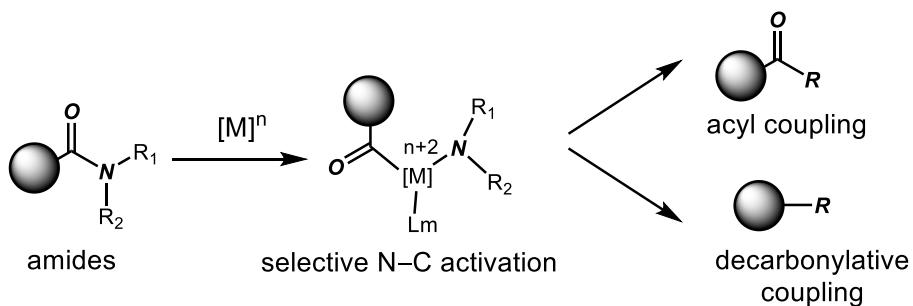


**Figure 1.7** Metal-catalyzed acyl and aryl cross-coupling of amides.

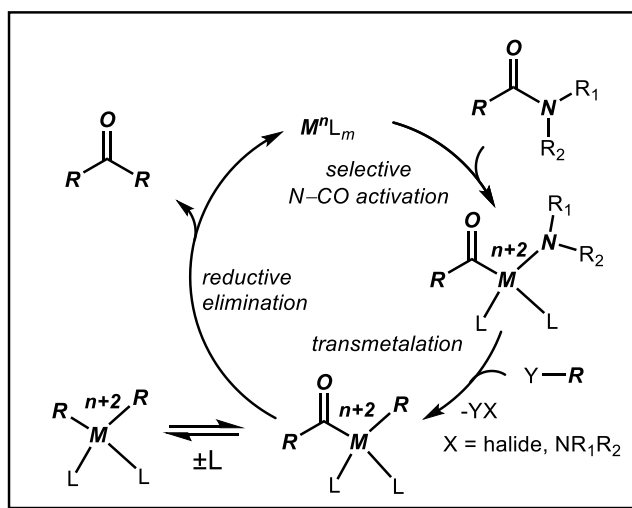


**Figure 1.8** Mechanism of metal-catalyzed acyl cross-coupling of amides.

The generic cycle for cross-coupling of amides by acyl-metal intermediates is shown in Figure 1.8. The key step involves a controlled metal insertion into the N–C amide bond. In this mechanism, bench-stable, readily accessible amides serve as acyl-precursor equivalents to other acyl-electrophiles, such as acyl halides, anhydrides, thioesters or esters.<sup>10,11</sup> The advantages of using amides as cross-coupling electrophilic partners

include (i) low-price; (ii) stability; (iii) low toxicity; (iv) orthogonal cross-coupling conditions; (v) the potential to functionalize biologically-active amide-containing molecules.

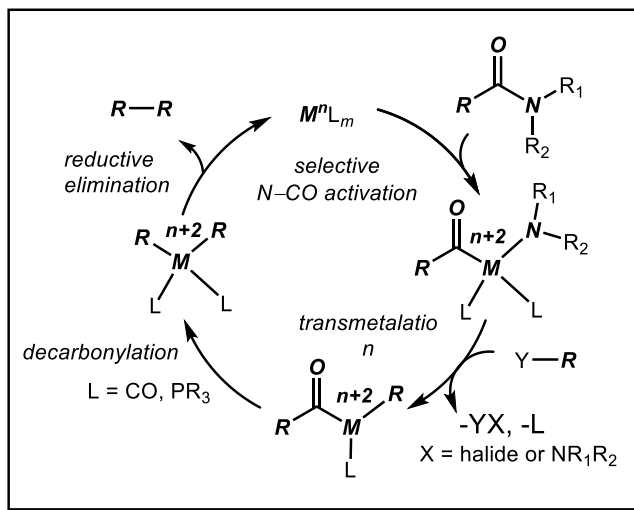


**Figure 1.9** Mechanism of metal catalyzed aryl cross-coupling of amides.

The general mechanism for decarbonylative amide N–C cross-coupling is shown in Figure 1.9. In general, decarbonylative cross-couplings are significantly more challenging than acyl-cross-couplings,<sup>14,15</sup> as these reactions must accommodate selective metal insertion into the N–C bond, and controlled decarbonylation. The major advantages of using amides as aryl electrophile equivalents involve low price and stability of amide precursors (air, moisture), halide-free cross-coupling conditions, and the potential for orthogonal C–N/C–X cross-coupling.

### 1.5 N-Heterocyclic carbene (NHC) ligands in amide bond activation

The research interest in acyl and aryl cross-coupling has mainly centered on two aspects:

(1) the discovery of a wide range of new cross-coupling partners, and (2) the development of new more effective catalyst systems.<sup>34</sup> In the sections above (Sections 1.2-1.4), the importance and the potential advantages of amides as electrophiles has been outlined. Equally important is the development of new catalyst systems for cross-coupling reactions of amide electrophiles.

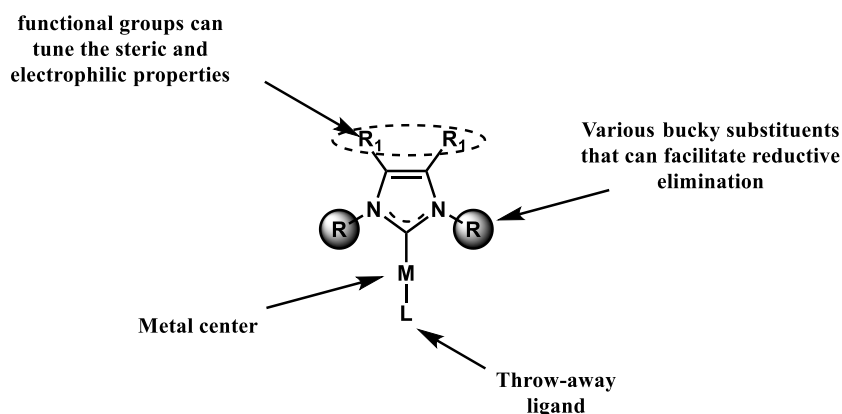


**Figure 1.10** General structure of NHC-metal precatalysts.

The most often used catalyst systems in cross-coupling chemistry are based on palladium-phosphine systems.<sup>35-37</sup> In our first reports on amide cross-coupling, we were successful in achieving the previously unknown transformations of amides by exploiting Pd-phosphine catalyst systems.<sup>19</sup> However, the deficiencies of this catalyst system have become very obvious, for example, the cross-coupling of amides using Pd-phosphines always necessitates high temperature, the use of relatively strong bases and excess of phosphine ligands, which altogether are a major limitation of the amide bond activation. Compared to phosphine ligands, NHC (N-heterocycle carbenes) ligands have been recognized as powerful ligands in cross-coupling reactions. Since the first free-NHC was

isolated in 1991 by Arduengo,<sup>38</sup> the interest of the synthetic community in these complexes has been growing almost exponentially.

Initially, NHC ligands were regarded as phosphine mimics. After almost 30 years of studies, the unique advantages of NHC ligands over phosphines have become apparent: (1) NHCs are more strongly  $\sigma$ -donating and have larger, more flexible steric bulk; (2) NHC ligands as salts most often are easily handled, bench-stable solids; (3) the use of NHCs permits for the the exact 1:1 ratio of NHC to metal; (4) NHC ligands are easy to synthesize; (5) there are more ways to control the steric and electronic properties of NHCs than of phosphines (Figure 1.10).<sup>39-43</sup> With the help of NHC ligands (Figure 1.11), we have successfully achieved several new methods for cross-coupling of amides, including cross-coupling at ambient temperature and cross-coupling of planar amides.<sup>44,45</sup>

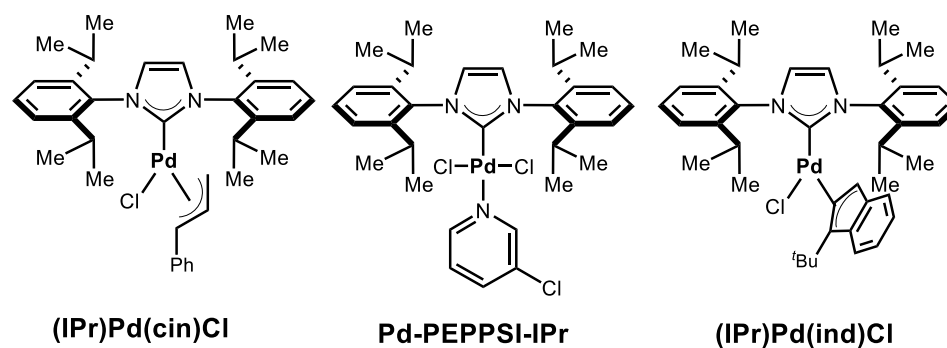


**Figure 1.11** NHC precatalysts employed in amide activation.

The general mechanism of NHC-Pd catalyzed cross-coupling reaction is shown in Figure 1.12. The departure of a throw-away ligand initiates the catalytic cycle by forming NHC-stabilized catalytically active, monoligated Pd. The oxidative addition and reductive elimination steps benefit from the strong  $\sigma$ -donation and flexible bulk of NHC ligands,

respectively.<sup>46</sup>

## 1.6 Brief summary of the work in this thesis

Building upon our new concept for activation of amide bonds, we have made several key contributions to amide bond cross-coupling reactions in past five years. In our initial communication, in 2015, we reported the first example of palladium-catalyzed Suzuki-Miyaura ketone synthesis from amides by N–C(O) bond activation.<sup>19,20</sup> Subsequently, we reported the first palladium-catalyzed decarbonylative Heck reaction<sup>47</sup> of amides for the synthesis of olefins via N–C activation. These two reactions established that amides can serve as generic acyl and aryl electrophiles for the construction of C–C bonds using palladium. The latter method represented the first example of a general decarbonylative cross-coupling of amides of any type. Next, we discovered the first rhodium-catalyzed C–H bond activation by using amides as aryl electrophiles. This reaction further demonstrated the wide utility of amides as cross-coupling partners.<sup>48</sup>

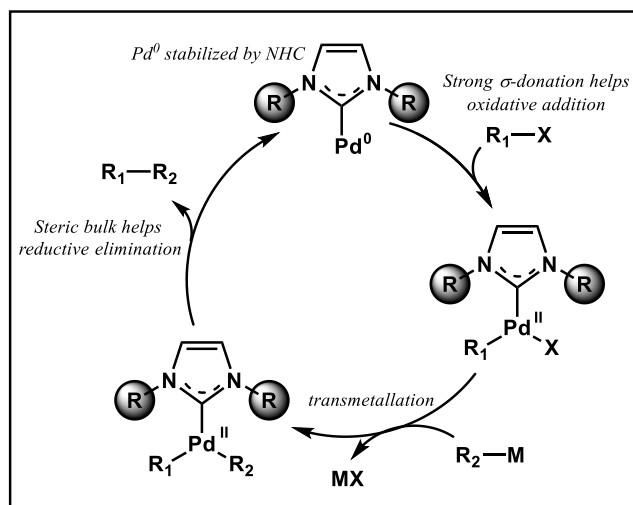


**Figure 1.12** General mechanism of Pd-NHC-catalyzed cross-couplings.

The research outlined in this thesis aims to employ amides as electrophiles in metal catalyzed acyl and decarbonylative cross-coupling reactions, and also to find more efficient ways for the transformation of generic amides that would provide alternative methods for chemists to construct complex molecular structures by manipulation of ubiquitous amide bonds. Chapter II will discuss the palladium-catalyzed acyl Suzuki cross-coupling of amides by N–C bond activation. This chapter will include a detailed study of three separate projects: (1) palladium-catalyzed Suzuki cross-coupling of N-acyl-glutarimides; (2) palladium-catalyzed Suzuki cross-coupling of planar primary amides by cooperative cross-coupling strategy; (3) the study of reversible twisting of primary amides.<sup>49-50</sup> Chapter III will discuss the metal-catalyzed decarbonylative cross-coupling reactions of amides.<sup>51</sup> This chapter will focus on three separate projects: (1) palladium-catalyzed Heck cross-coupling reactions; (2) rhodium-catalyzed C–H bond activation employing N-acyl-glutarimides by decarbonylation; (3) rhodium-catalyzed C–

H bond functionalization with primary amides via cooperative decarbonylative cross-coupling strategy. Chapter IV will discuss the development of new amides as acyl precursors for cross-coupling reactions using Pd-NHC catalyst systems. This chapter will focus on three projects: (1) the development of planar N-acyl-pyrroles as cross-coupling amide based reagents; (2) the development of N-methylamino pyrimidyl amides (MAPA) as acyl electrophiles; (3) the development of the first palladium- catalyzed C(sp<sup>3</sup>)-C(sp<sup>2</sup>) carbon–carbon bond construction from amides by using B-alkyl-9-BBN reagents.



## References

- (1) Greenberg, A.; Breneman, C. M.; Liebman, J. F. *The Amide Linkage: Structural Significance in Chemistry, Biochemistry and Materials Science*; Wiley-VCH: New York, **2003**.
- (2) Pattabiraman, V. R.; Bode, J. W. *Nature* **2011**, 480, 471.
- (3) Brunton, L.; Chabner, B.; Knollman, B. *Goodman and Gilman's The Pharmacological Basis of Therapeutics*, MacGraw-Hill, **2010**.
- (4) Roughley, S. D.; Jordan, A. M. *J. Med. Chem.* **2011**, 54, 3451.
- (5) Beller, M.; Blaser, H. U. *Top. Organomet. Chem.* **2012**, 42, 1.
- (6) Marchildon, K. *Macromol. React. Eng.* **2011**, 5, 22.
- (7) Trost, B. M.; Fleming, I. *Comprehensive Organic Synthesis*; Pergamon Press: Oxford, **1991**.
- (8) Smith, M. B.; March, J. *Advanced Organic Chemistry*; Wiley: Hoboken, **2007**.
- (9) Zabicky, J. *The Chemistry of Amides*; Interscience, **1970**.
- (10) Dieter, R. K. *Tetrahedron* **1999**, 55, 4177.
- (11) Zapf, A. *Angew. Chem. Int. Ed.* **2003**, 42, 5394.
- (12) Gooßen, L. J.; Rodriguez, N.; Gooßen, K. *Angew. Chem. Int. Ed.* **2008**, 47, 3100.
- (13) Brennfürer, A.; Neumann, H.; Beller, M. *Angew. Chem. Int. Ed.* **2009**, 48, 4114.

- (14) Johnson, J. B.; Rovis, T. *Acc. Chem. Res.* **2008**, *41*, 327.
- (15) Muto, K.; Yamaguchi, J.; Musaev, D. G.; Itami, K. *Nat. Commun.* **2015**, *6*, 7508.
- (16) Tasker, S. Z.; Standley, E. A.; Jamison, T. F. *Nature* **2014**, *509*, 299.
- (17) Rosen, B. M.; Quasdorf, K. W.; Wilson, D. A.; Zhang, N.; Resmerita, A. M.; Garg, N. K.; Perec, V. *Chem. Rev.* **2011**, *111*, 1346.
- (18) Kemnitz, C. R.; Loewen, M. J. *J. Am. Chem. Soc.* **2007**, *129*, 2521.
- (19) Meng, G.; Szostak, M. *Org. Lett.* **2015**, *17*, 4364.
- (20) Meng, G.; Szostak, M. *Org. Biomol. Chem.* **2016**, *14*, 5690.
- (21) Szostak, M.; Aubé, J. *Chem. Rev.* **2013**, *113*, 5701.
- (22) Hartwig, J. F. *Organotransition Metal Chemistry: From Bonding to Catalysis*, University Science Books, **2010**.
- (23) Mahatthananchai, J.; Dumas, A.; Bode, J. W. *Angew. Chem. Int. Ed.* **2012**, *51*, 10954.
- (24) Kirby, A. J.; Komarov, I. V.; Wothers, P. D.; Feeder, N. *Angew. Chem. Int. Ed.* **1998**, *37*, 785.
- (25) Tani, K.; Stoltz, B. M. *Nature* **2006**, *441*, 731.
- (26) Lei, Y.; Wroblewski, A. D.; Golden, J. E.; Powell, D. R.; Aubé, J. *J. Am. Chem. Soc.* **2005**, *127*, 4552.

- (27) Eliel, E. L.; Wilen, S. H. *Stereochemistry of Organic Compounds*; Wiley: **1994**.
- (28) Greenberg, A.; Venanzi, C. A. *J. Am. Chem. Soc.* **1993**, *115*, 6951.
- (29) Greenberg, A.; Moore, D. T.; DuBois, T. D. *J. Am. Chem. Soc.* **1996**, *118*, 8658.
- (30) Cox, C.; Lectka, T. *Acc. Chem. Res.* **2000**, *33*, 849.
- (31) K. B. Wiberg, *Acc. Chem. Res.* **1999**, *32*, 922.
- (32) Szostak, R.; Aubé, J.; Szostak, M. *Chem. Commun.* **2015**, *51*, 6395.
- (33) Szostak, R.; Aubé, J.; Szostak, M. *J. Org. Chem.* **2015**, *80*, 7905.
- (34) Fortman, G. C.; Nolan, S. P. *Chem. Soc. Rev.* **2011**, *40*, 5151.
- (35) Surry, D. S.; Buchwald, S. L. *Chem. Sci.* **2011**, *2*, 27.
- (36) Fleckenstein, C. A.; Plenio, H. *Chem. Soc. Rev.* **2010**, *39*, 694.
- (37) Chen, L.; Ren, P.; Carrow, B. P. *J. Am. Chem. Soc.* **2016**, *138*, 6392.
- (38) Arduengo, A. J.; Harlow, R. L.; Kline, M. *J. Am. Chem. Soc.* **1991**, *113*, 361.
- (39) Meng, G.; Kakalis, L.; Nolan, S. P.; Szostak, M. *Tetrahedron Letter* **2019**, *60*, 378.
- (40) Lei, P.; Meng, G.; Szostak, M. *ACS Catal.* **2017**, *7*, 1960.
- (41) Shi, S.; Nolan, S. P.; Szostak, M. *Acc. Chem. Res.* **2018**, *51*, 2589.
- (42) Gonzalez, S. D.; Marion, N.; Nolan, S. P. *Chem. Rev.* **2009**, *109*, 3612.

- (43) Kantchev, E. A. B.; O'Brien, C. J.; Organ, M. G. *Angew. Chem. Int. Ed.* **2007**, *46*, 2768.
- (44) Meng, G.; Lalancette, R.; Szostak, R.; Szostak, M. *Org. Lett.* **2017**, *19*, 4656.
- (45) Meng, G.; Szostak, R.; Szostak, M. *Org. Lett.* **2017**, *19*, 3596.
- (46) Wurtz, S.; Glorius, F. *Acc. Chem. Res.* **2007**, *21*, 1.
- (47) Meng, G.; Szostak, M. *Angew. Chem. Int. Ed.* **2015**, *127*, 14726.
- (48) Meng, G.; Szostak, M. *ACS Catal.* **2017**, *7*, 7251.
- (49) Meng, G.; Shi, S.; Lalancette, R.; Szostak, R.; Szostak, M. *J. Am. Chem. Soc.* **2018**, *140*, 727.
- (50) Meng, G.; Szostak, M. *Eur. J. Org. Chem.* **2018**, *20*, 2352.
- (51) Meng, G.; Shi, S.; Szostak, M. *Synlett* **2016**, *27*, 2530.

## Chapter 2

### Acyl Cross-Coupling of Amides by N–C Bond Activation

#### 2.1 Pd-catalyzed acyl cross-coupling of amides

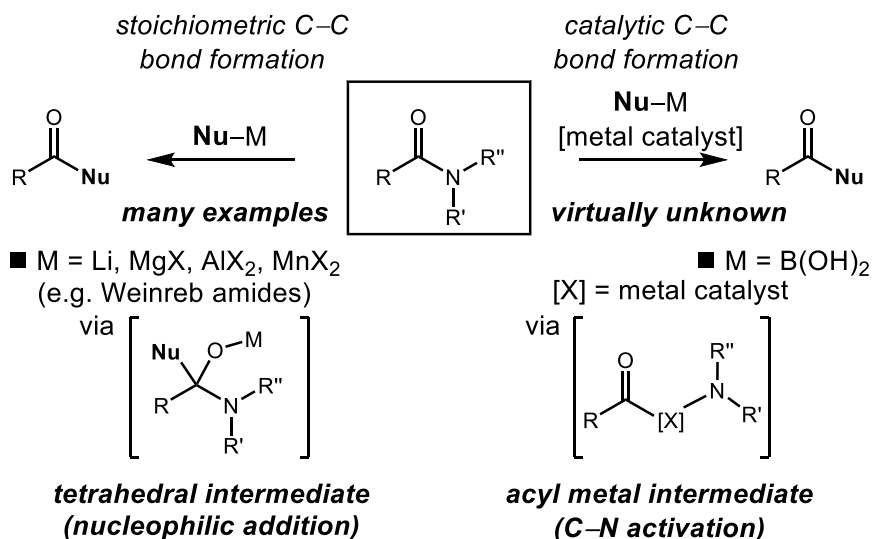
Parts of this section were adapted with permission from the article: “Sterically-Controlled Pd-Catalyzed Chemoselective Ketone Synthesis via N–C Cleavage in Twisted Amides” (*Org. Lett.* **2015**, *17*, 4364). Copyright ©2015, American Chemical Society and from the article: “Palladium-Catalyzed Suzuki-Miyaura Coupling of Amides by Carbon–Nitrogen Cleavage: General Strategy for Amide N–C Bond Activation” (*Org. Biomol. Chem.* **2016**, *14*, 5690). Copyright ©2016, The Royal Society of Chemistry.

##### 2.1.1 Research background

Palladium-catalyzed cross-couplings have markedly changed bond forming strategies in modern organic chemistry.<sup>1</sup> In particular, cross-couplings of carboxylic acid derivatives that forge new carbon-acyl bonds are among the most powerful transformations for the chemoselective formation of ketones that have been extensively utilized in the synthesis of pharmaceuticals, functional materials, peptides, and complex target synthesis.<sup>2</sup> Importantly, the downstream products of these technologies are often not available by other methods.<sup>3</sup> A number of elegant solutions to increase the substrate scope and include a wide range of cross-coupling partners has been reported by the groups of Negishi,<sup>4a,b</sup> Fukuyama,<sup>4c</sup> Liebeskind and Srogl,<sup>4d,e</sup> Yamamoto,<sup>4f</sup> and Gooßen,<sup>4g</sup> among others.<sup>4h–j</sup> Despite these significant advances, however, the use of amides as electrophilic precursors

to form acyl-palladium intermediates for catalytic cross-coupling reactions with organometallic reagents had remained unknown prior to 2015 (Figure 2.1.1).<sup>5</sup>

### A. General reaction pathways in the nucleophilic addition to amides



### B. This work: C–N activation of amides via ground-state destabilization

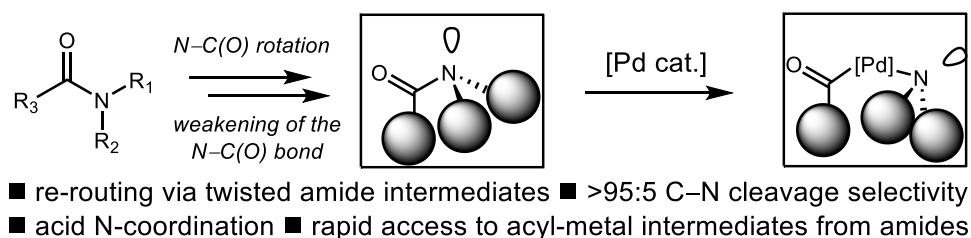


**Figure 2.1.1** (a) General strategies for nucleophilic addition to amides. (b) Our work: the first general Pd-catalyzed addition of boronic acids to amides via ground-state distortion.

This surprising gap in synthetic methodology was due to the high activation energy required for the N–C(O) bond scission in amides as a consequence of  $n_{\text{N}} \rightarrow \pi_{\text{C=O}}^*$  conjugation<sup>6</sup> as well as low propensity of amines to act as leaving groups.<sup>7</sup> The use of amides as acyl electrophiles in metal-catalyzed reactions with organometallic reagents offers a unique opportunity to expand the scope of ketone synthesis by providing new

strategic C–C bond disconnection, especially when high stability of the acyl precursor, directing effect of the amide bond or orthogonal cross-coupling conditions are required.<sup>8</sup>

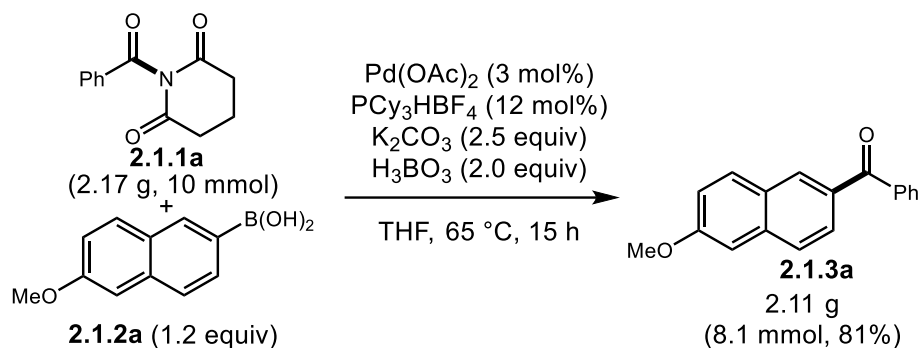


**Figure 2.1.2** Representative gram scale synthesis of the ketone product.

In this project we have developed the first general highly chemoselective palladium(0)-catalyzed cross-coupling of amides with boronic acids by exploiting the ground state amide distortion. The method provided direct access to ketone products, tolerating sensitive functionalities such as ketones, esters, aldehydes, N-heterocycles, halides, and proceeded with a complete N–C(O) (cf. R–NC(O)) selectivity. We demonstrated that the rate of metal insertion into the N–C(O) bond is controlled by the ground-state destabilization (Winkler-Dunitz distortion parameters:  $\tau$ ,  $\chi_N$ ,  $\chi_C$ ).<sup>9</sup> Notably, this first study set the stage for the development of numerous transition-metal-catalyzed reactions of amide bonds via acyl-metal intermediates reported subsequently by our group and other laboratories.

Most generally, twisted amides are amides in which the classical  $n_N \rightarrow \pi^*_{C=O}$  conjugation (barrier to rotation of ca. 15–20 kcal/mol) has been changed by geometrical features.<sup>10</sup> Seminal studies by Pracejus,<sup>11a</sup> Kirby,<sup>11b</sup> Stoltz,<sup>11c</sup> and others have demonstrated the

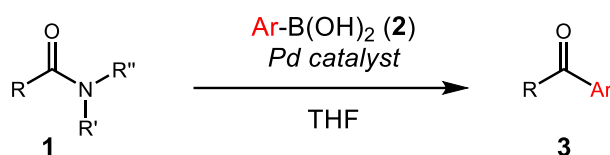
utility of these amides in the formation of C–C and C–X (X = O, N) bonds. Developments in the functionalization of the R–NC(O) bond and further mechanistic insights have been provided by the groups of Aubé,<sup>11d</sup> Greenberg,<sup>11e,f</sup> Brown<sup>11g,h</sup> and Lectka.<sup>11i</sup> Our group has demonstrated that the N-/O-protonation aptitude in such amides is directly correlated with additive distortion parameters ( $\Sigma\tau+\chi_N$ ).<sup>12</sup> Considerable advancements in the synthesis and reactivity of sterically-distorted amides have been reported.<sup>13</sup> Booker-Milburn and co-workers have developed an elegant method for solvolysis of amides by a proton-switch mechanism utilizing sterically-distorted tmp (tmp = 2,2,6,6-tetramethylpiperidine) amides.<sup>14</sup> However, prior to our studies, no method had existed for the metal-catalyzed cross-coupling of amides destabilized in the ground state despite the ready availability of an array of amides characterized by a wide range of distortion and the fact that such a process could open new vistas in transition-metal-catalyzed C–C bond formation.

### 2.1.2 Reaction discovery

Our strategy to achieve a broadly useful, modular, sterically-controlled cross-coupling of amides to access ketones involved the following steps: (i) oxidative addition of Pd into the N–C(O) bond; (ii) transmetallation with organoboron organometallic; (iii) reductive elimination to give the ketone product.<sup>1,2</sup> Importantly, we hypothesized from the beginning that amide can be used as a precursor to access a wide variety of end-products by functionalization and/or elementary reactions of the acyl metal intermediate.<sup>1,2</sup> A critical feature of our design was the capacity of amides to undergo N-activation via N-coordination (cf. O-coordination),<sup>10–12</sup> a well-established process that results in a



disruption of the amide bond resonance and could facilitate palladium insertion into the inert N–C(O) bond.<sup>15</sup> We anticipated that in amides in which the sum of distortion parameters ( $\Sigma\tau+\chi_N$ ) is close to 50°, palladium insertion would be thermodynamically favorable.<sup>12</sup> We hypothesized that the use of electron-rich ligands on Pd would favor insertion into the N–C(O) bond.<sup>16</sup> As a third feature, we anticipated that acidic additives would activate the N–C(O) bond and favor ligand dissociation from the acyl metal intermediate.<sup>10</sup>



Entry	2.1.1	$\tau$ (deg)	$\chi_N$ (deg)	Conv (%)	yield (%)
1	<b>2.1.1b</b>	1.2	16.3	<5	<5
2	<b>2.1.1c</b>	34.1	17.0	10	9
3	<b>2.1.1d</b>	39.7	8.4	25	<5
4	<b>2.1.1a</b>	87.8	6.8	>98	98
5	<b>2.1.1e</b>	45.9	10.7	55	54
6	<b>2.1.1f</b>	14.3	69.6	<5	<5
7	<b>2.1.1g</b>	5.1	33.1	<5	<5

**2.1.1b**

**2.1.1c**

**2.1.1d**

**2.1.1a**

**2.1.1e**

**2.1.1f**

**2.1.1g**

**Table 2.1.1** Optimization of the amide bond geometry.

While our study was in the final stages, a Pd-catalyzed cross-coupling of electronically-activated amides was reported.<sup>17</sup> The method reported by us showed a number of advantages: (1) mild reaction conditions, including room temperature; (2) high functional

group tolerance (ketones, aldehydes, halides); (3) generality of the activation mode across amide functions; (4) fully-tunable N–C(O) bond activation mode.<sup>10–13</sup> Moreover, since N-acylation of amides is well-established,<sup>3</sup> the our method can be used to cross-couple RC(O)–NH<sub>2</sub> bonds, which is not possible via electronic activation. Finally, complete recovery of electronically-activated amides<sup>17</sup> is observed under our conditions, which set the first stage for reagent-controlled sequential transformations.

We demonstrated that the following gram scale procedure is representative: a mixture of **2.1.1a** (2.17 g, 10 mmol), boronic acid (2.42 g, 12 mmol), Pd(OAc)<sub>2</sub> (67.4 mg, 0.30 mmol) was stirred in the presence of PCy<sub>3</sub>HBF<sub>4</sub>, K<sub>2</sub>CO<sub>3</sub> and H<sub>3</sub>BO<sub>3</sub> in THF at 65 °C to afford 2.11 g of ketone **2.1.3a** (81% yield) (Figure 2.1.2).

We first examined the amide-bond cross-coupling strategy by screening a range of electronically- and sterically-distorted amides<sup>10–23</sup> in the reactions with phenylboronic acid as a coupling partner<sup>18</sup> in the presence of palladium catalytic systems under various conditions (Table 2.1.1). While Weinreb amides (entry 1),<sup>19</sup> tmp amides (entry 2),<sup>14</sup> and acylpyrroles (entry 3)<sup>11g</sup> provided trace or no quantities of the desired ketone product, we were delighted to find that by using the previously unknown six-membered imide derivative **2.1.1a** (entry 4)<sup>13</sup> the proposed cross-coupling was indeed feasible, providing the ketone product in excellent 98% yield. Furthermore, less distorted systems such as five-membered imide **2.1.1e** (entry 5)<sup>13</sup> resulted in a dramatic decrease in efficiency, consistent with studies on amide bond activation. A survey of pyramidalized aziridinyl (entry 6) and azetidiny (entry 7) amides resulted in little or no product formation, consistent with the reactive properties of pyramidalized (cf. twisted) amides.<sup>20</sup> The

optimization results as outlined in Table 2.1.1 demonstrated for the first time that metal insertion into the N–C(O) bond of twisted amides is feasible, and that the rate of coupling is proportional to the degree of distortion. Importantly, under these conditions cleavage of the alternative R–NC(O) bond was not observed, attesting to the high chemoselectivity and/or reversibility of the insertion.<sup>11d</sup>

### 2.1.3 Reaction optimization

Encouraged by the successful coupling of amide **2.1.1d**, we undertook comprehensive optimization studies in order to provide insights into the factors controlling this new Suzuki-Miyaura coupling protocol. Key results obtained during optimization of the reaction are presented in Tables 2.1.2-2.1.8. Again, we chose the reaction of amide **2.1.1d** (Ar = Ph) with phenylboronic acid (**2.1.2a**, Ar = Ph) as our model system.

entry	ligand	yield (%)
1	PCy <sub>3</sub> HBF <sub>4</sub>	>95
2	PCy <sub>3</sub>	40
3	P( <i>n</i> -Bu) <sub>3</sub>	5
4	PMet-Bu <sub>2</sub> HBF <sub>4</sub>	80
5	PMe <sub>3</sub> HBF <sub>4</sub>	-
6	P( <i>n</i> -Bu) <sub>3</sub> HBF <sub>4</sub>	-
7	P <i>t</i> -Bu <sub>3</sub> HBF <sub>4</sub>	8
8	PCy <sub>2</sub> (CH <sub>2</sub> ) <sub>2</sub> PCy <sub>2</sub> HBF <sub>4</sub>	-
9	PCy <sub>2</sub> (CH <sub>2</sub> ) <sub>4</sub> PCy <sub>2</sub> HBF <sub>4</sub>	-
10	BINAP	-
11	PCy <sub>2</sub> Ph	56
12	PCyPh <sub>2</sub>	-
13	PPh <sub>3</sub>	7
14	P(4-CF <sub>3</sub> -C <sub>6</sub> H <sub>4</sub> ) <sub>3</sub>	34
15	P(4-MeO-C <sub>6</sub> H <sub>4</sub> ) <sub>3</sub>	-
16	P(2-Me-C <sub>6</sub> H <sub>4</sub> ) <sub>3</sub>	-
17	P(3-Me-C <sub>6</sub> H <sub>4</sub> ) <sub>3</sub>	11
18	P(4-Me-C <sub>6</sub> H <sub>4</sub> ) <sub>3</sub>	11
19	P(2-Fur) <sub>3</sub>	-
20	Xphos	-
21	DIPHOS	-
22	DPPF	-
23	DPPP	10
24	DPPB	-

<sup>a</sup>Conditions: amide (0.2 mmol), Ph-B(OH)<sub>2</sub> (2.0 equiv), Pd(OAc)<sub>2</sub> (3 mol%), ligand (12 mol%), (6 mol%) for chelating ligands, K<sub>2</sub>CO<sub>3</sub> (2.5 equiv), H<sub>3</sub>BO<sub>3</sub> (2.0 equiv), THF (0.25 M), 65 °C, 15 h. R<sup>1</sup>R<sup>2</sup> = **(2.1.1d)**. Conversions were determined by <sup>1</sup>H NMR or GC vs. internal standard.

**Table 2.1.2** Effect of ligands on Suzuki-Miyaura cross-coupling of amides.<sup>a</sup>

As in the mechanistically related cross-couplings of carboxylic acid derivatives, we anticipated that the choice of a phosphane ligand would have a significant effect on the reaction efficiency. Evaluation of the effect of ligand on the Suzuki-Miyaura coupling of amides is presented in Table 2.1.2. Among a variety of phosphane ligands screened, PCy<sub>3</sub>HBF<sub>4</sub> provided optimal results (entry 1). Notably, the phosphonium salt showed higher efficiency than in the absence of cocatalytic additive (entries 1-2). A range of other phosphane ligands furnished the desired Suzuki-Miyaura coupling product in

promising yields (entries 4, 11, 14); however, it appeared that both steric and electronic effects played a critical role in the observed coupling. We found that increasing steric demand around the metal center resulted in a decrease of the coupling selectivity (e.g. *Pt*-Bu<sub>3</sub>, entry 7; *PMet*-Bu<sub>2</sub>, entry 4). However, less sterically demanding and bidentate alkyl phosphane ligands (e.g. *Pn*-Bu<sub>3</sub>, entry 3; *PMe*<sub>3</sub>, entry 5; *dcpe*, entry 8) also resulted in a dramatic decrease in efficiency, showing that subtle changes in the ligand structure influence elementary steps of the C–N coupling. The latter suggested that a *trans* configuration of the ligand might be required for the efficient coupling, albeit this point requires further study. Moreover, the coupling was achieved using the aromatic diphosphane ligand PCy<sub>2</sub>Ph (entry 11). The related PCyPh<sub>2</sub> did not generate substantial amounts of the ketone product (entry 12). Steric hindrance on the aromatic monophosphane ligands had a significant influence on the coupling (tri(*o*-tolyl)phosphane, entry 16), while higher conversions were observed with tri(*m*-tolyl)phosphane (entry 17) and tri(*p*-tolyl)phosphane (entry 18), showing an increase of reactivity with small cone angles. Moreover, varying the electronic property at the position para to the phosphorus in tri(aryl)phosphane ligands had a great impact on the reaction, with electron withdrawing substituents facilitating the coupling (entry 14), and electron donating substituents giving a trace quantity of the desired product (entry 15). The reaction with other ligands known to promote Suzuki-Miyaura coupling of related acyl electrophiles (entries 19-24) did not generate significant amounts of the ketone products, suggesting interplay between the steric and electronic environment of the ligand in our protocol, and emphasizing the challenge of N–C amide bond activation. Overall, the bench-stable PCy<sub>3</sub>HBF<sub>4</sub> was found to be the best ligand in terms of reaction

efficiency, stability and low cost, comparing very favourably with the Ni(cod)<sub>2</sub>/SIPr system.

entry	K <sub>2</sub> CO <sub>3</sub> (equiv)	Ph-B(OH) <sub>2</sub> (equiv)	additive	T (°C)	yield (%)
1	-	2.0	H <sub>2</sub> O (2.5)	65	<5
2	2.5	2.0	H <sub>2</sub> O (2.5)	65	-
3	2.5	2.0	-	65	71
4	2.5	2.0	-	rt	8
5	2.5	2.0	H <sub>3</sub> BO <sub>3</sub> (2.5)	65	>95
6	-	2.0	H <sub>3</sub> BO <sub>3</sub> (2.5)	65	45
7	2.5	2.0	H <sub>3</sub> BO <sub>3</sub> (2.5)	rt	83
8	2.5	1.2	H <sub>3</sub> BO <sub>3</sub> (2.5)	65	93
9	2.5	2.0	H <sub>3</sub> BO <sub>3</sub> (1.0)	65	70
10 <sup>b</sup>	-	2.0	H <sub>3</sub> BO <sub>3</sub> (2.5)	65	-
11 <sup>b</sup>	2.5	2.0	H <sub>3</sub> BO <sub>3</sub> (2.5)	65	-
12 <sup>c</sup>	2.5	2.0	H <sub>3</sub> BO <sub>3</sub> (2.5)	65	91

<sup>a</sup>Conditions: amide (0.2 mmol), Ph-B(OH)<sub>2</sub> (1.2-2.0 equiv), Pd(OAc)<sub>2</sub> (3 mol%), ligand (12 mol%), K<sub>2</sub>CO<sub>3</sub> (2.5 equiv), additive (0-2.5 equiv), THF (0.25 M), rt-65 °C, 15 h. R'R'' = **(2.1.1d)**. Conversions were determined by <sup>1</sup>H NMR or GC vs. internal standard.

<sup>b</sup>Without PCy<sub>3</sub>HBF<sub>4</sub>. <sup>c</sup>With 5.0 equiv of H<sub>2</sub>O.

**Table 2.1.3** General optimization of Suzuki-Miyaura cross-coupling of amides.<sup>a</sup>

It is important to note that we have not observed any other by-products such as decarbonylated products of over-addition products in the reaction mixture. Control experiments demonstrated that all of the reaction parameters (Pd, ligand) are essential for efficient coupling, in line with our mechanistic proposal.

Next, key optimization results evaluating the effect of acidic additives are presented in Table 2.1.3. In line with our original hypothesis, we anticipated that the use of acidic additives would have a significant impact on the reaction efficiency by protonating the amide nitrogen and facilitating ligand dissociation during the catalytic cycle. Moreover, a study by Gooßen on the Suzuki-Miyaura coupling of anhydrides suggested a non-innocent behaviour of water on the catalyst turnover.<sup>4g</sup> In contrast, we determined that catalyst turnover was not observed under aqueous conditions and that the base was required for coupling in our case (Table 2.1.3, entries 1-2). Optimization of the temperature revealed that catalytic turnover of Pd ensues at room temperature, but the process was inefficient under these conditions (entries 3-4). Careful optimization of acidic additives revealed that  $\text{H}_3\text{BO}_3$  gave the best results in terms of yield and reaction efficiency (entry 5, *vide infra*). Notably, under these new conditions, the base was not required for the coupling (entry 6). Remarkably, 83% yield of the ketone product was observed at room temperature (entry 7). Control experiments demonstrated that 1 equiv of acid is required for the coupling (entry 8-9). The coupling did not take place in the absence of phosphane ligand under these conditions (entries 10-11), consistent with the proposed catalytic cycle. Furthermore, the reaction was surprisingly robust in the presence of few equivalents water (entry 12). Interestingly, in contrast to previous reports on Suzuki-Miyaura coupling of anhydrides, amide recovery was observed under aqueous conditions (entries 1-2), highlighting a potential to achieve orthogonal cross-coupling of these two classes of acyl electrophiles (entries 1-2 vs. 12).

entry	catalyst	yield (%)
1	Pd(OAc) <sub>2</sub>	>95
2	PdCl <sub>2</sub> (PPh) <sub>2</sub>	-
3	PdCl <sub>2</sub>	47
4	Pd(dba) <sub>2</sub>	85
5	Pd <sub>2</sub> (dba) <sub>3</sub>	87
6	Pd <sub>2</sub> (dba) <sub>3</sub> CHCl <sub>3</sub>	61
7	Pd(PPh <sub>3</sub> ) <sub>4</sub>	-
8	Pd/C	-

<sup>a</sup>Conditions: amide (0.2 mmol), Ph-B(OH)<sub>2</sub> (2.0 equiv), catalyst (3 mol%), ligand (12 mol%), K<sub>2</sub>CO<sub>3</sub> (2.5 equiv), H<sub>3</sub>BO<sub>3</sub> (2.0 equiv), THF (0.25 M), 65 °C, 15 h. R'R'' = (2.1.1d). Conversions were determined by <sup>1</sup>H NMR or GC vs. internal standard.

**Table 2.1.4** Effect of catalysts on Suzuki-Miyaura cross-coupling of amides.<sup>a</sup>

Optimization of palladium complexes is shown in Table 2.1.4. Various palladium catalysts were tested, and Pd(OAc)<sub>2</sub> showed the best catalytic activity (entry 1). Other palladium complexes were also found to catalyze the reaction (entries 2-8). Of particular note is the fact that Pd(PPh<sub>3</sub>)<sub>2</sub>Cl<sub>2</sub> (entry 2) and Pd(PPh<sub>3</sub>)<sub>4</sub> (entry 7) precatalysts failed to give the desired coupling product, in contrast to related Suzuki-Miyaura cross-coupling of acyl electrophiles.<sup>4f</sup> However, other Pd(II) and Pd(0) precatalysts such as PdCl<sub>2</sub>, Pd(dba)<sub>2</sub>, Pd<sub>2</sub>(dba)<sub>3</sub> and Pd<sub>2</sub>(dba)<sub>3</sub> CHCl<sub>3</sub> (entries 3-6) afforded the coupling product in good to high yields, highlighting the importance of ligand coordination to the metal center in our N–C activation protocol. The coupling with a heterogenous catalyst, Pd/C (10 wt%), was ineffective (entry 8).

Next, the effect of base on the cross-coupling of amides is summarized in Table 2.1.5. It is well-established that a choice of base plays a critical role in the Suzuki-Miyaura cross-coupling reactions.<sup>36</sup> We have determined that the highest yields in our palladium-catalyzed Suzuki-Miyaura coupling of amides are observed in the presence of base, with K<sub>2</sub>CO<sub>3</sub> giving the best results (entry 1). Importantly, a range of bases featuring different



counterions afforded the coupling product in good to high yields (entries 2-7), suggesting a non-specific role of this additive. Remarkably, high yield were still obtained in the absence of a base (entry 12), which provided an entry point to the highly useful Suzuki-Miyaura cross-coupling under neutral conditions. Interestingly, some bases were found to have a deleterious effect on the cross-coupling, thus revealing a non-innocent behaviour of the base under these conditions (entries 8-11). The coupling in a presence of only 1.0 equiv of  $K_2CO_3$  indicated high reactivity of the catalyst system for N–C activation (entry 13).

entry	base	yield (%)
1	$K_2CO_3$	>95
2	$K_2HPO_4$	74
3	$KH_2PO_4$	76
4	KOAc	64
5	$KHCO_3$	61
6	$NaHCO_3$	70
7	$CaCO_3$	48
8	$K_3PO_4$	5
9	$CsCO_3$	-
10	NaOAc	5
11	KF	-
12	-	47
13	$K_2CO_3$	89

<sup>a</sup>Conditions: amide (0.2 mmol), Ph-B(OH)<sub>2</sub> (2.0 equiv), Pd(OAc)<sub>2</sub> (3 mol%), ligand (12 mol%), base (2.5 equiv), H<sub>3</sub>BO<sub>3</sub> (2.0 equiv), THF (0.25 M), 65 °C, 15 h. R'R'' = (2.1.1d). Conversions were determined by <sup>1</sup>H NMR or GC vs. internal standard. <sup>b</sup> $K_2CO_3$  (1.0 equiv).

**Table 2.1.5** Effect of bases on Suzuki-Miyaura cross-coupling of amides.<sup>a</sup>

Next, the effect of solvents on the Suzuki-Miyaura cross-coupling of amides is presented in Table 2.1.6. THF was found to be the optimum solvent for the reaction (entry 1). Importantly, a number of other solvents proved to be effective for the reaction, including toluene, dioxane, acetone and benzene (entries 2-5). In contrast, lower yields were

obtained for reactions performed in polar solvents such as acetonitrile and DMSO (entries 5-7), suggesting incompatibility with the reagent system. Consequently, THF was selected as the best solvent for optimization experiments.

entry	solvent	yield (%)
1	THF	>95
2	Toluene	84
3	Dioxane	82
4	Acetone	64
5	Benzene	75
6	CH <sub>3</sub> CN	42
7	DMSO	24

<sup>a</sup>Conditions: amide (0.2 mmol), Ph-B(OH)<sub>2</sub> (2.0 equiv), Pd(OAc)<sub>2</sub> (3 mol%), ligand (12 mol%), K<sub>2</sub>CO<sub>3</sub> (2.5 equiv), H<sub>3</sub>BO<sub>3</sub> (2.0 equiv), solvent (0.25 M), 65 °C, 15 h. R'R'' = **(2.1.1d)**. Conversions were determined by <sup>1</sup>H NMR or GC vs. internal standard.

**Table 2.1.6** Effect of solvents on Suzuki-Miyaura cross-coupling of amides.<sup>a</sup>

Then, the effect of solvent concentration on the reaction efficiency is shown in Table 2.1.7. A study across four different concentrations indicated that the cross-coupling could be performed at reasonably high concentrations without any negative impact on the reaction efficiency and N–C coupling selectivity (entries 1-4).

entry	concentration (M)	yield (%)
1	0.05	20
2	0.10	80
3	0.25	>95
4	1.0	49

<sup>a</sup>Conditions: amide (0.2 mmol), Ph-B(OH)<sub>2</sub> (2.0 equiv), Pd(OAc)<sub>2</sub> (3 mol%), ligand (12 mol%), K<sub>2</sub>CO<sub>3</sub> (2.5 equiv), H<sub>3</sub>BO<sub>3</sub> (2.0 equiv), THF (x M), 65 °C, 15 h. R'R'' = **(2.1.1d)**. Conversions were determined by <sup>1</sup>H NMR or GC vs. internal standard.

**Table 2.1.7** Effect of concentration on Suzuki-Miyaura cross-coupling of amides.<sup>a</sup>

Finally, optimization of the palladium/phosphane ratio is presented in Table 2.1.8. The screening of five different phosphane loadings revealed that equimolar ratio was

sufficient for the reaction (entry 1); however, the best results were obtained using 3 and 4 equivalents of the phosphane ligand with respect to Pd(OAc)<sub>2</sub> (entries 3-4). Interestingly, higher phosphane loading resulted in a decrease of the reaction efficiency (entry 5), which suggested saturation of the coordination sphere of a catalytically-active Pd(0) species in the catalytic cycle. Saturation of Pd(0) by additional phosphane ligands in the Suzuki-Miyaura cross-coupling of anhydrides has been reported by Yamamoto.<sup>4f</sup> The requirement for 1 equiv of phosphane ligand in the Suzuki-Miyaura coupling of amides (entry 1) was later confirmed in the stoichiometric ESI-MS experiments.

entry	Pd(OAc) <sub>2</sub> :PCy <sub>3</sub> HBF <sub>4</sub> (x:y)	yield (%)
1	1:1	65
2	1:2	60
3	1:3	93
4	1:4	>95
5	1:5	68

<sup>a</sup>Conditions: amide (0.2 mmol), Ph-B(OH)<sub>2</sub> (2.0 equiv), Pd(OAc)<sub>2</sub> (3 mol%), ligand (y mol%), K<sub>2</sub>CO<sub>3</sub> (2.5 equiv), H<sub>3</sub>BO<sub>3</sub> (2.0 equiv), THF (0.25 M), 65 °C, 15 h. R'R'' = (2.1.1d). Conversions were determined by <sup>1</sup>H NMR or GC vs. internal standard.

**Table 2.1.8** Effect of catalyst/ligand stoichiometry on cross-coupling of amides.<sup>a</sup>

### 2.1.4 Substrate scope

With the optimized conditions in hand, we tested the preparative scope of the reaction using **2.1.1a** as a standard electrophile (Figure 2.1.3). We found that the reaction tolerated a wide range of aromatic boronic acids bearing sensitive functional groups, such as ketones (**2.1.3d**), nitriles (**2.1.3h**) and aryl halides (**2.1.3i**) that provided synthetic handles for further functionalization. Electron-donating (**2.1.3c**) and electron-withdrawing (**2.1.3e**) boronic acids gave products in high yields. Steric-hindrance on the boronic acid component (**2.1.3f**) and (**2.1.3g**) was well-tolerated. Heteroaromatic boronic acids, such

as thienyl (**2.1.3j**), furyl (**2.1.3k**), benzothieryl (**2.1.3l**) and indolyl (**2.1.3m**), underwent coupling with high reaction efficiency.<sup>21</sup> Additional examples of the boronic acid substrate scope are presented in Figure 2.1.4, and included other functional groups poised for synthetic manipulations, such as aldehydes, nitro groups, esters and vinyl moieties.

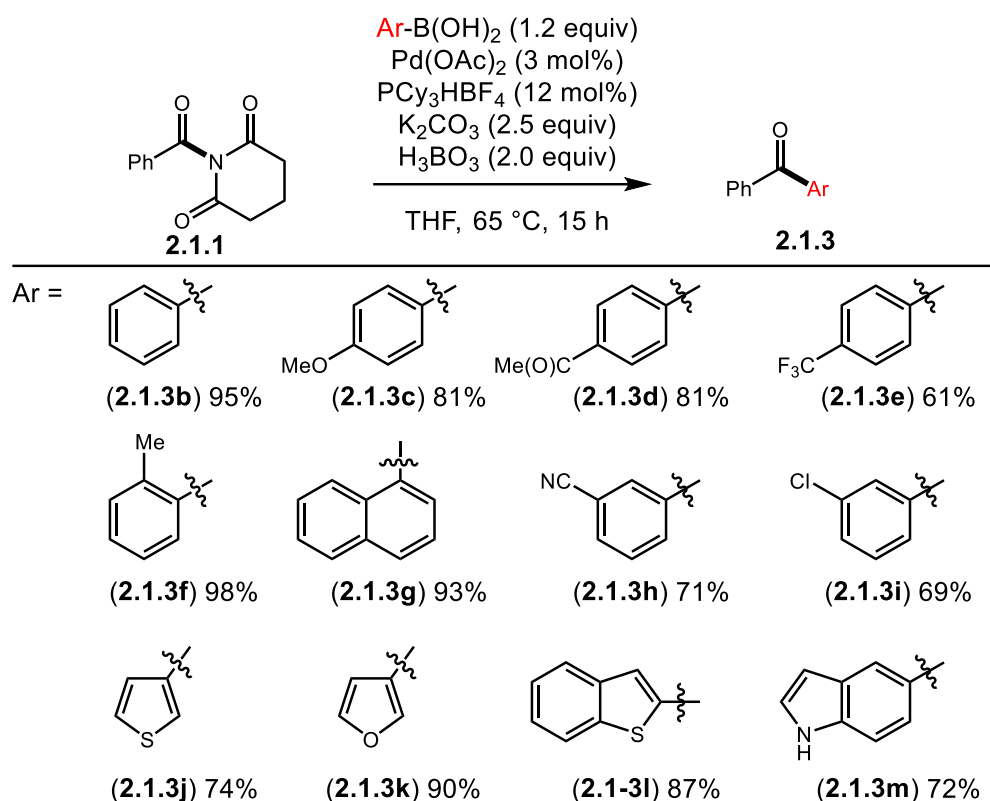


**Figure 2.1.3** Boronic acid scope.

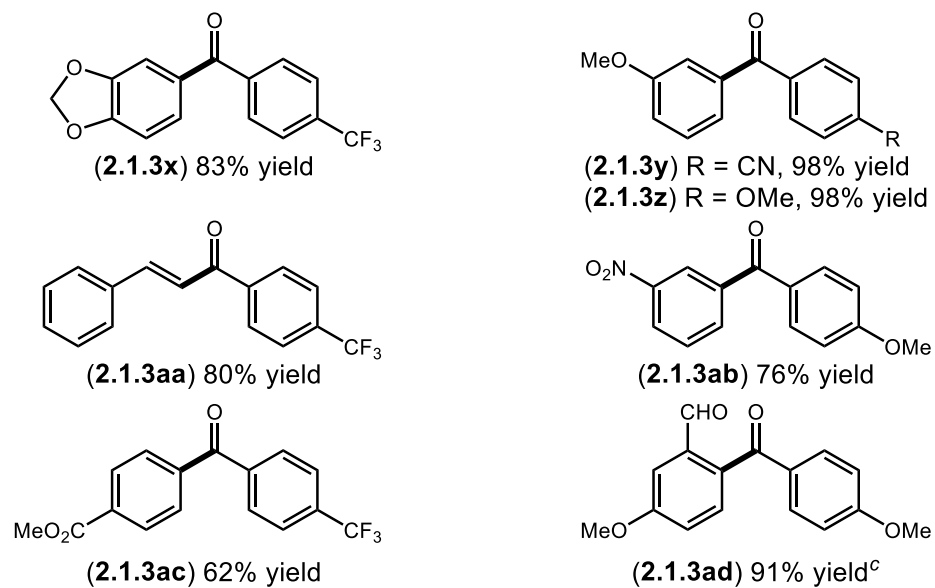


**Figure 2.1.4** Additional substrate scope.

Next, we turned our attention to the scope of amides (Figure 2.1.5). Particularly noteworthy was the functional group tolerance of our protocol, accommodating para-cyano- (**2.1.3o**), nitro- (**2.1.3p**), chloro- (**2.1.3q**), and fluoro- (**2.1.3r**) substituents. Steric hindrance in the ortho-position on the aromatic ring was well-tolerated (**2.1.3f**).

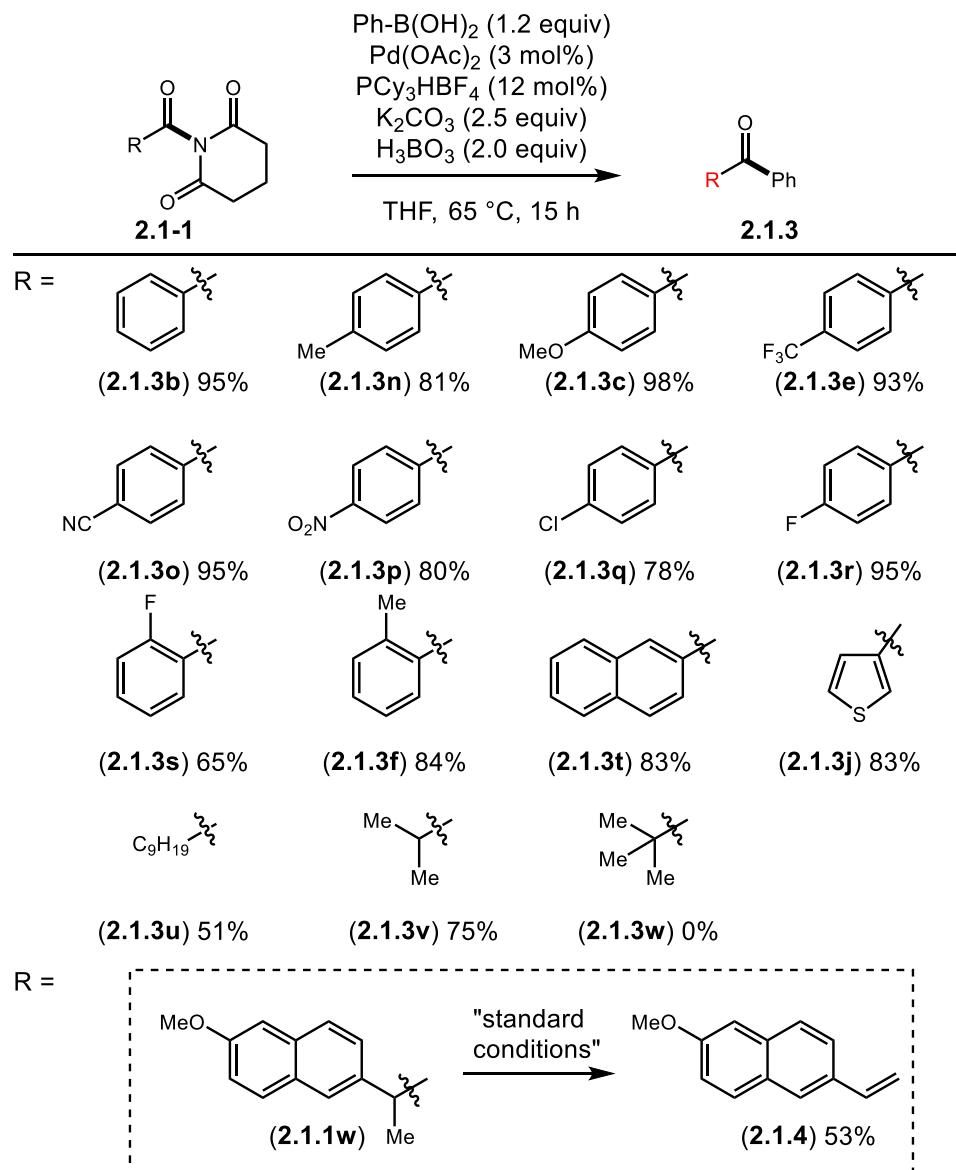


**Figure 2.1.5** Scope of amides

Naphthyl- (**2.1.3t**) and heteroaromatic (**2.1.3j**) amides underwent coupling with high reaction efficiency. Primary (**2.1.3u**) and secondary (**2.1.3v**) aliphatic amides coupled in moderate to good yields; however, a tertiary aliphatic amide (**2.1.3w**) was unreactive under these reaction conditions.<sup>4g</sup> Interestingly, a substrate bearing activated  $\beta$ -hydrogens

(2.1.3w) underwent tandem decarbonylation/ $\beta$ -hydride elimination to give the styrenyl derivative in good yield.<sup>22</sup> Decarbonylation, followed by  $\beta$ -hydride elimination has been reported in related reactions of aliphatic carboxylic acid derivatives.<sup>22</sup> The high efficiency of this Pd-catalyzed dehydrogenative decarbonylation could find application in biomass conversion. Additional examples of the cross-coupling are shown in Figure 2.1.4. These examples further included a variety of functionalized boronic acids that could be coupled with a range of distorted amides to give electronically-diverse products in high yields.

### 2.1.5 Mechanistic studies

We conducted several studies to gain insight into the reaction mechanism (Figure 2.1.6 and Figure 2.1.7). (1) Intermolecular competition experiments with differently substituted amides (Figure 2.1.6A) revealed that electron-deficient arenes are inherently more reactive substrates, consistent with metal insertion into the N–C(O) bond.<sup>1,2</sup> (2) Intermolecular competition experiments with differently substituted boronic acids (Figure 2.1.6B) indicated no preference for electron-donating nucleophiles, consistent with coordination of the amino group to the boron atom.<sup>23</sup> (3) Intermolecular competition experiments with sterically-differentiated amides and boronic acids revealed that steric effects on the nucleophile play an important role in these cross-couplings, consistent with boron coordination.<sup>1,2</sup> (4) Electrospray ionization mass spectrometry (ESI/MS) analysis using stoichiometric palladium revealed intermediates corresponding to the acyl-Pd species containing a single phosphane ligand, consistent with the proposed mechanism and optimization studies.<sup>24</sup> (5) The effect of the acidic additive was probed by using

substituted aryl carboxylic acids (Figure 2.1.6D). The cross-coupling rate was found to be inversely proportional to the  $pK_a$  of the acid.<sup>25</sup>

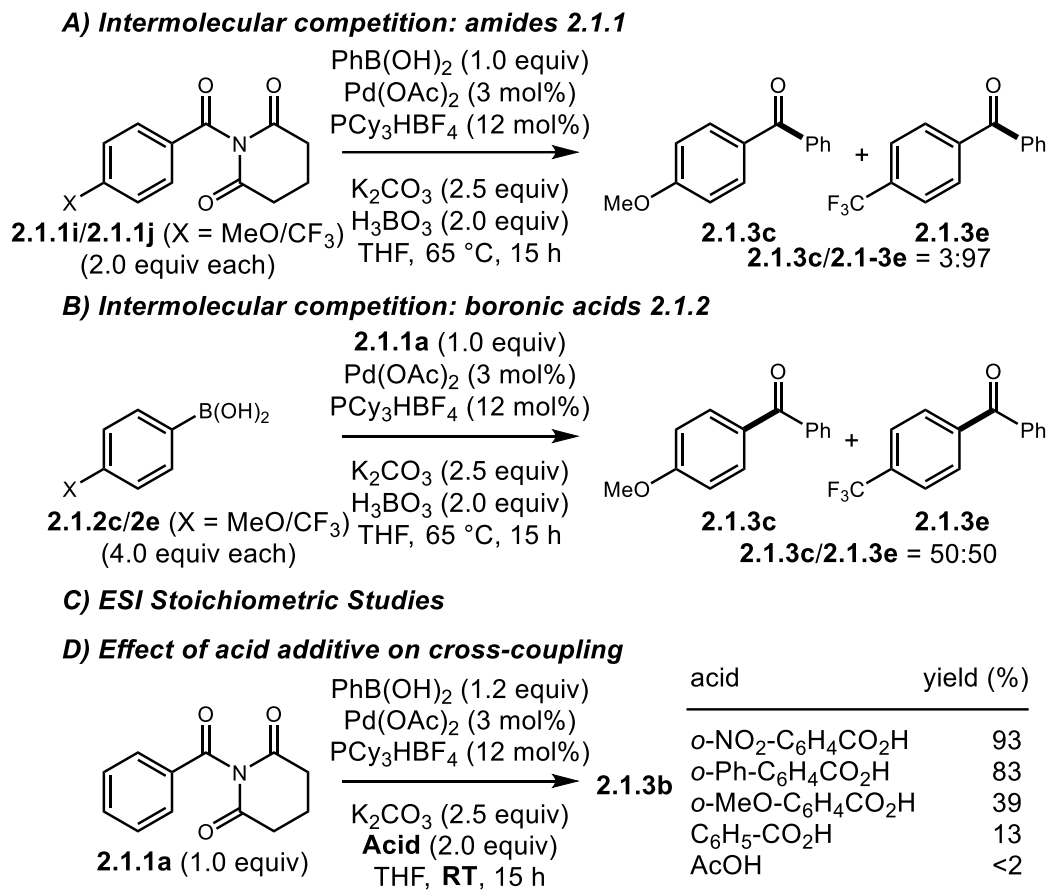


**Figure 2.1.6** Mechanistic studies.

A Hammett correlation study, employing cross-coupling of differently substituted amides **2.1.1d** with phenylboronic acid, showed a large positive  $\rho$ -value of 2.06 ( $R^2 = 0.94$ ) (Fig. 2.1.8), which can be compared with the  $\rho$ -value of 0.89 for the palladium-catalyzed



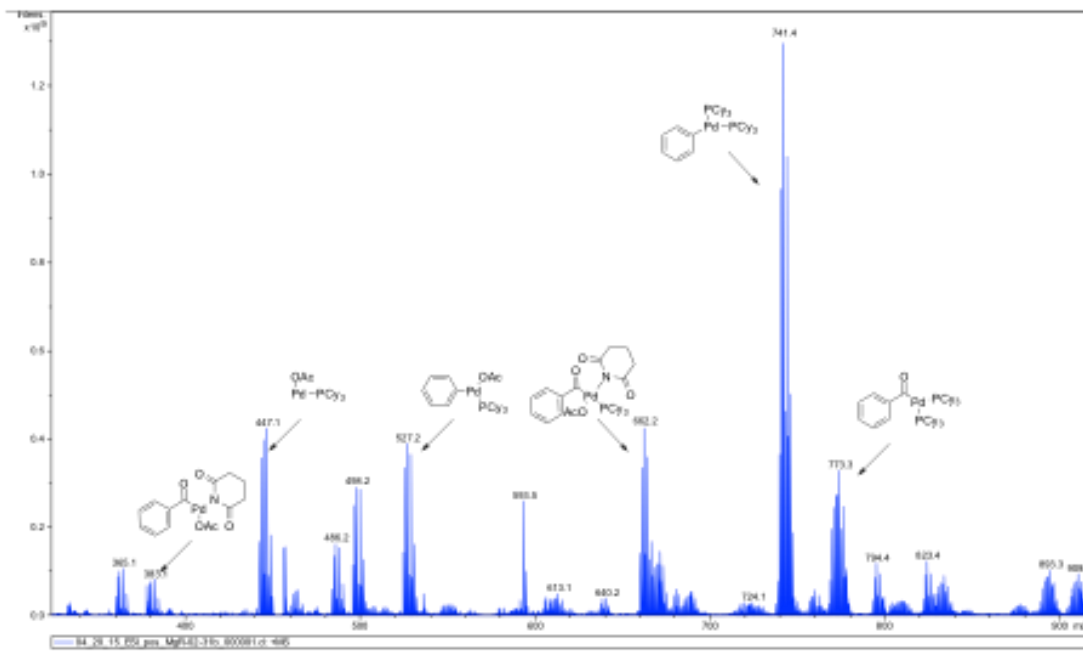


**Figure 2.1.7** ESI studies.

Suzuki-Miyaura coupling of benzoic anhydrides using  $\text{PhB(OH)}_2$  and the  $\rho$ -value of 2.0 for the nickel-catalyzed Suzuki-Miyaura coupling of aryl tosylates using 4-TolB(OH)<sub>2</sub>.<sup>4f</sup> In addition, a good correlation was obtained by plotting  $\log(k_{\text{obs}})$  vs. Hammett-Brown $\sigma^+$  constants ( $\rho$ -value of 1.31,  $R^2 = 0.99$ ), which suggests that resonance effects are involved in stabilization of the reactive center. The large positive  $\rho$ -value suggested that electron-deficient arenes are inherently more reactive substrates, consistent with metal insertion into the N–C(O) bond. As expected, electron-withdrawing groups facilitated oxidative addition; resonance effects were involved in stabilization of the acyl-Pd(II) intermediate.

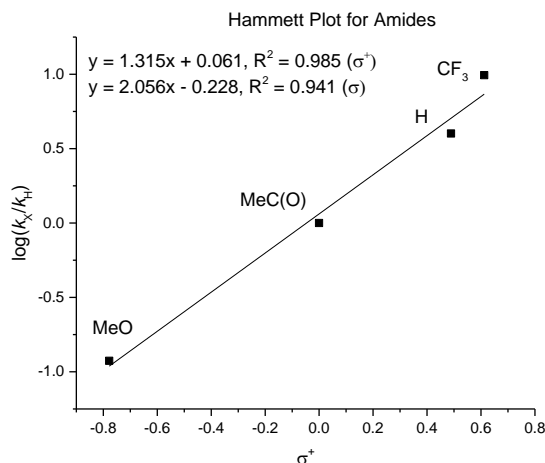


**Figure. 2.1.8** Plot of  $\log k$  vs.  $\sigma^+$  in Suzuki-Miyaura arylation of amides with boronic acids: effects of substituents on aryl amide.

A Hammett correlation study, employing cross-coupling of differently substituted aryl boronic acids with phenyl amide **2.1.1d**, showed a small positive  $\rho$ -value of 0.24 ( $R^2 = 0.99$ ) (Fig. 2.1.9), which can be compared with the  $\rho$ -value of 0.72 for the palladium-catalyzed Suzuki-Miyaura coupling of boronic acids with acetic benzoic anhydride and the  $\rho$ -value of 0.81 for the nickel-catalyzed Suzuki-Miyaura coupling of phenyl tosylate.<sup>4f</sup> Plotting of  $\log(k_{\text{obs}})$  vs. Hammett-Brown  $\sigma^+$  constants gives a  $\rho$ -value of 0.14, ( $R^2 = 0.87$ ). A small positive  $\rho$ -value indicated that electron deficient boronic acids were more reactive in the cross-coupling. This electronic effect has been described in the literature and is consistent with coordination of the amino group to boronic acids with high Lewis acidity.

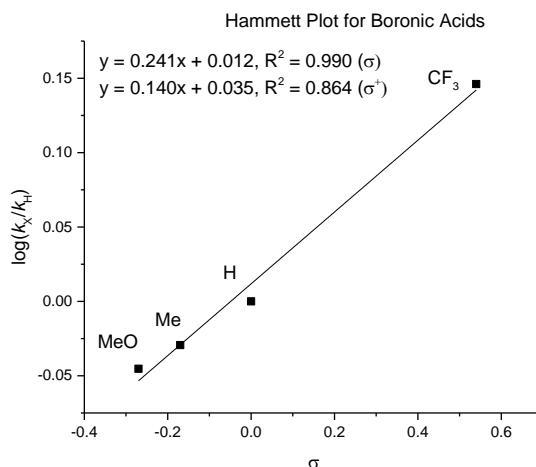


**Figure. 2.1.9** Plot of  $\log k$  vs.  $\sigma^+$  for Suzuki-Miyaura arylation of amides with boronic acids: effects of substituents on boronic acid.

To gain insight into the factors involved in transmetallation, cross-coupling of amide **2.1.1d** with phenylboronic acid with the increasing amount of base and boronic acid was performed (Table 2.1.9). As shown, the cross-coupling proceeded more rapidly when the amount of boronic acid and base was increased ( $K_2CO_3$ , 2.0 equiv,  $PhB(OH)_2$ , 1.5 equiv, 2 h, 54% conversion;  $K_2CO_3$ , 4.0 equiv,  $PhB(OH)_2$ , 3.0 equiv, 2 h, >98% conversion), consistent with the importance of transmetallation in the catalytic cycle.

entry	$K_2CO_3$ (equiv)	$Ph-B(OH)_2$ (equiv)	time (h)	conversion (%)
1	1.5	2.0	2	54
2	3.0	4.0	2	98

<sup>a</sup>Conditions: amide (0.2 mmol),  $Ph-B(OH)_2$  (2.0-4.0 equiv),  $Pd(OAc)_2$  (3 mol%), ligand (12 mol%),  $K_2CO_3$  (1.5-3.0 equiv),  $H_3BO_3$  (2.0 equiv), THF (0.25 M), 65 °C, 2 h. R'R'' = (**2.1.1d**).

**Table 2.1.9** Effect of base/boronic acid stoichiometry on the reaction rate.<sup>a</sup>

Catalyst turnover number (TON) in the cross-coupling of amide **2.1.1d** with phenylboronic acid at 0.1-0.2 mol% Pd(OAc)<sub>2</sub> loading was determined (Table 2.1.10). The observed reactivity compared favourably with the previously reported examples of Suzuki-Miyaura cross-coupling of carboxylic acid derivatives,<sup>4g</sup> and indicated highly efficient catalysis. At the time of the study, this was the highest TON observed to date for N–C amide bond activation.

entry	Pd(OAc) <sub>2</sub> (mol%)	yield (%)	TON
1	3.0	>98	33
2	0.2	69	345
2	0.1	32	320

<sup>a</sup>Conditions: amide (0.2 mmol), Ph-B(OH)<sub>2</sub> (2.0 equiv), Pd(OAc)<sub>2</sub> (x mol%), ligand (12 mol%), K<sub>2</sub>CO<sub>3</sub> (2.5 equiv), H<sub>3</sub>BO<sub>3</sub> (2.0 equiv), THF (0.25 M), 65 °C, 15 h. R'R'' = (**2.1.1d**).

**Table 2.1.10** Determination of TON.<sup>a</sup>

Overall, these studies were consistent with a mechanism involving activation of the amide N–C(O) bond.<sup>26,27</sup> The high chemoselectivity of the N–C(O) cleavage resulted from ground-state-destabilization of the amide bond by rotation.<sup>27</sup> Cleavage of the alternative R–NC(O) bond was thermodynamically-disfavored due to steric hindrance and conjugation of the imide carbonyl groups.<sup>13</sup> Furthermore, in the acyl-Pd intermediate the ligand dissociation was favored by low nucleophilicity of amines that are eliminated,<sup>7</sup> and by coordination of acid to the nitrogen,<sup>26</sup> enhancing the overall N–C(O) coupling selectivity.

**Proposed mechanism.** A possible mechanism is presented in Figure 2.1.10. The first step involved oxidative addition of Pd(0) into the amide N–C bond to afford acyl-Pd(II) intermediate. Step two of the proposed catalytic cycle involved ligand exchange and

transmetallation to give acyl-palladium intermediate, which equilibrated with aryl-palladium(II) species. The final step involved base-mediated C–C bond formation by reductive elimination to afford the ketone product and regenerate the catalyst. An alternative mechanism involving Pd(II) cycle was ruled out on the basis of ESI/MS experiments and control experiments using conditions typical for Pd(II) catalytic cycle.

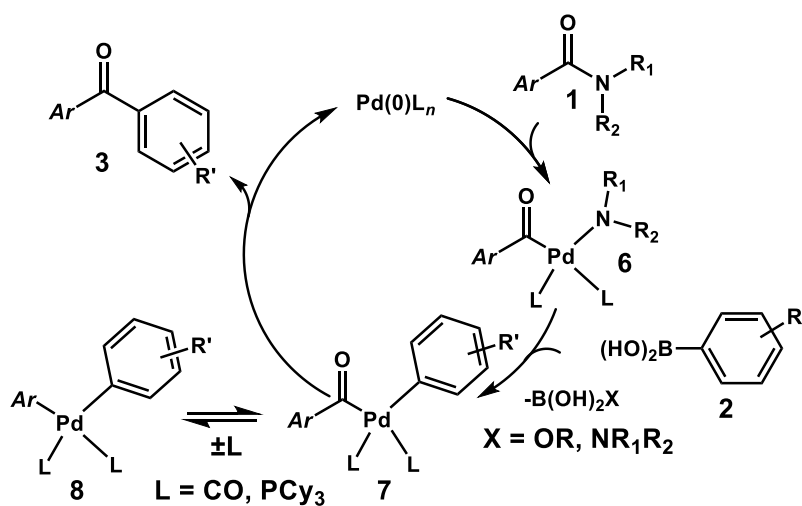


**Figure 2.1.10** Proposed catalytic cycle.

It is important to emphasize that the key step in the mechanism is activation of the amide N–C bond. In the cross-coupling, acid coordination to the amidic nitrogen appeared to play a substantial role in assisting the N–C cleavage. In the acyl-Pd intermediate, ligand dissociation was favoured by low nucleophilicity of amines that are eliminated, and by coordination of acid to the Lewis basic nitrogen, enhancing the overall N–C(O) cleavage selectivity.

### 2.1.6 Conclusion

This part of Chapter II outlined the discovery of the first palladium-catalyzed Suzuki-Miyaura cross-coupling of amides with boronic acids for the synthesis of ketones by sterically-controlled N–C bond activation. The method provided versatile ketone products in excellent yields from readily available amides, tolerated a wide range of functional groups, steric hindrance and electronic variation on both coupling partners, including an array of sensitive functionalities (ester, ketone, aldehyde, cyano, nitro, chloride, olefin, heterocycles), and was characterized by operational simplicity utilizing bench-stable, commercially available reagents and catalysts. The scope and limitations of this methodology were presented in the synthesis of >60 functionalized ketones. Mechanistic studies provided insight into the catalytic cycle of the cross-coupling, including the first experimental evidence for Pd insertion into the amide N–C bond. The synthetic utility was further showcased by a gram-scale cross-coupling and cross-coupling at room temperature. Furthermore, catalyst turnover number exceeding 300 was demonstrated for the reaction.

In a broader sense, this first study outlined a general strategy for transition-metal-catalyzed activation of amide N–C bonds. Classically, the large rotation barrier around planar N–C amide bonds (amide bond resonance of 15-20 kcal/mol) resulting from the partial double bond character of amides (approx. 40%  $sp^2$ - $sp^2$  double bond) renders metal insertion into the amide bond energetically unfavourable. Thus, in order to achieve metal insertion into the amide N–C bond, the amide bond  $n_N \rightarrow \pi^*_{C=O}$  conjugation must be disrupted. This represented a new generic activation mode of amide bonds because the

acyl metal species generated by metal insertion could be utilized across many transition-metal-catalyzed reactions in organic synthesis, as exemplified by ketone synthesis under catalytic conditions.

In light of the key role of amides as bench-stable intermediates in organic chemistry and the importance of amides in biology as building blocks of proteins and peptides, the study has triggered the important field of transition-metal-catalyzed amide bond activation. The importance of practical, direct and catalytic methods for amide bond manipulation is highlighted by the fact that reactions involving amide bonds account for 20% of all reactions performed in pharmaceutical research laboratories world-wide, with the amide functional group present in 55% of potential pharmaceuticals.

### 2.1.7 Experimental section

**General methods.** All experiments involving transition-metals were performed using Schlenk or glovebox techniques under argon or nitrogen atmosphere unless stated otherwise. All solvents were purchased at the highest commercial grade and used as received or after purification by passing through activated alumina columns or distillation from sodium/benzophenone under nitrogen. All chemicals were purchased at the highest commercial grade and used as received. Reaction glassware was oven-dried at 140 °C for at least 24 h or flame-dried prior to use, allowed to cool under vacuum and purged with argon (three cycles).  $^1\text{H}$  NMR and  $^{13}\text{C}$  NMR spectra were recorded in  $\text{CDCl}_3$  on Bruker spectrometers at 500 ( $^1\text{H}$  NMR) and 125 MHz ( $^{13}\text{C}$  NMR). All shifts are reported in parts per million (ppm) relative to residual  $\text{CHCl}_3$  peak (7.27 and 77.2 ppm,  $^1\text{H}$  NMR and  $^{13}\text{C}$

NMR, respectively). All coupling constants (J) are reported in hertz (Hz). Abbreviations are: s, singlet; d, doublet; t, triplet; q, quartet; brs, broad singlet. GC-MS chromatography was performed using Agilent HP6890 GC System and Agilent 5973A inert XL EI/CI MSD using helium as the carrier gas at a flow rate of 1 mL/min and an initial oven temperature of 50 °C. High-resolution mass spectra (HRMS) were measured on a 7T Bruker Daltonics FT-MS instrument. All flash chromatography was performed using silica gel, 60 Å, 300 mesh. TLC analysis was carried out on glass plates coated with silica gel 60 F254, 0.2 mm thickness. The plates were visualized using a 254 nm ultraviolet lamp or aqueous potassium permanganate solutions.

**General procedure for amide synthesis.** An oven-dried round-bottomed flask (100 mL) equipped with a stir bar was charged with amine (8.84 mmol, 1.0 equiv), triethylamine (2.0 equiv), 4-dimethylaminopyridine (0.25 equiv) and dichloromethane (50 mL), placed under a positive pressure of argon, and subjected to three evacuation/backfilling cycles under high vacuum. Acyl chloride (typically, 1.1 equiv) was added dropwise to the reaction mixture with vigorous stirring at 0 °C, and the reaction mixture was stirred overnight at room temperature. After the indicated time, the reaction mixture was diluted with Et<sub>2</sub>O (20 mL) and filtered. The organic layer was washed with HCl (1.0 N, 30 mL), brine (30 mL), dried, and concentrated. The crude product was purified by recrystallization to give analytically pure amide.

**General procedure for Pd-catalyzed Suzuki-Miyaura coupling.** An oven-dried vial equipped with a stir bar was charged with an amide substrate (1.0 equiv), potassium carbonate (2.5 equiv), boric acid (2.0 equiv), boronic acid (1.2 equiv), Pd(OAc)<sub>2</sub> (0.03



equiv), and  $\text{PCy}_3\text{HBF}_4$  (0.12 equiv), placed under a positive pressure of argon, and subjected to three evacuation/backfilling cycles under high vacuum. Tetrahydrofuran (0.80 mL) was added with vigorous stirring at room temperature, the reaction mixture was placed in a preheated oil bath at 65 °C, and stirred for the indicated time at 65 °C. After the indicated time, the reaction mixture was cooled down to room temperature, diluted with  $\text{CH}_2\text{Cl}_2$  (10 mL), filtered, and concentrated. The sample was analyzed by  $^1\text{H}$  NMR ( $\text{CDCl}_3$ , 500 MHz) and GC-MS to obtain selectivity, conversion and yield using internal standard and comparison with authentic samples. Purification by chromatography on silica gel afforded the title product.

**2.1.1a.** White solid.  $^1\text{H}$  NMR (500 MHz,  $\text{CDCl}_3$ )  $\delta$  7.89 (d,  $J$  = 7.8 Hz, 2 H), 7.67 (t,  $J$  = 7.5 Hz, 1 H), 7.52 (t,  $J$  = 7.7 Hz, 2 H), 2.80 (t,  $J$  = 6.6 Hz, 4 H), 2.17 (q,  $J$  = 6.5 Hz, 2 H).  $^{13}\text{C}$  NMR (125 MHz,  $\text{CDCl}_3$ )  $\delta$  171.90, 170.74, 134.97, 131.78, 130.16, 129.14, 32.41, 17.51. MS = 182.1 (EI). HRMS calcd for  $\text{C}_{13}\text{H}_{10}\text{ONa}$  ( $\text{M}^+ + \text{Na}$ ) 205.0624, found 205.0631.

**2.1.1b.** Colorless oil.  $^1\text{H}$  NMR (500 MHz,  $\text{CDCl}_3$ )  $\delta$  7.68 (dt,  $J$  = 7.0, 1.5 Hz, 2 H), 7.45-7.43 (m, 1 H), 7.42-7.37 (m, 2 H), 3.55 (s, 3 H), 3.36 (s, 3 H).  $^{13}\text{C}$  NMR (125 MHz,  $\text{CDCl}_3$ )  $\delta$  169.94, 134.09, 130.55, 128.10, 128.00, 61.01, 33.79. MS = 165.1 (EI). HRMS calcd for  $\text{C}_{18}\text{H}_{22}\text{N}_2\text{O}_4\text{Na}$  ( $2\text{M}^+ + \text{Na}$ ) 353.1472, found 353.1496.

**2.1.1c.** White solid.  $^1\text{H}$  NMR (500 MHz,  $\text{CDCl}_3$ )  $\delta$  7.49-7.42 (m, 2 H), 7.37 (qd,  $J$  = 8.6, 7.5, 4.3 Hz, 3 H), 1.81 (s, 6 H), 1.39 (s, 6 H), 1.38 (s, 6 H).  $^{13}\text{C}$  NMR (125 MHz,  $\text{CDCl}_3$ )

$\delta$  176.74, 143.30, 129.33, 127.81, 127.74, 56.51, 37.02, 30.57, 14.95. MS = 245.1 (EI). HRMS calcd for  $C_{16}H_{23}NONa$  ( $M^+ + Na$ ) 268.1672, found 268.1678.

**2.1.1d.** Colorless oil.  $^1H$  NMR (500 MHz,  $CDCl_3$ )  $\delta$  7.78-7.67 (m, 2 H), 7.66-7.59 (m, 1 H), 7.50 (t,  $J = 7.9$  Hz, 2 H), 5.90 (s, 2 H), 2.10 (s, 3 H), 2.09 (s, 3 H).  $^{13}C$  NMR (125 MHz,  $CDCl_3$ )  $\delta$  171.18, 135.68, 133.18, 130.34, 130.12, 128.67, 110.14, 99.98, 14.69. MS = 199.1 (EI). HRMS calcd for  $C_{13}H_{13}NONa$  ( $M^+ + Na$ ) 222.0889, found 222.0894.

**2.1.1e.** White solid.  $^1H$  NMR (500 MHz,  $CDCl_3$ )  $\delta$  7.88 (d,  $J = 7.2$  Hz, 2 H), 7.69 (t,  $J = 7.5$  Hz, 1 H), 7.53 (t,  $J = 7.8$  Hz, 2 H), 2.96 (s, 4 H).  $^{13}C$  NMR (125 MHz,  $CDCl_3$ )  $\delta$  174.54, 167.62, 135.15, 131.40, 130.53, 128.97, 29.08. MS = 203.1 (EI). HRMS calcd for  $C_{11}H_9NO_3Na$  ( $M^+ + Na$ ) 226.0475, found 226.0483.

**2.1.1f.** Colorless oil.  $^1H$  NMR (500 MHz,  $CDCl_3$ )  $\delta$  8.08-8.02 (m, 2 H), 7.57 (td,  $J = 7.2$ , 1.5 Hz, 1 H), 7.48 (t,  $J = 7.8$  Hz, 2 H), 2.66-2.54 (m, 2 H), 2.17 (d,  $J = 3.6$  Hz, 1 H), 1.42 (d,  $J = 5.4$  Hz, 3 H).  $^{13}C$  NMR (125 MHz,  $CDCl_3$ )  $\delta$  179.30, 133.54, 132.62, 129.05, 128.40, 34.61, 32.14, 17.79. MS = 161.1 (EI). HRMS calcd for  $C_{10}H_{11}NONa$  ( $M^+ + Na$ ) 184.0733, found 184.0715.

**2.1.1g.** Colorless oil.  $^1H$  NMR (500 MHz,  $CDCl_3$ )  $\delta$  7.68-7.57 (m, 2 H), 7.51-7.35 (m, 3 H), 4.26 (dt,  $J = 15.0$ , 7.8 Hz, 4 H), 2.41-2.25 (m, 2H).  $^{13}C$  NMR (125 MHz,  $CDCl_3$ )  $\delta$  170.24, 133.26, 130.82, 128.31, 127.78, 30.92, 16.03. MS = 161.1 (EI). HRMS calcd for  $C_{10}H_{11}NONa$  ( $M^+ + Na$ ) 184.0733, found 184.0737.

**2.1.1h.** White solid.  $^1H$  NMR (500 MHz,  $CDCl_3$ )  $\delta$  7.78 (d,  $J = 8.0$  Hz, 2 H), 7.331 (d,  $J = 8.0$  Hz, 2 H), 2.79 (t,  $J = 6.6$  Hz, 4 H), 2.45 (s, 3 H), 2.16 (p,  $J = 6.6$  Hz, 2 H).  $^{13}C$

NMR (125 MHz,  $\text{CDCl}_3$ )  $\delta$  171.87, 170.39, 146.32, 130.32, 129.87, 129.24, 32.42, 21.89, 17.52. MS = 231.1 (EI). HRMS calcd for  $\text{C}_{13}\text{H}_{13}\text{NO}_3\text{Na}$  ( $\text{M}^+ + \text{Na}$ ) 254.0788, found 254.0799.

**2.1.1i.** White solid.  $^1\text{H}$  NMR (500 MHz,  $\text{CDCl}_3$ )  $\delta$  7.87-7.82 (d,  $J = 7.5$  Hz, 2 H), 6.99-6.94 (d,  $J = 7.5$  Hz, 2 H), 3.90 (s, 3 H), 2.78 (t,  $J = 6.6$  Hz, 4 H), 2.15 (p,  $J = 6.6$  Hz, 2 H).  $^{13}\text{C}$  NMR (125 MHz,  $\text{CDCl}_3$ )  $\delta$  171.88, 169.48, 165.09, 132.75, 124.51, 114.49, 55.69, 32.45, 17.52. MS = 247.1 (EI). HRMS calcd for  $\text{C}_{13}\text{H}_{13}\text{NO}_4\text{Na}$  ( $\text{M}^+ + \text{Na}$ ) 270.0737, found 270.0743.

**2.1.1j.** White solid.  $^1\text{H}$  NMR (500 MHz,  $\text{CDCl}_3$ )  $\delta$  8.00 (d,  $J = 8.1$  Hz, 2 H), 7.79 (d,  $J = 8.0$  Hz, 2 H), 2.83 (t,  $J = 6.5$  Hz, 4 H), 2.20 (q,  $J = 6.6$  Hz, 2 H).  $^{13}\text{C}$  NMR (125 MHz,  $\text{CDCl}_3$ )  $\delta$  171.97, 170.17, 135.93 (q,  $J^2 = 36.7$  Hz), 134.80, 130.36, 126.21 (q,  $J^3 = 3.5$  Hz), 123.27 (q,  $J^1 = 272.4$  Hz).  $^{19}\text{F}$  (471 MHz,  $\text{CDCl}_3$ )  $\delta$  -63.4. MS = 285.1 (EI). HRMS calcd for  $\text{C}_{13}\text{H}_{10}\text{F}_3\text{NO}_3\text{Na}$  ( $\text{M}^+ + \text{Na}$ ) 308.0505, found 308.0512.

**2.1.1k.** White solid.  $^1\text{H}$  NMR (500 MHz,  $\text{CDCl}_3$ )  $\delta$  7.97 (d,  $J = 8.5$  Hz, 2 H), 7.82 (d,  $J = 8.5$  Hz, 2 H), 2.82 (t,  $J = 6.5$  Hz, 4 H), 2.20 (p,  $J = 6.6$  Hz, 2 H).  $^{13}\text{C}$  NMR (125 MHz,  $\text{CDCl}_3$ )  $\delta$  171.89, 169.88, 135.23, 132.86, 130.30, 117.97, 117.48, 32.38, 17.43. MS = 242.1 (ESI). HRMS calcd for  $\text{C}_{13}\text{H}_{10}\text{N}_2\text{O}_3\text{Na}$  ( $\text{M}^+ + \text{Na}$ ) 265.0584, found 265.0591.

**2.1.1l.** Yellow solid.  $^1\text{H}$  NMR (500 MHz,  $\text{CDCl}_3$ )  $\delta$  8.36 (d,  $J = 7.5$  Hz, 2 H), 8.04 (d,  $J = 7.5$  Hz, 2 H), 2.84 (t,  $J = 6.5$  Hz, 4 H), 2.21 (p,  $J = 6.6$  Hz, 2 H).  $^{13}\text{C}$  NMR (125 MHz,  $\text{CDCl}_3$ )  $\delta$  171.91, 169.70, 151.20, 136.73, 131.00, 124.25, 32.39, 17.42. MS = 262.1 (EI). HRMS calcd for  $\text{C}_{12}\text{H}_{10}\text{N}_2\text{O}_5\text{Na}$  ( $\text{M}^+ + \text{Na}$ ) 285.0560, found 285.0558.

**2.1.1m.** White solid.  $^1\text{H}$  NMR (500 MHz,  $\text{CDCl}_3$ )  $\delta$  7.81 (d,  $J = 8.5$  Hz, 2 H), 7.48 (d,  $J = 8.5$  Hz, 2 H), 2.80 (t,  $J = 6.5$  Hz, 4 H), 2.17 (p,  $J = 6.6$  Hz, 2 H).  $^{13}\text{C}$  NMR (125 MHz,  $\text{CDCl}_3$ )  $\delta$  171.91, 169.89, 141.68, 131.44, 130.31, 129.55, 32.40, 17.47. MS = 251.0 (EI). HRMS calcd for  $\text{C}_{12}\text{H}_{11}\text{ClNO}_3$  ( $\text{M}^+ + \text{H}$ ) 252.0422, found 252.0433.

**2.1.1n.** White solid.  $^1\text{H}$  NMR (500 MHz,  $\text{CDCl}_3$ )  $\delta$  7.91 (dd,  $J = 8.5, 5.2$  Hz, 2 H), 7.18 (t,  $J = 8.4$  Hz, 2 H), 2.79 (t,  $J = 6.5$  Hz, 4 H), 2.15 (p,  $J = 6.5$  Hz, 2 H).  $^{13}\text{C}$  NMR (125 MHz,  $\text{CDCl}_3$ )  $\delta$  171.94, 169.59, 166.84 (d,  $J^I = 258.4$  Hz), 133.01 (d,  $J^3 = 10.2$  Hz), 128.30 (d,  $J^4 = 2.7$  Hz), 116.52 (d,  $J^2 = 22.1$  Hz), 32.37, 17.46.  $^{19}\text{F}$  (471 MHz,  $\text{CDCl}_3$ )  $\delta$  -101.31. MS = 235.1 (EI). HRMS calcd for  $\text{C}_{12}\text{H}_{10}\text{FNO}_3\text{Na}$  ( $\text{M}^+ + \text{Na}$ ) 258.0537, found 258.0547.

**2.1.1o.** White solid.  $^1\text{H}$  NMR (500 MHz,  $\text{CDCl}_3$ )  $\delta$  8.11 (td,  $J = 7.8, 1.8$  Hz, 1 H), 7.63 (dddd,  $J = 8.3, 7.1, 5.0, 1.8$  Hz, 1 H), 7.36-7.30 (m, 1 H), 7.13 (ddd,  $J = 12.0, 8.4, 1.1$  Hz, 1 H), 2.76 (t,  $J = 6.5$  Hz, 4 H), 2.13 (p,  $J = 6.6$  Hz, 2 H).  $^{13}\text{C}$  NMR (125 MHz,  $\text{CDCl}_3$ )  $\delta$  171.68, 166.86, 161.79 (d,  $J^I = 255.9$  Hz), 136.79 (d,  $J^3 = 10.0$  Hz), 132.95, 125.09 (d,  $J^4 = 3.6$  Hz), 120.36 (d,  $J^3 = 7.0$  Hz), 117.08 (d,  $J^2 = 23.6$  Hz), 32.41, 17.24.  $^{19}\text{F}$  NMR (471 MHz,  $\text{CDCl}_3$ )  $\delta$  -113.49. MS = 235.1 (ESI). HRMS calcd for  $\text{C}_{12}\text{H}_{10}\text{FNO}_3$  ( $\text{M}^+ + \text{Na}$ ) 285.0537, found 285.0548.

**2.1.1p.** White solid.  $^1\text{H}$  NMR (500 MHz,  $\text{CDCl}_3$ )  $\delta$  7.54-7.46 (m, 2 H), 7.35 (d,  $J = 7.6$  Hz, 1 H), 7.29-7.25 (m, 1 H), 2.77 (t,  $J = 6.6$  Hz, 4 H), 2.70 (s, 3 H), 2.14 (p,  $J = 6.6$  Hz, 2 H).  $^{13}\text{C}$  NMR (125 MHz,  $\text{CDCl}_3$ )  $\delta$  171.98, 170.66, 142.53, 133.75, 132.44, 131.19,

130.70, 126.19, 32.48, 21.89, 17.45. MS = 231.1 (ESI). HRMS calcd for  $C_{13}H_{13}NO_3Na$  ( $M^+ + Na$ ) 254.0788, found 254.0793.

**2.1.1q.** White solid.  $^1H$  NMR (500 MHz,  $CDCl_3$ )  $\delta$  8.37 (s, 1 H), 7.99-7.93 (m, 3 H), 7.91 (d,  $J = 8.2$  Hz, 1 H), 7.66 (ddd,  $J = 8.2, 6.8, 1.3$  Hz, 1 H), 7.59 (ddd,  $J = 8.1, 6.9, 1.3$  Hz, 1 H), 2.85 (t,  $J = 6.5$  Hz, 4 H), 2.22 (p,  $J = 6.6$  Hz, 2 H).  $^{13}C$  NMR (125 MHz,  $CDCl_3$ )  $\delta$  172.02, 170.89, 136.42, 132.65, 132.45, 129.83, 129.51, 129.20, 127.91, 127.17, 124.75, 32.50, 17.57. MS = 267.1 (EI). HRMS calcd for  $C_{16}H_{13}NO_3Na$  ( $M^+ + Na$ ) 290.0788, found 290.0804.

**2.1.1r.** White solid.  $^1H$  NMR (500 MHz,  $CDCl_3$ )  $\delta$  8.08 (d,  $J = 2.8$  Hz, 1 H), 7.50 (d,  $J = 5.2$  Hz, 1 H), 7.39 (dd,  $J = 5.3, 2.9$  Hz, 1 H), 2.79 (t,  $J = 6.6$  Hz, 4 H), 2.15 (p,  $J = 6.6$  Hz, 2 H).  $^{13}C$  NMR (125 MHz,  $CDCl_3$ )  $\delta$  171.73, 164.49, 136.54, 136.39, 127.77, 127.43, 32.43, 17.50. MS = 223.0 (EI). HRMS calcd for  $C_{10}H_9NO_3SNa$  ( $M^+ + Na$ ) 246.0195, found 246.0170.

**2.1.1s.** White solid.  $^1H$  NMR (500 MHz,  $CDCl_3$ )  $\delta$  3.12 (t,  $J = 7.3$  Hz, 2 H), 2.69 (t,  $J = 7.0$  Hz, 4 H), 2.04 (p,  $J = 6.6$  Hz, 2 H), 1.72 (p,  $J = 7.4$  Hz, 2 H), 1.44 (t,  $J = 7.3$  Hz, 1 H), 1.41-1.22 (m, 11 H), 0.90 (t,  $J = 6.8$  Hz, 3 H).  $^{13}C$  NMR (125 MHz,  $CDCl_3$ )  $\delta$  178.20, 171.55, 45.78, 41.01, 32.26, 31.85, 29.37, 29.26, 28.62, 23.43, 22.67, 17.32, 14.12. MS = 267.1 (EI). HRMS calcd for  $C_{15}H_{25}NO_3Na$  ( $M^+ + Na$ ) 290.1727, found 290.1739.

**2.1.1t.** White solid.  $^1H$  NMR (500 MHz,  $CDCl_3$ )  $\delta$  2.92 (hept,  $J = 7.0$  Hz, 1 H), 2.69 (t,  $J = 6.5$  Hz, 4 H), 2.05 (p,  $J = 6.5$  Hz, 2 H), 1.25 (d,  $J = 7.1$  Hz, 6 H).  $^{13}C$  NMR (125 MHz,

$\text{CDCl}_3$ )  $\delta$  181.85, 171.78, 39.77, 32.36, 17.81, 17.38. MS = 183.1 (EI). HRMS calcd for  $\text{C}_{18}\text{H}_{26}\text{N}_2\text{O}_6\text{Na}$  ( $2\text{M}^+ + \text{Na}$ ) 389.1683, found 389.1709.

**2.1.1u.** White solid.  $^1\text{H}$  NMR (500 MHz,  $\text{CDCl}_3$ )  $\delta$  2.67 (t,  $J$  = 6.5 Hz, 4 H), 2.05 (p,  $J$  = 6.5 Hz, 2 H), 1.28 (s, 9 H).  $^{13}\text{C}$  NMR (125 MHz,  $\text{CDCl}_3$ )  $\delta$  185.57, 171.86, 43.75, 32.17, 27.14, 17.44. MS = 197.1 (EI). HRMS calcd for  $\text{C}_{10}\text{H}_{15}\text{NO}_3\text{Na}$  ( $\text{M}^+ + \text{Na}$ ) 220.0944, found 220.0952.

**2.1.1w.** Yellow solid.  $^1\text{H}$  NMR (500 MHz,  $\text{CDCl}_3$ )  $\delta$  7.72 (dd,  $J$  = 8.7, 3.0 Hz, 2 H), 7.63 (d,  $J$  = 1.8 Hz, 1 H), 7.34 (dd,  $J$  = 8.5, 1.8 Hz, 1 H), 7.17 (dd,  $J$  = 8.9, 2.5 Hz, 1 H), 7.13 (d,  $J$  = 2.5 Hz, 1 H), 4.29 (q,  $J$  = 7.1 Hz, 1 H), 3.94 (s, 3 H), 2.39 (t,  $J$  = 6.5 Hz, 4 H), 1.70 (d,  $J$  = 7.0 Hz, 3 H), 1.64-1.71 (m, 2 H).  $^{13}\text{C}$  NMR (125 MHz,  $\text{CDCl}_3$ )  $\delta$  178.72, 171.24, 157.87, 133.99, 133.26, 129.30, 128.73, 127.34, 127.10, 126.66, 119.20, 105.62, 55.33, 50.56, 32.15, 17.23, 16.98. MS = 325.1 (EI). HRMS calcd for  $\text{C}_{19}\text{H}_{19}\text{NO}_4\text{Na}$  ( $\text{M}^+ + \text{Na}$ ) 348.1206, found 348.1232.

**2.1.3b.** White solid.  $^1\text{H}$  NMR (500 MHz,  $\text{CDCl}_3$ )  $\delta$  7.84 (dd,  $J$  = 8.5, 1.5 Hz, 4 H), 7.62 (tt,  $J$  = 7.5, 1.5 Hz, 2 H), 7.51 (t,  $J$  = 7.7 Hz, 4 H).  $^{13}\text{C}$  NMR (125 MHz,  $\text{CDCl}_3$ )  $\delta$  196.74, 137.62, 132.41, 130.06, 128.31. MS = 182.1 (EI). HRMS calcd for  $\text{C}_{13}\text{H}_{10}\text{ONa}$  ( $\text{M}^+ + \text{Na}$ ) 205.0624 found 205.0631.

**2.1.3c.** White solid.  $^1\text{H}$  NMR (500 MHz,  $\text{CDCl}_3$ )  $\delta$  7.86 (d,  $J$  = 8.0 Hz, 2 H), 7.78 (d,  $J$  = 7.6 Hz, 2 H), 7.59 (t,  $J$  = 7.5 Hz, 1 H), 7.50 (t,  $J$  = 7.5 Hz, 2 H), 6.99 (d,  $J$  = 7.5 Hz, 2 H), 3.92 (s, 3 H).  $^{13}\text{C}$  NMR (125 MHz,  $\text{CDCl}_3$ )  $\delta$  195.56, 163.23, 138.30, 132.57, 131.89,

130.17, 129.74, 128.19, 113.56, 55.51. MS = 212.1 (EI). HRMS calcd for  $C_{14}H_{13}O_2$  ( $M^+ + H$ ) 213.0910 found 213.0917.

**2.1.3d.** White solid.  $^1H$  NMR (500 MHz,  $CDCl_3$ )  $\delta$  8.09 (d,  $J$  = 8.2 Hz, 2 H), 7.89 (d,  $J$  = 8.3 Hz, 2 H), 7.83 (d,  $J$  = 7.5 Hz, 2 H), 7.65 (t,  $J$  = 6.5 Hz, 1 H), 7.53 (t,  $J$  = 7.7 Hz, 2 H), 2.70 (s, 3 H).  $^{13}C$  NMR (125 MHz,  $CDCl_3$ )  $\delta$  197.52, 195.96, 141.34, 139.57, 136.92, 133.00, 130.11, 130.05, 128.49, 128.17, 26.92. MS = 224.1 (EI). HRMS calcd for  $C_{15}H_{12}O_2Na$  ( $M^+ + Na$ ) 247.0730 found 247.0741.

**2.1.3e.** White solid.  $^1H$  NMR (500 MHz,  $CDCl_3$ )  $\delta$  7.93 (d,  $J$  = 8.0 Hz, 2 H), 7.84 (d,  $J$  = 7.7 Hz, 2 H), 7.79 (d,  $J$  = 8.0 Hz, 2 H), 7.66 (t,  $J$  = 7.4 Hz, 1 H), 7.54 (t,  $J$  = 7.6 Hz, 2 H).  $^{13}C$  NMR (125 MHz,  $CDCl_3$ )  $\delta$  195.53, 140.74, 136.74, 133.46 (q,  $J^2$  = 32.0 Hz), 133.09, 130.14, 130.11, 128.54, 125.36 (q,  $J^3$  = 3.5 Hz), 123.68 (q,  $J^I$  = 271.5 Hz).  $^{19}F$  (471 MHz,  $CDCl_3$ )  $\delta$  -63.0. MS = 250.1 (EI). HRMS calcd for  $C_{14}H_9F_3ONa$  ( $M^+ + Na$ ) 273.0498 found 273.0510.

**2.1.3f** Colorless oil.  $^1H$  NMR (500 MHz,  $CDCl_3$ )  $\delta$  7.84 (d,  $J$  = 8.5 Hz, 2 H), 7.61 (t,  $J$  = 6.5 Hz, 1 H), 7.49 (t,  $J$  = 7.0 Hz, 2 H), 7.42 (t,  $J$  = 7.5 Hz, 1 H), 7.33 (m, 2 H), 7.29 (m, 1 H), 2.35 (s, 3 H).  $^{13}C$  NMR (125 MHz,  $CDCl_3$ )  $\delta$  198.64, 138.63, 137.75, 136.75, 133.14, 131.00, 130.24, 130.14, 128.52, 128.46, 125.20, 20.00. MS = 196.1 (EI). HRMS calcd for  $C_{14}H_{12}ONa$  ( $M^+ + Na$ ) 219.0780 found 219.0782.

**2.1.3g.** Colorless oil.  $^1H$  NMR (500 MHz,  $CDCl_3$ )  $\delta$  8.13 (d,  $J$  = 8.2 Hz, 1 H), 8.04 (d,  $J$  = 8.2 Hz, 1 H), 7.96 (dd,  $J$  = 7.8, 1.7 Hz, 1 H), 7.91-7.88 (d,  $J$  = 7.0 Hz, 2 H), 7.65-7.59 (m, 2 H), 7.59-7.51 (m, 3 H), 7.49 (t,  $J$  = 7.7 Hz, 2 H).  $^{13}C$  NMR (125 MHz,  $CDCl_3$ )  $\delta$  198.03,

138.33, 136.37, 133.73, 133.23, 131.27, 130.97, 130.42, 128.46, 128.41, 127.77, 127.26, 126.47, 125.71, 124.34. MS = 232.1 (EI). HRMS calcd for  $C_{17}H_{12}ONa$  ( $M^+ + Na$ ) 255.0780 found 255.0790.

**2.1.3h.** White solid.  $^1H$  NMR (500 MHz,  $CDCl_3$ )  $\delta$  8.10 (s, 1 H), 8.06 (d,  $J = 8.0$  Hz, 1 H), 7.90 (dt,  $J = 7.7, 1.4$  Hz, 1 H), 7.81 (dd,  $J = 8.2, 1.4$  Hz, 2 H), 7.67 (q,  $J = 7.7$  Hz, 2 H), 7.55 (t,  $J = 7.6$  Hz, 2 H).  $^{13}C$  NMR (125 MHz,  $CDCl_3$ )  $\delta$  194.40, 138.63, 136.33, 135.35, 133.84, 133.47, 133.29, 130.00, 129.41, 128.69, 117.95, 112.86. MS = 207.1 (EI). HRMS calcd for  $C_{28}H_{18}N_2O_2Na$  ( $2M^+ + Na$ ) 437.1260 found 437.1295.

**2.1.3i.** White solid.  $^1H$  NMR (500 MHz,  $CDCl_3$ )  $\delta$  7.84-7.80 (m, 3 H), 7.70 (dt,  $J = 7.7, 1.3$  Hz, 1 H), 7.64 (t,  $J = 7.5$  Hz, 1 H), 7.59 (dd,  $J = 8.5, 1.5$  Hz, 1 H), 7.53 (t,  $J = 7.7$  Hz, 2 H), 7.46 (t,  $J = 7.9$  Hz, 1 H).  $^{13}C$  NMR (125 MHz,  $CDCl_3$ )  $\delta$  195.27, 139.27, 136.96, 134.58, 132.84, 132.36, 130.03, 129.91, 129.64, 128.47, 128.11. MS = 216.0 (EI). HRMS calcd for  $C_{13}H_9ClONa$  ( $M^+ + Na$ ) 239.0234 found 239.0243.

**2.1.3j.** Colorless oil.  $^1H$  NMR (500 MHz,  $CDCl_3$ )  $\delta$  7.96 (dd,  $J = 2.8, 1.2$  Hz, 1 H), 7.88 (dd,  $J = 8.0, 1.5$  Hz, 2 H), 7.66-7.58 (m, 2 H), 7.52 (t,  $J = 7.6$  Hz, 2 H), 7.41 (dd,  $J = 5.1, 2.9$  Hz, 1 H).  $^{13}C$  NMR (125 MHz,  $CDCl_3$ )  $\delta$  190.01, 141.31, 138.64, 133.92, 132.31, 129.38, 128.62, 128.39, 126.21. MS = 188.0 (EI). HRMS calcd for  $C_{22}H_{16}O_2S_2Na$  ( $2M^+ + Na$ ) 399.0484 found 399.0498.

**2.1.3k.** Colorless oil.  $^1H$  NMR (500 MHz,  $CDCl_3$ )  $\delta$  7.95 (d,  $J = 1.3$  Hz, 1 H), 7.88 (d,  $J = 7.0$  Hz, 2 H), 7.62 (t,  $J = 7.0$  Hz, 1 H), 7.56-7.49 (m, 3 H), 6.94 (d,  $J = 1.8$  Hz, 1 H).  $^{13}C$  NMR (125 MHz,  $CDCl_3$ )  $\delta$  189.44, 148.57, 143.96, 138.83, 132.48, 128.83, 128.56,



126.53, 110.23. MS = 172.1 (EI). HRMS calcd for  $C_{22}H_{16}O_4Na$  ( $2M^+ + Na$ ) 367.0941, found 367.0954.

**2.1.3l.** Colorless oil.  $^1H$  NMR (500 MHz,  $CDCl_3$ )  $\delta$  7.95 (dd,  $J = 7.5, 1.0$  Hz, 3 H), 7.90 (d,  $J = 7.5$  Hz, 1 H), 7.89 (s, 1 H), 7.66 (t,  $J = 7.0$  Hz, 1 H), 7.57 (t,  $J = 7.6$  Hz, 2 H), 7.52 (ddd,  $J = 8.1, 7.1, 1.2$  Hz, 1 H), 7.45 (ddd,  $J = 8.1, 7.1, 1.1$  Hz, 1 H).  $^{13}C$  NMR (125 MHz,  $CDCl_3$ )  $\delta$  189.66, 143.14, 142.73, 139.07, 137.88, 132.49, 132.23, 129.28, 128.53, 127.46, 126.06, 125.05, 122.93. MS = 238.1 (EI). HRMS calcd for  $C_{15}H_{10}OSNa$  ( $M^+ + Na$ ) 261.0345, found 261.0353.

**2.1.3m.** Colorless oil.  $^1H$  NMR (500 MHz,  $CDCl_3$ )  $\delta$  8.58 (br, 1 H), 8.17 (d,  $J = 1.5$  Hz, 1 H), 7.84 (d,  $J = 8.0$  Hz, 2 H), 7.83 (m, 1 H), 7.61 (t,  $J = 7.0$  Hz, 1 H), 7.52 (t,  $J = 8.0$  Hz, 2 H), 7.49 (d,  $J = 9.0$  Hz, 1 H), 7.32 (t,  $J = 2.8$  Hz, 1 H), 6.68 (t,  $J = 2.6$  Hz, 1 H).  $^{13}C$  NMR (125 MHz,  $CDCl_3$ )  $\delta$  197.36, 139.01, 138.27, 131.64, 129.93, 129.79, 128.10, 127.16, 125.70, 125.28, 124.27, 111.00, 104.30. MS = 221.1 (EI). HRMS calcd for  $C_{15}H_{11}NONa$  ( $M^+ + Na$ ) 244.0733, found 244.0741.

**2.1.3n.** White solid.  $^1H$  NMR (500 MHz,  $CDCl_3$ )  $\delta$  7.82 (d,  $J = 7.5$  Hz, 2 H), 7.75 (d,  $J = 7.9$  Hz, 2 H), 7.60 (t,  $J = 7.5$  Hz, 1 H), 7.50 (t,  $J = 7.6$  Hz, 2 H), 7.31 (d,  $J = 7.9$  Hz, 2 H), 2.47 (s, 3 H).  $^{13}C$  NMR (125 MHz,  $CDCl_3$ )  $\delta$  196.50, 143.23, 137.98, 134.90, 132.15, 130.31, 129.93, 128.98, 128.21, 21.67. MS = 196.1 (EI). HRMS calcd for  $C_{14}H_{12}ONa$  ( $M^+ + Na$ ) 219.0780 found 219.0786.

**2.1.3o.** White solid.  $^1H$  NMR (500 MHz,  $CDCl_3$ )  $\delta$  7.91 (d,  $J = 9.0$  Hz, 2 H), 7.85-7.78 (m, 4 H), 7.67 (t,  $J = 7.5$  Hz, 1 H), 7.55 (t,  $J = 7.6$  Hz, 2 H).  $^{13}C$  NMR (125 MHz,  $CDCl_3$ )

$\delta$  195.04, 141.24, 136.34, 133.34, 132.18, 130.25, 130.08, 128.65, 118.02, 115.68. MS = 207.1 (EI). HRMS calcd for  $C_{14}H_9NO$  ( $M^+$ ) 207.0679 found 207.0705.

**2.1.3p.** White solid.  $^1H$  NMR (500 MHz,  $CDCl_3$ )  $\delta$  8.37 (d,  $J = 9.0$  Hz, 2 H), 7.97 (d,  $J = 9.0$  Hz, 2 H), 7.82 (dd,  $J = 7.5, 1.0$  Hz, 2 H), 7.68 (tt,  $J = 7.5, 1.5$  Hz, 1 H), 7.56 (t,  $J = 7.8$  Hz, 2 H).  $^{13}C$  NMR (125 MHz,  $CDCl_3$ )  $\delta$  194.80, 149.82, 142.90, 136.30, 133.48, 130.71, 130.11, 128.70, 123.56. MS = 227.1 (EI). HRMS calcd for  $C_{26}H_{18}N_2O_6Na$  ( $2 M^+ + Na$ ) 477.1057 found 477.1083.

**2.1.3q.** White solid.  $^1H$  NMR (500 MHz,  $CDCl_3$ )  $\delta$  7.80 (td,  $J = 7.7, 7.1, 1.7$  Hz, 4 H), 7.63 (t,  $J = 7.0$  Hz, 1 H), 7.55-7.47 (m, 4 H).  $^{13}C$  NMR (126 MHz,  $CDCl_3$ )  $\delta$  195.50, 138.91, 137.27, 135.89, 132.64, 131.46, 129.93, 128.64, 128.40. MS = 216.0 (EI). HRMS calcd for  $C_{26}H_{18}N_2O_6Na$  ( $M^+ + Na$ ) 239.0234 found 239.0347.

**2.1.3r.** White solid.  $^1H$  NMR (500 MHz,  $CDCl_3$ )  $\delta$  7.92-7.84 (m, 2 H), 7.80 (dd,  $J = 7.5, 1.0$  Hz, 2 H), 7.62 (t,  $J = 8.0$  Hz, 1 H), 7.52 (t,  $J = 7.7$  Hz, 2 H), 7.19 (tt,  $J = 8.5, 2.0$  Hz, 2 H).  $^{13}C$  NMR (125 MHz,  $CDCl_3$ )  $\delta$  195.29, 165.40 (d,  $J^I = 125.4$  Hz), 137.51, 133.82, 132.68 (d,  $J^3 = 9.1$  Hz), 132.48, 129.89, 128.37, 115.47 (d,  $J^2 = 22.5$  Hz).  $^{19}F$  (471 MHz,  $CDCl_3$ )  $\delta$  -106.00. MS = 200.1 (EI). HRMS calcd for  $C_{26}H_{18}F_2O_2Na$  ( $2 M^+ + Na$ ) 423.1167 found 423.1178.

**2.1.3s.** White solid.  $^1H$  NMR (500 MHz,  $CDCl_3$ )  $\delta$  7.87 (d,  $J = 7.7$  Hz, 2 H), 7.63 (t,  $J = 7.0$  Hz, 1 H), 7.58-7.54 (m, 2 H), 7.51 (t,  $J = 7.7$  Hz, 2 H), 7.30 (t,  $J = 7.0$  Hz, 1 H), 7.19 (t,  $J = 9.1$  Hz, 1 H).  $^{13}C$  NMR (125 MHz,  $CDCl_3$ )  $\delta$  193.47, 160.10 (d,  $J^I = 252.1$  Hz), 137.41, 133.41, 133.05 (d,  $J^3 = 8.1$  Hz), 130.76 (d,  $J^3 = 2.9$  Hz), 129.82, 128.47, 127.11

(d,  $J^2 = 14.1$  Hz), 124.29 (d,  $J^4 = 3.5$  Hz), 116.28 (d,  $J^2 = 21.5$  Hz).  $^{19}\text{F}$  (470.6 MHz,  $\text{CDCl}_3$ )  $\delta$  -111.2. MS = 200.1 (EI). HRMS calcd for  $\text{C}_{13}\text{H}_9\text{FONa}$  ( $\text{M}^+ + \text{Na}$ ) 223.0530 found 223.0536.

**2.1.3t.** White solid.  $^1\text{H}$  NMR (500 MHz,  $\text{CDCl}_3$ )  $\delta$  8.30 (s, 1 H), 7.98 (s, 2 H), 7.95 (dd,  $J = 8.0, 2.0$  Hz, 1 H), 7.90 (d,  $J = 7.0$  Hz, 1 H), 7.92-7.87 (m, 2 H), 7.65 (td,  $J = 7.7, 4.5$  Hz, 2 H), 7.57 (dt,  $J = 18.3, 7.7$  Hz, 3 H).  $^{13}\text{C}$  NMR (125 MHz,  $\text{CDCl}_3$ )  $\delta$  196.76, 137.92, 135.28, 134.84, 132.39, 132.27, 131.88, 130.11, 129.43, 128.35, 128.34, 128.31, 127.84, 126.81, 125.80. MS = 232.1 (EI). HRMS calcd for  $\text{C}_{17}\text{H}_{12}\text{ONa}$  ( $\text{M}^+ + \text{Na}$ ) 255.0780 found 255.0790.

**2.1.3u.** Colorless oil.  $^1\text{H}$  NMR (500 MHz,  $\text{CDCl}_3$ )  $\delta$  7.99 (d,  $J = 8.5$  Hz, 2 H), 7.58 (t,  $J = 7.4$  Hz, 1 H), 7.49 (t,  $J = 7.6$  Hz, 2 H), 2.99 (t,  $J = 7.4$  Hz, 2 H), 1.76 (p,  $J = 7.4$  Hz, 2 H), 1.48-1.37 (m, 1 H), 1.40-1.23 (m, 11 H), 0.91 (t,  $J = 6.8$  Hz, 3 H).  $^{13}\text{C}$  NMR (125 MHz,  $\text{CDCl}_3$ )  $\delta$  200.64, 137.12, 132.85, 128.55, 128.06, 38.66, 31.89, 29.50, 29.49, 29.40, 29.30, 24.42, 22.68, 14.12. MS = 232.1 (EI). HRMS calcd for  $\text{C}_{16}\text{H}_{24}\text{ONa}$  ( $\text{M}^+ + \text{Na}$ ) 255.1719 found 255.1706.

**2.1.3v.** Colorless oil.  $^1\text{H}$  NMR (500 MHz,  $\text{CDCl}_3$ )  $\delta$  7.99 (d,  $J = 8.5$  Hz, 2 H), 7.58 (t,  $J = 7.0$  Hz, 1 H), 7.50 (t,  $J = 8.0$  Hz, 2 H), 3.59 (hept,  $J = 6.9$ , 1 H), 1.25 (d,  $J = 6.7$  Hz, 6 H).  $^{13}\text{C}$  NMR (125 MHz,  $\text{CDCl}_3$ )  $\delta$  204.51, 136.23, 132.78, 128.60, 128.31, 35.37, 19.16. MS = 148.1 (EI). HRMS calcd for  $\text{C}_{10}\text{H}_{12}\text{OK}$  ( $\text{M}^+ + \text{K}$ ) 187.0520 found 187.0490.

**2.1.4.** Colorless oil.  $^1\text{H}$  NMR (500 MHz,  $\text{CDCl}_3$ )  $\delta$  7.81-7.69 (m, 3 H), 7.63 (dd,  $J = 8.6, 1.7$  Hz, 1 H), 7.18-7.15 (m, 2 H), 6.88 (dd,  $J = 17.6, 10.9$  Hz, 1 H), 5.85 (d,  $J = 17.6$  Hz,

1 H), 5.30 (d,  $J = 10.9$  Hz, 1 H), 3.95 (s, 3 H).  $^{13}\text{C}$  NMR (125 MHz,  $\text{CDCl}_3$ )  $\delta$  157.79, 136.95, 134.31, 132.99, 129.55, 128.95, 127.00, 126.16, 123.78, 118.95, 113.10, 105.87, 55.32. MS = 184.1 (EI). HRMS calcd for  $\text{C}_{13}\text{H}_{12}\text{ONa}$  ( $\text{M}^+ + \text{Na}$ ) 207.0780 found 207.0792.

**2.1.3x.** White solid.  $^1\text{H}$  NMR (500 MHz,  $\text{CDCl}_3$ )  $\delta$  7.86 (d,  $J = 8.0$  Hz, 2 H), 7.77 (d,  $J = 8.0$  Hz, 2 H), 7.45-7.34 (m, 2 H), 6.90 (d,  $J = 8.0$  Hz, 1 H), 6.12 (s, 2 H).  $^{13}\text{C}$  NMR (125 MHz,  $\text{CDCl}_3$ )  $\delta$  193.89, 152.14, 148.28, 141.24, 133.53 (q,  $J^2 = 30.6$  Hz), 131.19, 129.77, 127.19, 125.32, 123.74 (q,  $J^1 = 254.1$  Hz), 109.72, 107.88, 102.05.  $^{19}\text{F}$  (470.6 MHz,  $\text{CDCl}_3$ )  $\delta$  -63.0. MS = 294.1 (EI). HRMS calcd for  $\text{C}_{15}\text{H}_{10}\text{O}_3\text{F}_3$  ( $\text{M}^+ + \text{H}$ ) 295.0577 found 295.0586.

**2.1.3y.** White solid.  $^1\text{H}$  NMR (500 MHz,  $\text{CDCl}_3$ )  $\delta$  7.90 (d,  $J = 8.2$  Hz, 2 H), 7.82 (d,  $J = 8.1$  Hz, 2 H), 7.43 (t,  $J = 7.9$  Hz, 1 H), 7.37 (dd,  $J = 2.7, 1.5$  Hz, 1 H), 7.31 (dt,  $J = 7.6, 1.2$  Hz, 1 H), 7.22-7.19 (m, 1 H), 3.90 (s, 3 H).  $^{13}\text{C}$  NMR (125 MHz,  $\text{CDCl}_3$ )  $\delta$  194.83, 159.83, 141.29, 137.61, 132.15, 130.22, 129.57, 122.87, 119.73, 118.02, 115.68, 114.30, 55.55. MS = 237.1 (EI). HRMS calcd for  $\text{C}_{15}\text{H}_{11}\text{NO}_2\text{Na}$  ( $\text{M}^+ + \text{Na}$ ) 260.0682 found 260.0692.

**2.1.3z.** White solid.  $^1\text{H}$  NMR (500 MHz,  $\text{CDCl}_3$ )  $\delta$  7.87 (d,  $J = 8.5$  Hz, 2 H), 7.40 (t,  $J = 8.5$  Hz, 1 H), 7.35-7.27 (m, 2 H), 7.14 (ddd,  $J = 8.2, 2.6, 1.2$  Hz, 1 H), 6.99 (d,  $J = 8.5$  Hz, 2 H), 3.91 (s, 3 H), 3.89 (s, 3 H).  $^{13}\text{C}$  NMR (125 MHz,  $\text{CDCl}_3$ )  $\delta$  195.31, 163.25, 159.50, 139.62, 132.57, 130.17, 129.13, 122.42, 118.26, 114.19, 113.55, 55.51, 55.46. MS = 242.1 (EI). HRMS calcd for  $\text{C}_{15}\text{H}_{14}\text{O}_3\text{Na}$  ( $\text{M}^+ + \text{Na}$ ) 265.0835 found 265.0838.

**2.1.3aa.** Yellow solid.  $^1\text{H}$  NMR (500 MHz,  $\text{CDCl}_3$ )  $\delta$  8.13 (d,  $J = 8.1$  Hz, 2 H), 7.86 (d,  $J = 15.7$  Hz, 1 H), 7.80 (d,  $J = 8.1$  Hz, 2 H), 7.69 (dd,  $J = 6.6, 2.9$  Hz, 2 H), 7.52 (d,  $J = 15.7$  Hz, 1 H), 7.49-7.45 (m, 3 H).  $^{13}\text{C}$  NMR (125 MHz,  $\text{CDCl}_3$ )  $\delta$  189.68, 146.13, 141.08, 134.53, 134.04 (q,  $J^2 = 30.6$  Hz), 130.98, 129.07, 128.78, 128.61, 125.69 (q,  $J^3 = 3.6$  Hz), 123.68 (q,  $J^1 = 272.3$  Hz), 121.62.  $^{19}\text{F}$  (471 MHz,  $\text{CDCl}_3$ )  $\delta$  -63.0. MS = 276.1 (EI). HRMS calcd for  $\text{C}_{16}\text{H}_{14}\text{O}_4\text{Na}$  ( $\text{M}^+ + \text{Na}$ ) 299.0654 found 299.0659.

**2.1.3ab.** Yellow solid.  $^1\text{H}$  NMR (500 MHz,  $\text{CDCl}_3$ )  $\delta$  8.60 (t,  $J = 2.0$  Hz, 1 H), 8.45 (ddd,  $J = 8.3, 2.3, 1.1$  Hz, 1 H), 8.12 (dt,  $J = 7.7, 1.4$  Hz, 1 H), 7.85 (d,  $J = 9.5$  Hz, 2 H), 7.72 (t,  $J = 7.9$  Hz, 1 H), 7.03 (d,  $J = 8.5$  Hz, 2 H), 3.94 (s, 3 H).  $^{13}\text{C}$  NMR (125 MHz,  $\text{CDCl}_3$ )  $\delta$  192.86, 163.94, 148.00, 139.81, 135.20, 132.59, 129.55, 128.88, 126.26, 124.45, 114.04, 55.63. MS = 257.1 (EI). HRMS calcd for  $\text{C}_{14}\text{H}_{11}\text{NO}_4\text{Na}$  ( $\text{M}^+ + \text{Na}$ ) 280.0580 found 280.0585.

**2.1.3ac.** White solid.  $^1\text{H}$  NMR (500 MHz,  $\text{CDCl}_3$ )  $\delta$  8.19 (d,  $J = 9.0$  Hz, 2 H), 7.93 (d,  $J = 8.1$  Hz, 2 H), 7.86 (d,  $J = 8.0$  Hz, 2 H), 7.80 (d,  $J = 8.1$  Hz, 2 H), 4.00 (s, 3 H).  $^{13}\text{C}$  NMR (125 MHz,  $\text{CDCl}_3$ )  $\delta$  195.31, 163.25, 159.50, 139.62, 132.57, 130.17, 129.13, 122.42, 118.26, 114.19, 113.55, 55.46.  $^{19}\text{F}$  (471 MHz,  $\text{CDCl}_3$ )  $\delta$  -63.1. MS = 308.1 (EI). HRMS calcd for  $\text{C}_{16}\text{H}_{11}\text{F}_3\text{O}_3\text{Na}$  ( $\text{M}^+ + \text{Na}$ ) 331.0552 found 331.0561.

**2.1.3ad.** White solid.  $^1\text{H}$  NMR (500 MHz,  $\text{CDCl}_3$ )  $\delta$  10.09 (s, 1 H), 7.84 (d,  $J = 9.5$  Hz, 2 H), 7.56 (d,  $J = 2.5$  Hz, 1 H), 7.54 (d,  $J = 8.5$  Hz, 1 H), 7.18 (dd,  $J = 8.4, 2.7$  Hz, 1 H), 6.99 (d,  $J = 9.0$  Hz, 2 H), 3.96 (s, 3 H), 3.92 (s, 3 H).  $^{13}\text{C}$  NMR (125 MHz,  $\text{CDCl}_3$ )  $\delta$  194.06, 190.67, 163.90, 161.45, 138.02, 134.58, 132.61, 131.53, 130.68, 119.26, 113.89,

112.21, 55.79, 55.59. MS = 270.1 (EI). HRMS calcd for  $C_{16}H_{14}O_4Na$  ( $M^+ + Na$ ) 293.0784 found 293.0789.

**2.1.3ae.** Colorless oil.  $^1H$  NMR (500 MHz,  $CDCl_3$ )  $\delta$  7.92-7.87 (m, 2 H), 7.75 (d,  $J = 4.9$  Hz, 1 H), 7.68 (d,  $J = 3.8$  Hz, 1 H), 7.62 (t,  $J = 7.5$  Hz, 1 H), 7.53 (t,  $J = 7.6$  Hz, 2 H), 7.20 (t,  $J = 4.3$  Hz, 1 H).  $^{13}C$  NMR (125 MHz,  $CDCl_3$ )  $\delta$  188.24, 143.66, 138.17, 134.85, 134.21, 132.27, 129.18, 128.42, 127.96. MS = 188.0 (EI). HRMS calcd for  $C_{22}H_{16}O_2S_2Na$  ( $2 M^+ + Na$ ) 399.0484 found 399.0497.

**2.1.3af.** Colorless oil.  $^1H$  NMR (500 MHz,  $CDCl_3$ )  $\delta$  7.93-7.89 (m, 2 H), 7.73 (d,  $J = 4.0$  Hz, 1 H), 7.69-7.63 (m, 2 H), 7.55 (t,  $J = 7.7$  Hz, 2 H), 2.65 (d,  $J = 1.1$  Hz, 3 H).  $^{13}C$  NMR (125 MHz,  $CDCl_3$ )  $\delta$  190.84, 188.09, 149.30, 148.32, 137.25, 134.12, 132.97, 131.64, 129.34, 128.63, 27.24. MS = 230.0 (EI). HRMS calcd for  $C_{13}H_{10}O_2SNa$  ( $M^+ + Na$ ) 253.0294 found 253.0296.

## References

- (1) (a) *Metal-Catalyzed Cross-Coupling Reactions and More*, de Meijere, A.; Bräse, S.; Oestreich, M., Eds.; Wiley: New York, 2014. (b) *Science of Synthesis: Cross-Coupling and Heck-Type Reactions*, Molader, G.; Wolfe, J. P.; Larhed, M., Eds.; Thieme: Stuttgart, 2013. (c) *Handbook of Organopalladium Chemistry for Organic Synthesis*, Negishi, E., Ed.; Wiley: New York, 2002.
- (2) (a) Dieter, R. K. *Tetrahedron* **1999**, *55*, 4177. (b) Zapf, A. *Angew. Chem. Int. Ed.* **2003**, *42*, 5394. (c) Gooßen, L. J.; Rodriguez, N.; Gooßen, K. *Angew. Chem. Int. Ed.* **2008**, *47*, 3100.
- (3) (a) Trost, B. M.; Fleming, I. *Comprehensive Organic Synthesis*; Pergamon Press: 1991. (b) Smith, M. B.; March, J. *Advanced Organic Chemistry*; Wiley: Hoboken, 2007.
- (4) (a) Negishi, E.; Bagheri, V.; Chatterjee, S.; Luo, F. T.; Miller, J. A.; Stoll, A. T. *Tetrahedron Lett.* **1983**, *24*, 5181. See, also: (b) Milstein, D.; Stille, J. K. *J. Org. Chem.* **1979**, *44*, 1613. (c) Fukuyama, T.; Tokuyama, H. *Aldrichim. Acta* **2004**, *37*, 87. (d) Liebeskind, L. S.; Srogl, J. *J. Am. Chem. Soc.* **2000**, *122*, 11260. (e) Prokopcova, H.; Kappe, C. O. *Angew. Chem. Int. Ed.* **2009**, *48*, 2276. (f) Kakino, R.; Yasumi, S.; Shimizu, I.; Yamamoto, A. *Bull. Chem. Soc. Jpn.* **2002**, *75*, 137. (g) Gooßen, L. J.; Ghosh, K. *Angew. Chem. Int. Ed.* **2001**, *40*, 3458. (h) Tatamidani, H.; Yokota, K.; Kakiuchi, F.; Chatani, N. *J. Org. Chem.* **2004**, *69*, 5615. (i) Tadamidami, H.; Kakiuchi, F.; Chatani, N. *Org. Lett.* **2004**, *6*, 3597. (j) Xin, B.; Zhang, Y.; Cheng, K. *J. Org. Chem.* **2006**, *71*, 5725.

- (5) (a) Brennführer, A.; Neumann, H.; Beller, M. *Angew. Chem. Int. Ed.* **2009**, *48*, 4114.  
(b) Hermanage, P.; Lindhardt, A. T.; Taaning, R. H.; Bjerglund, K.; Lupp, D.; Skrydstrup, T. *J. Am. Chem. Soc.* **2011**, *133*, 6061.
- (6) Greenberg, A.; Breneman, C. M.; Liebman, J. F. *The Amide Linkage: Structural Significance in Chemistry, Biochemistry and Materials Science*; Wiley-VCH: 2003.
- (7) Laurence, C.; Gal, J. F. *Lewis Basicity and Affinity Scales: Data and Measurement*; Wiley-Blackwell: 2009.
- (8) *New Trends in Cross-Coupling*; Colacot, T. J., Ed.; The Royal Society of Chemistry: Cambridge, 2015.
- (9) Winkler, F. K.; Dunitz, J. D. *J. Mol. Biol.* **1971**, *59*, 169. Winkler-Dunitz distortion parameters:  $\tau$  (twist angle),  $\chi_N$  (pyramidalization at N) and  $\chi_C$  (pyramidalization at C) describe the magnitude of rotation around the N–C(O) bond, pyramidalization at N, and C;  $\tau$  is 0° for planar amide bonds and 90° for fully orthogonal bonds;  $\chi_N$  and  $\chi_C$  are 0° for planar bonds, and 60° for fully pyramidalized amide bonds.
- (10) Szostak, M.; Aubé, J. *Chem. Rev.* **2013**, *113*, 5701.
- (11) (a) Pracejus, H. *Ber.* **1959**, *92*, 988. (b) Kirby, A. J.; Komarov, I. V.; Wothers, P. D.; Feeder, N. *Angew. Chem. Int. Ed.* **1998**, *37*, 785. (c) Tani, K.; Stoltz, B. M. *Nature* **2006**, *441*, 731. (d) Lei, Y.; Wroblewski, A. D.; Golden, J. E.; Powell, D. R.; Aubé, J. *J. Am. Chem. Soc.* **2005**, *127*, 4552. (e) Greenberg, A.; Venanzi, C. A. *J. Am. Chem. Soc.* **1993**, *115*, 6951. (f) Greenberg, A.; Moore, D. T.; DuBois, T. D. *J. Am. Chem. Soc.* **1996**, *118*,



8658. (g) Bennet, A. J.; Wang, Q. P.; Slebocka-Tilk, H.; Somayaji, V.; Brown, R. S.; Santarsiero, B. D. *J. Am. Chem. Soc.* **1990**, *112*, 6383. (h) Bennet, A. J.; Somayaji, V.; Brown, R. S.; Santarsiero, B. D. *J. Am. Chem. Soc.* **1991**, *113*, 7563. (i) Cox, C.; Lectka, T. *Acc. Chem. Res.* **2000**, *33*, 849.

(12) Szostak, R.; Aubé, J.; Szostak, M. *Chem. Commun.* **2015**, *51*, 6395.

(13) Yamada, S. *Rev. Heteroat. Chem.* **1999**, *19*, 203.

(14) Hutchby, M.; Houlden, C. E.; Haddow, M. F.; Tyler, S. N.; Lloyd-Jones, G. C.; Booker-Milburn, K. I. *Angew. Chem. Int. Ed.* **2012**, *51*, 548.

(15) (a) Blakey, S. B.; MacMillan, D. W. C. *J. Am. Chem. Soc.* **2003**, *125*, 6046. (b) Xie, L. G.; Wang, Z. X. *Angew. Chem. Int. Ed.* **2011**, *50*, 4901. (c) Tobisu, M.; Nakamura, K.; Chatani, N. *J. Am. Chem. Soc.* **2014**, *136*, 5587.

(16) Littke, A. F.; Fu, G. C. *Angew. Chem. Int. Ed.* **2002**, *41*, 4176.

(17) (a) Li, X.; Zou, G. *Chem. Commun.* **2015**, *51*, 5089. (b) Hie, L.; Nathel, N. F. F.; Shah, T. K.; Baker, E. L.; Hong, X.; Yang, Y. F.; Liu, P.; Houk, K. N.; Garg, N. K. *Nature* **2015**, *524*, 79.

(18) Lennox, A. J. J.; Lloyd-Jones, G. C. *Chem. Soc. Rev.* **2014**, *43*, 412.

(19) Sato, T.; Chida, N. *Org. Biomol. Chem.* **2014**, *12*, 3147.

(20) Otani, Y.; Nagae, O.; Naruse, Y.; Inagaki, S.; Ohno, M.; Yamaguchi, K.; Yamamoto, G.; Uchiyama, M.; Ohwada, T. *J. Am. Chem. Soc.* **2003**, *125*, 15191.

- (21) Kinzel, T.; Zhang, Y.; Buchwald, S. L. *J. Am. Chem. Soc.* **2010**, *132*, 14073.
- (22) (a) Gooßen, L. J.; Rodriguez, N. *Chem. Commun.* **2004**, 724. (b) Liu, Y.; Kim, K. E.; Herbert, M. B.; Fedorov, A.; Grubbs, R. H.; Stoltz, B. M. *Adv. Synth. Catal.* **2014**, 356, 130. (c) John, A.; Hogan, L. T.; Hillmyer, M. A.; Tolman, W. B. *Chem. Commun.* **2015**, 51, 2731.
- (23) Moriya, T.; Miyaura, N.; Suzuki, A. *Synlett* **1994**, 149.
- (24) Santos, L. S. *Eur. J. Org. Chem.* **2008**, 235.
- (25) Lebrasseur, N.; Larrosa, I. *J. Am. Chem. Soc.* **2008**, *130*, 2926.
- (26) Preliminary DFT studies (B3LYP/6-311++g(d,p) level, **2.1.1a**, gas phase), indicated the energy minimum for 87.0° O–C–N–C dihedral angle, consistent with the ground-state destabilization.
- (27) (a) Gooßen, L. J.; Koley, D.; Hermann, H. L.; Thiel, W. *J. Am. Chem. Soc.* **2005**, *127*, 11102. (b) Lennox, A. J. J.; Lloyd-Jones, G. C. *Angew. Chem. Int. Ed.* **2013**, *52*, 7362. (c) Partyka, D. V. *Chem. Rev.* **2011**, *111*, 1529.

## 2.2 Cooperative strategy for amide bond activation-acyl coupling

Parts of this section were adapted with permission from the article “Palladium-Catalyzed Suzuki-Miyaura Cross-Coupling of Amides via Site-Selective N–C Bond Cleavage by Cooperative Catalysis” (*ACS Catal.* **2016**, 6, 7335). Copyright ©2016, American Chemical Society.

### 2.2.1 Research background

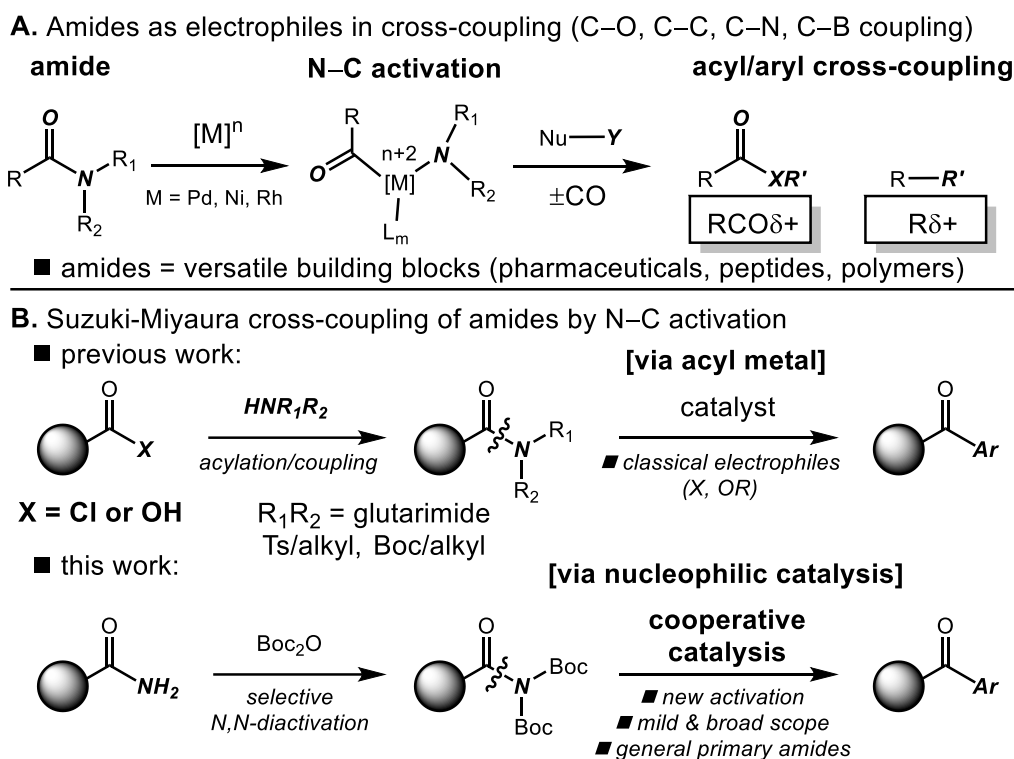


**Figure 2.2.1** (a) Amide cross-coupling by N–C bond activation. (b) Suzuki-Miyaura cross-coupling of amides: previous work and this study.

In 2016, catalytic functionalization of amides has already emerged as a powerful strategy in organic synthesis.<sup>1,2</sup> In particular, given that amides are ubiquitous in

pharmaceuticals,<sup>3</sup> biomolecules<sup>4</sup> and polymers,<sup>5</sup> the selective cross-coupling of amides by N–C bond cleavage showed a unique opportunity to expand the portfolio of organometallic reactions<sup>6</sup> and provide a general solution to the construction of complex organic molecules from amides in a modular fashion.<sup>1–5</sup>

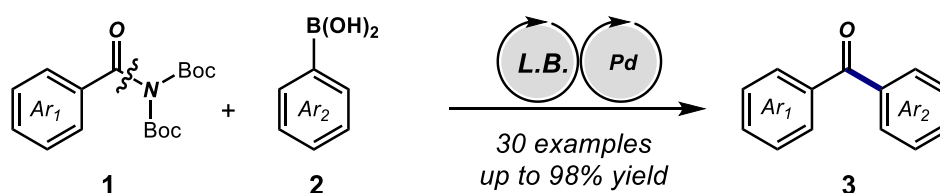
In particular, in 2015, the Garg group reported a nickel catalyst system for mild and highly selective esterification of amides.<sup>7</sup> Concurrent to this report, new methods for the cross-coupling of amides to forge carbon–carbon,<sup>8</sup> carbon–nitrogen<sup>9</sup> and carbon–boron<sup>10</sup> bonds have been developed. The amide N–C coupling approach enables low-valent metal insertion into the amide N–C(O) bond to catalytically generate acyl-metal intermediates<sup>6,11</sup> directly from amides. In this way, the catalytic amide N–C bond functionalization circumvents the use of highly reactive stoichiometric reagents<sup>12</sup> and creates new and valuable bonds by employing inert amides to actively participate in a broad range of chemoselective,<sup>13</sup> transition-metal-catalyzed manifolds (Figure 2.2.1).<sup>7–11</sup> However, when we initiated this study, the field of amide bond cross-coupling had remained essentially limited to the coupling of Boc-activated secondary amides and less common tertiary amides that were ultimately derived from carboxylic acids or aroyl chlorides.

### **2.2.2 Reaction discovery**

We were aware of a significant progress that has been made in the development of new cooperative catalytic strategies for organic synthesis.<sup>14</sup> In particular, cooperative catalysis has enabled novel reactivity of otherwise benign substrates by lowering energy barriers

associated with the individual steps. In many examples cooperative catalysis mechanism resulted in previously unattainable transformations and offered new methods for the reaction development of broadly applicable substrates.<sup>15</sup>

**A. N–C Cross-coupling of primary benzamides by cooperative catalysis**



**B. Proposed catalytic cycle**

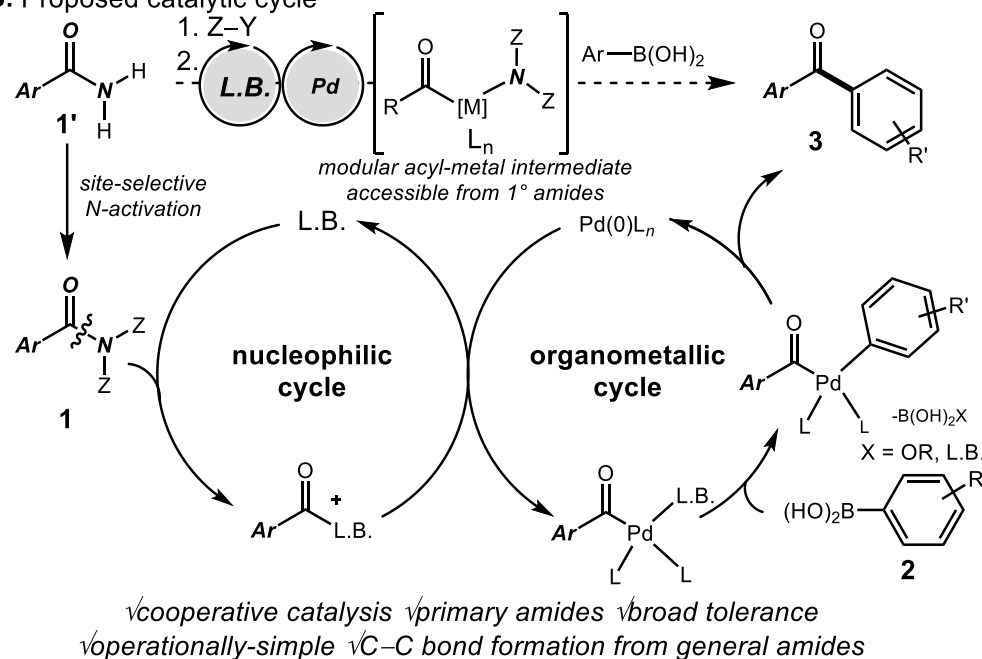


**Figure 2.2.2** Proposed mechanism for site-selective N,N-di-activation and cross-coupling of amides by cooperative catalysis.

In our research on amide bond activation,<sup>8c-e,g-i</sup> we became interested in selective N–C bond cleavage of primary amides by transition-metal-catalysis. In this part of Chapter II, we outline the development of a new cooperative catalysis platform for the palladium-

catalyzed Suzuki-Miyaura cross-coupling of generic amides enabled by a merger of site-selective N,N-di-Boc-activation and cooperative catalysis via N–C bond cleavage. The following features made this study notable: (1) Conceptually, the new catalytic strategy by-passed the direct metal insertion into the amide bond,<sup>16</sup> providing a powerful synergistic approach to employing amide bond functionalization in less reactive amide substrates. (2) All amides were prepared directly from the corresponding common benzamides, while the product biaryl ketones represent versatile linchpins in organic chemistry that can be converted into a broad range of functional groups.<sup>17,18</sup>

In the most general sense, the Suzuki-Miyaura cross-coupling represents one of the most powerful methods for the construction of carbon–carbon bonds in organic synthesis.<sup>19</sup> Primary amide substrates constitute the most fundamental amide building blocks in pharmaceutical and agrochemical industry.<sup>20</sup> Moreover, primary amides are widely available from a distinct pool of precursors than secondary and tertiary amides.<sup>21</sup> The reactivity pathway of amides by the direct metal insertion is ultimately limited by the facility of oxidative addition into the N–C amide bond.<sup>7,16</sup> Our study on cooperative catalysis has provided a mechanistically distinct approach for amide N–C functionalization by the combination of Lewis base and organometallic catalysis that can be triggered using reactivity complementary to the standard activation approach.<sup>7–10</sup>

Our proposed mechanism for the cooperative catalytic activation of amides is shown in Figure 2.2.2. Considering the high barrier to rotation in primary amides,<sup>22</sup> we postulated that the site-selective N,N-diacylation of the amide would enable amide transacylation by an appropriate Lewis base (nucleophilic cycle).<sup>23</sup> In sharp contrast to amide O-activation,

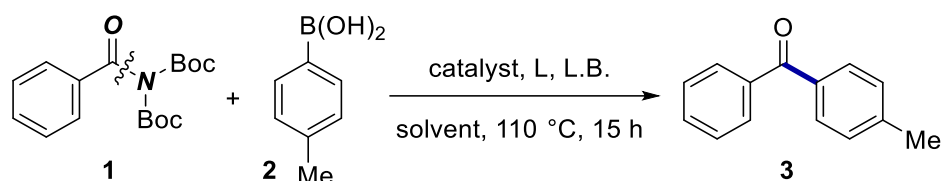
the site-selective N-coordination of amides is significantly more challenging.<sup>24</sup> The feasibility of this approach relied on the propensity of amides to undergo selective transacylation of the nitrogen atom. In a simultaneous organometallic cycle, an appropriate metal catalyst, for example Pd(0), would undergo selective oxidative addition into the weak acylammonium bond<sup>25</sup> to generate a highly reactive acyl-Pd(II) intermediate. This intermediate would be intercepted by an appropriate organometallic reagent, resulting in transmetallation and releasing the Lewis base catalyst. Reductive elimination would generate the ketone product and release the Pd(0) catalyst to complete the cycle. Crucially, this cooperative merger enables general primary amides to become available for a range of organometallic transformations for the first time.<sup>6-11</sup> Furthermore, we postulated that this unified approach by two independent catalytic events could potentially be extended to other amide substrates, resulting in a new broadly general activation platform of amide bonds.<sup>1-5</sup>

### 2.2.3 Reaction optimization

Our initial efforts focused on examination of the coupling of amide **2.2.1** prepared directly from benzamide<sup>26</sup> with 4-tolylboronic acid in the presence of various Lewis bases and organometallic catalysts. We identified N,N-di-Boc site-selective diactivation as a process that renders these reactions synthetically useful.<sup>26</sup> It should be noted that all substrates for this study were prepared directly from the corresponding benzamides (average 71% yield, including substrates with Lewis basic sites). We found after very extensive experimentation that the proposed cooperative coupling was indeed feasible under the simultaneous action of triethylamine as a Lewis base and a palladium catalyst.

The optimized system utilized Pd(OAc)<sub>2</sub> (3 mol%), PCy<sub>3</sub>HBF<sub>4</sub> (12 mol%), Et<sub>3</sub>N (30 mol%), potassium carbonate (2.5 equiv) and H<sub>3</sub>BO<sub>3</sub> (2.0 equiv) in THF at 110 °C, affording the desired product in quantitative yield. Selected key optimization results are presented in Table 2.2.1. Other Lewis bases could also be used; however, Et<sub>3</sub>N provided consistently the best results (entries 1-7). THF was found to be the optimal solvent for the reaction (entries 8-11). As expected, no product formation was observed in the absence of palladium catalyst and marginal product formation was observed in the absence of Lewis base (<7%) (entries 12-13). It is worth noting that decarbonylation products were not detected.<sup>8g-i,10</sup> The use of acid was critical for high activity (entry 14). We proposed that the role of acid was to activate the amide bond by switchable O-/O-coordination.<sup>27</sup> The optimized Lewis base stoichiometry and nucleophilicity was critical to match the efficiency of both cycles (entries 16-17). The use of polar solvents and strong bases resulted in lower reaction efficiency due to amide degradation (not shown). Finally, we noted that the reaction proceeded at temperatures as low as 65 °C with high efficiency (85% yield, entry 18). Notably, the overall process was catalytic in amine since it could be regenerated after transmetallation/ligand exchange.<sup>19</sup>





entry	catalyst	Lewis base	solvent	yield (%) <sup>b</sup>
1	Pd(OAc) <sub>2</sub>	Et <sub>3</sub> N	THF	>98
2	Pd(OAc) <sub>2</sub>	DMAP	THF	15
3	Pd(OAc) <sub>2</sub>	DIEA	THF	51
4	Pd(OAc) <sub>2</sub>	Bu <sub>3</sub> N	THF	65
5	Pd(OAc) <sub>2</sub>	quinoline	THF	44
6	Pd(OAc) <sub>2</sub>	isoquinoline	THF	18
7	Pd(OAc) <sub>2</sub>	pyridine	THF	11
8	Pd(OAc) <sub>2</sub>	Et <sub>3</sub> N	toluene	40
9	Pd(OAc) <sub>2</sub>	Et <sub>3</sub> N	dioxane	15
10	Pd(OAc) <sub>2</sub>	Et <sub>3</sub> N	CH <sub>3</sub> CN	38
11	Pd(OAc) <sub>2</sub>	Et <sub>3</sub> N	DMF	<5
12	Pd(OAc) <sub>2</sub>	-	THF	<7
13	-	Et <sub>3</sub> N	THF	<5
14 <sup>c</sup>	Pd(OAc) <sub>2</sub>	Et <sub>3</sub> N	THF	26
15 <sup>d</sup>	Pd(OAc) <sub>2</sub>	Et <sub>3</sub> N	THF	37
16 <sup>e</sup>	Pd(OAc) <sub>2</sub>	Et <sub>3</sub> N	THF	74
17 <sup>f</sup>	Pd(OAc) <sub>2</sub>	Et <sub>3</sub> N	THF	64
18 <sup>g</sup>	Pd(OAc) <sub>2</sub>	Et <sub>3</sub> N	THF	85

<sup>a</sup>Conditions: amide (1.0 equiv), R-B(OH)<sub>2</sub> (2.0 equiv), catalyst (3 mol%), L.B. (30 mol%), K<sub>2</sub>CO<sub>3</sub> (2.5 equiv), PCy<sub>3</sub>HBF<sub>4</sub> (12 mol%), H<sub>3</sub>BO<sub>3</sub> (2.0 equiv), solvent (0.25 M), 110 °C, 15 h. <sup>b</sup>GC/<sup>1</sup>H NMR yields. <sup>c</sup>Without H<sub>3</sub>BO<sub>3</sub>. <sup>d</sup>Without K<sub>2</sub>CO<sub>3</sub>. <sup>e</sup>Et<sub>3</sub>N (0.10 equiv). <sup>f</sup>Et<sub>3</sub>N (1.0 equiv). <sup>g</sup>65 °C. L.B. = Lewis base.

**Table 2.2.1** Optimization of the reaction conditions.<sup>a</sup>

## 2.2.4 Substrate scope

With the optimal conditions in hand, we next evaluated the preparative scope of our strategy for activation of N–C bonds (Figure 2.2.3). Particularly noteworthy was broad functional group compatibility and the use of generic primary amide substrates in all cases studied. The reaction tolerated electron-rich, electron-neutral and electron-deficient

functional groups on both coupling partners, providing the desired ketone products in uniformly high yields. Boronic acids bearing alkyl (**2.2.3b-2.2.3c**), ether (**2.2.3d**), ester (**2.2.3e**), ketone (**2.2.3f**), nitro (**2.2.3g**), cyano (**2.2.3h**), trifluoromethyl (**2.2.3i**), and fluoro (**2.2.3j**) groups were perfectly tolerated. Of note, our protocol readily tolerated electrophilic functional groups such as ketones, esters, nitro and cyano that are problematic in the nucleophilic addition to classic Weinreb amides.<sup>12</sup> Electronically-diverse substituents in the meta-position (**2.2.3k-2.2.3l**) were well-accommodated. Furthermore, our protocol tolerated coordinating functional groups in the ortho-position (**2.2.3m**) and polyarenes with diverse substitution (**2.2.3n-2.2.3p**).

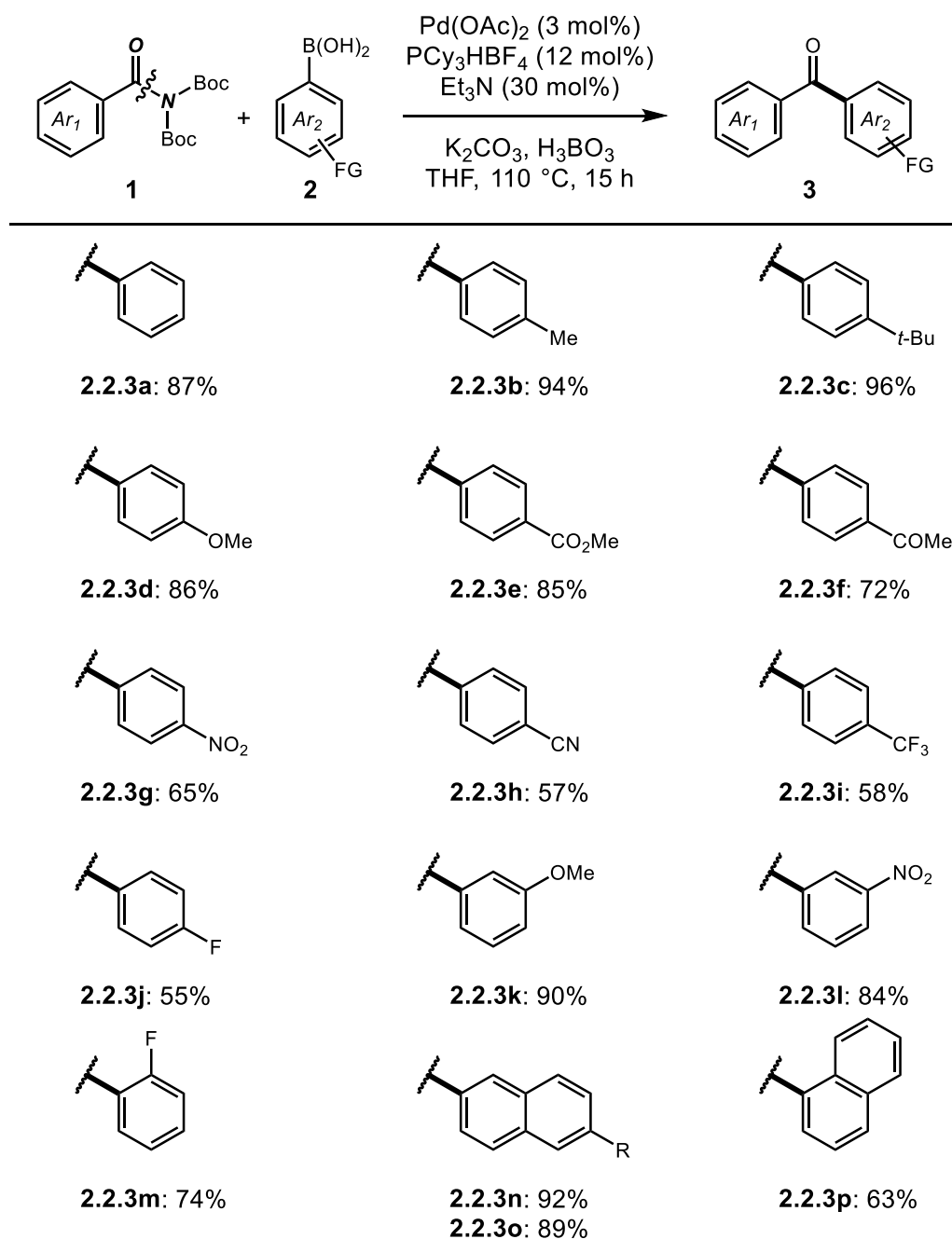


**Figure 2.2.3** Suzuki-Miyaura cross-coupling of amides: scope of boronic acids.

The scope of the amide component was also very broad (Figure 2.2.4). Our conditions were amenable to the coupling of neutral (**2.2.3b**), electron-rich (**2.2.3d**) and

electron.poor (**2.2.3i**, **2.2.3h**, **2.2.3e**) amides bearing an array of electrophilic functional groups, including cyano (**2.2.3h**), ester (**2.2.3e**), nitro (**2.2.3g**), chloro (**2.2.3q**), and fluoro (**2.2.3j**) at the para-position of the aromatic ring, enabling selective installation of the electrophilic functional handle from the preferred coupling partner.<sup>12,13</sup>

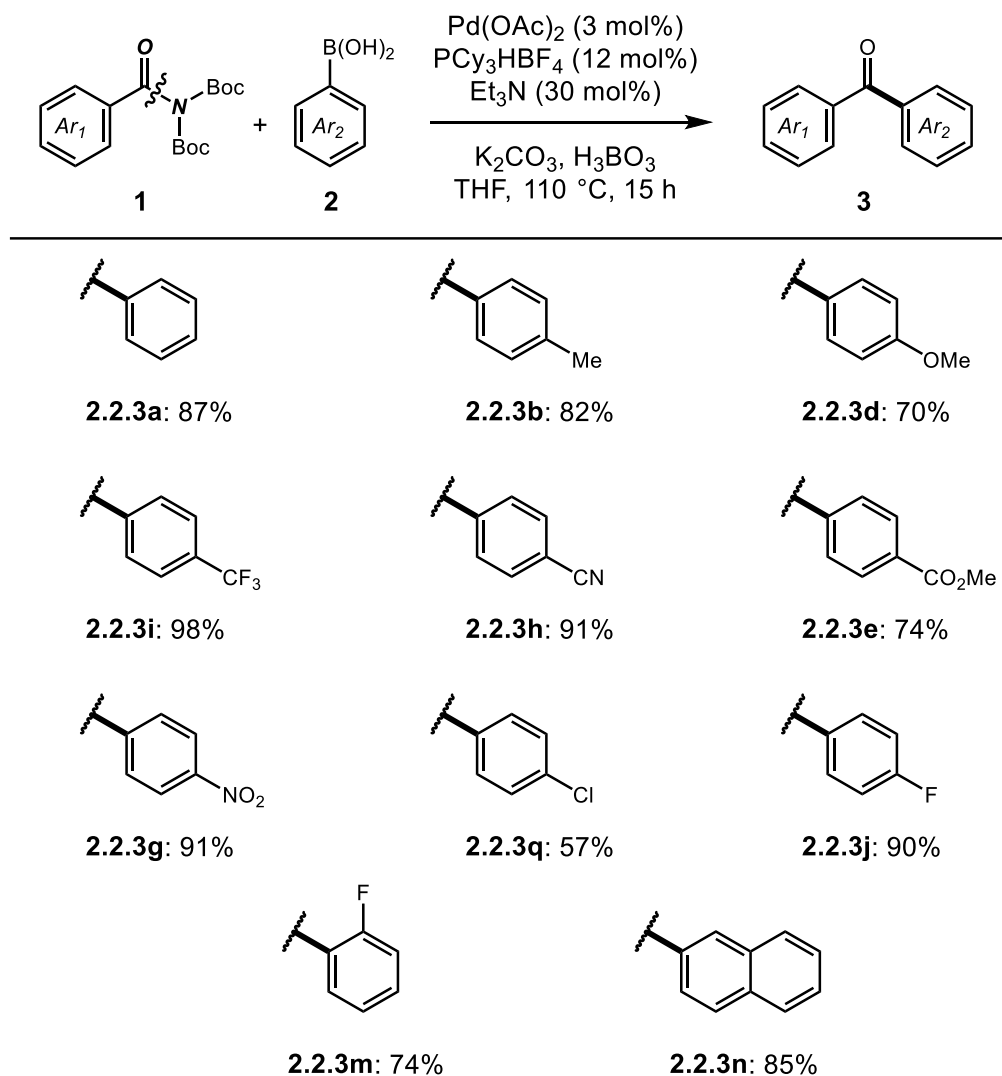


**Figure 2.2.4** Suzuki-Miyaura cross-coupling of amides: scope of amides.

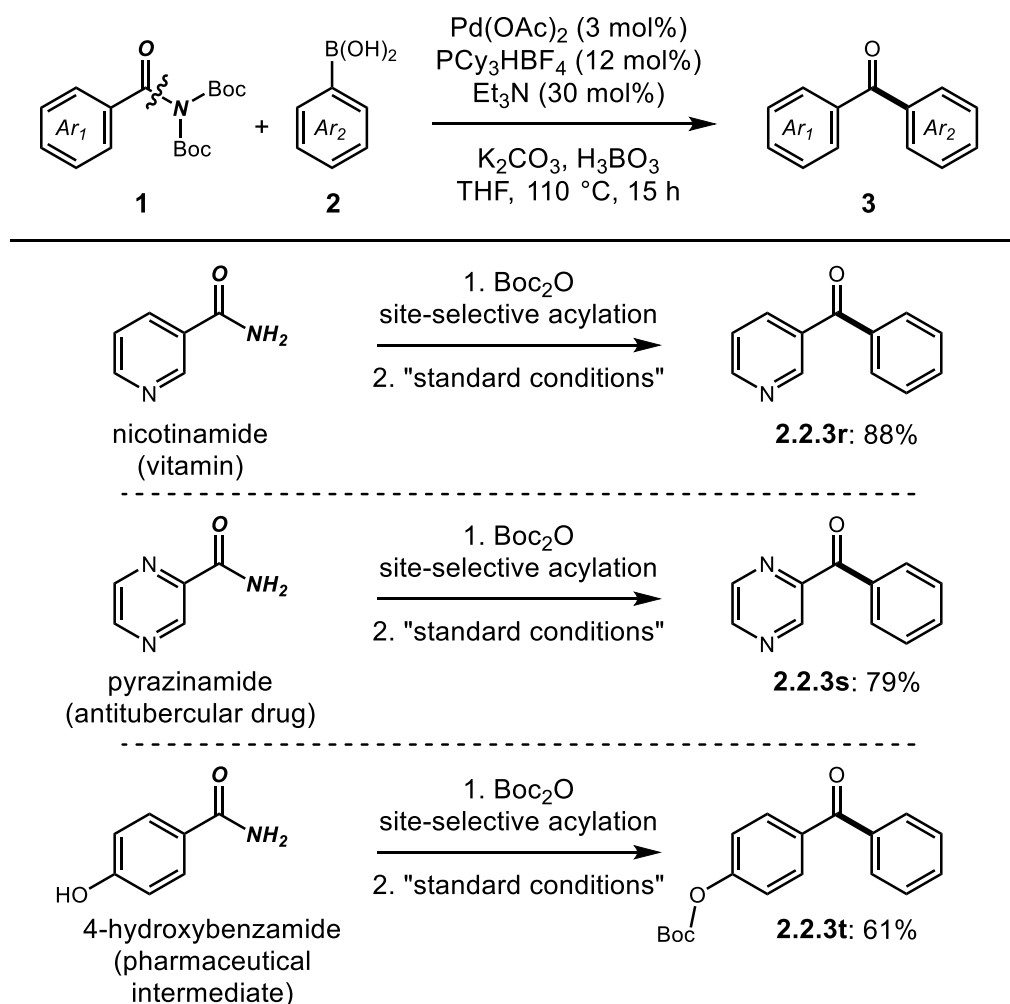


**Figure 2.2.5** Suzuki-Miyaura cross-coupling of amides: cross-coupling of pharmaceuticals.

Furthermore, the amide component could also tolerate an ortho-fluoro functional group (**2.2.3m**) poised for S<sub>N</sub>Ar post-coupling functionalization and conjugated polyarenes (**2.2.3n**).

The synthetic value of our method was highlighted by the coupling of biologically active molecules and pharmaceutical intermediates bearing 1° amide functional groups (Figure

2.2.5) as demonstrated by the successful cross-coupling of nicotinamide (vitamin with anti-inflammatory properties),<sup>28</sup> pyrazinamide (antitubercular drug),<sup>29</sup> and 4-hydroxycarboxamide (pharmaceutical feedstock).<sup>30</sup> Clear advantages of our protocol included the ease of primary amide bond activation for the N–C coupling, and tolerance of functional groups that would be problematic in stoichiometric techniques employing reactive organometallic reagents.

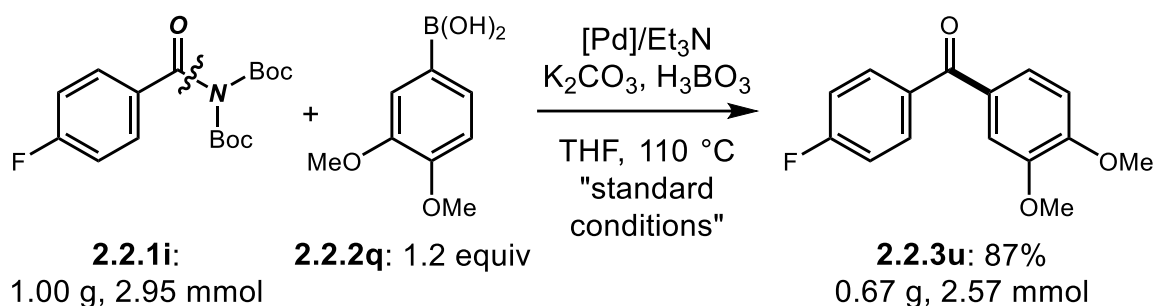
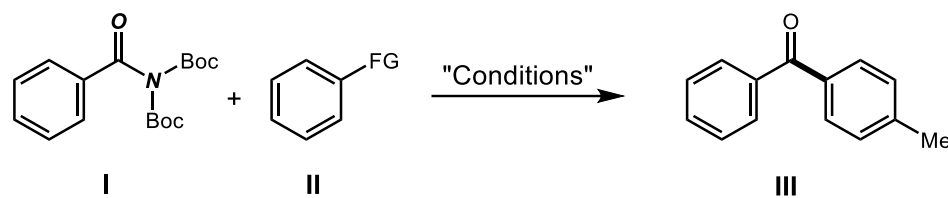


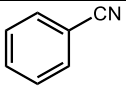
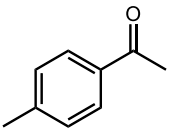
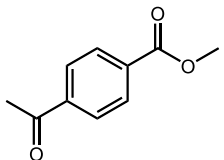
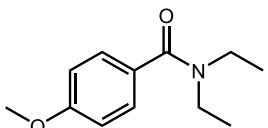
**Figure 2.2.6** Large scale cross-coupling.

The scalability of the method was evaluated (Figure 2.2.6). A gram scale coupling was performed to furnish **2.2.3u**, the intermediate in the commercial synthesis of Flumorph, a new generation pesticide,<sup>31</sup> and gave the product in 87% isolated yield without any modifications of the standard conditions.

### 2.2.5 Mechanistic studies

Studies were performed to gain insight into the reaction mechanism.



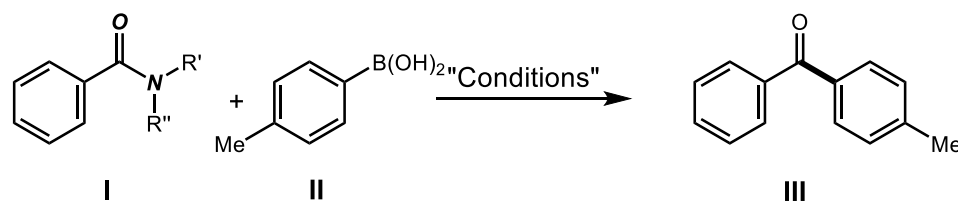
entry	substrate <b>II</b>	recovery of <b>II</b> (%) <sup>b</sup>	yield of <b>III</b> (%) <sup>b</sup>
1		>98	80
2		>98	98
3		>95	81
4		>98	68

<sup>a</sup>Conditions: amide (0.1 mmol), boronic acid (2.0 equiv), Pd(OAc)<sub>2</sub> (3 mol%), PCy<sub>3</sub>HBF<sub>4</sub> (12 mol%), base (2.5 equiv), H<sub>3</sub>BO<sub>3</sub> (2.0 equiv), Et<sub>3</sub>N (0.30 equiv), THF (0.20 M), 110 °C, 15 h. All reactions carried out using standard Schlenk techniques. <sup>b</sup>Determined by <sup>1</sup>H NMR and/or GC-MS.

**Table 2.2.2** Selectivity study in the Pd-catalyzed Suzuki-Miyaura cross-coupling of N,N-Boc<sub>2</sub>-amides.<sup>a</sup>

(1) Electrospray ionization mass spectrometry (ESI/MS) analysis under stoichiometric conditions revealed intermediates corresponding to the acylammonium and acyl-Pd species, consistent with the proposed mechanism and optimization studies. Decarbonylation intermediates were not detected.<sup>8g-i,10</sup> (2) Selectivity studies with carbonyl substrates demonstrated exquisite selectivity over nitrile, ketone, ester, and tertiary amide functional groups (Table 2.2.2). (3) Moreover, >95:5 selectivity was

obtained in the cross-coupling of **1** over activated tertiary amides that have been engaged in the N–C cross-coupling by oxidative addition (e.g., N-Boc/alkyl, N-Ts/Ph) (Table 2.2.3), attesting to the potential of the method in chemoselective synthesis.<sup>7,8a,b,9</sup> (4) A TON of 164 in Pd has been determined, showing efficient turnover.



entry	amide <b>I</b>	recovery of <b>I</b> (%) <sup>b</sup>	yield of <b>III</b> (%) <sup>b</sup>
1		>95	<5
2		>95	<5

<sup>a</sup>Conditions: amide (0.1 mmol), boronic acid (2.0 equiv), Pd(OAc)<sub>2</sub> (3 mol%), PCy<sub>3</sub>·HBF<sub>4</sub> (12 mol%), base (2.5 equiv), H<sub>3</sub>BO<sub>3</sub> (2.0 equiv), Et<sub>3</sub>N (0.30 equiv), THF (0.20 M), 110 °C, 15 h. All reactions carried out using standard Schlenk techniques. <sup>b</sup>Determined by <sup>1</sup>H NMR and/or GC-MS.

**Table 2.2.3** Selectivity study in the Pd-catalyzed Suzuki-Miyaura cross-coupling of N,N-Boc<sub>2</sub>-amides.<sup>a</sup>

## 2.2.6 Conclusion

In conclusion, in this project we demonstrated the first Suzuki-Miyaura cross-coupling of amides by a combination of site-selective N,N-di-Boc-activation and cooperative catalysis via N–C cleavage. The primary amide starting materials are particularly common in pharmaceuticals and biologically active intermediates. This strategy provided



a new method for the Suzuki-Miyaura cross-coupling by exploiting a synergistic mechanism. The synthetic potential of this method was demonstrated through the direct functionalization of amide-containing pharmaceuticals. This new activation concept of amide bonds permits the synthesis of versatile ketone building blocks, and could enable the development of a broad range of amide N–C bond functionalization reactions through acyl-metal intermediates.

### 2.2.7 Experimental section

**General procedure for amide synthesis.** An oven-dried round-bottomed flask (100 mL) equipped with a stir bar was charged with primary amide (8.26 mmol, 1.0 equiv), 4-dimethylaminopyridine (typically, 0.10 equiv) and dichloromethane (typically, 25 mL), placed under a positive pressure of argon, and subjected to three evacuation/backfilling cycles under high vacuum. Di-*tert*-butyl dicarbonate (typically, 2.0 equiv) was added portion-wise to the reaction mixture with vigorous stirring at 0 °C, and the reaction mixture was stirred overnight at room temperature. After the indicated time, the reaction mixture was concentrated and unless stated otherwise purified directly by chromatography on silica gel (hexanes/ethyl acetate) to give analytically pure product.

**General procedure for Suzuki-Miyaura cross-coupling of amides.** An oven-dried vial equipped with a stir bar was charged with an amide substrate (neat, 1.0 equiv), potassium carbonate (typically, 2.5 equiv), boric acid (typically, 2.0 equiv), boronic acid (typically, 2.0 equiv), Pd(OAc)<sub>2</sub> (typically, 3 mol%), and PCyHBF<sub>4</sub> (typically, 12 mol%), placed under a positive pressure of argon, and subjected to three evacuation/backfilling cycles

under high vacuum. Triethylamine (TEA, typically, 0.30 equiv) and tetrahydrofuran (0.20 M) were added with vigorous stirring at room temperature, the reaction mixture was placed in a preheated oil bath at 110 °C, and stirred for the indicated time at 110 °C. After the indicated time, the reaction mixture was diluted with CH<sub>2</sub>Cl<sub>2</sub> (10mL), filtered, and concentrated. The sample was analyzed by <sup>1</sup>H NMR (CDCl<sub>3</sub>, 500 MHz) and GC-MS to obtain conversion, yield and selectivity using internal standard and comparison with authentic samples. Purification by chromatography on silica gel (hexanes/ethyl acetate) afforded the title product.

**2.2.1a.** Yield 85%. White solid. Mp = 58-60°C. <sup>1</sup>H NMR (500 MHz, CDCl<sub>3</sub>) δ 7.85 (d, *J* = 7.7 Hz, 2 H), 7.61 (t, *J* = 7.4 Hz, 1 H), 7.49 (t, *J* = 7.3 Hz, 2 H), 1.39 (s, 18 H). <sup>13</sup>C NMR (125 MHz, CDCl<sub>3</sub>) δ 149.77, 133.41, 129.09, 128.67, 84.27, 27.59. HRMS calcd for C<sub>34</sub>H<sub>46</sub>N<sub>2</sub>O<sub>10</sub>Na (2 M<sup>+</sup> + Na) 665.3045, found 665.3066.

**2.2.1b.** Yield 79%. White solid. Mp = 65-67 °C. <sup>1</sup>H NMR (500 MHz, CDCl<sub>3</sub>) δ 7.75 (d, *J* = 8.1 Hz, 2 H), 7.28 (d, *J* = 8.2 Hz, 2 H), 2.44 (s, 3 H), 1.39 (s, 18 H). <sup>13</sup>C NMR (125 MHz, CDCl<sub>3</sub>) δ 169.02, 149.81, 144.53, 129.41, 129.35, 84.05, 27.62, 21.73. HRMS calcd for C<sub>36</sub>H<sub>50</sub>N<sub>2</sub>O<sub>10</sub>Na (2 M<sup>+</sup> + Na) 693.3358, found 693.3368.

**2.2.1c.** Yield 40%. White solid. Mp = 71-73 °C. <sup>1</sup>H NMR (500 MHz, CDCl<sub>3</sub>) δ 7.85 (d, *J* = 8.4 Hz, 2 H), 6.97 (d, *J* = 8.5 Hz, 2 H), 3.91 (s, 3 H), 1.40 (s, 18 H). <sup>13</sup>C NMR (125 MHz, CDCl<sub>3</sub>) δ 168.24, 164.03, 149.80, 131.75, 126.38, 114.00, 83.94, 55.58, 27.68. HRMS calcd for C<sub>18</sub>H<sub>25</sub>NO<sub>6</sub>Na (M<sup>+</sup> + Na) 374.1574, found 374.1584.

**2.2.1d.** Yield 73%. Oil.  $^1\text{H}$  NMR (500 MHz,  $\text{CDCl}_3$ )  $\delta$  7.93 (d,  $J = 7.9$  Hz, 2 H), 7.75 (d,  $J = 7.9$  Hz, 2 H), 1.43 (s, 18 H).  $^{13}\text{C}$  NMR (125 MHz,  $\text{CDCl}_3$ )  $\delta$  168.40, 149.55, 137.52, 134.57 ( $J^2 = 32.5$  Hz), 129.14, 125.67 ( $J^3 = 7.5$  Hz), 123.43 ( $J^1 = 271.3$  Hz), 84.92, 27.57.  $^{19}\text{F}$  NMR (471 MHz,  $\text{CDCl}_3$ )  $\delta$  -63.15. HRMS calcd for  $\text{C}_{18}\text{H}_{22}\text{NO}_5\text{F}_3\text{Na}$  ( $\text{M}^+ + \text{Na}$ ) 412.1342, found 412.1359.

**2.2.1e.** Yield 85%. White solid.  $\text{Mp} = 72\text{-}74$   $^\circ\text{C}$ .  $^1\text{H}$  NMR (500 MHz,  $\text{CDCl}_3$ )  $\delta$  7.89 (d,  $J = 8.1$  Hz, 2 H), 7.79 (d,  $J = 8.0$  Hz, 2 H), 1.43 (s, 18 H).  $^{13}\text{C}$  NMR (125 MHz,  $\text{CDCl}_3$ )  $\delta$  168.12, 149.43, 138.14, 132.39, 129.12, 117.68, 116.39, 85.18, 27.58. HRMS calcd for  $\text{C}_{18}\text{H}_{22}\text{N}_2\text{O}_5\text{Na}$  ( $\text{M}^+ + \text{Na}$ ) 369.1421, found 369.1427.

**2.2.1f.** Yield 48%. White solid.  $\text{Mp} = 66\text{-}68$   $^\circ\text{C}$ .  $^1\text{H}$  NMR (500 MHz,  $\text{CDCl}_3$ )  $\delta$  8.15 (d,  $J = 7.6$  Hz, 2 H), 7.88 (d,  $J = 7.6$  Hz, 2 H), 3.98 (s, 3 H), 1.41 (s, 18 H).  $^{13}\text{C}$  NMR (125 MHz,  $\text{CDCl}_3$ )  $\delta$  168.76, 165.98, 149.57, 138.05, 134.06, 129.81, 128.78, 84.76, 52.55, 27.58. HRMS calcd for  $\text{C}_{38}\text{H}_{50}\text{N}_2\text{O}_{14}\text{Na}$  ( $2\text{ M}^+ + \text{Na}$ ) 781.3154, found 781.3131.

**2.2.1g.** Yield 83%. Yellow solid.  $\text{Mp} = 63\text{-}65$   $^\circ\text{C}$ .  $^1\text{H}$  NMR (500 MHz,  $\text{CDCl}_3$ )  $\delta$  8.33 (d,  $J = 8.5$  Hz, 2 H), 7.95 (d,  $J = 8.5$  Hz, 2 H), 1.45 (s, 18 H).  $^{13}\text{C}$  NMR (125 MHz,  $\text{CDCl}_3$ )  $\delta$  167.89, 150.19, 149.41, 139.73, 129.59, 123.77, 85.30, 27.58. HRMS calcd for  $\text{C}_{17}\text{H}_{22}\text{N}_2\text{O}_7\text{Na}$  ( $\text{M}^+ + \text{Na}$ ) 389.1319, found 389.1324.

**2.2.1h.** Yield 68%. White solid.  $\text{Mp} = 58\text{-}61$   $^\circ\text{C}$ .  $^1\text{H}$  NMR (500 MHz,  $\text{CDCl}_3$ )  $\delta$  7.79 (d,  $J = 7.6$  Hz, 2 H), 7.47 (d,  $J = 7.6$  Hz, 2 H), 1.42 (s, 18 H).  $^{13}\text{C}$  NMR (125 MHz,  $\text{CDCl}_3$ )  $\delta$  168.35, 149.59, 139.92, 132.59, 130.44, 129.05, 84.57, 27.63. HRMS calcd for  $\text{C}_{17}\text{H}_{22}\text{NO}_5\text{ClNa}$  ( $\text{M}^+ + \text{Na}$ ) 378.1079, found 378.1093.

**2.2.1i.** Yield 73%. White solid. Mp = 67-68 °C.  $^1\text{H}$  NMR (500 MHz,  $\text{CDCl}_3$ )  $\delta$  7.90-7.85 (m, 2 H), 7.17 (t,  $J$  = 8.1 Hz, 2 H), 1.41 (s, 18 H).  $^{13}\text{C}$  NMR (125 MHz,  $\text{CDCl}_3$ )  $\delta$  168.09, 165.89 ( $J^1$  = 253.8 Hz), 149.64, 131.76 ( $J^3$  = 10.0 Hz), 130.43 ( $J^4$  = 2.5 Hz), 115.96 ( $J^2$  = 22.5 Hz), 84.43, 27.62.  $^{19}\text{F}$  NMR (471 MHz,  $\text{CDCl}_3$ )  $\delta$  -104.00. HRMS calcd for  $\text{C}_{17}\text{H}_{22}\text{NO}_5\text{FNa}$  ( $\text{M}^+ + \text{Na}$ ) 362.1374, found 362.1384.

**2.2.1j.** Yield 70%. Colorless oil.  $^1\text{H}$  NMR (500 MHz,  $\text{CDCl}_3$ )  $\delta$  7.71 (t,  $J$  = 7.4 Hz, 1 H), 7.54 (q,  $J$  = 7.3 Hz, 1H), 7.25 (t,  $J$  = 7.6 Hz, 1 H), 7.12 (t,  $J$  = 9.4 Hz, 1 H), 1.46 (s, 18 H).  $^{13}\text{C}$  NMR (125 MHz,  $\text{CDCl}_3$ )  $\delta$  165.48, 160.03 ( $J^1$  = 252.5 Hz), 149.53, 134.10 ( $J^3$  = 8.8 Hz), 130.81( $J^4$  = 2.5 Hz), 124.40 ( $J^4$  = 3.8 Hz), 123.16 ( $J^3$  = 12.5 Hz), 116.02 ( $J^2$  = 21.3 Hz), 84.72, 27.50.  $^{19}\text{F}$  NMR (471 MHz,  $\text{CDCl}_3$ )  $\delta$  -113.04. HRMS calcd for  $\text{C}_{17}\text{H}_{22}\text{NO}_5\text{FNa}$  ( $\text{M}^+ + \text{Na}$ ) 362.1374, found 362.1389.

**2.2.1k.** Yield 91%. White solid. Mp = 69-71 °C.  $^1\text{H}$  NMR (500 MHz,  $\text{CDCl}_3$ )  $\delta$  8.40 (s, 1 H), 7.95 (dd,  $J$  = 19.7, 9.1 Hz, 4 H), 7.65 (t,  $J$  = 7.5 Hz, 1 H), 7.60 (t,  $J$  = 7.4 Hz, 1 H), 1.38 (s, 18 H).  $^{13}\text{C}$  NMR (125 MHz,  $\text{CDCl}_3$ )  $\delta$  169.29, 149.84, 135.68, 132.40, 131.40, 130.69, 129.41, 128.82, 128.69, 127.88, 127.12, 124.73, 84.30, 27.63. HRMS calcd for  $\text{C}_{21}\text{H}_{25}\text{NO}_5\text{Na}$  ( $\text{M}^+ + \text{Na}$ ) 394.1625, found 394.1641.

**2.2.1l.** Yield 57%. White solid. Mp = 78-80 °C.  $^1\text{H}$  NMR (500 MHz,  $\text{CDCl}_3$ )  $\delta$  8.97 (s, 1 H), 8.78 (d,  $J$  = 4.8 Hz, 1 H), 8.07 (d,  $J$  = 7.9 Hz, 1 H), 7.42 (dd,  $J$  = 7.8, 4.9 Hz, 1 H), 1.41 (s, 18 H).  $^{13}\text{C}$  NMR (125 MHz,  $\text{CDCl}_3$ )  $\delta$  167.95, 153.47, 149.79, 149.49, 136.23, 130.17, 123.42, 84.97, 27.56. HRMS calcd for  $\text{C}_{16}\text{H}_{22}\text{N}_2\text{O}_5\text{Na}$  ( $\text{M}^+ + \text{Na}$ ) 345.1421, found 345.1428.

**2.2.1m.** Yield 79%. White solid. Mp = 62-64 °C.  $^1\text{H}$  NMR (500 MHz,  $\text{CDCl}_3$ )  $\delta$  9.19 (s, 1 H), 8.77 (brs, 1 H), 8.61 (brs, 1 H), 1.47 (s, 18 H).  $^{13}\text{C}$  NMR (125 MHz,  $\text{CDCl}_3$ )  $\delta$  167.03, 149.75, 147.56, 145.93, 145.57, 143.00, 84.84, 27.56. HRMS calcd for  $\text{C}_{15}\text{H}_{21}\text{N}_3\text{O}_5\text{Na}$  ( $\text{M}^+ + \text{Na}$ ) 346.1373, found 346.1375.

**2.2.1n.** Yield 67%. Colorless oil.  $^1\text{H}$  NMR (500 MHz,  $\text{CDCl}_3$ )  $\delta$  7.87 (d,  $J = 8.4$  Hz, 2 H), 7.31 (d,  $J = 8.5$  Hz, 2 H), 1.58 (s, 9 H), 1.39 (s, 18 H).  $^{13}\text{C}$  NMR (125 MHz,  $\text{CDCl}_3$ )  $\delta$  168.26, 150.75, 149.61, 131.40, 130.71, 121.42, 84.38, 84.29, 27.65, 27.61. HRMS calcd for  $\text{C}_{44}\text{H}_{62}\text{N}_2\text{O}_{16}\text{Na}$  ( $2 \text{M}^+ + \text{Na}$ ) 897.3992, found 897.4013.

**2.2.3a.** White solid.  $^1\text{H}$  NMR (500 MHz,  $\text{CDCl}_3$ )  $\delta$  7.86-7.81 (m, 2 H), 7.64-7.59 (m, 1 H), 7.51 (t,  $J = 7.7$  Hz, 2 H).  $^{13}\text{C}$  NMR (125 MHz,  $\text{CDCl}_3$ )  $\delta$  196.74, 137.62, 132.41, 130.06, 128.31.

**2.2.3b.** White solid.  $^1\text{H}$  NMR (500 MHz,  $\text{CDCl}_3$ )  $\delta$  7.81 (d,  $J = 7.7$  Hz, 2 H), 7.75 (d,  $J = 7.5$  Hz, 2 H), 7.60 (t,  $J = 7.4$  Hz, 1 H), 7.50 (t,  $J = 7.2$  Hz, 2 H), 7.31 (d,  $J = 7.7$  Hz, 2 H), 2.47 (s, 3 H).  $^{13}\text{C}$  NMR (125 MHz,  $\text{CDCl}_3$ )  $\delta$  196.49, 143.22, 137.98, 134.90, 132.14, 130.31, 129.93, 128.97, 128.20, 21.66.

**2.2.3c.** White solid.  $^1\text{H}$  NMR (500 MHz,  $\text{CDCl}_3$ )  $\delta$  7.83 (d,  $J = 7.3$  Hz, 2 H), 7.79 (d,  $J = 8.3$  Hz, 2 H), 7.60 (t,  $J = 7.4$  Hz, 1 H), 7.54-7.48 (m, 4 H), 1.39 (s, 9 H).  $^{13}\text{C}$  NMR (125 MHz,  $\text{CDCl}_3$ )  $\delta$  196.46, 156.18, 137.95, 134.82, 132.17, 130.14, 129.98, 128.20, 125.25, 35.13, 31.16.

**2.2.3d.** White solid.  $^1\text{H}$  NMR (500 MHz,  $\text{CDCl}_3$ )  $\delta$  7.86 (d,  $J = 8.5$  Hz, 2 H), 7.78 (d,  $J = 7.8$  Hz, 2 H), 7.59 (t,  $J = 7.0$  Hz, 1 H), 7.50 (t,  $J = 7.5$  Hz, 2 H), 6.99 (d,  $J = 8.5$  Hz, 2 H),

3.92 (s, 3 H).  $^{13}\text{C}$  NMR (125 MHz,  $\text{CDCl}_3$ )  $\delta$  195.56, 163.22, 138.30, 132.57, 131.89, 130.17, 129.73, 128.19, 113.56, 55.51.

**2.2.3e.** White solid.  $^1\text{H}$  NMR (500 MHz,  $\text{CDCl}_3$ )  $\delta$  8.17 (d,  $J = 8.2$  Hz, 2 H), 7.87 (d,  $J = 8.2$  Hz, 2 H), 7.83 (d,  $J = 7.5$  Hz, 2 H), 7.64 (t,  $J = 7.4$  Hz, 1 H), 7.53 (t,  $J = 7.6$  Hz, 2 H), 3.99 (s, 3 H).  $^{13}\text{C}$  NMR (125 MHz,  $\text{CDCl}_3$ )  $\delta$  196.03, 166.32, 141.33, 136.96, 133.22, 132.95, 130.11, 129.78, 129.50, 128.47, 52.48.

**2.2.3f.** White solid.  $^1\text{H}$  NMR (500 MHz,  $\text{CDCl}_3$ )  $\delta$  8.08 (d,  $J = 7.6$  Hz, 2 H), 7.89 (d,  $J = 7.8$  Hz, 2 H), 7.83 (d,  $J = 7.8$  Hz, 2 H), 7.65 (t,  $J = 7.4$  Hz, 1 H), 7.53 (t,  $J = 7.4$  Hz, 2 H), 2.70 (s, 3 H).  $^{13}\text{C}$  NMR (125 MHz,  $\text{CDCl}_3$ )  $\delta$  197.51, 195.95, 141.34, 139.57, 136.93, 132.99, 130.10, 130.05, 128.48, 128.17, 26.91.

**2.2.3g.** Yellow solid.  $^1\text{H}$  NMR (500 MHz,  $\text{CDCl}_3$ )  $\delta$  8.37 (d,  $J = 8.2$  Hz, 2 H), 7.97 (d,  $J = 8.3$  Hz, 2 H), 7.83 (d,  $J = 7.9$  Hz, 2 H), 7.68 (t,  $J = 7.4$  Hz, 1 H), 7.55 (t,  $J = 7.5$  Hz, 2 H).  $^{13}\text{C}$  NMR (125 MHz,  $\text{CDCl}_3$ )  $\delta$  194.80, 149.84, 142.89, 136.29, 133.48, 130.70, 130.11, 128.69, 123.55.

**2.2.3h.**  $^1\text{H}$  NMR (500 MHz,  $\text{CDCl}_3$ )  $\delta$  7.90 (d,  $J = 7.2$  Hz, 2 H), 7.84-7.78 (m, 4 H), 7.67 (t,  $J = 7.4$  Hz, 1 H), 7.54 (t,  $J = 7.3$  Hz, 2 H).  $^{13}\text{C}$  NMR (125 MHz,  $\text{CDCl}_3$ )  $\delta$  195.03, 141.25, 136.34, 133.33, 132.17, 130.24, 130.07, 128.64, 118.01, 115.69.

**2.2.3i.** White solid.  $^1\text{H}$  NMR (500 MHz,  $\text{CDCl}_3$ )  $\delta$  7.92 (d,  $J = 7.9$  Hz, 2 H), 7.83 (d,  $J = 7.8$  Hz, 2 H), 7.78 (d,  $J = 7.9$  Hz, 2 H), 7.66 (t,  $J = 7.3$  Hz, 1 H), 7.54 (t,  $J = 7.5$  Hz, 2 H).  $^{13}\text{C}$  NMR (125 MHz,  $\text{CDCl}_3$ )  $\delta$  195.53, 140.73, 136.74, 133.73 ( $J^2 = 32.5$  Hz), 133.09,

130.13 ( $J^4 = 3.8$  Hz), 128.53, 125.36 ( $J^3 = 7.5$  Hz), 123.68 ( $J^1 = 271.3$  Hz).  $^{19}\text{F}$  NMR (471 MHz,  $\text{CDCl}_3$ )  $\delta$  -63.01.

**2.2.3j.** White solid.  $^1\text{H}$  NMR (500 MHz,  $\text{CDCl}_3$ )  $\delta$  7.90-7.84 (m, 2 H), 7.79 (d,  $J = 7.7$  Hz, 2 H), 7.62 (t,  $J = 6.9$  Hz, 1 H), 7.51 (t,  $J = 7.4$  Hz, 2 H), 7.18 (t,  $J = 8.2$  Hz, 2 H).  $^{13}\text{C}$  NMR (125 MHz,  $\text{CDCl}_3$ )  $\delta$  195.26, 165.39 ( $J^1 = 252.5$  Hz), 137.51, 133.81 ( $J^4 = 2.5$  Hz), 132.67 ( $J^3 = 8.8$  Hz), 132.47, 129.88, 128.36, 115.46 ( $J^2 = 21.3$  Hz).  $^{19}\text{F}$  NMR (471 MHz,  $\text{CDCl}_3$ )  $\delta$  -105.98.

**2.2.3k.** White solid.  $^1\text{H}$  NMR (500 MHz,  $\text{CDCl}_3$ )  $\delta$  7.83 (d,  $J = 7.2$  Hz, 2 H), 7.61 (t,  $J = 7.4$  Hz, 1 H), 7.50 (t,  $J = 7.7$  Hz, 2 H), 7.42-7.34 (m, 3 H), 7.16 (dd,  $J = 8.0, 2.6$  Hz, 1 H), 3.88 (s, 3 H).  $^{13}\text{C}$  NMR (125 MHz,  $\text{CDCl}_3$ )  $\delta$  196.51, 159.58, 138.91, 137.63, 132.43, 130.04, 129.22, 128.26, 122.87, 118.86, 114.33, 55.48.

**2.2.3l.** Yellow solid.  $^1\text{H}$  NMR (500 MHz,  $\text{CDCl}_3$ )  $\delta$  8.65 (s, 1 H), 8.47 (d,  $J = 8.2$  Hz, 1 H), 8.17 (d,  $J = 7.6$  Hz, 1 H), 7.83 (d,  $J = 8.2$  Hz, 2 H), 7.73 (t,  $J = 7.9$  Hz, 1 H), 7.69 (t,  $J = 7.0$  Hz, 1 H), 7.56 (t,  $J = 7.6$  Hz, 2 H).  $^{13}\text{C}$  NMR (125 MHz,  $\text{CDCl}_3$ )  $\delta$  194.18, 148.10, 139.08, 136.27, 135.44, 133.38, 130.02, 129.65, 128.75, 126.73, 124.74.

**2.2.3m.** White solid.  $^1\text{H}$  NMR (500 MHz,  $\text{CDCl}_3$ )  $\delta$  7.87 (d,  $J = 7.6$  Hz, 2 H), 7.63 (t,  $J = 7.3$  Hz, 1 H), 7.57 (dt,  $J = 14.2, 6.8$  Hz, 2 H), 7.50 (t,  $J = 7.6$  Hz, 2 H), 7.30 (d,  $J = 7.5$  Hz, 1 H), 7.19 (t,  $J = 9.1$  Hz, 1 H).  $^{13}\text{C}$  NMR (125 MHz,  $\text{CDCl}_3$ )  $\delta$  193.47, 160.09 ( $J^1 = 250.0$  Hz), 137.41, 133.40, 133.04 ( $J^3 = 8.8$  Hz), 130.75 ( $J^4 = 2.5$  Hz), 129.81, 128.46, 126.99, 124.27 ( $J^4 = 2.5$  Hz), 116.33 ( $J^3 = 8.8$  Hz).  $^{19}\text{F}$  NMR (471 MHz,  $\text{CDCl}_3$ )  $\delta$  -111.04.

**2.2.3n.** White solid.  $^1\text{H}$  NMR (500 MHz,  $\text{CDCl}_3$ )  $\delta$  8.30 (s, 1 H), 7.98 (s, 2 H), 7.95 (dd,  $J$  = 8.1, 2.9 Hz, 2 H), 7.89 (d,  $J$  = 7.1 Hz, 2 H), 7.67-7.62 (m, 2 H), 7.61-7.57 (m, 1 H), 7.55 (t,  $J$  = 7.7 Hz, 2 H).  $^{13}\text{C}$  NMR (125 MHz,  $\text{CDCl}_3$ )  $\delta$  196.76, 137.92, 135.28, 134.84, 132.38, 132.27, 131.87, 130.10, 129.43, 128.35, 128.33, 128.31, 127.83, 126.80, 125.79.

**2.2.3o.** 89% yield. White solid.  $^1\text{H}$  NMR (500 MHz,  $\text{CDCl}_3$ )  $\delta$  8.24 (s, 1 H), 7.97 (d,  $J$  = 8.5 Hz, 1 H), 7.89-7.82 (m, 4 H), 7.64 (t,  $J$  = 7.1 Hz, 1 H), 7.54 (t,  $J$  = 7.4 Hz, 2 H), 7.23 (d,  $J$  = 9.7 Hz, 2 H), 3.99 (s, 3 H).  $^{13}\text{C}$  NMR (125 MHz,  $\text{CDCl}_3$ )  $\delta$  196.58, 159.69, 138.22, 137.01, 132.70, 132.12, 131.99, 131.04, 129.98, 128.29, 127.61, 127.02, 126.57, 119.74, 105.77, 55.46.

**2.2.3p.** White solid.  $^1\text{H}$  NMR (500 MHz,  $\text{CDCl}_3$ )  $\delta$  8.12 (d,  $J$  = 8.2 Hz, 1 H), 8.04 (d,  $J$  = 8.1 Hz, 1 H), 7.95 (d,  $J$  = 8.0 Hz, 1 H), 7.90 (d,  $J$  = 7.8 Hz, 2 H), 7.64-7.60 (m, 2 H), 7.58-7.52 (m, 3 H), 7.49 (t,  $J$  = 7.3 Hz, 2 H).  $^{13}\text{C}$  NMR (125 MHz,  $\text{CDCl}_3$ )  $\delta$  198.02, 138.33, 136.37, 133.73, 133.23, 131.26, 130.96, 130.42, 128.45, 128.41, 127.77, 127.26, 126.46, 125.70, 124.34.

**2.2.3q.** White solid.  $^1\text{H}$  NMR (500 MHz,  $\text{CDCl}_3$ )  $\delta$  7.79 (t,  $J$  = 7.7 Hz, 4 H), 7.63 (t,  $J$  = 7.0 Hz, 1 H), 7.54-7.48 (m, 4 H).  $^{13}\text{C}$  NMR (125 MHz,  $\text{CDCl}_3$ )  $\delta$  195.50, 138.90, 137.26, 135.88, 132.64, 131.47, 129.93, 128.64, 128.41.

**2.2.3r.** Colorless oil.  $^1\text{H}$  NMR (500 MHz,  $\text{CDCl}_3$ )  $\delta$  9.03 (s, 1 H), 8.84 (d,  $J$  = 4.6 Hz, 1 H), 8.15 (d,  $J$  = 7.8 Hz, 1 H), 7.85 (d,  $J$  = 7.9 Hz, 2 H), 7.67 (t,  $J$  = 7.2 Hz, 1 H), 7.55 (t,  $J$  = 7.4 Hz, 2 H), 7.48 (dd,  $J$  = 7.2, 5.0 Hz, 1 H).  $^{13}\text{C}$  NMR (125 MHz,  $\text{CDCl}_3$ )  $\delta$  194.89, 152.86, 150.98, 137.18, 136.74, 133.18, 130.03, 128.63, 123.36.



**2.2.3s.** White solid.  $^1\text{H}$  NMR (500 MHz,  $\text{CDCl}_3$ )  $\delta$  9.28 (s, 1 H), 8.81 (s, 1 H), 8.72 (s, 1 H), 8.11 (d,  $J = 7.9$  Hz, 2 H), 7.67 (t,  $J = 7.3$  Hz, 1 H), 7.55 (t,  $J = 7.5$  Hz, 2 H).  $^{13}\text{C}$  NMR (125 MHz,  $\text{CDCl}_3$ )  $\delta$  192.28, 149.96, 146.81, 146.13, 142.91, 133.56, 130.89, 128.39.

**2.2.3t.** White solid.  $^1\text{H}$  NMR (500 MHz,  $\text{CDCl}_3$ )  $\delta$  7.87 (d,  $J = 8.1$  Hz, 2 H), 7.81 (d,  $J = 7.8$  Hz, 2 H), 7.62 (t,  $J = 7.3$  Hz, 1 H), 7.51 (t,  $J = 7.5$  Hz, 2 H), 7.32 (d,  $J = 8.1$  Hz, 2 H), 1.61 (s, 9 H).  $^{13}\text{C}$  NMR (125 MHz,  $\text{CDCl}_3$ )  $\delta$  195.52, 154.20, 151.20, 137.50, 134.94, 132.47, 131.65, 129.96, 128.33, 121.12, 84.21, 27.69.

**2.2.3u.** White solid.  $^1\text{H}$  NMR (500 MHz,  $\text{CDCl}_3$ )  $\delta$  7.82 (t,  $J = 5.8$  Hz, 2 H), 7.48 (s, 1 H), 7.36 (d,  $J = 6.2$  Hz, 1 H), 7.18 (t,  $J = 8.3$  Hz, 2 H), 6.92 (d,  $J = 8.05$  Hz, 1 H), 3.99 (s, 3 H), 3.96 (s, 3 H).  $^{13}\text{C}$  NMR (125 MHz,  $\text{CDCl}_3$ )  $\delta$  194.13, 165.06 ( $J^1 = 252.5$  Hz), 153.07, 149.09, 134.45, 132.27 ( $J^3 = 8.75$  Hz), 130.11, 125.22, 115.32 ( $J^2 = 22.5$  Hz), 112.08, 109.77, 56.12, 56.07.  $^{19}\text{F}$  NMR (471 MHz,  $\text{CDCl}_3$ )  $\delta$  -106.9.

## References

- (1) (a) Ruider, S.; Maulide, N. *Angew. Chem. Int. Ed.* **2015**, *54*, 13856. (b) Ouyang, K.; Hao, W.; Zhang, W. X.; Xi, Z. *Chem. Rev.* **2015**, *115*, 12045. (c) Wang, Q.; Su, Y.; Li, L.; Huang, H. *Chem. Soc. Rev.* **2016**, *45*, 1257.
- (2) (a) Greenberg, A.; Breneman, C. M.; Liebman, J. F. *The Amide Linkage: Structural Significance in Chemistry, Biochemistry and Materials Science*; Wiley-VCH: New York, 2003. (b) Pattabiraman, V. R.; Bode, J. W. *Nature* **2011**, *480*, 471.
- (3) (a) Roughley, S. D.; Jordan, A. M. *J. Med. Chem.* **2011**, *54*, 3451. (b) *Pharmaceutical Process Chemistry for Synthesis*, Harrington, P. J., Ed.; Wiley: Hoboken, 2011.
- (4) Kaspar, A. A.; Reichert, J. M. *Drug Discov. Today* **2013**, *18*, 807.
- (5) Marchildon, K. *Macromol. React. Eng.* **2011**, *5*, 22.
- (6) (a) *Metal-Catalyzed Cross-Coupling Reactions and More*, de Meijere, A.; Bräse, S.; Oestreich, M., Eds.; Wiley: New York, 2014. (b) *Science of Synthesis: Cross-Coupling and Heck-Type Reactions*, Molander, G.; Wolfe, J. P.; Larhed, M., Eds.; Thieme: Stuttgart, 2013. (c) *Handbook of Organopalladium Chemistry for Organic Synthesis*, Negishi, E., Ed.; Wiley: New York, 2002.
- (7) Hie, L.; Nathel, N. F. F.; Shah, T. K.; Baker, E. L.; Hong, X.; Yang, Y. F.; Liu, P.; Houk, K. N.; Garg, N. K. *Nature* **2015**, *524*, 79.
- (8) (a) Weires, N. A.; Baker, E. L.; Garg, N. K. *Nat. Chem.* **2016**, *8*, 75. (b) Li, X.; Zou, G. *Chem. Commun.* **2015**, *51*, 5089. (c) Meng, G.; Szostak, M. *Org. Lett.* **2015**, *17*, 4364.

- (d) Meng, G.; Szostak, M. *Org. Biomol. Chem.* **2016**, *14*, 5690. (e) S. Shi, M. Szostak, *Chem. Eur. J.* **2016**, *22*, 10420. (f) Simmons, B. J.; Weires, N. A.; Dander, J. E.; Garg, N. K. *ACS Catal.* **2016**, *6*, 3176. (g) Meng, G.; Szostak, M. *Angew. Chem. Int. Ed.* **2015**, *54*, 14518. (h) Meng, G.; Szostak, M. *Org. Lett.* **2016**, *18*, 796. (i) Shi, S.; Meng, G.; Szostak, M. *Angew. Chem. Int. Ed.* **2016**, *55*, 6959. (j) Dander, J. E.; Weires, N. A.; Garg, N. K. *Org. Lett.* **2016**, *22*, 3934.
- (9) Baker, E. L.; Yamano, M. M.; Zhou, Y.; Anthony, S. M.; Garg, N. K. *Nat. Commun.* **2016**, *7*, 11554.
- (10) Hu, J.; Zhao, Y.; Liu, J.; Zhang, Y.; Shi, Z. *Angew. Chem. Int. Ed.* **2016**, *55*, 8718.
- (11) (a) Dieter, R. K. *Tetrahedron* **1999**, *55*, 4177. (b) Zapf, A. *Angew. Chem. Int. Ed.* **2003**, *42*, 5394. (c) Gooßen, L. J.; Rodriguez, N.; Gooßen, K. *Angew. Chem. Int. Ed.* **2008**, *47*, 3100. (d) Brennführer, A.; Neumann, H.; Beller, M. *Angew. Chem. Int. Ed.* **2009**, *48*, 4114. (e) Liebeskind, L. S.; Srogl, J. *J. Am. Chem. Soc.* **2000**, *122*, 11260. (f) Prokopcova, H.; Kappe, C. O. *Angew. Chem. Int. Ed.* **2009**, *48*, 2276. (g) Gooßen, L. J.; Ghosh, K. *Angew. Chem. Int. Ed.* **2001**, *40*, 3458. (h) Refs. 11b and 11c. (i) Blangetti, M.; Rosso, H.; Prandi, C.; Deagostino, A.; Venturello, P. *Molecules* **2013**, *18*, 1188.
- (12) (a) Nahm, S.; Weinreb, S. M. *Tetrahedron Lett.* **1981**, *22*, 3815-3818. (b) Bechara, W. S.; Pelletier, G.; Charette, A. B. *Nat. Chem.* **2012**, *4*, 228.
- (13) (a) Afagh, N. A.; Yudin, A. K. *Angew. Chem. Int. Ed.* **2010**, *49*, 262. (b) Mahatthananchai, J.; Dumas, A.; Bode, J. W. *Angew. Chem. Int. Ed.* **2012**, *51*, 10954.

- (14) (a) Peters, R. *Cooperative Catalysis: Designing Efficient Catalysts for Synthesis*; Wiley-VCH: Weinheim, 2015. (b) Du, Z.; Shao, Z. *Chem. Soc. Rev.* **2013**, *42*, 1337. (c) Allen, A. E.; MacMillan, D. W. C. *Chem. Sci.* **2012**, *3*, 633.
- (15) (a) Nicewicz, D.; MacMillan, D. W. C. *Science* **2008**, *322*, 77. (b) Gooßen, L. J.; Deng, G.; Levy, L. M. *Science* **2006**, *313*, 662. (c) Mo, F.; Dong, G. *Science* **2014**, *345*, 68. (d) Tellis, J. C.; Primer, D. N.; Molander, G. A. *Science* **2014**, *345*, 433. (e) Zuo, Z.; Ahneman, D. T.; Chu, L.; Terret, J. A.; Doyle, A. G.; MacMillan, D. W. C. *Science* **2014**, *345*, 437.
- (16) Szostak, R.; Shi, S.; Meng, G.; Lalancette, R.; Szostak, M. *J. Org. Chem.* **2016**, *81*, 8091.
- (17) (a) Trost, B. M.; Fleming, I. *Comprehensive Organic Synthesis*; Pergamon Press: Oxford, 1991. (b) Smith, M. B.; March, J. *Advanced Organic Chemistry*; Wiley: Hoboken, 2007.
- (18) (a) Jabeen, I.; Pleban, K.; Rinner, U.; Chiba, P.; Ecker, G. F. *J. Med. Chem.* **2012**, *55*, 3261. (b) Sharmoukh, W.; Kol, K. C.; Noh, C.; Lee, J. Y.; Son, S. U. *J. Org. Chem.* **2010**, *75*, 6708 (c) Kameswaran, V. WO2001051440 A1, Jul 19, **2001**. (d) Brunton, L.; Chabner, B.; Knollman, B. *Goodman and Gilman's The Pharmacological Basis of Therapeutics*; MacGraw-Hill: New York, 2010.
- (19) (a) Miyaura, N.; Suzuki, A. *Chem. Rev.* **1995**, *95*, 2457. (b) Lennox, A. J. J.; Lloyd-Jones, G. C. *Chem. Soc. Rev.* **2014**, *43*, 412.

- (20) (a) Larock, R. C. *Comprehensive Organic Transformations*; Wiley: New York, 1999. (b) Zabicky, J. *The Chemistry of Amides*; Interscience: New York, 1970. (c) Moorthy, J. N.; Singhal, N. *J. Org. Chem.* **2005**, *70*, 1926.
- (21) (a) Gooßen, L. J.; Gooßen, K.; Stanciu, C. *Angew. Chem. Int. Ed.* **2009**, *48*, 3569. (b) Knappke, C. E. I.; Jacobi von Wangelin, A. *Angew. Chem. Int. Ed.* **2010**, *49*, 3568.
- (22) Kemnitz, C. R.; Loewen, M. J. *J. Am. Chem. Soc.* **2007**, *129*, 2521.
- (23) (a) Allen, C. L.; Atkinson, B. N.; Williams, J. M. *Angew. Chem. Int. Ed.* **2012**, *51*, 1383. (b) Dineen, T. A.; Zajac, M. A.; Myers, A. G. *J. Am. Chem. Soc.* **2006**, *128*, 16406. (c) Eldred, S. E.; Stone, D. A.; Gellman, S. H.; Stahl, S. S. *J. Am. Chem. Soc.* **2003**, *125*, 3422.
- (24) (a) Tani, K.; Stoltz, B. M. *Nature* **2006**, *441*, 731. (b) Szostak, R.; Aubé, J.; Szostak, M. *Chem. Commun.* **2015**, *51*, 6395. (c) Hu, F.; Lalancette, R.; Szostak, M. *Angew. Chem. Int. Ed.* **2016**, *55*, 5062.
- (25) Blakey, S. B.; MacMillan, D. W. C. *J. Am. Chem. Soc.* **2003**, *125*, 6046. (b) Buszek, K. R.; Brown, N. *Org. Lett.* **2007**, *9*, 707.
- (26) Davidsen, S. K.; May, P. D.; Summers, J. B. *J. Org. Chem.* **1991**, *56*, 5482.
- (27) (a) Greenberg, A.; Venanzi, C. A. *J. Am. Chem. Soc.* **1993**, *115*, 6951. (b) Szostak, R.; Aubé, J.; Szostak, M. *J. Org. Chem.* **2015**, *80*, 7905. (c) Cox, C.; Lectka, T. *Acc. Chem. Res.* **2000**, *33*, 849.
- (28) Bogan, K. L.; Brenner, C. *Annu. Rev. Nutr.* **2008**, *28*, 115.

(29) (a) Beena; Rawat, D. S. *Med. Res. Rev.* **2013**, *33*, 693. (b) Rivers, E. C.; Mancera, R. L. *Drug Discov. Today* **2008**, *13*, 1090.

(30) Magano, J.; Dunetz, J. R. *Chem. Rev.* **2011**, *111*, 2177.

(31) Zhu, S. S.; Liu, X. L.; Liu, P. F.; Li, Y.; Li, J. Q.; Wang, H. M.; Yuan, S. K.; Si, N. G. *Phytopathology* **2007**, *97*, 643.

## 2.3 Reversible twisting of primary amides

Parts of this section were adapted with permission from the article “Reversible Twisting of Primary Amides via Ground State N–C(O) Destabilization: Highly Twisted Rotationally-Inverted Acyclic Amides” (*J. Am. Chem. Soc.* **2018**, *140*, 727). Copyright ©2018, American Chemical Society.

### 2.3.1 Research background

As already outlined in the introduction, the amide bond represents one of the most crucial functional groups in chemistry and biology.<sup>1–3</sup> As predicted by the Pauling’s resonance theory,<sup>4</sup> the vast majority of amides are planar,<sup>5</sup> which has important implications for their reactivity (e.g. neutral hydrolysis of unactivated amides has a half-life of ca. 500 years),<sup>6</sup> structure (e.g.  $\alpha$ -helix as a fundamental building block of proteins)<sup>7</sup> and chemical properties (e.g. vastly preferred O-protonation).<sup>8</sup> Previous extensive studies have shown that deviations of the amide bond from planarity greatly affect the stability and reactivity of amides.<sup>9</sup> Furthermore, amide bond twisting has been proposed as a central design element of enzymatic processes, including cis-trans isomerization,<sup>10</sup> amide hydrolysis<sup>11</sup> and protein splicing.<sup>12</sup> Recently, amide bond twisting has been demonstrated as a part of the mechanism in protein N-glycosylation involving primary carboxamide groups.<sup>13</sup> Moreover, recent work has shown that amide bond deformations are a controlling factor for selective amide bond activation/cross-coupling,<sup>14</sup> thus emphasizing the role of amide bond twist as an enabling pathway in modern organic synthesis.<sup>15</sup>

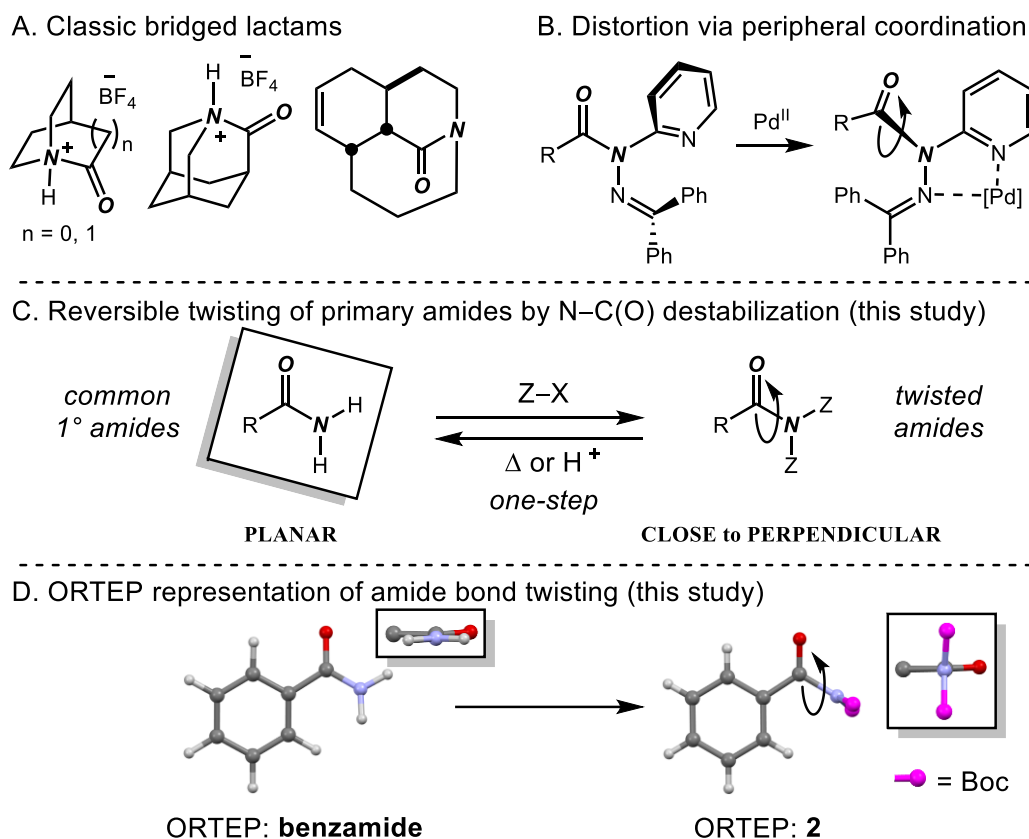


**Figure 2.3.1** (a) Examples of highly distorted amides in cyclic frameworks (classic bridged lactams). (b) Amide distortion by peripheral coordination (Shibasaki et al.). (c-d) Reversible twisting of acyclic primary amides by ground-state N–C(O) destabilization. (this study, insets show view along N–C(O) axis).

In principle, the most common method to achieve amide bond twisting relies on the incorporation of the amide function into a rigid cyclic ring system (Figure 2.3.1A).<sup>9a-c</sup> These bicyclic bridgehead lactams feature extreme geometric properties of structurally-characterized amide bonds<sup>16</sup> (Winkler-Dunitz distortion parameters,<sup>17</sup> up to  $\tau = 90^\circ$ ,  $\chi_N = 60^\circ$ ). However, the synthesis of these lactams is challenging<sup>1-3</sup> due to severe decrease of amidic resonance (e.g. the landmark syntheses of the parent 2-quinuclidonium



tetrafluoroborate<sup>2</sup> and 1-aza-2-adamantanone<sup>16c</sup> featured unique amide forming transforms), and typically this distortion method cannot be adapted to more readily-available common acyclic amides.

Recently, Kumagai, Shibasaki et al. devised a new type of non-planar amides bearing predominantly pyramidalized amide bonds in which reversible deformation has been achieved by peripheral coordination of Pd(II) to Lewis basic nitrogen moieties (Figure 2.3.1B).<sup>18</sup> The method resulted in amides with remarkable deformations from planarity of up to  $\chi_N = 56^\circ$  and  $\tau = 19^\circ$ . However, the identification of peripheral coordination in these structurally intriguing amides rendered the direct distortion of common acyclic amides more challenging. In addition, the emergence of specifically-tailored N-tetramethylpiperidine (TMP),<sup>19</sup> N-glutarimide<sup>20</sup> and N-1,3-thiazolidine-2-thione amides<sup>21</sup> has provided controlled access to non-planar amide bond geometries; however, these compounds were synthesized from the corresponding carboxylic acids and derivatives and often suffered from high susceptibility to hydrolysis as exemplified by TMP amides.<sup>19</sup>

With these considerations in mind and having discovered the unusual properties of N,N-di-Boc amides as general electrophiles for cooperative catalysis (Section 2.2), we developed the first class of acyclic twisted amides that could be prepared, fully reversibly, from common primary amides<sup>22</sup> in a single, operationally-trivial step (Figure 2.3.1C-D). In these examples, amide bond distortion was triggered by selective di-*tert*-butoxycarbonylation of the amide nitrogen atom furnishing twisted amides in which the amide bond exhibited nearly perpendicular twist (up to  $\tau = 82^\circ$ ). We demonstrated

through reactivity studies unusual properties of the amide bond in this new class of twisted amides, wherein selective cleavage of the N–C(O) or N–Boc bond could be achieved by a judicious choice of the reaction conditions. We further demonstrated that the amide bond deformation could be attributed to ground-state destabilization,<sup>3</sup> which resulted in the most twisted acyclic amide bonds reported at the time of this investigation.<sup>1–3,9</sup> Most importantly, this project demonstrated the ability to selectively induce twist of common primary amides, in a reversible manner, which represents a new concept for the design and application of non-planar amides in biochemistry, organic synthesis and molecular switching.<sup>24</sup>

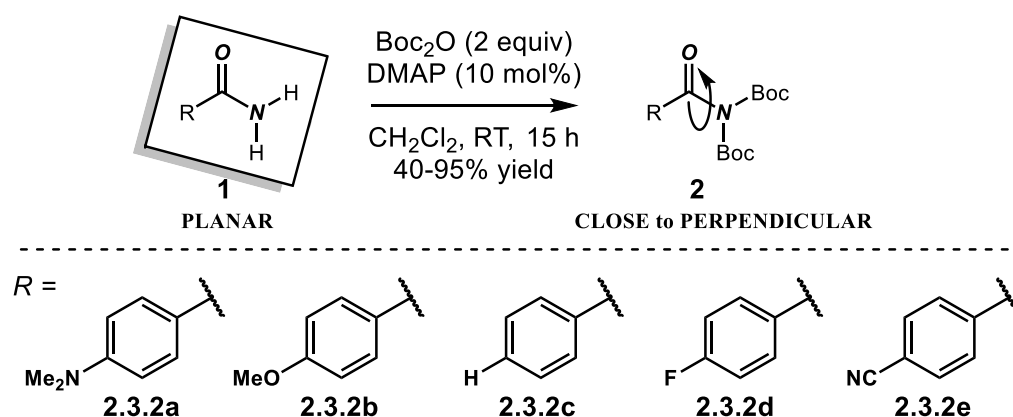


**Figure 2.3.2** One-step synthesis of twisted amides.

### 2.3.2 Synthesis and proof of structure

Based on our previous experience gained in the synthesis of non-planar amides and their cross-coupling, we began our study by isolating N,N-di-Boc amides and growing single crystals of **2.3.2** (Figure 2.3.2). All amides **2.3.2** were prepared directly in one-step from the corresponding benzamides<sup>25,26</sup> by site-selective N,N-di-*tert*-butoxycarbonylation of

the amide bond under mild conditions. This widely-applicable process enables to directly engage common primary amides in amide bond twisting.<sup>27</sup> Since primary amides are among the most ubiquitous amide derivatives in organic synthesis and constitute widespread structural motifs in pharmaceutical industry,<sup>22</sup> our method of preparation put emphasis on the use of common acyclic amides<sup>28</sup> as models for amide bond distortion and established a distinguishing feature of this approach.

entry	<b>2.3.2</b>	N-C(O) (Å)	C=O (Å)	$\tau$ (deg)	$\chi_N$ (deg)	$\tau+\chi_N$ (deg)
1	<b>2.3.2a</b>	1.483	1.201	81.9	1.1	83.0
2	<b>2.3.2b</b>	1.458	1.205	59.2	0.2	59.4
3	<b>2.3.2c</b>	1.467	1.200	72.5	3.6	76.1
4	<b>2.3.2d</b>	1.433	1.206	38.3	4.7	43.0
5 <sup>b</sup>	<b>2.3.2e</b>	1.418	1.205	28.9	19.5	48.4
6 <sup>b</sup>	<b>2.3.2e'</b>	1.414	1.209	20.0	26.8	46.8
7 <sup>c</sup>	<b>benzamide</b>	1.342	1.265	0.0	0.1	0.1

Crystallographic data have been deposited with the Cambridge Crystallographic Data Center. See SI for details and expanded tables.<sup>b</sup>Two independent molecules in the unit cell. <sup>c</sup>Benzamide, ref. 30.

**Table 2.3.1** Summary of structural parameters for the X-ray structures of **2.3.2a-2.3.2e** and reference benzamide<sup>a</sup>

We found that amides **2.3.2a-2.3.2e** (R = NMe<sub>2</sub>, OMe, H, F, CN) were crystalline and their structures could be confirmed by X-ray crystallography (Tables 2.3.1-2, Figure 2.3.3). Table 2.3.1 summarizes the Winkler-Dunitz distortion parameters ( $\tau$ ,  $\chi_N$ ), the additive distortion parameter  $\Sigma(\tau + \chi_N)$ ,<sup>29</sup> and selected bond lengths of the N,N-Boc<sub>2</sub>-amides. The table also includes geometric parameters of the corresponding parent benzamide.<sup>30</sup> The structures of amides **2.3.2a-2.3.2e** together with Newman projections along the N-C(O) axis are presented in Figure 2.3.3. The structure of the corresponding

parent benzamide is shown in Figure 2.3.1D. Notably, the well-studied availability of the crystal structure of benzamide (**2.3.1c**, PhCONH<sub>2</sub>) permitted comparison of the parent amide and its N,N-Boc<sub>2</sub> twisted amide product.

entry	<b>2.3.2</b>	X1□X2 (Å)	ω <sub>1</sub> (deg)	ω <sub>2</sub> (deg)	ω <sub>3</sub> (deg)	ω <sub>4</sub> (deg)
1	<b>2.3.2a</b>	1.452	-98.4	-97.9	81.0	82.7
2	<b>2.3.2b</b>	1.470	-58.8	-59.6	120.5	121.0
3	<b>2.3.2c</b>	1.479	71.6	73.4	-110.2	-104.8
4	<b>2.3.2d</b>	1.479	-41.7	-34.9	140.4	143.0
5	<b>2.3.2e</b>	1.493	39.7	18.1	-142.4	-159.9
6	<b>2.3.2e'</b>	1.495	-33.6	-6.4	146.8	173.2

**Table 2.3.2** Summary of additional bond lengths (Å) and angles (deg) for the X-ray structures of **2.3.2a-2.3.2e**.

Remarkably, the structure of **2.3.2a** (R = NMe<sub>2</sub>) showed that this compound belonged to the most twisted amides isolated and fully-structurally characterized at the time of this investigation ( $\tau = 81.9^\circ$ ).<sup>1-3,9</sup> Moreover, the N–CO amide bond length of 1.483 Å in **2.3.2a** was the longest recorded so far for an acyclic amide derivative. The observed length for the C=O bond was 1.201 Å. Interestingly, nitrogen in **2.3.2a** was basically sp<sup>2</sup> hybridized ( $\chi_N = 1.1^\circ$ ), indicating that **2.3.2a** belonged to classic twisted amides as defined by Yamada et. al. The X-ray structures of **2.3.2b-2.3.2e** (R = OMe, H, F, CN) revealed substantial twisting of the amide bond.

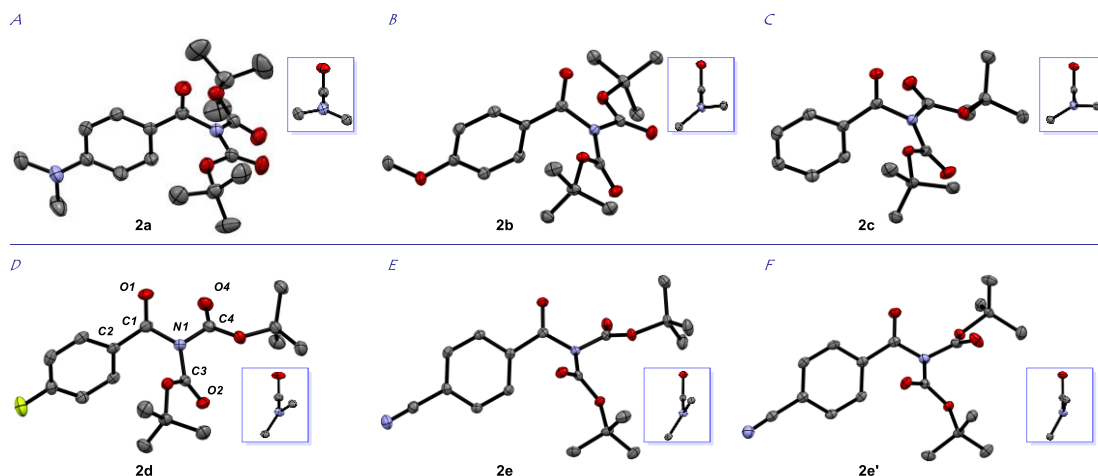


**Figure 2.3.3** Crystal structures of amides **2.3.2a-2.3.2e**: two molecules in the unit cell.

insets show Newman projections along N–C(O) bonds.

The amide **2.3.2e** ( $R = \text{CN}$ ) was crystallized as two independent molecules in the unit cell. Analysis of the pyramidalization at nitrogen angle revealed significant pyramidalization in **2.3.2e** (up to  $\chi_{\text{N}} = 26.8^\circ$  in **2.3.2e'**). Pyramidalization at nitrogen has historically been one of the most valuable parameters to describe structural distortion of the amide bond.<sup>1–9</sup> More recent studies demonstrated that the additive amide bond distortion parameter,  $\Sigma(\tau + \chi_{\text{N}})$ , provides a more accurate description of non-planarity of the amide linkage.<sup>29</sup>

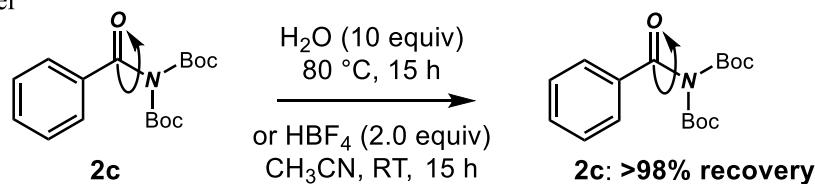
We thought it instructive to compare structural parameters of the parent benzamide<sup>30</sup> (**2.3.1c**,  $R = \text{H}$ ;  $\tau = 0.0^\circ$ ;  $\chi_{\text{N}} = 0.1^\circ$ ;  $\text{N–C(O)} = 1.342 \text{ \AA}$ ;  $\text{C=O} = 1.265 \text{ \AA}$ , X-ray data) with the corresponding N,N-Boc<sub>2</sub> twisted amide **2.3.2c** ( $R = \text{H}$ ;  $\tau = 72.5^\circ$ ;  $\chi_{\text{N}} = 3.6^\circ$ ;  $\text{N–C(O)} = 1.467 \text{ \AA}$ ;  $\text{C=O} = 1.200 \text{ \AA}$ ). As shown in Table 2.3.1, N,N-di-*tert*-butoxycarbonylation dramatically enhanced the twist angle (from  $0^\circ$  to  $72.5^\circ$ ). This was accompanied by a significant increase of the N–C(O) bond length (by  $0.125 \text{ \AA}$ ) and a considerable

shortening of the C=O bond (by 0.065 Å). Moreover, the observed N–C(O) bond length in **2.3.2e'** (1.414 Å) was shorter by 0.069 Å than the N–C(O) bond length in **2.3.2a** (1.483 Å), while the C=O bond lengths in **2.3.2a** (1.201 Å) and **2.3.2e'** (1.209 Å) differed by only 0.008 Å. Overall, these structural features in **2.3.2a-2.3.2e** indicated substantial amide bond deviation from planarity upon N,N-di-*tert*-butoxycarbonylation.<sup>1–3,23</sup>

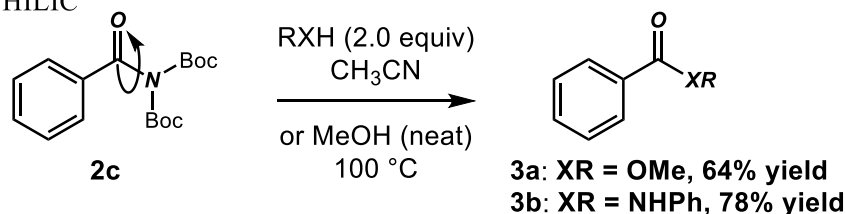
### 2.3.3 Chemical reactivity

Having established a survey of structural properties of acyclic twisted amides, next, we examined their chemical reactivity. The parent amide **2.3.2c** (R = H) was used as a model substrate. It is well-established that deviations of the amide bond from planarity lead to unusual reactivity of amides as a result of diminished resonance, including (1) hypersensitivity to hydrolysis, (2) N-protonation, and (3) high susceptibility to nucleophilic addition.<sup>1–3,9</sup>

## A. ACID/Water



## B. NUCLEOPHILIC



## C. ORGANOMETALLIC

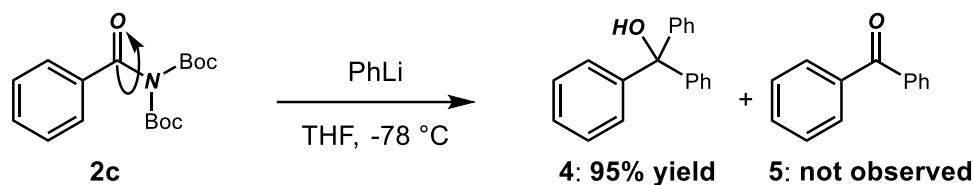
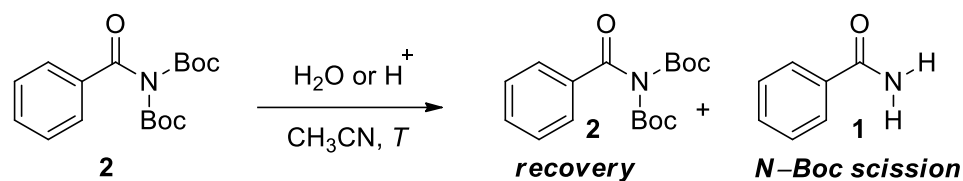


**Figure 2.3.4** N–C(O) Cleavage reactivity of amide **2.3.2c**.

As expected, we found the chemical reactivity of amide **2.3.2c** to be remarkable. Most notably, although twisted amides with a similar amide bond distortion are hypersensitive to hydrolysis,<sup>9</sup> we found that incubation of amide **2.3.2c** in aqueous CH<sub>3</sub>CN (10 equiv of H<sub>2</sub>O) at 80 °C for 15 h afforded only recovered starting material (Figure 2.3.5A). Importantly, these acyclic twisted amides do not benefit from the thermodynamic stability afforded by a scaffolding effect of the medium-sized ring,<sup>16f,g</sup> which ruled out reversibility of the amide bond hydrolysis. Furthermore, **2.3.2c** was remarkably stable to acidic conditions (Figure 2.3.5 A and Table 2.3.3).



entry	H <sub>2</sub> O/acid	H <sub>2</sub> O/acid (equiv)	temp (°C)	time (h)	conversion <sup>b</sup> (%)	yield <sup>b</sup> (%)	notes
1	H <sub>2</sub> O	5	23	15	<2	>98	-
2	H <sub>2</sub> O	5	80	15	<2	>98	-
3	H <sub>2</sub> O	5	100	15	71	29	71% NH <sub>2</sub> amide
4	HBFe <sub>4</sub>	2	23	15	<2	>98	-
5	HBFe <sub>4</sub>	5	23	15	40	60	40% NHBoc amide
6	TFA	2	23	15	<2	>98	-
7	TFA	5	23	15	41	59	41% NHBoc amide
8	AcOH	2	23	15	<2	>98	-
9	<i>p</i> TsOH	5	23	15	>98	<2	>98% NH <sub>2</sub> amide
10	HCl	2	23	15	44	56	44% NH <sub>2</sub> amide
11	HCl	2	23	1	<2	>98	-
12	HCl	2	80	15	>98	<2	>98% NH <sub>2</sub> amide
13 <sup>c</sup>	HCl	2	100	15	>98	<2	>98% NH <sub>2</sub> amide

<sup>a</sup>All reactions carried out using standard Schlenk techniques. Conditions: **2.3.2c** (0.10 mmol), H<sub>2</sub>O/acid (2-5 equiv), CH<sub>3</sub>CN (0.25 M), T, 1-15 h. <sup>b</sup>Determined by <sup>1</sup>H NMR. Yield indicates recovery yield of **2.3.2c**.

**Table 2.3.3** Comparison of stability of amide **2.3.2c** under aqueous and acidic conditions.<sup>a</sup>



entry	solvent	temp (°C)	time (h)	conversion <sup>b</sup> (%)	yield <sup>b</sup> (%)	notes
1	CH <sub>3</sub> CN	80	24	<2	>98	-
2 <sup>c</sup>	CH <sub>3</sub> CN	120	24	>98	<2	>98% NH <sub>2</sub> amide
3	CH <sub>3</sub> CN	150	24	>98	<2	>98% NH <sub>2</sub> amide
4	CDCl <sub>3</sub>	23	24	<2	>98	-
5	CDCl <sub>3</sub>	23	120	<2	>98	-
6	CDCl <sub>3</sub>	23	168	<2	>98	-
7	C <sub>6</sub> D <sub>6</sub>	23	24	<2	>98	-
8	C <sub>6</sub> D <sub>6</sub>	23	120	<2	>98	-
9	C <sub>6</sub> D <sub>6</sub>	23	168	<2	>98	-
10	Acetone- <i>d</i> <sub>6</sub>	23	24	<2	>98	-
11	Acetone- <i>d</i> <sub>6</sub>	23	120	<2	>98	-
12	Acetone- <i>d</i> <sub>6</sub>	23	168	<2	>98	-
13	CD <sub>3</sub> OD	23	24	<2	>98	-
14	CD <sub>3</sub> OD	23	120	<2	>98	-
15	CD <sub>3</sub> OD	23	168	<2	>98	-
16	CH <sub>3</sub> CN/D <sub>2</sub> O 1:1	23	24	<2	>98	-
17	CH <sub>3</sub> CN/D <sub>2</sub> O 1:1	23	120	16	84	16% NH <sub>2</sub> amide
18	CH <sub>3</sub> CN/D <sub>2</sub> O 1:1	23	168	25	75	25% NH <sub>2</sub> amide
19	DMSO- <i>d</i> <sub>6</sub>	23	24	<2	>98	-
20	DMSO- <i>d</i> <sub>6</sub>	23	120	<2	>98	-
21	DMSO- <i>d</i> <sub>6</sub>	23	168	<2	>98	-

<sup>a</sup>All reactions carried out using standard Schlenk techniques. Conditions: **2.3.2c**(0.10 mmol), solvent (0.25M), *T*, 1-7d.<sup>b</sup>Determined by <sup>1</sup>H NMR. Yield indicates recovery yield of **2.3.2c**. <sup>c</sup>70% recovery, 100 °C, 24 h.

**Table 2.3.4** Comparison of stability of amide **2.3.2c** in different solvents.<sup>a</sup>

For example, incubation of **2.3.2c** with HBF<sub>4</sub> (2 equiv) in CH<sub>3</sub>CN at 23 °C for 15 h had no impact of the recovery of starting material. In addition, amide **2.3.2c** was recovered unchanged from common nucleophilic solvents (e.g., DMSO, MeOH, 23 °C, 7 days, see table 2.3.4). Amide **2.3.2c** was also very stable in aqueous solutions (e.g., D<sub>2</sub>O:CH<sub>3</sub>CN, 1:1, v/vol, 75% recovery, 23 °C, 7 days). Collectively, these studies unambiguously

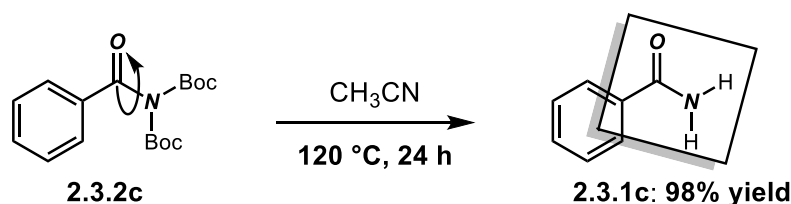
demonstrated that acyclic twisted amides of the type **2.3.2** show substantially higher stability to nucleophilic N–C(O) cleavage than classical bridged lactams. The high stability of amides **2.3.2** is critical to the development of synthetically-valuable reactivity governed by amide bond twist in easily accessible from 1° amides twisted acyclic amides.<sup>27</sup>

Despite high stability to nucleophilic cleavage relative to other classes of twisted amides, amide **2.3.2c** reacted with nucleophiles under neutral conditions, i.e. in the absence of additional Lewis bases (Figure 2.3.5B). For instance, the reaction of **2.3.2c** with MeOH (neat, 100 °C) or aniline (2.0 equiv, CH<sub>3</sub>CN, 100 °C) cleanly afforded the corresponding ester or amide by N–C(O) nucleophilic opening. Moreover, amide **2.3.2c** reacted instantaneously with organometallic reagents, such as PhLi, at -78 °C resulting in exhaustive nucleophilic addition (Figure 2.3.5C). The formation of acetophenone was not observed, even when limiting organometallic reagent was used. This reactivity contrasted with bridged lactams, which react by stable tetrahedral intermediates due to the lack of  $\sigma^*_{\text{C-N}}$  overlap,<sup>31</sup> but also differed from N,N-dialkylbenzamides (e.g. dimethylbenzamide), which give approx. 2:1 mixture of ketone : alcohol using the organometallic reagent in excess.<sup>32</sup>

However, the most remarkable feature of the reactivity of amides of the type **2.3.2** was their capacity to revert to benzamides upon a judicious choice of the reaction conditions (Figure 2.3.6).<sup>33</sup> We found that a simple exposure of amide **2.3.2c** to thermal (120 °C, CH<sub>3</sub>CN, 24 h) or acidic (HCl, 2 equiv, CH<sub>3</sub>CN, 80 °C, 24 h) conditions resulted in fully chemo- and regioselective (vs. amide acyl N–C(O) bond) cleavage of the carbamate N–

Boc bonds via thermal/acid-mediated deprotection of the carbamate group. The reaction was completely regioselective with respect to the C–N bond that was less distorted from the C=O  $\pi$  system, in contrast to the previous examples of N–C cleavage of twisted amides.<sup>16g,34</sup>

A. THERMAL



B. ACID-MEDIATED

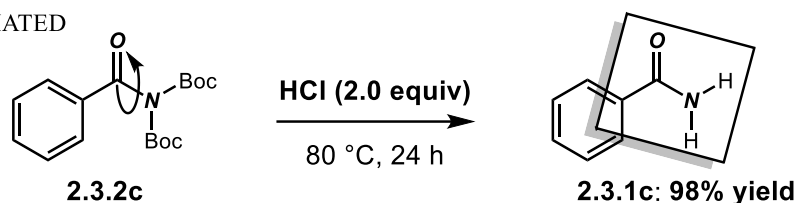


**Figure 2.3.5** Thermal and acid-mediated deconstruction of N,N-Boc<sub>2</sub>amides: N–Boc cleavage of amide **2.3.2c**.

Overall, these results demonstrated novel reactivity of non-planar acyclic amides **2.3.2**. Importantly, in combination with the rapid access to N,N-Boc<sub>2</sub> twisted amides from common primary amides (Figure 2.3.2),<sup>25</sup> our studies illustrated the capacity to readily change molecular conformation around the amide bond in a highly efficient manner. To the best of our knowledge, this was the first example of a rapid formation/deconstruction of a twisted amide bond from the corresponding primary amide.<sup>1–3,9</sup> The abundance of primary amides<sup>22</sup> renders this process particularly attractive for a plethora of synthetic applications.

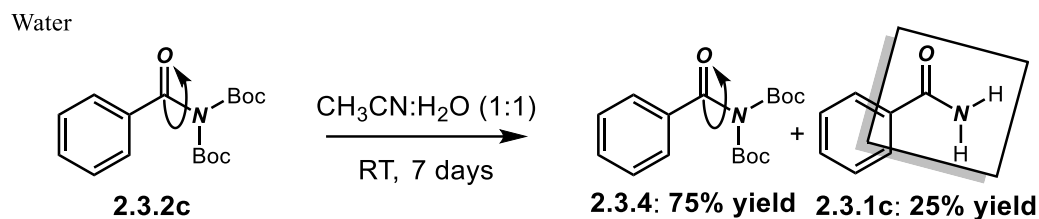


**Figure 2.3.6** Stability of amides **2.3.2c** in aqueous solutions.

As noted earlier, amides **2.3.2** are very stable to aqueous conditions. We showed that the reaction of **2.3.2c** with  $\text{D}_2\text{O}:\text{CH}_3\text{N}$  (1:1, v/vol) at room temperature led to the recovery of **2.3.2c** and production of the parent benzamide **2.3.1c** in a 3:1 ratio after 7 days (Figure 2.3.7). Thus, deconstruction of these twisted amides under mild, aqueous, thermodynamic conditions also appeared to be synthetically accessible.

### 2.3.4 Conclusion

In conclusion, we have developed the first class of acyclic twisted amides that can be prepared directly, in a reversible manner, from ubiquitous primary amides in a single operationally-trivial step. More importantly, our data demonstrated the propensity of common acyclic amides to participate in amide bond deformation pathways that can be attributed to ground-state destabilization of the amide bond, resulting in the most twisted acyclic amide bonds isolated and fully characterized at the time of this study. Mechanistic and synthetic studies have provided insight into the structural and energetic properties of the amide bond and showed evidence for controlled generation/ deconstruction of acyclic twisted amides, wherein selective cleavage of the  $\text{N}-\text{C}(\text{O})$  or  $\text{N}-\text{Boc}$  bond could be achieved by controlling the reaction conditions. On a fundamental level, our studies show that these structures are best represented as classic twisted amides as defined by Yamada

et al., providing an alternative to generating substantial non-planarity of the amide bond without resorting to complex frameworks. We believe that the results obtained in the structural characterization and reactivity of N,N-Boc<sub>2</sub> amides will permit a better understanding of the properties of the amide bond in structural chemistry and metal catalyzed reactions of amides.

### 2.3.5 Experimental section

**Details of crystal structure analysis of amides.** Crystallographic information for all of the compounds is given in Tables 2.3.5 and 2.3.6. All compounds were colorless single crystals. Full datasets were collected using graphite-monochromated CuK  $\alpha$  radiation ( $\lambda = 1.54178 \text{ \AA}$ ) on a Bruker SMART APEX2 single crystal diffractometer. X-rays were provided by a fine-focus sealed X-ray tube operated at 48kV and 30mA. Lattice constants were all determined using the Bruker SAINT software package using all available reflections (after data collection, ORTEP files, see Figures 2.3.13-2.3.17). All data were corrected for absorption by measuring the faces of each crystal and doing a numerical absorption correction. The Bruker software package SHELXTL-2014 was used to solve all of the structures using the direct methods technique and difference electron density maps. All stages of weighted full-matrix least-squares refinement were conducted using  $F_o^2$  data with the same software package. The final structural model for each compound was refined using anisotropic thermal parameters for all non-hydrogen atoms; all of the H atoms were located in difference maps, but were placed in geometrically idealized positions and allowed to “ride” on their parent C, O or N atoms, with bond lengths of 0.95, 1.00, 0.99, 0.98, and 0.84  $\text{\AA}$  for aromatic, methine, methylene, methyl, and

hydroxyl, respectively. The isotropic thermal parameters for these H atoms were fixed to be 1.2 times the  $U_{\text{iso}}$  for C or N and 1.5 times the  $U_{\text{iso}}$  for O.

Details for all of the structures are given in Tables 2.3.5 and 2.3.6. Also included in this table are the largest shifts/s.u. for the final cycle of refinement and the largest maxima and minima in any of the final difference maps.

compound	<b>2.3.2a</b>	<b>2.3.2b</b>	<b>2.3.2c</b>
Empirical Formula	C <sub>19</sub> H <sub>28</sub> N <sub>2</sub> O <sub>5</sub>	C <sub>18</sub> H <sub>25</sub> NO <sub>6</sub>	C <sub>17</sub> H <sub>23</sub> NO <sub>5</sub>
Fw	364.43	351.39	321.36
Space Group	P 21	P 21	P b c a
Hall Group	P 2yb	P 2yb	-P 2ac 2ab
a (Å)	10.1592(7)	8.680(2)	16.7598(3)
b (Å)	11.0638(8)	11.203(2)	16.5657(3)
c (Å)	10.3109(7)	10.273(2)	12.5706(2)
α (deg)	90	90	90
β (deg)	113.208(4)	110.19(3)	90
γ (deg)	90	90	90
V (Å <sup>3</sup> )	1065.16(13)	937.6(4)	3490.07(10)
Z	2	2	8
Diffractometer	Bruker APEX2	Bruker APEX2	Bruker APEX2
d <sub>calcd</sub> (g/cm <sup>3</sup> )	1.136	1.245	1.223
λ	1.54178	1.54178	1.54178
Bond precision (Å)	0.0046	0.0028	0.0020
T (K)	296	100	100
F(000)	392.0	376.0	1376.0
Abs coeff (mm <sup>-1</sup> )	0.675	0.775	0.742
Abs corr	Numerical	Numerical	Numerical
Max, Min Transm.	0.800,0.890	0.751,0.902	0.835,0.947
Frame time (s)	10 sec	10 sec	10 sec
h, k, l max	11, 13, 12	10,13,12	19,19,14
θ max (deg)	68.284	68.550	68.965
Reflns collected	3546	2718	3151
Independent reflections	3345	2700	2933
Completeness	1.72/0.91	1.49/0.79	0.973
Params	244	234	215
R <sub>1</sub> (obsd); wR <sub>2</sub> (all)	0.0376; 0.1031	0.0227; 0.0576	0.0373; 0.0956
GOF (F <sup>2</sup> )	1.071	1.050	1.083

**Table 2.3.5** Crystal data and structure refinement summaries for **2.3.2a-2.3.2c**.

compound	<b>2.3.2d</b>	<b>2.3.2e</b>
Empirical Formula	C <sub>17</sub> H <sub>22</sub> FNO <sub>5</sub>	C <sub>18</sub> H <sub>22</sub> N <sub>2</sub> O <sub>5</sub>
Fw	339.35	346.37
Space Group	C 2/c	P -1
Hall Group	-C 2yc	-P 1
a (Å)	20.988(3)	11.7945(3)
b (Å)	11.0644(13)	12.5579(3)
c (Å)	15.974(2)	12.9994(3)
$\alpha$ (deg)	90	91.316(1)
$\beta$ (deg)	104.590(3)	101.162(1)
$\gamma$ (deg)	90	102.764(1)
V (Å <sup>3</sup> )	3589.9(8)	1837.94(8)
Z	8	4
Diffractometer	Bruker APEX2	Bruker APEX2
d <sub>calcd</sub> (g/cm <sup>3</sup> )	1.256	1.252
$\lambda$	1.54178	1.54178
Bond precision (Å)	0.0019	0.0018
T (K)	100	100
F(000)	1440.0	736.0
Abs coeff (mm <sup>-1</sup> )	0.832	0.761
Abs corr	Numerical	Numerical
Max, Min Transm.	0.815,0.918	0.835,0.918
Frame time (s)	10 sec	10 sec
h, k, l max	24, 13, 18	13,14,15
$\theta$ max (deg)	68.695	68.736
Reflns collected	3180	6128
Independent reflections	2911	5773
Completeness	0.955	0.902
Params	224	464
R <sub>1</sub> (obsd); wR <sub>2</sub> (all)	0.0337; 0.0896	0.327; 0.0890
GOF (F <sup>2</sup> )	1.047	1.023

**Table 2.3.6** Crystal data and structure refinement summaries for **2.3.2d** and **2.3.2e**.





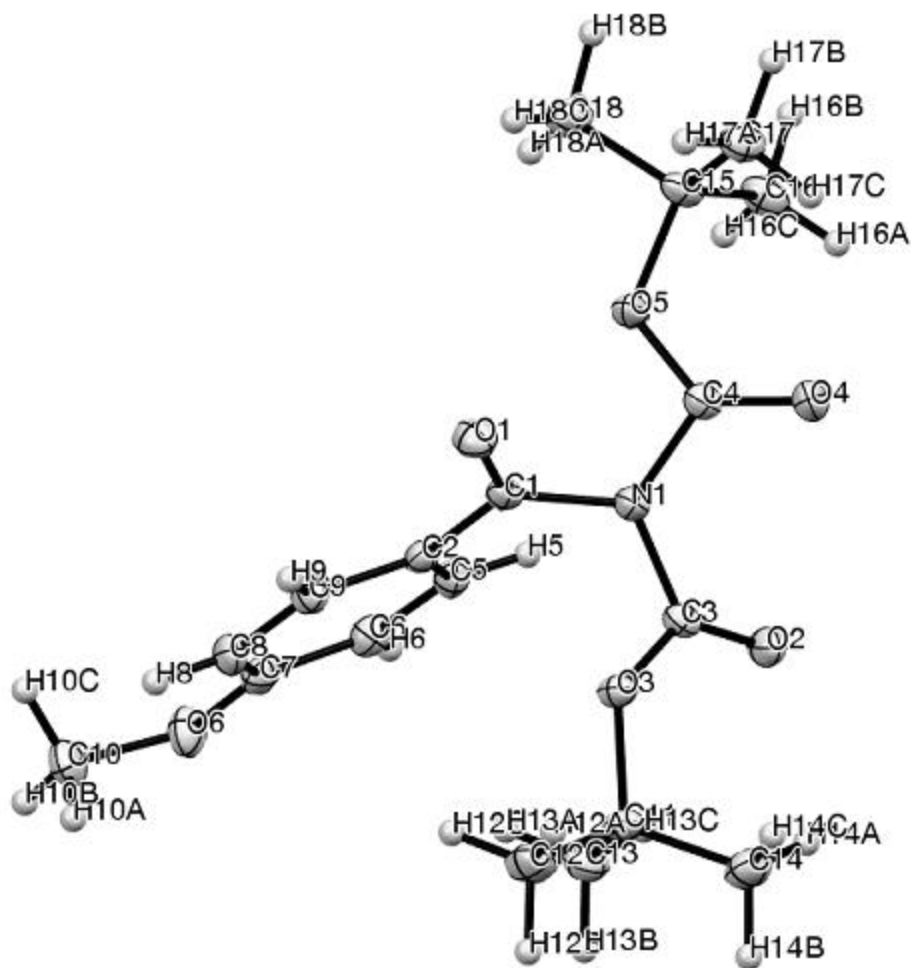


**Figure 2.3.8** ORTEP structure of **2.3.2b** (CCDC 1552720). Selected bond lengths (Å) and angles (deg): N1–C1, 1.458(2); C1–O1, 1.205(2); C1–C2, 1.470(3); N1–C3, 1.411(2); N1–C4, 1.409(2); C2–C1–N1–C3, –58.8(2); O1–C1–N1–C4, –59.6(2); O1–C1–N1–C3, 120.5(2); C2–C1–N1–C4, 121.0(2).

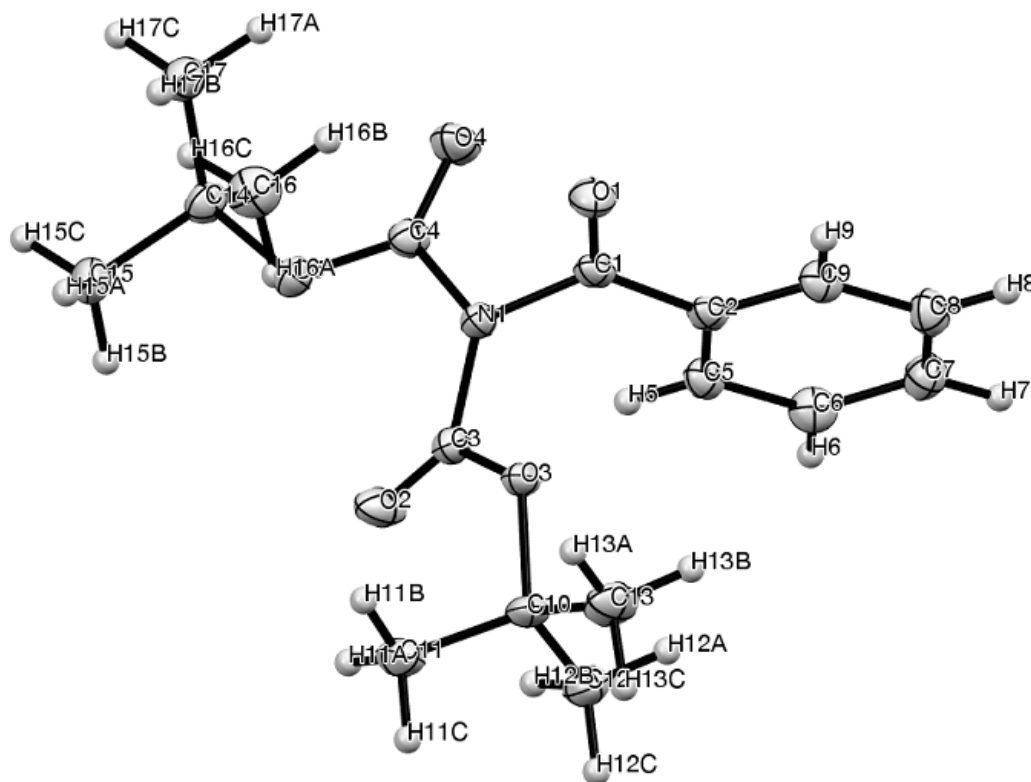


**Figure 2.3.9** ORTEP structure of **2.3.2c** (CCDC 1552721). Selected bond lengths (Å) and angles (deg). N1–C1, 1.467(2); C1–O1, 1.200(2); C1–C2, 1.479(2); N1–C3, 1.410(2); N1–C4, 1.408(2); C2–C1–N1–C3, 71.6(1); O1–C1–N1–C4, 73.4(2); O1–C1–N1–C3, –110.2(1); C2–C1–N1–C4, –104.8(1).

**Figure 2.3.10** ORTEP structure of **2.3.2d** (*CCDC 1552722*). Selected bond lengths (Å) and angles (deg): N1–C1, 1.433(2); C1–O1, 1.206(1); C1–C2, 1.479(2); N1–C3, 1.427(1); N1–C4, 1.423(2); C2–C1–N1–C3, –41.7(2); O1–C1–N1–C4, –34.9(2); O1–C1–N1–C3, 140.4(1); C2–C1–N1–C4, 143.0(1).

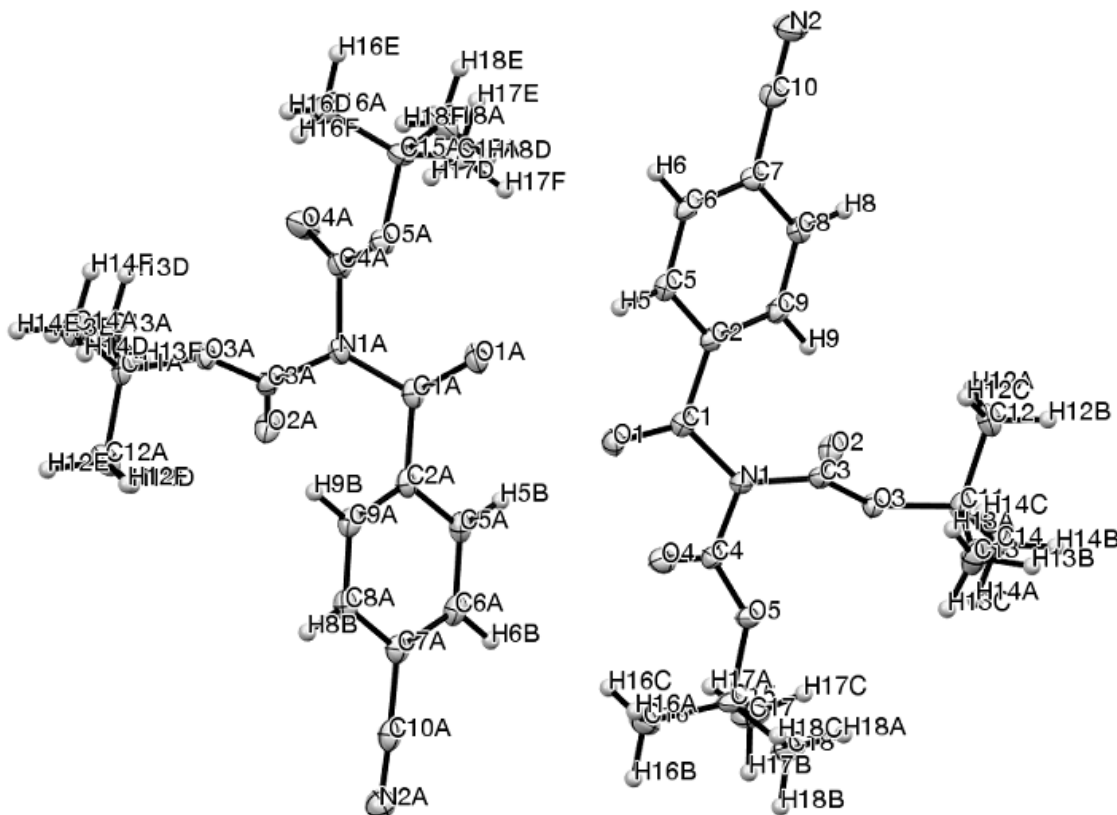


**Figure 2.3.11** ORTEP structure of **2.3.2e** (CCDC 1552723). Selected bond lengths (Å) and angles (deg), two molecules were observed in the asymmetric unit: (I) N1–C1, 1.418(1); C1–O1, 1.205(2); C1–C2, 1.493(2); N1–C3, 1.431(1); N1–C4, 1.435(1); C2–C1–N1–C3, 39.7(1); O1–C1–N1–C4, 18.1(2); O1–C1–N1–C3, –142.4(1); C2–C1–N1–C4, –159.9(1). (II) N1A–C1A, 1.414(1); C1A–O1A, 1.209(2); C1A–C2A, 1.495(2); N1A–C3A, 1.435(2); N1A–C4A, 1.437(1); C2A–C1A–N1A–C3A, –33.6(2); O1A–C1A–N1A–C4A, –6.4(2); O1A–C1A–N1A–C3A, 146.8(1); C2A–C1A–N1A–C4A, 173.2(1).

**General procedure for amide synthesis.** An oven-dried round-bottomed flask (100 mL) equipped with a stir bar was charged with primary amide (8.26 mmol, 1.0 equiv), 4-dimethylaminopyridine (typically, 0.10 equiv) and dichloromethane (typically, 25 mL),

placed under a positive pressure of argon, and subjected to three evacuation/backfilling cycles under high vacuum. Di-*tert*-butyl dicarbonate (typically, 2.0 equiv) was added portion-wise to the reaction mixture with vigorous stirring at 0 °C, and the reaction mixture was stirred overnight at room temperature. After the indicated time, the reaction mixture was concentrated and unless stated otherwise purified directly by chromatography on silica gel (hexanes/ethyl acetate) to give analytically pure product.

It should be noted that all N,N-Boc<sub>2</sub>-benzamides were prepared by site-selective double N-acylation of the amide bond. This well-established procedure afforded N,N-Boc<sub>2</sub>-amides in average 70-75% yields on gram scale.

**2.3.2a.** Yield 95%. White solid. Mp = 169-170°C. <sup>1</sup>H NMR (500 MHz, CDCl<sub>3</sub>) δ 7.76 (d, *J* = 9.0 Hz, 2 H), 6.64 (d, *J* = 9.0 Hz, 2 H), 3.08 (s, 6 H), 1.38 (s, 18 H). <sup>13</sup>C NMR (125 MHz, CDCl<sub>3</sub>) δ 168.01, 154.01, 150.13, 132.15, 120.44, 110.88, 83.45, 40.17, 27.89.

**2.3.2b.** Yield 40%. White solid. Mp = 71-73 °C. <sup>1</sup>H NMR (500 MHz, CDCl<sub>3</sub>) δ 7.85 (d, *J* = 8.4 Hz, 2 H), 6.97 (d, *J* = 8.5 Hz, 2 H), 3.91 (s, 3 H), 1.40 (s, 18 H). <sup>13</sup>C NMR (125 MHz, CDCl<sub>3</sub>) δ 168.24, 164.03, 149.80, 131.75, 126.38, 114.00, 83.94, 55.58, 27.68.

**2.3.2c.** Yield 85%. White solid. Mp = 58-60 °C. <sup>1</sup>H NMR (500 MHz, CDCl<sub>3</sub>) δ 7.85 (d, *J* = 7.7 Hz, 2 H), 7.61 (t, *J* = 7.4 Hz, 1 H), 7.49 (t, *J* = 7.3 Hz, 2 H), 1.39 (s, 18 H). <sup>13</sup>C NMR (125 MHz, CDCl<sub>3</sub>) δ 149.77, 133.41, 129.09, 128.67, 84.27, 27.59.

**2.3.2d.** Yield 73%. White solid. Mp = 67-68 °C. <sup>1</sup>H NMR (500 MHz, CDCl<sub>3</sub>) δ 7.90-7.85 (m, 2 H), 7.17 (t, *J* = 8.1 Hz, 2 H), 1.41 (s, 18 H). <sup>13</sup>C NMR (125 MHz, CDCl<sub>3</sub>) δ 168.09,

165.89 (d,  $J = 253.8$  Hz), 149.64, 131.76 (d,  $J = 10.0$  Hz), 130.43 (d,  $J = 2.5$  Hz), 115.96 (d,  $J = 22.5$  Hz), 84.43, 27.62.  $^{19}\text{F}$  NMR (471 MHz,  $\text{CDCl}_3$ )  $\delta$  -104.00.

**2.3.2e.** Yield 85 %. White solid. Mp = 72-74 °C.  $^1\text{H}$  NMR (500 MHz,  $\text{CDCl}_3$ )  $\delta$  7.89 (d,  $J = 8.1$  Hz, 2 H), 7.79 (d,  $J = 8.0$  Hz, 2 H), 1.43 (s, 18 H).  $^{13}\text{C}$  NMR (125 MHz,  $\text{CDCl}_3$ )  $\delta$  168.12, 149.43, 138.14, 132.39, 129.12, 117.68, 116.39, 85.18, 27.58.

**2.3.1c.**  $^1\text{H}$  NMR (500 MHz,  $\text{CDCl}_3$ )  $\delta$  8.20-8.14 (m, 2 H), 7.65 (t,  $J = 7.4$  Hz, 1 H), 7.51 (t,  $J = 7.8$  Hz, 2 H).  $^{13}\text{C}$  NMR (125 MHz,  $\text{CDCl}_3$ )  $\delta$  172.47, 133.85, 130.24, 129.33, 128.51.

***tert*-Butyl benzoylcarbamate.**  $^1\text{H}$  NMR (500 MHz,  $\text{CDCl}_3$ )  $\delta$  7.91 (s, 1 H), 7.84-7.76 (m, 2 H), 7.57 (t,  $J = 7.2$  Hz, 1 H), 7.47 (t,  $J = 7.8$  Hz, 2 H), 1.54 (s, 9 H).  $^{13}\text{C}$  NMR (125 MHz,  $\text{CDCl}_3$ )  $\delta$  165.31, 149.64, 133.55, 132.89, 128.94, 127.61, 82.95, 28.17.

**Benzoic acid.**  $^1\text{H}$  NMR (500 MHz,  $\text{CDCl}_3$ )  $\delta$  8.20-8.14 (m, 2 H), 7.65 (t,  $J = 7.4$  Hz, 1 H), 7.51 (t,  $J = 7.8$  Hz, 2 H).  $^{13}\text{C}$  NMR (125 MHz,  $\text{CDCl}_3$ )  $\delta$  172.47, 133.85, 130.24, 129.33, 128.51.

**2.3.3a.**  $^1\text{H}$  NMR (500 MHz,  $\text{CDCl}_3$ )  $\delta$  8.05 (d,  $J = 6.4$  Hz, 2 H), 7.60-7.51 (m, 1 H), 7.48-7.39 (m, 2 H), 3.91 (s, 3 H).  $^{13}\text{C}$  NMR (125 MHz,  $\text{CDCl}_3$ )  $\delta$  166.99, 132.88, 130.15, 129.55, 128.33, 52.03.

**2.3.3b.**  $^1\text{H}$  NMR (500 MHz,  $\text{CDCl}_3$ )  $\delta$  8.01 (s, 1 H), 7.87 (d,  $J = 7.5$  Hz, 2 H), 7.66 (d,  $J = 8.0$  Hz, 2 H), 7.54 (t,  $J = 7.5$  Hz, 1 H), 7.46 (t,  $J = 7.5$  Hz, 2 H), 7.36 (t,  $J = 8.0$  Hz, 2 H),

7.16 (t,  $J = 7.5$  Hz, 1 H).  $^{13}\text{C}$  NMR (125 MHz,  $\text{CDCl}_3$ )  $\delta$  165.98, 138.07, 135.10, 131.92, 129.18, 128.86, 127.17, 124.67, 120.41.

**Triphenylmethanol (2.3.4).**  $^1\text{H}$  NMR (500 MHz,  $\text{CDCl}_3$ )  $\delta$  7.34-7.28 (m, 15 H), 2.81 (s, 1 H).  $^{13}\text{C}$  NMR (125 MHz,  $\text{CDCl}_3$ )  $\delta$  146.98, 128.06, 128.05, 127.39, 82.16.



## References

- (1) Greenberg, A.; Breneman, C. M.; Liebman, J. F., Eds. *The Amide Linkage: Structural Significance in Chemistry, Biochemistry, and Materials Science*; Wiley: New York, 2000.
- (2) Tani, K.; Stoltz, B. M. *Nature* **2006**, *441*, 731.
- (3) Aubé, J. *Angew. Chem., Int. Ed.* **2012**, *51*, 3063.
- (4) Pauling, L. *The Nature of the Chemical Bond*; Oxford University Press: London, 1940.
- (5) (a) Kemnitz, C. R.; Loewen, M. J. *J. Am. Chem. Soc.* **2007**, *129*, 2521. (b) Mujika, J. I.; Mercero, J. M.; Lopez, X. *J. Am. Chem. Soc.* **2005**, *127*, 4445. (c) Mujika, J. I.; Matxain, J. M.; Eriksson, L. A.; Lopez, X. *Chem. Eur. J.* **2006**, *12*, 7215. (d) Mucsi, Z.; Tsai, A.; Szori, M.; Chass, G. A.; Viskolcz, B.; Csizmadia, I. G. *J. Phys. Chem. A* **2007**, *111*, 13245. (e) Mucsi, Z.; Chass, G. A.; Viskolcz, B.; Csizmadia, I. G. *J. Phys. Chem. A* **2008**, *112*, 9153. (f) Glover, S. A.; Rosser, A. A. *J. Org. Chem.* **2012**, *77*, 5492. (g) Morgan, J.; Greenberg, A.; Liebman, J. F. *Struct. Chem.* **2012**, *23*, 197. (h) Morgan, J.; Greenberg, A. *J. Chem. Thermodynamics* **2014**, *73*, 206. (i) Morgan, J. P.; Weaver-Guevara, H. M.; Fitzgerald, R. W.; Dunlap-Smith, A.; Greenberg, A. *Struct. Chem.* **2017**, *28*, 327.
- (6) Somayaji, V.; Brown, R. S. *J. Org. Chem.* **1986**, *51*, 2676.
- (7) Ramachandran, G. N. *Biopolymers* **1968**, *6*, 1494.
- (8) Cox, C.; Lectka, T. *Acc. Chem. Res.* **2000**, *33*, 849.

- (9) (a) Hall, H. K., Jr.; El-Shekeil, A. *Chem. Rev.* **1983**, 83, 549. (b) Yamada, S. *Rev. Heteroat. Chem.* **1999**, 19, 203. (c) Szostak, M.; Aubé, J. *Chem. Rev.* **2013**, 113, 5701. (d) Glover, S. A. *Adv. Phys. Org. Chem.* **2007**, 42, 35.
- (10) (a) Williams, A. *J. Am. Chem. Soc.* **1976**, 98, 5645. (b) Perrin, C. L. *Acc. Chem. Res.* **1989**, 22, 268.
- (11) (a) Liu, J.; Albers, M. W.; Chen, C. M.; Schreiber, S. L.; Walsh, C. T. *Proc. Natl. Acad. Sci. U. S. A.* **1990**, 87, 2304. (b) Fischer, G. *Chem. Soc. Rev.* **2000**, 29, 119. (c) Eakin, C. M.; Berman, A. J.; Miranker, A. D. *Nat. Struct. Mol. Biol.* **2006**, 13, 202.
- (12) (a) Poland, B. W.; Xu, M. Q.; Quioco, F. A. *J. Biol. Chem.* **2000**, 275, 16408. (b) Romanelli, A.; Shekhtman, A.; Cowburn, D.; Muir, T. W. *Proc. Natl. Acad. Sci. U.S.A.* **2004**, 101, 6397. (c) Shemella, P.; Pereira, B.; Zhang, Y. M.; van Roey, P.; Belfort, G.; Garde, S.; Nayak, S. K.; *Biophys. J.* **2007**, 92, 847.
- (13) (a) Lizak, C.; Gerber, S.; Numao, S.; Aebi, M.; Locher, K. P. *Nature* **2011**, 474, 350. (b) Lizak, C.; Gerber, S.; Michaud, G.; Schubert, M.; Fan, Y. Y.; Bucher, M.; Darbare, T.; Aebi, M.; Reymond, J. L.; Locher, K. P. *Nat. Commun.* **2013**, 4, 2627.
- (14) (a) Takise, R.; Muto, K.; Yamaguchi, J. *Chem. Soc. Rev.* **2017**, 46, 5864. (b) Meng, G.; Shi, S.; Szostak, M. *Synlett* **2016**, 27, 2530. (c) Liu, C.; Szostak, M. *Chem. Eur. J.* **2017**, 23, 7157. (d) Dander, J. E.; Garg, N. K. *ACS Catal.* **2017**, 7, 1413.
- (15) (a) *Science of Synthesis: Cross-Coupling and Heck-Type Reactions*, Molander, G. A.; Wolfe, J. P.; Larhed, M., Eds.; Thieme: Stuttgart, 2013. (b) *Metal-Catalyzed Cross-*

*Coupling Reactions and More*, de Meijere, A.; Bräse, S.; Oestreich, M., Eds.; Wiley: New York, 2014.

(16) (a) Ref. 2. (b) Liniger, M.; VanderVelde, D. G.; Takase, M. K.; Shahgholi, M.; Stoltz, B. M. *J. Am. Chem. Soc.* **2016**, *138*, 969. (c) Liniger, M.; Liu, Y.; Stoltz, B. *J. Am. Chem. Soc.* **2017**, *139*, 13944. (d) Kirby, A. J.; Komarov, I. V.; Wothers, P. D.; Feeder, N. *Angew. Chem., Int. Ed.* **1998**, *37*, 785. (e) Komarov, I. V.; Yanik, S.; Ishchenko, A. Y.; Davies, J. E.; Goodman, J. M.; Kirby, A. J. *J. Am. Chem. Soc.* **2015**, *137*, 926. (f) Golden, J.; Aubé, J. *Angew. Chem. Int. Ed.* **2002**, *41*, 4316. (g) Lei, Y.; Wroblewski, A. D.; Golden, J. E.; Powell, D. R.; Aubé, J. *J. Am. Chem. Soc.* **2005**, *127*, 4552. (h) Sliter, B.; Morgan, J.; Greenberg, A. *J. Org. Chem.* **2011**, *76*, 2770 (i) Artacho, J.; Ascic, E.; Rantanen, T.; Karlsson, J.; Wallentin, C. J.; Wang, R.; Wendt, O. F.; Harmata, M.; Snieckus, V.; Wärnmark, K. *Chem. Eur. J.* **2012**, *18*, 1038.

(17) Winkler, F. K.; Dunitz, J. D. *J. Mol. Biol.* **1971**, *59*, 169.

(18) Adachi, S.; Kumagai, N.; Shibasaki, M. *Chem. Sci.* **2017**, *8*, 85.

(19) Hutchby, M.; Houlden, C. E.; Haddow, M. F.; Tyler, S. N.; Lloyd-Jones, G. C.; Booker-Milburn, K. I. *Angew. Chem., Int. Ed.* **2012**, *51*, 548.

(20) (a) Meng, G.; Szostak, M. *Org. Lett.* **2015**, *17*, 4364. (b) Pace, V.; Holzer, W.; Meng, G.; Shi, S.; Lalancette, R.; Szostak, R.; Szostak, M. *Chem. Eur. J.* **2016**, *22*, 14494.

(21) (a) Yamada, S. *Angew. Chem. Int. Ed.* **1993**, *32*, 1083. (b) Yamada, S. *Angew. Chem., Int. Ed.* **1995**, *34*, 1113.

(22) (a) Roughley, S. D.; Jordan, A. M. *J. Med. Chem.* **2011**, *54*, 3451. (b) Pattabiraman, V. R.; Bode, J. W. *Nature* **2011**, *480*, 471. (c) Kaspar, A. A.; Reichert, J. M. *Drug Discov. Today* **2013**, *18*, 807.

(23) (a) Greenberg, A.; Venanzi, C. A. *J. Am. Chem. Soc.* **1993**, *115*, 6951. (b) Greenberg, A.; Moore, D. T.; DuBois, T. D. *J. Am. Chem. Soc.* **1996**, *118*, 8658.

(24) (a) Clayden, J.; Lund, A.; Vallverdu, L.; Helliwell, M. *Nature* **2004**, *431*, 966. (b) Clayden, J. *Chem. Soc. Rev.* **2009**, *38*, 817. (c) Sola, J.; Fletcher, S. P.; Castellanos, A.; Clayden, J. *Angew. Chem. Int. Ed.* **2010**, *49*, 6836. (d) Knipe, P. C.; Thompson, S.; Hamilton, A. D. *Chem. Sci.* **2015**, *6*, 1630. (e) Volz, N.; Clayden, J. *Angew. Chem. Int. Ed.* **2011**, *50*, 12148.

(25) Davidsen, S. K.; May, P. D.; Summers, J. B. *J. Org. Chem.* **1991**, *56*, 5482.

(26) See the Experimental section.

(27) (a) Meng, G.; Shi, S.; Szostak, M. *ACS Catal.* **2016**, *6*, 7335. (b) Shi, S.; Szostak, M. *Org. Lett.* **2016**, *18*, 5872. (c) Meng, G.; Szostak, M. *ACS Catal.* **2017**, *7*, 7251.

(28) (a) Larock, R. C. *Comprehensive Organic Transformations*; Wiley: New York, 1999.

(b) Zabicky, J. *The Chemistry of Amides*; Interscience: New York, 1970.

(29) (a) Szostak, R.; Aubé, J.; Szostak, M. *Chem. Commun.* **2015**, *51*, 6395. (b) Szostak, R.; Shi, S.; Meng, G.; Lalancette, R.; Szostak, M. *J. Org. Chem.* **2016**, *81*, 8091. (c) Szostak, R.; Meng, G.; Szostak, M. *J. Org. Chem.* **2017**, *82*, 6373.

(30) Johansson, K. E.; van de Streek, J. *Cryst. Growth Des.* **2016**, *16*, 1366 .

(31) (a) Szostak, M.; Yao, L.; Aubé, J. *J. Am. Chem. Soc.* **2010**, *132*, 2078. (b) Adler, M.; Adler, S.; Boche, G. *J. Phys. Org. Chem.* **2005**, *18*, 193.

(32) (a) Izzo, P. T.; Safir, S. R. *J. Org. Chem.* **1959**, *24*, 701; (b) Dieter, R. K. *Tetrahedron* **1999**, *55*, 4177. (c) Wang, X. J.; Zhang, L.; Sun, X.; Xu, Y.; Krishnamurthy, D.; Senanayake, C. H. *Org. Lett.* **2005**, *7*, 5593.

(33) (a) Corbett, P. T.; Leclaire, J.; Vial, L.; West, K. R.; Wietor, J. L.; Sanders, J. K. M.; Otto, S. *Chem. Rev.* **2006**, *106*, 3652. (b) See, Refs. 24a-d.

(34) Hu, F.; Lalancette, R.; Szostak, M. *Angew. Chem. Int. Ed.* **2016**, *55*, 5062.

(35) (a) Hegarty, A. F.; McCormack, M. T.; Brady, K.; Ferguson, G.; Roberts, P. J. *J. Chem. Soc., Perkin Trans. 2* **1980**, 867. (b) Brady, K.; Hegarty, A. F. *J. Chem. Soc., Perkin Trans. 2* **1980**, 121. (c) Tailhades, J.; Patil, N. A.; Hossain, M. A.; Wade, J. D. *J. Pept. Sci.* **2015**, *21*, 139.

(36) (a) Gibson, F. S.; Bergmeier, S. C.; Rapoport, H. *J. Org. Chem.* **1994**, *59*, 3216. (b) See, Ref. 16e.

(37) Additional computational studies were conducted. Geometry optimization was performed at the B3LYP/6-311++G(d,p) level. Extensive studies have shown that this level is accurate in predicting properties and resonance energies of amides. This method was further verified by obtaining good correlations between the calculated structures and available X-ray structures in the series.

- (38) (a) Itai, A.; Toriumi, Y.; Saito, S.; Kagechika, H.; Shudo, K. *J. Am. Chem. Soc.* **1992**, *114*, 10649. (b) Forbes, C. C.; Beatty, A. M.; Smith, B. D. *Org. Lett.* **2001**, *3*, 3595. (c) Dugave, C.; Demange, L. *Chem. Rev.* **2003**, *103*, 2475.
- (39) Etter, M. C.; Britton, D.; Reutzel, S. M. *Acta Cryst.* **1991**, *C47*, 556.
- (40) (a) Eliel, E. L.; Wilen, S. H. *Stereochemistry of Organic Compounds*; Wiley: New York, 1994. (b) Gawley, R.; Aubé, J. *Principles of Asymmetric Synthesis*; Elsevier: Oxford, 2012.
- (41) (a) Brameld, K. A.; Kuhn, B.; Reuter, D. C.; Stahl, M. *J. Chem. Inf. Model.* **2008**, *48*, 1. (b) Price, S. L. *Chem. Soc. Rev.* **2014**, *43*, 2098.
- (42) Bailey, T.; Blakemore, P. R.; Cesare, V.; Cha, J. K.; Cook, G. *Science of Synthesis Vol. 21*; Thieme: Stuttgart, 2014.
- (43) IUPAC Gold Book, International Union of Pure and Applied Chemistry. <http://goldbook.iupac.org>, accessed on Dec, 10, 2017.

## Chapter 3

### Decarbonylative Cross-Coupling of Amides

#### 3.1 Pd-catalyzed Heck cross-coupling of amides via N–C cleavage

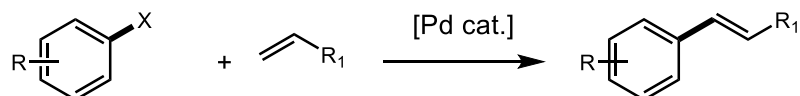
Parts of this section were adapted with permission from the article: “General Olefin Synthesis by the Pd-Catalyzed Heck Reaction of Amides: Sterically-Controlled Chemoselective N–C Activation” (*Angew. Chem. Int. Ed.* **2015**, 127, 14726). Copyright ©2015, Wiley-VCH Verlag GmbH & Co. KGaA, Weinheim.

##### 3.1.1 Research background

The Heck reaction represents one of the most powerful methods for the catalytic construction of C–C bonds under mild conditions.<sup>1,2</sup> As recognized by the 2010 Nobel Prize in chemistry, this method has been widely utilized for the synthesis of small molecules, natural products, polymers and pharmaceuticals on both the laboratory and industrial scale.<sup>3,4</sup> Over the last four decades, a variety of aryl halides,<sup>5a–d</sup> aryl triflates,<sup>5e</sup> aryl phosphates,<sup>5f</sup> aryl diazonium salts,<sup>5g,h</sup> arylsulfonyl halides,<sup>5i</sup> aroyl halides,<sup>5j,k</sup> anhydrides<sup>5l</sup> and esters<sup>5m</sup> have been shown to participate as aryl electrophiles in this reaction.<sup>6</sup> Significant advances in the development of new catalytic systems<sup>7</sup> and mechanistic studies have been reported.<sup>8</sup> However, when we started our study, the use of amides as electrophilic coupling partners in the Heck reaction was unknown.<sup>1–8</sup> We hypothesized that the successful application of bench-stable amide building blocks as olefination precursors could significantly broaden the scope of electrophilic partners for

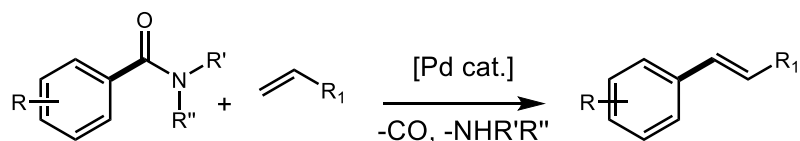
the Heck reaction of carboxylic acid electrophiles and represent an attractive opportunity for the development of new activation modes of inert N–C bonds.<sup>9</sup>

### A. Classic electrophiles in the Heck reaction



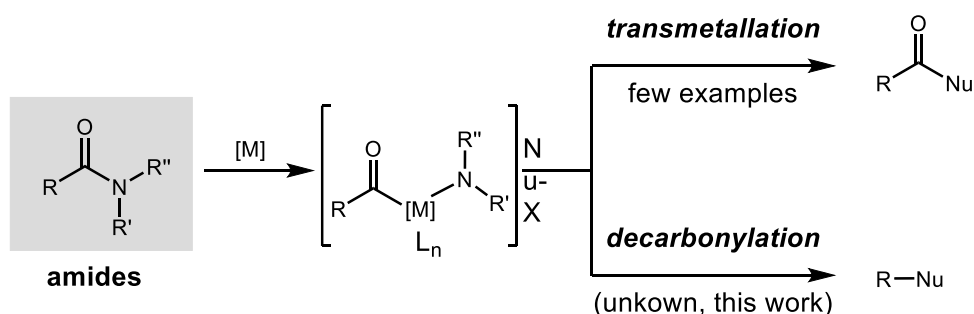
■ X = Hal (I, Br, Cl, F), OTs, N<sub>2</sub>, OTf, COCl, COCOR, CO<sub>2</sub>R

### This work: the Heck reaction of amides



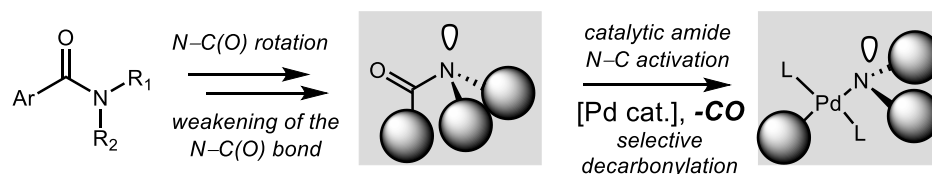
■ no ligand ■ no base ■ wide scope ■ high FG tolerance ■ halide-free

### B. General reaction pathways in metal-catalyzed activation of amides



■ key building blocks ■ bench stable ■ easily available ■ orthogonal selectivity  
 ■ challenge:  $n_N \rightarrow \pi^*_{CO}$  conjugation ■ unexplored potential in metal catalysis

### C. This work: aryl electrophiles from amides via ground-state destabilization



■ re-routing via twisted amide intermediates ■ >95:5 C–N cleavage selectivity  
 ■ twist-controlled selectivity ■ access to aryl-metal intermediates from amides

**Figure 3.1.1.** (a) Electrophiles in the Heck reaction. (b) Transition-metal-catalyzed activation of amides. (c) Our study: the first Heck reaction of amides via ground-state distortion.



Metal-catalyzed reactions of amides proceeding via metal insertion into the N–CO bond are challenging due to  $n_N \rightarrow \pi^*_{C=O}$  stabilization.<sup>10</sup> As outlined in Chapter I, we successfully implemented the use of amide ground-state distortion,<sup>11</sup> a well-recognized property of non-planar amides,<sup>12</sup> to promote metal insertion into the amide N–CO bond under mild and chemoselective conditions.<sup>13</sup> This reactivity delivers the acyl-metal intermediate capable of participating in a myriad of catalytic cross-coupling manifolds by either acyl or decarbonylative pathways.<sup>13,14</sup> Furthermore, our group has recently demonstrated that the N-/O-coordination aptitude in amides could be directly correlated with the additive distortion parameter ( $\Sigma\tau + \chi_N$ ),<sup>15</sup> which allows to rationally design new classes of amides for catalytic cross-coupling methodologies.<sup>16</sup> At the beginning of this project, we hypothesized that the acyl-Pd(II) intermediate<sup>17</sup> formed after Pd(0) insertion into the inert amide N–CO bond could undergo controlled decarbonylation<sup>18</sup> to give the aryl-Pd(II) electrophile, thereby providing access a wide variety of valuable end-products by functionalization and/or elementary reactions.<sup>19</sup>

### 3.1.2 Reaction discovery

This part of Chapter III outlines the discovery of the first Heck reaction of amides proceeding via highly chemoselective N–CO cleavage catalyzed by Pd(0). The following features of this study are notable: (1) We found that the reaction proceeded with an excellent N–CO bond cleavage selectivity (>95:5 in all cases examined).<sup>11c</sup> (2) We demonstrated that the protocol was characterized by a broad substrate scope with respect to amide and alkene coupling partners, showing the highest functional group tolerance of all Heck reactions of aroyl precursors examined.<sup>5j-m</sup> (3) We established that high yields

and coupling selectivity were achieved under base-free and ligand-free conditions, leading to an operationally-simple protocol, reduction of waste and cost of the process.<sup>5</sup> (4) Stoichiometric corrosive halide waste was not formed in the reaction (waste-free Heck), demonstrating new opportunities for industrial olefination processes.<sup>4a</sup> (5) The method constituted the first general method for the synthesis of aryl electrophiles from amides under mild catalytic conditions.<sup>9–14</sup> Perhaps most importantly, this transformation opened up the field of decarbonylative cross-couplings of amides and permitted the direct construction of C–C bonds from amides via N–C activation<sup>20</sup> with potential applications ranging from functionalization of biomolecules (amino acids, peptides, proteins)<sup>2</sup> to industrial olefinations for the production of fine chemicals.<sup>4b</sup>

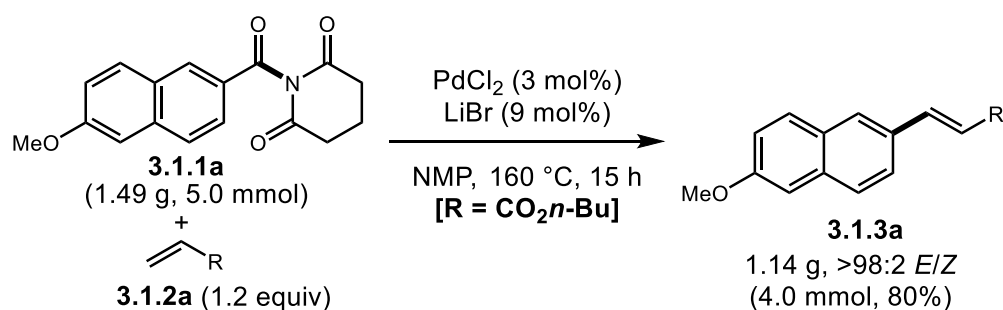
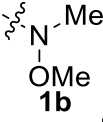


**Figure 3.1.2** Gram scale reaction.

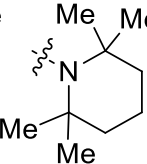
The following gram scale procedure was representative: a mixture of **3.1.1a** (1.49 g, 5 mmol), olefin (0.77 g, 6 mmol), PdCl<sub>2</sub> (26.6 mg, 0.15 mmol) was stirred in the presence of LiBr (39.1 mg, 0.45 mmol) in NMP at 160 °C to afford 1.14 g of **3.1.3a** (80% yield) (Figure 3.1.2).

### 3.1.3 Reaction optimization

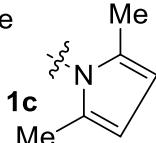
entry	NR'R''	$\tau$ [deg]	$\chi_N$ [deg]	conv. [%]	yield [%]
1	<b>3.1.1b</b>	1.2	16.3	<5	<5
2	<b>3.1.1c</b>	34.1	17.0	<5	<5
3	<b>3.1.1d</b>	39.7	8.4	<5	<5
4	<b>3.1.1e</b>	45.9	10.7	<5	<5
5	<b>3.1.1f</b>	87.8	6.8	>98	95
6	<b>3.1.1g</b>	14.3	69.6	<5	<5
7	<b>3.1.1h</b>	5.1	33.1	<5	<5
8	<b>3.1.1i</b>	5.1	33.1	<5	<5



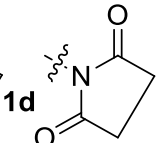
**1b**



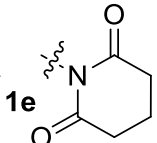
**1c**



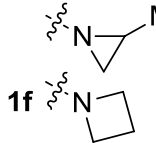
**1d**



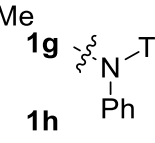
**1e**



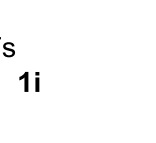
**1f**



**1g**



**1h**



**1i**

**Table 3.1.1** Optimization of twisted amides.

At the outset, we screened a range of electronically- and sterically-distorted amides in the reaction with *n*-butyl acrylate as a coupling partner in the presence of palladium catalytic systems under various conditions (Table 3.1.1). We hypothesized that (1) metal insertion into the N–C bond in amides in which the sum of distortion parameters ( $\Sigma\tau + \chi_N$ ) is close to  $50^\circ$  should be thermodynamically favorable;<sup>15</sup> (2) less coordinating ligands should favor decarbonylation of the acyl-metal intermediate;<sup>18c</sup> (3) the leaving group should regenerate Pd(0),<sup>1,2</sup> thus obviating the need for a stoichiometric amount of external base.

The optimization results in Table 3.1.1 revealed that no reaction or low yields were observed with Weinreb amides (entry 1),<sup>22a</sup> tmp amides (entry 2),<sup>22b</sup> acylpyrroles (entry 3),<sup>22c</sup> and five-membered imide derivatives (entry 4).<sup>22d</sup> We found that by using the six-

membered imide derivative **3.1.1f** (entry 5),<sup>22d</sup> the proposed Heck reaction was indeed feasible delivering the desired olefin in excellent 95% yield (2,1/1,2 >98:2; *E/Z*>98:2). Pyramidalized aziridinyl (entry 6) and azetidiny (entry 7) amides<sup>22e</sup> resulted in no product formation. It is worth noting that N–C bond activation was not observed using electronically-activated amide substrates (entry 8),<sup>14</sup> which presented an early attractive opportunity for chemoselective transformations using complementary amide bond activation modes. Overall, our optimization results in Table 3.1.1 validated the feasibility of the N–C activation/decarbonylation platform of sterically-activated amides for the first time. The results showed that the rate of olefination was proportional to the degree of distortion,<sup>15</sup> which generalized our previous studies on the amide bond activation.<sup>13</sup> Importantly, under these conditions, reductive elimination from the acyl-Pd intermediate was not observed, suggesting that decarbonylation was facile. Tables 3.1.2-3.1.5 present selected results obtained during optimization of the reaction conditions. Most importantly, palladium chloride was identified as the most active precatalyst. NMP was found to be the optimum solvent. In line with our mechanistic proposal, phosphane ligands and base were not required for the efficient coupling. Catalytic halide salts<sup>7a</sup> had small but beneficial effect on the reaction selectivity, consistent with ligand displacement on palladium prior to the reduction elimination during the catalytic cycle.<sup>8a</sup> Optimization of the temperature revealed that catalytic turnover of Pd ensued at lower temperatures, but the process was less efficient. Other products resulting from the acyl-Pd(II) intermediate were not detected in the reaction. As for related cross-couplings,<sup>5j-m</sup> we found that the addition to styrene was not completely regioselective; however, the observed selectivity compared very favorably with other reported olefinations.<sup>1,2</sup> Notably, olefin over-addition

products were not detected in the reaction, consistent with the highly chemoselective process.

entry	Pd source	additive	ligand	conversion (%)	selectivity (%)
1	Pd(OAc) <sub>2</sub>	-	-	13	73.3:26.7
2	Pd <sub>2</sub> (dba) <sub>3</sub>	-	-	<5	-
3	PdCl <sub>2</sub>	-	-	>98	87.0:13.0
4	PdBr <sub>2</sub>	-	-	>98	89.8:10.2
5	PdI <sub>2</sub>	-	-	>98	79.4:20.6
6	Pd(OAc) <sub>2</sub>	LiBr	-	76	90.7:9.3
7	Pd <sub>2</sub> (dba) <sub>3</sub>	LiBr	-	25	87.5:12.5
8	Pd(PPh <sub>3</sub> ) <sub>4</sub>	LiBr	-	>98	68.8:31.2
9	PdCl <sub>2</sub> (PPh <sub>3</sub> ) <sub>2</sub>	LiBr	-	72	73.3:26.7
10	PdCl <sub>2</sub>	KCl	-	>98	88.7:11.3
11	PdCl <sub>2</sub>	KBr	-	>98	87.6:12.4
12	PdCl <sub>2</sub>	NaCl	-	>98	88.5:11.5
13	PdCl <sub>2</sub>	NaBr	-	>98	86.1:13.9
14	PdCl <sub>2</sub>	LiBr	-	>98	93.8:6.2
15	PdCl <sub>2</sub>	LiCl	-	>98	90.1:9.9
16	PdCl <sub>2</sub>	TEAC	-	70	89.2:10.8
17	-	LiBr	-	<5	-
18	-	-	-	<5	-

**Table 3.1.2** General optimization studies.

entry	Pd source	additive	ligand	conversion (%)	Selectivity (%)
1	PdCl <sub>2</sub>	-	PPh <sub>3</sub>	10	-
2	PdCl <sub>2</sub>	LiBr	PPh <sub>3</sub>	>98	91.6:8.4
3	PdCl <sub>2</sub>	LiBr	DPPP	<5	-
4	PdCl <sub>2</sub>	LiBr	DPPF	94	79.6:20.4
5	PdCl <sub>2</sub>	LiBr	P <sup>n</sup> Bu <sub>3</sub>	<5	-
6	PdCl <sub>2</sub>	LiBr	P <sup>n</sup> Bu <sub>3</sub>	<5	-
7	PdCl <sub>2</sub>	LiBr	P(4-MeOPh) <sub>3</sub>	<5	-
8	PdCl <sub>2</sub>	LiBr	H <sub>3</sub> BO <sub>3</sub>	<5	-
9	PdCl <sub>2</sub>	LiBr	Quinoline	>98	87.3:12.7
10	PdCl <sub>2</sub>	LiBr	Isoquinoline	>98	86.2:13.8

**Table 3.1.3** Optimization of ligands.

entry	solvents	conversion (%)	selectivity (%)
1	NMP	>98	93.8:6.2
2	DMF	<5	-
3	DMSO	<5	-
4	Toluene	32	68.5:31.5
5	Dioxane	97	88.4:11.6
6	DCE	25	83.0:17.0
7	DMA	<5	-

**Table 3.1.4** Optimization of solvents.

entry	temperature (°C)	conversion (%)	selectivity (%)
1	160	>98	93.8:6.2
2	120	80	90.0:10.0
3	80	<5	-

**Table 3.1.5** Optimization of temperature.

### 3.1.4 Substrate scope

With the optimized conditions in hand, we next explored the scope of the reaction using styrene as a standard olefin (Figure 3.1.3). The reaction exhibited excellent chemoselectivity profile, tolerating a wide range of functional groups. The observed coupling selectivity was good to excellent in all cases examined. In all cases, single olefin isomers were obtained ( $E/Z$ >98:2). Electron-donating (**3.1.3d**, **3.1.3e**) and electron-withdrawing (**3.1.3f-3.1.3h**) substituents were well-tolerated. Amides containing sensitive functional groups at the para position of the aromatic ring such as cyano (**3.1.3g**), nitro

(**3.1.3h**), fluoro (**3.1.3i**), chloro (**3.1.3j**), and bromo (**3.1.3k**) were all successfully coupled in high yields, providing synthetic handles for further functionalization. Steric hindrance in the ortho-position was well-tolerated (**3.1.3m**). Naphthyl (**3.1.3n**) and heteroaromatic amides (**3.1.3o**) underwent olefination in high yields. Remarkably, the reaction was fully chemoselective for the C–N bond activation in the presence of other typically more reactive carboxylic acid derivatives such as esters (**3.1.3p**), ketones (**3.1.3q**) and aldehydes (**3.1.3r**); these moieties were poised for further functional group manipulation. The chemoselective coupling of amides illustrated the synthetic potential of the amide bond activation platform via distortion.<sup>12</sup> This decarbonylative Heck reaction could be readily extended to the  $\alpha,\beta$ -unsaturated amide substrate to yield the diene product with excellent selectivity ( $E/Z > 98:2$ ) (**3.1.3s**).

We found that the scope of olefin coupling partners was also very broad (Table 3.1.6). Electron-rich and electron-deficient olefins provided the products in high yields and with excellent regioselectivity.<sup>23</sup> Acrylic esters (entry 2-3), amides (entry 4) and nitriles (entry 5) were well-tolerated.<sup>23a</sup> Terminal olefins could be used as substrates (entry 6);<sup>23b</sup> in these cases, olefin isomerization resulted in a mixture of isomers, in agreement with previous studies.<sup>51</sup> Cyclooctane, the only cyclic olefin examined, gave isomeric arylcyclooctenes (entry 7).<sup>51</sup> Notably, sterically-demanding *n*-butyl methacrylate and  $\alpha$ -methylstyrene were arylated in high yields (entry 8-9);<sup>23c</sup> in these examples, double bond isomerization constituted a minor reaction pathway. Finally, the synthetically valuable *E*-stilbenes were also accessible in high yields by using trimethylvinylsilane as an ethylene equivalent (entry 10).<sup>23d</sup> Formation of styrenes was not observed under these conditions.

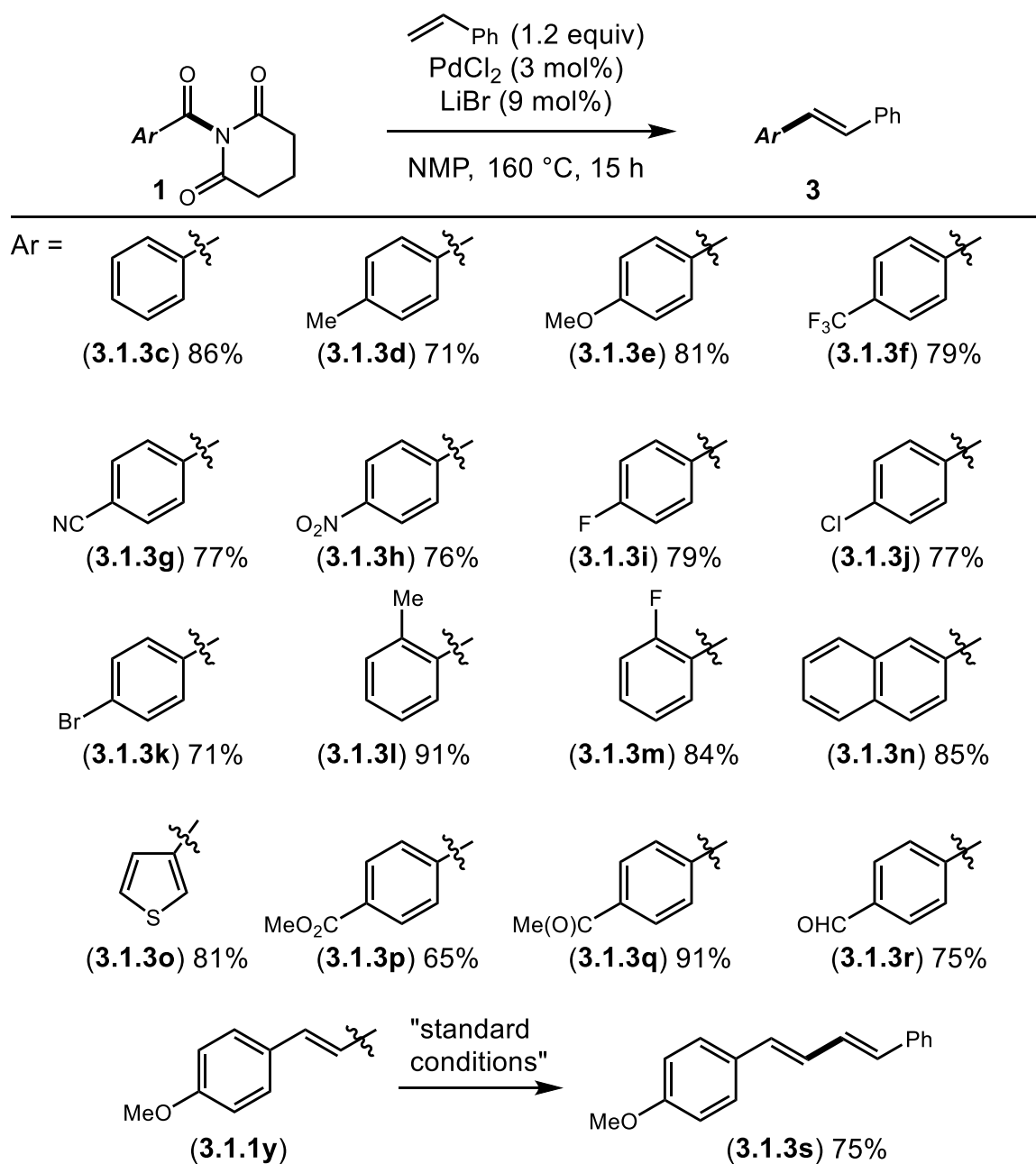


Figure 3.1.3 Scope of amides.



entry	3.1.1	2	olefin	yield [%]	selectivity
1	3.1.1f	3.1.2b		86	15:1
2	3.1.1f	3.1.2c		84	>20:1
3	3.1.1f	3.1.2a		81	>20:1
4	3.1.1f	3.1.2d		86	>20:1
5	3.1.1f	3.1.2e		93	13:1
6	3.1.1f	3.1.2f		85	_[c]
7	3.1.1f	3.1.2g		94	4:1
8	3.1.1f	3.1.2h		80	13:1
9	3.1.1f	3.1.2i		89	10:1
10	3.1.1f	3.1.2j		91	9:1

Table 3.1.6 Scope of olefins.

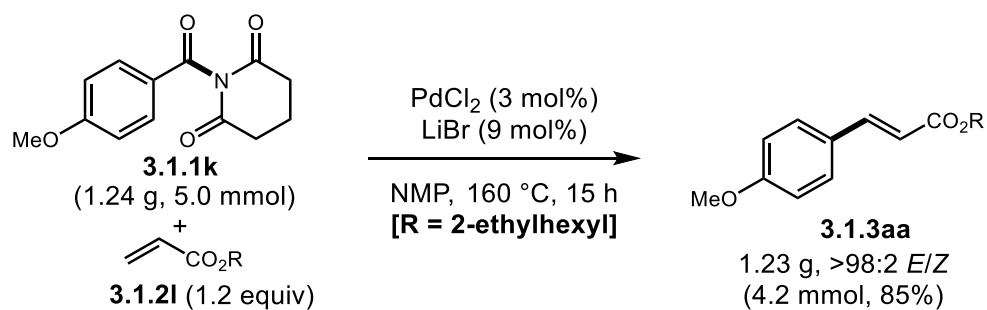
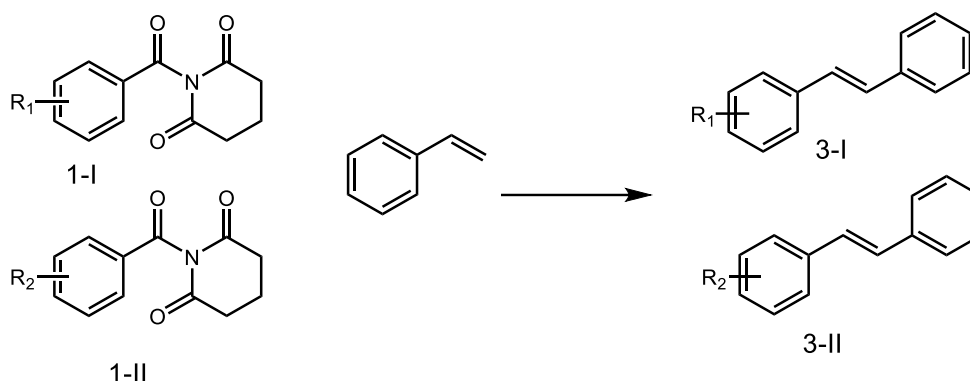


Figure 3.1.4 Large scale application.

### 3.1.5 Mechanistic studies

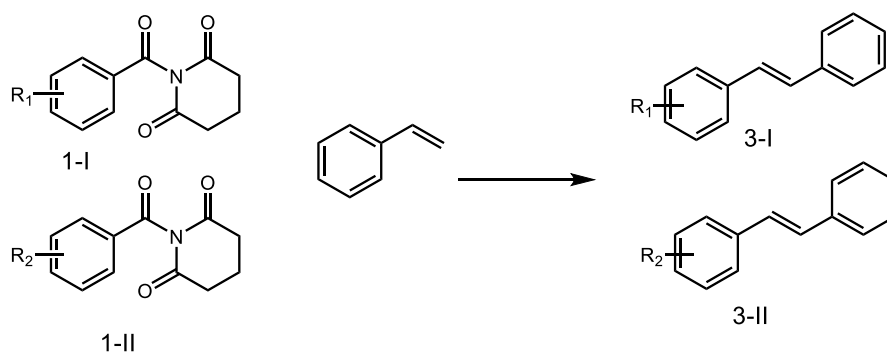


entry	<b>1-I</b> ( $R_1$ )	<b>1-II</b> ( $R_2$ )	amide (equiv)	<b>3-I:3-II</b> ( $R_1$ : $R_2$ )
1	CF <sub>3</sub> -	MeO-	2.0	81:19
2	NC-	MeO-	2.0	77:23

**Table 3.1.7** Selectivity studies – amides: electronics.

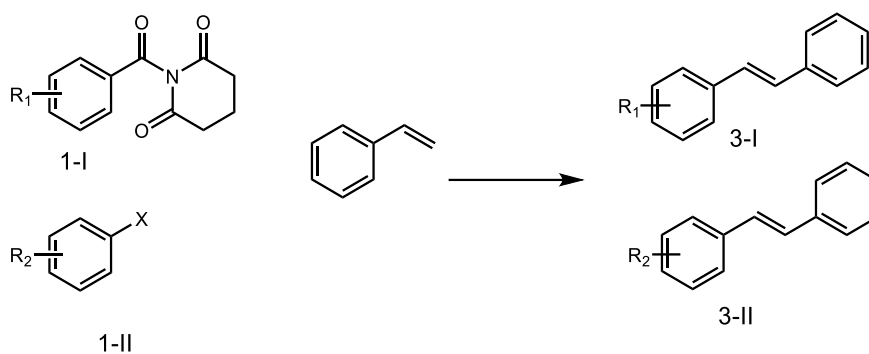
Previous studies on the Heck reaction of aryl anhydrides demonstrated that the reaction involved a cationic palladium complex with decarbonylation as the rate limiting step.<sup>24</sup> The presence of halide accelerated the reaction and increased the selectivity by acid to halide exchange. Thus, we conducted several studies to gain insight into the mechanism of the Heck reaction of amides (Table 3.1.7-3.1.11). In particular we conducted the following experiments: (1) Intermolecular competition experiments with differently substituted amides revealed that electron-deficient arenes were intrinsically more reactive substrates, consistent with an anionic intermediate in the oxidative addition.<sup>25</sup> (2) Competition experiments with sterically-demanding ortho aryl substrates revealed that steric effects played an important role in accelerating the reaction.<sup>18c</sup> (3) Intermolecular

competition experiments with different olefins ( $\text{H}_2\text{C}=\text{CHR}$ ) established the following order of reactivity:  $\text{CO}_2n\text{-Bu} > \text{Ph} > n\text{-C}_8\text{H}_{17}$ , which followed the reactivity in Heck reactions of aryl halides.<sup>1,2</sup> (4) Competition experiments established the following reactivity order:  $\text{Ar-I} > \text{Ar-C(O)NR}_2 \gg \text{Ph-Br}$ . Moreover, we established the following reactivity order of carboxylic acid electrophiles:  $\text{Ar-C(O)NR}_2 \approx (\text{Ar-CO})_2\text{O} \gg \text{Ar-CO}_2\text{R}$ . (5) Electrospray ionization mass spectrometry (ESI/MS) analysis using stoichiometric palladium was performed.<sup>26</sup> Intermediates corresponding to the aryl- $\text{Pd}^{\text{II}}$  species containing halide and amine ligands were detected, consistent with the proposed mechanism. (6) The role of halide was probed by kinetic studies using styrene and acrylate nucleophiles.<sup>5k</sup> The effect of halide salt on the cross-coupling rate was found to be negligible in both classes of olefins, consistent with amine coordination to the metal throughout the catalytic cycle.



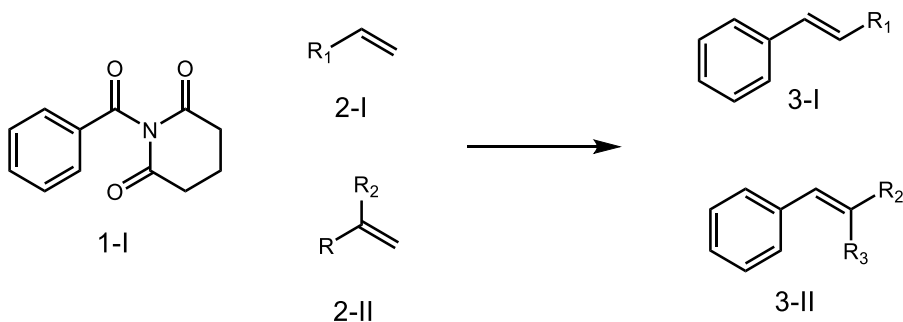
Entry	<b>1-I</b> ( $\text{R}_1$ )	<b>1-II</b> ( $\text{R}_2$ )	Amide (equiv)	<b>3-I:3-II</b> ( $\text{R}_1:\text{R}_2$ )
1	2-Me-	4-Me-	2.0	85:15
2	2-F-	4-F-	2.0	81:19

**Table 3.1.8** Selectivity studies – sterics.



entry	<b>1-I</b> (R <sub>1</sub> )	<b>1-II</b> (R <sub>2</sub> )	X	<b>3-I:3-II</b> (R <sub>1</sub> :R <sub>2</sub> )
1	Me-	H-	Br-	>99:1
2	Me-	H-	I-	7:93

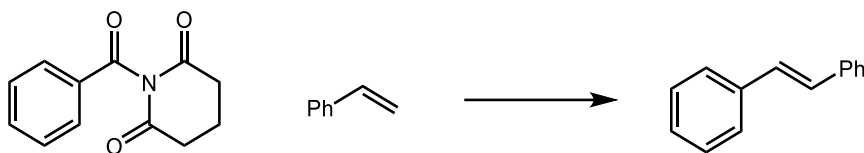
**Table 3.1.9** Additional selectivity studies.



entry	<b>2-I</b> (R <sub>1</sub> )	<b>2-II</b> (R <sub>2</sub> , R <sub>3</sub> )	Olefin (equiv)	<b>3-I:3-II</b> (R <sub>1</sub> :R <sub>2</sub> )
1	<i>n</i> -BuO <sub>2</sub> C-	<i>n</i> -C <sub>8</sub> H <sub>17</sub> -	2.0	80:20
2	<i>n</i> -BuO <sub>2</sub> C-	Ph-	2.0	77:23
3	<i>n</i> -BuO <sub>2</sub> C-	<i>n</i> -BuO <sub>2</sub> C(Me)-	2.0	67:33

**Table 3.1.10** Selectivity studies – olefins.

We concluded that the mechanistic studies were consistent with amide activation by ground-state distortion. It was particularly noteworthy that activation of the inert N–C bond took place in the absence of electron-rich ligands on metal. Decarbonylation of the acyl-Pd intermediate was favored by coordination of the sterically-demanding anionic amine ligand. Reductive elimination appeared to be a kinetically relevant step in the reaction.



entry	Pd(OAc) <sub>2</sub> (mol%)	conv. (%)
1	3.0	>98
2	0.25	>98
3	0.1	71

**Table 3.1.11** Determination of TON.

### 3.1.6 Conclusion

In conclusion, this part of Chapter III described the development of the first Heck reaction of amides via chemoselective N–C bond activation using amide ground-state destabilization. The reaction demonstrated a broad substrate scope and an excellent functional group tolerance. Remarkably, metal insertion into the amide bond and catalytic turnover were achieved without any added ligands and bases (waste-free Heck). This first

example of a decarbonylative cross-coupling of amides set the stage for the design of new catalytic reactions via metal insertion/decarbonylation using amides as aryl electrophiles.

### 3.1.7 Experimental section

**General procedure for the Heck reaction of amides.** An oven-dried vial equipped with a stir bar was charged with an amide substrate (1.0 equiv), olefin (1.2 equiv), PdCl<sub>2</sub> (typically, 0.03 equiv), and LiBr (typically, 0.09equiv), placed under a positive pressure of argon, and subjected to three evacuation/backfilling cycles under high vacuum. N-Methyl-2-pyrrolidone (NMP, typically, 0.8 mL) was added with vigorous stirring at room temperature, the reaction mixture was placed in a preheated oil bath at 160 °C, and stirred for the indicated time at 160 °C. After the indicated time, the reaction mixture was cooled down to room temperature and diluted with CH<sub>2</sub>Cl<sub>2</sub> (5 mL). The sample was analyzed by <sup>1</sup>H NMR and/or GC-MS to obtain conversion, selectivity and yield using internal standard and comparison with authentic samples. In all examples reported 2,1/1,2-selectivity was obtained by analysis of the crude reaction mixture. Unless indicated otherwise, in all examples reported single olefin isomers were observed (*E/Z*>98:2). Unless indicated otherwise, only mono-arylated products were observed (mono-/diarylation selectivity >98:2). All yields reported refer to isolated yields after purification by chromatography on silica gel. Unless indicated otherwise, in all examples reported single olefin regioisomers were obtained after the purification.

**3.1.3a.** Yield 80%. Colorless oil. <sup>1</sup>H NMR (500 MHz, CDCl<sub>3</sub>) δ 7.88 (s, 1 H), 7.84 (d, *J* = 15.9 Hz, 1 H), 7.76 (dd, *J* = 15.0, 8.7 Hz, 2 H), 7.66 (d, *J* = 8.7 Hz, 1 H), 7.19 (d, *J* =

8.9Hz, 1 H), 7.15 (d,  $J = 2.5$  Hz, 1 H), 6.53 (d,  $J = 16.0$ Hz, 1 H), 4.26 (t,  $J = 6.7$  Hz, 2 H), 3.96 (d,  $J = 2.2$  Hz, 3 H), 1.80-1.70 (m, 2 H), 1.57-1.43 (m, 2 H), 1.01 (t,  $J = 8.5$ Hz, 3 H).  $^{13}\text{C}$  NMR (125 MHz,  $\text{CDCl}_3$ )  $\delta$  167.33, 158.80, 144.78, 135.66, 130.10, 129.88, 129.68, 128.69, 127.46, 124.22, 119.45, 117.29, 105.98, 64.38, 55.38, 30.85, 19.25, 13.79.

**3.1.1a.** White solid.  $^1\text{H}$  NMR (500 MHz,  $\text{CDCl}_3$ )  $\delta$  8.29 (d,  $J = 2.7$  Hz, 1 H), 7.91(d,  $J = 8.5$  Hz, 1 H), 7.85 (d,  $J = 8.8$  Hz, 1 H), 7.81 (d,  $J = 8.7$ Hz, 1 H), 7.23 (d,  $J = 8.7$  Hz, 1 H), 7.18 (d,  $J = 2.7$  Hz, 1 H), 3.98 (t,  $J = 2.4$  Hz, 3 H), 2.85 (tt,  $J = 6.4, 2.5$  Hz, 4 H), 2.22 (qt,  $J = 6.7, 3.7$  Hz, 2 H).  $^{13}\text{C}$  NMR (125 MHz,  $\text{CDCl}_3$ )  $\delta$  171.98, 170.57, 160.60, 138.39, 132.53, 131.45, 127.81, 127.04, 125.64, 120.17, 105.97, 105.81, 55.50, 32.52, 17.59.

**3.1.1b.** Colorless oil.  $^1\text{H}$  NMR (500 MHz,  $\text{CDCl}_3$ )  $\delta$  7.68 (dt,  $J = 7.0, 1.5$  Hz, 2 H), 7.45-7.43 (m, 1 H), 7.42-7.37 (m, 2 H), 3.55 (s, 3 H), 3.36 (s, 3 H).  $^{13}\text{C}$  NMR (125 MHz,  $\text{CDCl}_3$ )  $\delta$  169.94, 134.09, 130.55, 128.10, 128.00, 61.01, 33.79.

**3.1.1c.** White solid.  $^1\text{H}$  NMR (500 MHz,  $\text{CDCl}_3$ )  $\delta$  7.49-7.42 (m, 2 H), 7.37 (qd,  $J = 8.6, 7.5, 4.3$  Hz, 3 H), 1.81 (s, 6 H), 1.39 (s, 6 H), 1.38 (s, 6 H).  $^{13}\text{C}$  NMR (125 MHz,  $\text{CDCl}_3$ )  $\delta$  176.74, 143.30, 129.33, 127.81, 127.74, 56.51, 37.02, 30.57, 14.95.

**3.1.1d.** Colorless oil.  $^1\text{H}$  NMR (500 MHz,  $\text{CDCl}_3$ )  $\delta$  7.78-7.67 (m, 2 H), 7.66-7.59 (m, 1 H), 7.50 (t,  $J = 7.9$  Hz, 2 H), 5.90 (s, 2 H), 2.10 (s, 3 H), 2.09 (s, 3 H).  $^{13}\text{C}$  NMR (125 MHz,  $\text{CDCl}_3$ )  $\delta$  171.18, 135.68, 133.18, 130.34, 130.12, 128.67, 110.14, 99.98, 14.69.

**3.1.1e.** White solid.  $^1\text{H}$  NMR (500 MHz,  $\text{CDCl}_3$ )  $\delta$  7.88 (d,  $J = 7.2$  Hz, 2 H), 7.69 (t,  $J = 7.5$  Hz, 1 H), 7.53 (t,  $J = 7.8$  Hz, 2 H), 2.96 (s, 4H).  $^{13}\text{C}$  NMR (125 MHz,  $\text{CDCl}_3$ )  $\delta$  174.54, 167.62, 135.15, 131.40, 130.53, 128.97, 29.08.

**3.1.1f.** White solid.  $^1\text{H}$  NMR (500 MHz,  $\text{CDCl}_3$ )  $\delta$  7.89 (d,  $J = 7.8$  Hz, 2 H), 7.67 (t,  $J = 7.5$  Hz, 1 H), 7.52 (t,  $J = 7.7$  Hz, 2 H), 2.80 (t,  $J = 6.6$  Hz, 4 H), 2.17 (q,  $J = 6.5$  Hz, 2 H).  $^{13}\text{C}$  NMR (125 MHz,  $\text{CDCl}_3$ )  $\delta$  171.90, 170.74, 134.97, 131.78, 130.16, 129.14, 32.41, 17.51.

**3.1.1g.** Colorless oil.  $^1\text{H}$  NMR (500 MHz,  $\text{CDCl}_3$ )  $\delta$  8.08-8.02 (m, 2 H), 7.57 (td,  $J = 7.2$ , 1.5 Hz, 1 H), 7.48 (t,  $J = 7.8$  Hz, 2 H), 2.66-2.54 (m, 2 H), 2.17 (d,  $J = 3.6$  Hz, 1 H), 1.42 (d,  $J = 5.4$  Hz, 3 H).  $^{13}\text{C}$  NMR (125 MHz,  $\text{CDCl}_3$ )  $\delta$  179.30, 133.54, 132.62, 129.05, 128.40, 34.61, 32.14, 17.79.

**3.1.1h.** Colorless oil.  $^1\text{H}$  NMR (500 MHz,  $\text{CDCl}_3$ )  $\delta$  7.68-7.57 (m, 2 H), 7.51-7.35 (m, 3H), 4.26 (dt,  $J = 15.0$ , 7.8 Hz, 4 H), 2.41-2.25 (m, 2 H).  $^{13}\text{C}$  NMR (125 MHz,  $\text{CDCl}_3$ )  $\delta$  170.24, 133.26, 130.82, 128.31, 127.78, 30.92.

**3.1.1j.** White solid.  $^1\text{H}$  NMR (500 MHz,  $\text{CDCl}_3$ )  $\delta$  7.78 (d,  $J = 8.0$  Hz, 2 H), 7.331 (d,  $J = 8.0$  Hz, 2 H), 2.79 (t,  $J = 6.6$  Hz, 4 H), 2.45 (s, 3 H), 2.16 (p,  $J = 6.6$  Hz, 2 H).  $^{13}\text{C}$  NMR (125 MHz,  $\text{CDCl}_3$ )  $\delta$  171.87, 170.39, 146.32, 130.32, 129.87, 129.24, 32.42, 21.89, 17.52.

**3.1.1k.** White solid.  $^1\text{H}$  NMR (500 MHz,  $\text{CDCl}_3$ )  $\delta$  7.87-7.82 (d,  $J = 7.5$  Hz, 2 H), 6.99-6.94 (d,  $J = 7.5$  Hz, 2 H), 3.90 (s, 3H), 2.78 (t,  $J = 6.6$  Hz, 4 H), 2.15 (p,  $J = 6.6$  Hz, 2 H).  $^{13}\text{C}$  NMR (125 MHz,  $\text{CDCl}_3$ )  $\delta$  171.88, 169.48, 165.09, 132.75, 124.51, 114.49, 55.69, 32.45, 17.52.

**3.1.1l.** White solid.  $^1\text{H}$  NMR (500 MHz,  $\text{CDCl}_3$ )  $\delta$  8.00 (d,  $J = 8.1$  Hz, 2 H), 7.79 (d,  $J = 8.0$  Hz, 2 H), 2.83 (t,  $J = 6.5$  Hz, 4 H), 2.20 (q,  $J = 6.6$  Hz, 2 H).  $^{13}\text{C}$  NMR (125 MHz,



$\text{CDCl}_3$ )  $\delta$  171.97, 170.17, 135.93(q,  $J^2 = 36.7$  Hz), 134.80, 130.36, 126.21(q,  $J^3 = 3.5$  Hz), 123.27(q,  $J^1 = 272.4$  Hz).  $^{19}\text{F}$  (471 MHz,  $\text{CDCl}_3$ )  $\delta$  -63.4.

**3.1.1m.** White solid.  $^1\text{H}$  NMR (500 MHz,  $\text{CDCl}_3$ )  $\delta$  7.97 (d,  $J = 8.5$  Hz, 2 H), 7.82 (d,  $J = 8.5$  Hz, 2 H), 2.82 (t,  $J = 6.5$  Hz, 4 H), 2.20 (p,  $J = 6.6$  Hz, 2 H).  $^{13}\text{C}$  NMR (125 MHz,  $\text{CDCl}_3$ )  $\delta$  171.89, 169.88, 135.23, 132.86, 130.30, 117.97, 117.48, 32.38, 17.43.

**3.1.1n.** Yellow solid.  $^1\text{H}$  NMR (500 MHz,  $\text{CDCl}_3$ )  $\delta$  8.36 (d,  $J = 7.5$  Hz, 2 H), 8.04 (d,  $J = 7.5$  Hz, 2 H), 2.84 (t,  $J = 6.5$  Hz, 4 H), 2.21 (p,  $J = 6.6$  Hz, 2 H).  $^{13}\text{C}$  NMR (125 MHz,  $\text{CDCl}_3$ )  $\delta$  171.91, 169.70, 151.20, 136.73, 131.00, 124.25, 32.39, 17.42.

**3.1.1o.** White solid.  $^1\text{H}$  NMR (500 MHz,  $\text{CDCl}_3$ )  $\delta$  7.91 (dd,  $J = 8.5, 5.2$  Hz, 2 H), 7.18 (t,  $J = 8.4$  Hz, 2 H), 2.79 (t,  $J = 6.5$  Hz, 4 H), 2.15 (p,  $J = 6.5$  Hz, 2 H).  $^{13}\text{C}$  NMR (125 MHz,  $\text{CDCl}_3$ )  $\delta$  171.94, 169.59, 166.84(d,  $J^1 = 258.4$  Hz), 133.01(d,  $J^3 = 10.2$  Hz), 128.30(d,  $J^4 = 2.7$  Hz), 116.52(d,  $J^2 = 22.1$  Hz), 32.37, 17.46.  $^{19}\text{F}$  (471 MHz,  $\text{CDCl}_3$ )  $\delta$  -101.31.

**3.1.1p.** White solid.  $^1\text{H}$  NMR (500 MHz,  $\text{CDCl}_3$ )  $\delta$  7.81 (d,  $J = 8.5$  Hz, 2 H), 7.48 (d,  $J = 8.5$  Hz, 2 H), 2.80 (t,  $J = 6.5$  Hz, 4 H), 2.17 (p,  $J = 6.6$  Hz, 2 H).  $^{13}\text{C}$  NMR (125 MHz,  $\text{CDCl}_3$ )  $\delta$  171.91, 169.89, 141.68, 131.44, 130.31, 129.55, 32.40, 17.47.

**3.1.1q.** White solid.  $^1\text{H}$  NMR (500 MHz,  $\text{CDCl}_3$ )  $\delta$  7.74 (d,  $J = 8.6$  Hz, 2 H), 7.67 (d,  $J = 8.6$  Hz, 2 H), 2.80 (t,  $J = 6.5$  Hz, 4 H), 2.18 (m, 2 H).  $^{13}\text{C}$  NMR (125 MHz,  $\text{CDCl}_3$ )  $\delta$  171.85, 170.14, 132.55, 131.45, 130.76, 130.51, 32.39, 17.47.

**3.1.1r.** White solid.  $^1\text{H}$  NMR (500 MHz,  $\text{CDCl}_3$ )  $\delta$  7.54-7.46 (m, 2 H), 7.35 (d,  $J = 7.6$  Hz, 1H), 7.29-7.25 (m, 1 H), 2.77 (t,  $J = 6.6$  Hz, 4 H), 2.70 (s, 3 H), 2.14 (p,  $J = 6.6$  Hz,

2 H).  $^{13}\text{C}$  NMR (125 MHz,  $\text{CDCl}_3$ )  $\delta$  171.98, 170.66, 142.53, 133.75, 132.44, 131.19, 130.70, 126.19, 32.48, 21.89, 17.45.

**3.1.1s.** White solid.  $^1\text{H}$  NMR (500 MHz,  $\text{CDCl}_3$ )  $\delta$  8.11 (td,  $J = 7.8, 1.8$  Hz, 1 H), 7.63 (dddd,  $J = 8.3, 7.1, 5.0, 1.8$  Hz, 1 H), 7.36-7.30 (m, 1 H), 7.13 (ddd,  $J = 12.0, 8.4, 1.1$  Hz, 1 H), 2.76 (t,  $J = 6.5$  Hz, 4 H), 2.13 (p,  $J = 6.6$  Hz, 2 H).  $^{13}\text{C}$  NMR (125 MHz,  $\text{CDCl}_3$ )  $\delta$  171.68, 166.86, 161.79 (d,  $J^1 = 255.9$  Hz), 136.79 (d,  $J^3 = 10.0$  Hz), 132.95, 125.09 (d,  $J^4 = 3.6$  Hz), 120.36 (d,  $J^3 = 7.0$  Hz), 117.08 (d,  $J^2 = 23.6$  Hz), 32.41, 17.24.  $^{19}\text{F}$  NMR (471 MHz,  $\text{CDCl}_3$ )  $\delta$  -113.49.

**3.1.1t.** White solid.  $^1\text{H}$  NMR (500 MHz,  $\text{CDCl}_3$ )  $\delta$  8.37 (s, 1 H), 7.99-7.93 (m, 3 H), 7.91 (d,  $J = 8.2$  Hz, 1 H), 7.66 (ddd,  $J = 8.2, 6.8, 1.3$  Hz, 1 H), 7.59 (ddd,  $J = 8.1, 6.9, 1.3$  Hz, 1 H), 2.85 (t,  $J = 6.5$  Hz, 4 H), 2.22 (p,  $J = 6.6$  Hz, 2 H).  $^{13}\text{C}$  NMR (125 MHz,  $\text{CDCl}_3$ )  $\delta$  172.02, 170.89, 136.42, 132.65, 132.45, 129.83, 129.51, 129.20, 127.91, 127.17, 124.75, 32.50, 17.57.

**3.1.1u.** White solid.  $^1\text{H}$  NMR (500 MHz,  $\text{CDCl}_3$ )  $\delta$  8.08 (d,  $J = 2.8$  Hz, 1 H), 7.50 (d,  $J = 5.2$  Hz, 1 H), 7.39 (dd,  $J = 5.3, 2.9$  Hz, 1 H), 2.79 (t,  $J = 6.6$  Hz, 4 H), 2.15 (p,  $J = 6.6$  Hz, 2 H).  $^{13}\text{C}$  NMR (125 MHz,  $\text{CDCl}_3$ )  $\delta$  171.73, 164.49, 136.54, 136.39, 127.77, 127.43, 32.43, 17.50.

**3.1.1v.** White solid.  $^1\text{H}$  NMR (500 MHz,  $\text{CDCl}_3$ )  $\delta$  8.16 (d,  $J = 8.5$  Hz, 2 H), 7.94 (d,  $J = 8.2$  Hz, 2 H), 3.98 (s, 3H), 2.81 (t,  $J = 6.5$  Hz, 4 H), 2.18 (q,  $J = 6.5$  Hz, 2 H).  $^{13}\text{C}$  NMR (125 MHz,  $\text{CDCl}_3$ )  $\delta$  171.90, 170.38, 165.75, 135.42, 130.21, 129.95, 129.58, 52.64, 32.40, 17.47.

**3.1.1w.** White solid.  $^1\text{H}$  NMR (500 MHz,  $\text{CDCl}_3$ )  $\delta$  8.17-8.02 (d,  $J = 8.2$  Hz, 2H), 7.97 (d,  $J = 8.2$  Hz, 2H), 2.82 (t,  $J = 6.5$  Hz, 4H), 2.67 (s, 3H), 2.19 (q,  $J = 6.5$  Hz, 2H).  $^{13}\text{C}$  NMR (125 MHz  $\text{CDCl}_3$ )  $\delta$  197.01, 171.88, 170.33, 141.40, 135.14, 130.27, 128.83, 32.40, 26.95, 17.47.

**3.1.1x.** White solid.  $^1\text{H}$  NMR (500 MHz,  $\text{CDCl}_3$ )  $\delta$  10.13 (s, 1 H), 8.10-7.97 (m, 4 H), 2.82 (t,  $J = 6.5$  Hz, 4 H), 2.19 (q,  $J = 6.6$  Hz, 2 H).  $^{13}\text{C}$  NMR (125 MHz  $\text{CDCl}_3$ )  $\delta$  191.12, 171.92, 170.36, 140.13, 136.25, 130.55, 130.06, 32.40, 17.45.

**3.1.1y.** White solid.  $^1\text{H}$  NMR (500 MHz,  $\text{CDCl}_3$ )  $\delta$  7.65 (d,  $J = 15.8$  Hz, 1 H), 7.53 (d,  $J = 8.4$  Hz, 2 H), 6.93 (d,  $J = 8.3$  Hz, 2 H), 6.58 (d,  $J = 15.7$  Hz, 1 H), 3.88 (s, 3 H), 2.76 (t,  $J = 6.6$  Hz, 4 H), 2.10 (m, 2 H).  $^{13}\text{C}$  NMR (500 MHz,  $\text{CDCl}_3$ )  $\delta$  171.74, 169.26, 162.52, 148.54, 130.93, 126.35, 118.76, 114.51, 55.47, 32.54, 17.40.

**3.1.3b.** Colorless oil. 2,1/1,2 >98:2.  $E/Z$  >98:2.  $^1\text{H}$  NMR (500 MHz,  $\text{CDCl}_3$ )  $\delta$  7.71 (d,  $J = 16.0$  Hz, 1 H), 7.55 (dd,  $J = 6.7, 2.9$  Hz, 2 H), 7.41 (m, 3 H), 6.47 (d,  $J = 16.0$  Hz, 1 H), 4.24 (t,  $J = 6.7$  Hz, 2 H), 1.80-1.66 (m, 2 H), 1.47 (m, 2 H), 0.99 (t,  $J = 7.4$  Hz, 3 H).  $^{13}\text{C}$  NMR (125 MHz,  $\text{CDCl}_3$ )  $\delta$  167.11, 144.55, 134.49, 130.21, 128.87, 128.05, 118.31, 64.45, 30.79, 19.22, 13.77.

**3.1.3c.** White solid. 2,1/1,2 = 93.8:6.2.  $E/Z$  >98:2.  $^1\text{H}$  NMR (500 MHz,  $\text{CDCl}_3$ )  $\delta$  7.56 (dd,  $J = 7.8, 3.2$  Hz, 4 H), 7.40 (td,  $J = 7.6, 3.1$  Hz, 4 H), 7.33-7.27 (m, 2 H), 7.15 (d,  $J = 3.2$  Hz, 2 H).  $^{13}\text{C}$  NMR (125 MHz,  $\text{CDCl}_3$ )  $\delta$  137.36, 128.72, 128.68, 127.62, 126.52.

**3.1.3d.** White solid. 2,1/1,2 = 87:13.  $E/Z$  >98:2.  $^1\text{H}$  NMR (500 MHz,  $\text{CDCl}_3$ )  $\delta$  7.55 (d,  $J = 7.7$  Hz, 2 H), 7.46 (d,  $J = 7.9$  Hz, 2 H), 7.39 (t,  $J = 7.5$  Hz, 2 H), 7.31-7.26 (m, 1 H),

7.22 (d,  $J = 7.9$  Hz, 2 H), 7.12 (d,  $J = 3.8$  Hz, 2 H), 2.40 (s, 3 H).  $^{13}\text{C}$  NMR (125 MHz,  $\text{CDCl}_3$ )  $\delta$  137.54, 137.54, 134.56, 129.4, 128.67, 128.64, 127.71, 127.42, 126.44, 126.41, 21.29.

**3.1.3e.** White solid. 2,1/1,2 = 83:17.  $E/Z > 98:2$ .  $^1\text{H}$  NMR (500 MHz,  $\text{CDCl}_3$ )  $\delta$  7.52 (d,  $J = 7.7$  Hz, 2 H), 7.49 (d,  $J = 8.2$  Hz, 2 H), 7.38 (t,  $J = 7.6$  Hz, 2 H), 7.26 (t,  $J = 7.3$  Hz, 1 H), 7.10 (d,  $J = 16.3$  Hz, 1 H), 7.01 (d,  $J = 16.3$  Hz, 1 H), 6.94 (d,  $J = 8.2$  Hz, 2 H), 3.86 (s, 3H).  $^{13}\text{C}$  NMR (125 MHz,  $\text{CDCl}_3$ )  $\delta$  159.33, 137.67, 130.18, 128.64, 128.23, 127.71, 127.21, 126.65, 126.25, 114.15, 55.34.

**3.1.3f.** White solid. 2,1/1,2 = 94:6.  $E/Z > 98:2$ .  $^1\text{H}$  NMR (500 MHz,  $\text{CDCl}_3$ )  $\delta$  7.64 (s, 4 H), 7.57 (d,  $J = 7.6$  Hz, 2 H), 7.41 (t,  $J = 7.6$  Hz, 2 H), 7.33 (t,  $J = 7.5$  Hz, 1 H), 7.23 (d,  $J = 16.3$  Hz, 1 H), 7.15 (d,  $J = 16.3$  Hz, 1 H).  $^{13}\text{C}$  NMR (125 MHz,  $\text{CDCl}_3$ )  $\delta$  140.81, 136.64, 131.21, 129.40, 128.97 (q,  $J^2 = 32.1$  Hz), 128.30, 127.13, 126.78, 126.58, 125.63 (q,  $J^3 = 3.7$  Hz), 124.20 (q,  $J^1 = 270.0$  Hz).  $^{19}\text{F}$  NMR (471 MHz,  $\text{CDCl}_3$ )  $\delta$  -62.5.

**3.1.3g.** White solid. 2,1/1,2 = 95.5:4.5.  $E/Z > 98:2$ .  $^1\text{H}$  NMR (500 MHz,  $\text{CDCl}_3$ )  $\delta$  7.69-7.64 (m, 2 H), 7.64-7.59 (m, 2 H), 7.57 (d,  $J = 7.7$  Hz, 2 H), 7.42 (td,  $J = 7.6, 2.6$  Hz, 2 H), 7.36 (t,  $J = 7.0$  Hz, 1 H), 7.25 (d,  $J = 16.2$ , 1 H), 7.12 (d,  $J = 16.2$ , 1 H).  $^{13}\text{C}$  NMR (125 MHz,  $\text{CDCl}_3$ )  $\delta$  141.85, 136.30, 132.51, 132.42, 128.88, 128.66, 126.93, 126.88, 126.74, 119.05, 110.60.

**3.1.3h.** Orange solid. 2,1/1,2 = 87.2:12.8.  $E/Z > 98:2$ .  $^1\text{H}$  NMR (500 MHz,  $\text{CDCl}_3$ )  $\delta$  8.25 (d,  $J = 10.0$  Hz, 2 H), 7.66 (d,  $J = 10.0$  Hz, 2 H), 7.59 (d,  $J = 10.0$  Hz, 2 H), 7.43 (t,  $J = 7.5$  Hz, 2 H), 7.37 (dd,  $J = 8.3, 6.4$  Hz, 1 H), 7.30 (d,  $J = 14.7$  Hz, 1 H), 7.17 (d,  $J = 16.3$  Hz,

1 H).  $^{13}\text{C}$  NMR (125 MHz,  $\text{CDCl}_3$ )  $\delta$  146.78, 143.86, 136.19, 133.32, 128.92, 128.87, 127.04, 126.88, 126.30, 124.17.

**3.1.3i.** White solid. 2,1/1,2 = 89:11. *E/Z*>98:2.  $^1\text{H}$  NMR (500 MHz,  $\text{CDCl}_3$ )  $\delta$  7.57-7.49 (m, 4 H), 7.40 (t,  $J = 7.5$  Hz, 2 H), 7.30 (d,  $J = 14.6$  Hz, 1 H), 7.14-7.02 (m, 4 H).  $^{13}\text{C}$  NMR (125 MHz,  $\text{CDCl}_3$ )  $\delta$  162.35 (d,  $J^I = 245.5$  Hz), 137.18, 128.73, 128.52, 128.50, 127.99 (d,  $J^3 = 8.0$  Hz), 127.69, 127.49, 126.46, 115.64 (d,  $J^2 = 21.6$  Hz).  $^{19}\text{F}$  NMR (471 MHz,  $\text{CDCl}_3$ )  $\delta$  -114.24.

**3.1.3j.** White solid. 2,1/1,2 = 91.4:8.6. *E/Z*>98:2.  $^1\text{H}$  NMR (500 MHz,  $\text{CDCl}_3$ )  $\delta$  7.54 (d,  $J = 8.5$  Hz, 2 H), 7.47 (d,  $J = 8.5$  Hz, 2 H), 7.40 (t,  $J = 7.5$  Hz, 2 H), 7.36 (d,  $J = 8.6$  Hz, 2 H), 7.30 (t,  $J = 9.0$  Hz, 1 H), 7.10 (d,  $J = 4.3$  Hz, 2 H).  $^{13}\text{C}$  NMR (125 MHz,  $\text{CDCl}_3$ )  $\delta$  137.00, 135.87, 133.19, 129.34, 128.85, 128.74, 127.88, 127.67, 127.38, 126.56.

**3.1.3k.** White solid. 2,1/1,2 = 85.6:14.4. *E/Z*>98:2.  $^1\text{H}$  NMR (500 MHz,  $\text{CDCl}_3$ )  $\delta$  7.58-7.48 (m, 4 H), 7.45-7.37 (m, 4 H), 7.31 (t,  $J = 7.5$  Hz, 1 H), 7.13 (d,  $J = 16.5$  Hz, 1 H), 7.06 (d,  $J = 16.3$  Hz, 1 H).  $^{13}\text{C}$  NMR (125 MHz,  $\text{CDCl}_3$ )  $\delta$  136.97, 136.30, 131.79, 129.45, 128.75, 127.98, 127.91, 127.42, 126.57, 121.32.

**3.1.3l.** White solid. 2,1/1,2 = 92:8. *E/Z*>98:2.  $^1\text{H}$  NMR (500 MHz,  $\text{CDCl}_3$ )  $\delta$  7.66 (d,  $J = 7.5$  Hz, 1 H), 7.59 (d,  $J = 7.7$  Hz, 2 H), 7.46-7.37 (m, 3 H), 7.33 (t,  $J = 7.2$  Hz, 1 H), 7.28-7.20 (m, 3 H), 7.06 (d,  $J = 16.2$  Hz, 1 H), 2.50 (s, 3 H).  $^{13}\text{C}$  NMR (125 MHz,  $\text{CDCl}_3$ )  $\delta$  137.72, 136.44, 135.85, 130.44, 130.05, 128.73, 127.64, 127.60, 126.61, 126.59, 126.25, 125.41, 19.98.

**3.1.3m.** White solid. 2,1/1,2 = 92:8. *E/Z*>98:2.  $^1\text{H}$  NMR (500 MHz,  $\text{CDCl}_3$ )  $\delta$  7.65 (t,  $J$  = 7.5 Hz, 1 H), 7.58 (d,  $J$  = 7.2 Hz, 2 H), 7.41 (dd,  $J$  = 9.2, 5.6 Hz, 2 H), 7.36-7.30 (m, 2 H), 7.26 (dd,  $J$  = 19.3, 5.2 Hz, 2 H), 7.22-7.17 (m, 1 H), 7.12 (dt,  $J$  = 14.4, 5.9 Hz, 1 H).  $^{13}\text{C}$  NMR (125 MHz,  $\text{CDCl}_3$ )  $\delta$  160.46 (d,  $J^1$  = 248.0 Hz), 137.25, 130.92 (d,  $J^3$  = 5.0 Hz), 128.80 (d,  $J^3$  = 8.8 Hz), 128.73, 127.95, 127.05 (d,  $J^4$  = 3.8 Hz), 126.69, 125.23 (d,  $J^2$  = 11.3 Hz), 124.21 (d,  $J^4$  = 3.8 Hz), 120.93 (d,  $J^4$  = 3.8 Hz), 115.84 (d,  $J^2$  = 22.1 Hz).  $^{19}\text{F}$  NMR (471 MHz,  $\text{CDCl}_3$ )  $\delta$  -117.94.

**3.1.3n.** White solid. 2,1/1,2 = 87.2:12.8. *E/Z*>98:2.  $^1\text{H}$  NMR (500 MHz,  $\text{CDCl}_3$ )  $\delta$  7.93-7.84 (m, 4 H), 7.80 (d,  $J$  = 8.4 Hz, 1 H), 7.62 (d,  $J$  = 7.7 Hz, 2 H), 7.55-7.48 (m, 2 H), 7.44 (t,  $J$  = 7.6 Hz, 2 H), 7.36-7.26 (m, 3 H).  $^{13}\text{C}$  NMR (125 MHz,  $\text{CDCl}_3$ )  $\delta$  137.39, 134.86, 133.75, 133.08, 129.06, 128.81, 128.77, 128.35, 128.04, 127.74, 127.72, 126.68, 126.59, 126.38, 125.94, 123.55.

**3.1.3o.** White solid. 2,1/1,2 = 95.4:4.6. *E/Z*>98:2.  $^1\text{H}$  NMR (500 MHz,  $\text{CDCl}_3$ )  $\delta$  7.51 (d,  $J$  = 7.6 Hz, 2 H), 7.41-7.33 (m, 4 H), 7.33-7.28 (m, 2 H), 7.16 (d,  $J$  = 16.2 Hz, 1 H), 6.99 (d,  $J$  = 16.3 Hz, 1 H).  $^{13}\text{C}$  NMR (125 MHz,  $\text{CDCl}_3$ )  $\delta$  140.12, 137.37, 131.73, 128.67, 127.46, 126.28, 126.20, 124.92, 122.89, 122.36.

**3.1.3p.** White solid. 2,1/1,2 = 84.1:15.9. *E/Z*>98:2.  $^1\text{H}$  NMR (500 MHz,  $\text{CDCl}_3$ )  $\delta$  8.06 (d,  $J$  = 8.5 Hz, 2 H), 7.60 (d,  $J$  = 8.5 Hz, 2 H), 7.57 (d,  $J$  = 10.0 Hz, 2 H), 7.41 (t,  $J$  = 10.0 Hz, 2 H), 7.33 (t,  $J$  = 6.9 Hz, 1 H), 7.25 (d,  $J$  = 16.5 Hz, 1 H), 7.16 (d,  $J$  = 16.2 Hz, 1 H), 3.96 (s, 3 H).  $^{13}\text{C}$  NMR (125 MHz,  $\text{CDCl}_3$ )  $\delta$  166.89, 141.84, 136.76, 131.25, 130.04, 128.92, 128.79, 128.25, 127.58, 126.79, 126.32, 52.09.

**3.1.3q.** White solid. 2,1/1,2 = 91.1:8.9. *E/Z* > 98:2.  $^1\text{H}$  NMR (500 MHz,  $\text{CDCl}_3$ )  $\delta$  7.99 (dd,  $J = 8.3, 3.7$  Hz, 2 H), 7.62 (d,  $J = 9.0$  Hz, 2 H), 7.58 (d,  $J = 8.5$  Hz, 2 H), 7.42 (dt,  $J = 11.0, 5.1$  Hz, 2 H), 7.34 (m, 1 H), 7.26 (d,  $J = 16.9$  Hz, 1 H), 7.17 (d,  $J = 16.4$  Hz, 1 H), 2.64 (s, 3 H).  $^{13}\text{C}$  NMR (125 MHz,  $\text{CDCl}_3$ )  $\delta$  197.47, 142.03, 136.71, 135.98, 131.48, 128.89, 128.81, 128.33, 127.46, 126.83, 126.51, 26.60.

**3.1.3r.** White solid. 2,1/1,2 = 87.0:13.0. *E/Z* > 98:2.  $^1\text{H}$  NMR (500 MHz,  $\text{CDCl}_3$ )  $\delta$  10.03 (d,  $J = 8.5$  Hz, 1 H), 7.91 (t,  $J = 8.3$  Hz, 2 H), 7.70 (t,  $J = 8.3$  Hz, 2 H), 7.59 (t,  $J = 8.3$  Hz, 2 H), 7.43 (q,  $J = 7.7$  Hz, 2 H), 7.38-7.29 (m, 2 H), 7.21-7.15 (m, 1 H).  $^{13}\text{C}$  NMR (125 MHz,  $\text{CDCl}_3$ )  $\delta$  191.61, 143.44, 136.56, 135.35, 132.22, 130.25, 128.84, 128.51, 127.35, 126.91, 126.91.

**3.1.3s.** White solid. 2,1/1,2 > 98:2. *E/Z* > 98:2.  $^1\text{H}$  NMR (500 MHz,  $\text{CDCl}_3$ )  $\delta$  7.46 (d,  $J = 7.5$  Hz, 2 H), 7.41 (d,  $J = 8.0$  Hz, 2 H), 7.35 (t,  $J = 7.5$  Hz, 2 H), 7.24 (t,  $J = 7.3$  Hz, 1 H), 7.01-6.82 (m, 4 H), 6.66 (d,  $J = 15.4$  Hz, 2 H), 3.85 (s, 3 H).  $^{13}\text{C}$  NMR (125 MHz,  $\text{CDCl}_3$ )  $\delta$  159.30, 137.58, 132.45, 131.68, 130.23, 129.53, 128.63, 127.63, 127.32, 127.29, 126.26, 114.16, 55.33.

**3.1.3t.** Colorless oil. 2,1/1,2 > 98:2. *E/Z* > 98:2.  $^1\text{H}$  NMR (500 MHz,  $\text{CDCl}_3$ )  $\delta$  7.73 (d,  $J = 16.0$  Hz, 1 H), 7.60-7.53 (d,  $J = 7.0$  Hz, 2 H), 7.47-7.37 (m, 3 H), 6.47 (d,  $J = 16.0$  Hz, 1 H), 3.84 (s, 3 H).  $^{13}\text{C}$  NMR (125 MHz,  $\text{CDCl}_3$ )  $\delta$  167.44, 144.88, 134.40, 130.30, 128.90, 128.08, 117.82, 51.72.

**3.1.3u.** Colorless oil. 2,1/1,2 > 98:2. *E/Z* > 98:2.  $^1\text{H}$  NMR (500 MHz,  $\text{CDCl}_3$ )  $\delta$  7.59 (d,  $J = 15.6$  Hz, 1 H), 7.49 (d,  $J = 8.0$  Hz, 2 H), 7.42-7.31 (m, 3 H), 6.38 (d,  $J = 15.5$  Hz, 1 H),

5.62 (s, 1 H), 1.45 (s, 9 H).  $^{13}\text{C}$  NMR (125 MHz,  $\text{CDCl}_3$ )  $\delta$  165.21, 140.19, 135.02, 129.43, 128.75, 127.70, 122.05, 51.50, 28.89.

**3.1.3v.** Colorless oil. 2,1/1,2 = 93.0:7.0.  $E/Z > 98:2$ .  $^1\text{H}$  NMR (500 MHz,  $\text{CDCl}_3$ )  $\delta$  7.45 (m, 6 H), 5.92 (d,  $J = 16.6$  Hz, 1 H).  $^{13}\text{C}$  NMR (125 MHz,  $\text{CDCl}_3$ )  $\delta$  150.60, 133.55, 131.23, 129.14, 127.37, 118.15, 96.38.

**3.1.3w.** Colorless oil. Selectivity = 100 : 40.87 : 7.64 : 4.70. Data for the major isomer.  $^1\text{H}$  NMR (500 MHz,  $\text{CDCl}_3$ )  $\delta$  7.33-7.26 (m, 3 H), 7.21 (d,  $J = 7.5$  Hz, 2 H), 2.63 (t,  $J = 8.0$  Hz, 1 H), 1.71-1.51 (m, 3 H), 1.42-1.18 (m, 14 H), 0.91 (t,  $J = 7.0$  Hz, 3 H).  $^{13}\text{C}$  NMR (125 MHz,  $\text{CDCl}_3$ )  $\delta$  142.97, 128.39, 128.20, 125.53, 36.00, 31.91, 31.53, 29.63, 29.60, 29.53, 29.36, 29.34, 22.69, 14.12.

**3.1.3x.** Colorless oil. Selectivity = 10.95 : 2.95. Data for the major isomer.  $^1\text{H}$  NMR (500 MHz,  $\text{CDCl}_3$ )  $\delta$  7.45 (d,  $J = 7.0$  Hz, 2 H), 7.34 (t,  $J = 7.5$  Hz, 2 H), 7.24 (t,  $J = 7.5$  Hz, 1 H), 6.05 (t,  $J = 8.5$  Hz, 1 H), 2.67 (t,  $J = 6.5$  Hz, 2 H), 2.36-2.31 (m, 2 H), 1.63-1.57 (m, 8 H).  $^{13}\text{C}$  NMR (125 MHz,  $\text{CDCl}_3$ )  $\delta$  143.22, 140.25, 128.19, 127.97, 126.41, 125.78, 29.99, 29.46, 28.48, 27.42, 26.93, 26.17.

**3.1.3y.** Colorless oil. Selectivity = 92.6 : 7.4.  $E/Z > 98:2$ .  $^1\text{H}$  NMR (500 MHz,  $\text{CDCl}_3$ )  $\delta$  7.72 (s, 1 H), 7.42 (m, 4 H), 7.35 (m, 1 H), 4.25 (t,  $J = 6.7$  Hz, 2 H), 2.15 (d,  $J = 1.7$  Hz, 3 H), 1.76-1.70 (m, 2 H), 1.57-1.41 (m, 2 H), 1.08-0.93 (t,  $J = 8.4$  Hz, 3 H).  $^{13}\text{C}$  NMR (125 MHz,  $\text{CDCl}_3$ )  $\delta$  168.77, 138.63, 135.99, 129.63, 128.70, 128.35, 128.23, 64.81, 30.80, 19.31, 14.07, 13.79.



**3.1.3z.** Colorless oil. Selectivity = 91.1 : 8.9. The minor isomers could not be separated by silica gel chromatography. Data for the major isomer.  $^1\text{H}$  NMR (500 MHz,  $\text{CDCl}_3$ )  $\delta$  7.57 (d,  $J = 7.6$  Hz, 2 H), 7.41 (m, 6 H), 7.32 (m, 2 H), 6.88 (s, 1 H), 2.33 (s, 3 H).  $^{13}\text{C}$  NMR (125 MHz,  $\text{CDCl}_3$ )  $\delta$  143.99, 138.37, 137.44, 129.16, 128.34, 128.18, 127.72, 127.19, 126.48, 126.02, 17.50.

**3.1.3aa.** Colorless oil.  $^1\text{H}$  NMR (500 MHz,  $\text{CDCl}_3$ )  $\delta$  7.66 (d,  $J = 15.9$  Hz, 1 H), 7.50 (d,  $J = 8.4$  Hz, 2 H), 6.92 (d,  $J = 8.2$  Hz, 2 H), 6.34 (d,  $J = 15.9$  Hz, 1 H), 4.13 (m, 2 H), 3.85 (s, 3 H), 1.63 (m, 1 H), 1.45 (m, 2 H), 1.26 (m, 6 H), 0.94 (m, 6 H).  $^{13}\text{C}$  NMR (125 MHz,  $\text{CDCl}_3$ )  $\delta$  167.53, 161.33, 144.14, 129.69, 127.24, 115.85, 114.30, 66.83, 55.35, 38.92, 30.51, 28.99, 23.89, 23.01, 14.07, 11.05.

## References

- (1) (a) Heck, R. F.; Nolley, J. P., *J. Org. Chem.* **1972**, *37*, 2320. (b) Mizoroki, T.; Mori, K.; Ozaki, A. *Bull. Chem. Soc. Jpn.* **1971**, *44*, 581.
- (2) (a) Heck, R. F.; *Org. React.* **1982**, *27*, 345. (b) Heck, R. F. *Comprehensive Organic Synthesis*, Trost, B. M.; Pergamon, E. D. **1991**, Vol. 4, Chapter 4.3. (c) Meijere, D. E.; Meyer, F. E. *Angew. Chem. Int. Ed.* **1994**, *33*, 2379. (d) Beletskaya, I. P.; Cheprakov, A. V. *Chem. Rev.* **2000**, *100*, 3009. (e) Oestreich, M. *The Mizoroki-Heck Reaction*, Wiley, **2009**. (f) McCartney, D.; Guiry, P. J. *Chem. Soc. Rev.* **2011**, *40*, 5122. (g) Ruan, J.; Xiao, J. *Acc. Chem. Res.* **2011**, *44*, 614.
- (3) Dounay, A. B.; Overman, L. E. *Chem. Rev.* **2003**, *103*, 2945.
- (4) (a) Vries, J. D. *Can. J. Chem.* **2001**, *79*, 1086. (b) Beller, M.; Blaser, H. U. *Top. Organomet. Chem.* **2012**, *42*, 1. (c) Magano, J.; Dunetz, J. R. *Chem. Rev.* **2011**, *111*, 2177.
- (5) (a) Herrmann, W. A.; Brossmer, C.; Öfele, K.; Reisinger, C. P.; Priermeier, T.; Beller, M.; Fischer, H. *Angew. Chem. Int. Ed.* **1995**, *34*, 1844. (b) Reetz, M. T.; Lohmer, G.; Schwickardi, R. *Angew. Chem. Int. Ed.* **1998**, *37*, 481. (c) Shaughnessy, K. H.; Kim, P.; Hartwig, J. F. *J. Am. Chem. Soc.* **1999**, *121*, 2123. (d) Littke, A. F.; Fu, G. C. *J. Am. Chem. Soc.* **2001**, *123*, 6989. (e) Cacchi, S. *Pure & Appl. Chem.* **1996**, *68*, 45. (f) Ebran, J. P.; Hansen, A. L.; Gøgsig, T. M.; Skrydstrup, T. *J. Am. Chem. Soc.* **2007**, *129*, 6931. (g) Kikukawa, K.; Matsuda, T. *Chem. Lett.* **1977**, 159. (h) Taylor, J. G.; Moro, A. V.; Correia, C. R. D. *Eur. J. Org. Chem.* **2011**, 1403. (i) Miura, M. Hashimoto, H.; Itoh, K.; Nomura, M. *J. Chem. Soc., Perkin Trans.* **1990**, 2207. (j) Blaser, H. U.; Spencer, A. *J. Organomet.*

*Chem.* **1982**, 233, 267. (k) Sugihara, T.; Satoh, T.; Miura, M.; Nomura, M. *Angew. Chem. Int. Ed.* **2003**, 42, 4672. (l) Stephan, M. S.; Teunissen, A. J. J. M.; Verzijl, G. K. M.; de Vries, J. G. *Angew. Chem. Int. Ed.* **1998**, 37, 662. (m) Gooßen, L. J.; Paetzold, J. *Angew. Chem. Int. Ed.* **2002**, 41, 1237.

(6) (a) Myers, A. G.; Tanaka, D.; Mannion, M. R. *J. Am. Chem. Soc.* **2002**, 124, 11250. (b) Dams, M.; De Vos, D. E.; Celen, S.; Jacobs, P. A. *Angew. Chem. Int. Ed.* **2003**, 42, 3512. (c) Inoue, A.; Shinokubo, H.; Oshima, K. *J. Am. Chem. Soc.* **2003**, 125, 1484.

(7) (a) Jeffrey, T. *Tetrahedron* **1996**, 52, 10113. (b) Whitcombe, N. J.; Hii, K. K.; Gibson, S. E. *Tetrahedron* **2001**, 57, 7449. (c) Littke, A. F.; Fu, G. C. *Angew. Chem. Int. Ed.* **2002**, 41, 4176. (d) Zapf, A.; Beller, M. *Chem. Commun.* **2005**, 431. (e) Delcamp, J. H.; Brucks, A. P.; White, M. C. *J. Am. Chem. Soc.* **2008**, 130, 11270. (f) Matsubara, R.; Gutierrez, A. C.; Jamison, T. F. *J. Am. Chem. Soc.* **2011**, 133, 19020. (g) Werner, E. W.; Mei, T. S.; Burckle, A. J.; Sigman, M. S. *Science* **2012**, 338, 1455.

(8) (a) Crisp, G. T. *Chem. Soc. Rev.* **1998**, 27, 427. (b) Amatore, C.; Jutand, A. *Acc. Chem. Res.* **2000**, 33, 314. (c) de Vries, J. G. *Dalton Trans.* **2006**, 421. (d) Phan, N. T. S.; Van Der Sluys, M.; Jones, C. W. *Adv. Synth. Catal.* **2006**, 348, 609. (e) Carrow, B. P.; Hartwig, J. F. *J. Am. Chem. Soc.* **2010**, 132, 79.

(9) Greenberg, A.; Breneman, C. M.; Liebman, J. F. *The Amide Linkage: Structural Significance in Chemistry, Biochemistry, and Materials Science*, Wiley, **2000**.

(10) Pauling, L. *The Nature of the Chemical Bond*, Cornell University Press, **1939**.

(11) (a) Kirby, A. J.; Komarov, I. V.; Wothers, P. D.; Feeder, N. *Angew. Chem. Int. Ed.* **1998**, *37*, 785. (b) Tani, K.; Stoltz, B. M. *Nature* **2006**, *441*, 731. (c) Lei, Y.; Wroblewski, A. D.; Golden, J. E.; Powell, D. R.; Aubé, J. *J. Am. Chem. Soc.* **2005**, *127*, 4552. (d) Cox, C.; Lectka, T. *Acc. Chem. Res.* **2000**, *33*, 849.

(12) Szostak, M.; Aubé, J. *Chem. Rev.* **2013**, *113*, 5701.

(13) Meng, G.; Szostak, M. *Org. Lett.* **2015**, *17*, 4364.

(14) (a) Li, X.; Zou, G. *Chem. Commun.* **2015**, *51*, 5089. (b) Hie, L.; Nathel, N. F. F.; Shah, T. K.; Baker, E. L.; Hong, X.; Yang, Y. F.; Liu, P.; Houk, K. N.; Garg, N. K. *Nature* **2015**, *524*, 79.

(15) (a) Szostak, R.; Aubé, J.; Szostak, M. *Chem. Commun.* **2015**, *51*, 6395. (b) Szostak, R.; Aubé, J.; Szostak, M. *J. Org. Chem.* **2015**, *80*, 7905.

(16) (a) Greenberg, A.; Venanzi, C. A. *J. Am. Chem. Soc.* **1993**, *115*, 6951. (b) Greenberg, A.; Moore, D. T.; DuBois, T. D. *J. Am. Chem. Soc.* **1996**, *118*, 8658.

(17) (a) Brennfürher, A.; Neumann, H.; Beller, M. *Angew. Chem. Int. Ed.* **2009**, *48*, 4114.

(b) Hermanage, P.; Lindhardt, A. T.; Taaning, R. H.; Bjerglund, K.; Lupp, D.; Skrydstrup, T. *J. Am. Chem. Soc.* **2011**, *133*, 6061.

(18) (a) de Meijere, A.; Bräse, S.; Oestreich, M. *Metal-Catalyzed Cross-Coupling Reactions and More*, Wiley, New York, **2014**. (b) Molander, G.; Wolfe, J. P.; Larhed, M. *Science of Synthesis: Cross-Coupling and Heck-Type Reactions*, Thieme, Stuttgart, **2013**.

(c) Negishi, E. *Handbook of Organopalladium Chemistry for Organic Synthesis*, Wiley, New York, **2002**.

(19) Colacot, T. J. *New Trends in Cross-Coupling*, The Royal Society of Chemistry, **2015**.

(20) (a) Blakey, S. B.; MacMillan, D. W. C. *J. Am. Chem. Soc.* **2003**, *125*, 6046. (b) Xie, L. G.; Wang, Z. X. *Angew. Chem. Int. Ed.* **2011**, *50*, 4901. (c) Tobisu, M.; Nakamura, K.; Chatani, N. *J. Am. Chem. Soc.* **2014**, *136*, 5587.

(21) Yang, H.; Li, H.; Wittenberg, R.; Egi, M.; Huang, W.; Liebeskind, L. S. *J. Am. Chem. Soc.* **2007**, *129*, 1132.

(22) (a) Sato, T.; Chida, N. *Org. Biomol. Chem.* **2014**, *12*, 3147. (b) Hutchby, M.; Houlden, C. E.; Haddow, M. F.; Tyler, S. N.; Lloyd-Jones, G. C.; Booker-Milburn, K. I. *Angew. Chem. Int. Ed.* **2012**, *51*, 548. (c) Bennet, A. J.; Somayaji, V.; Brown, R. S.; Santarsiero, B. D. *J. Am. Chem. Soc.* **1991**, *113*, 7563. (d) Yamada, S. *Rev. Heteroat. Chem.* **1999**, *19*, 203. (e) Otani, Y.; Nagae, O.; Naruse, Y.; Inagaki, S.; Ohno, M.; Yamaguchi, K.; Yamamoto, G.; Uchiyama, M.; Ohwada, T. *J. Am. Chem. Soc.* **2003**, *125*, 15191.

(23) (a) Cabri, W.; Candiani, I. *Acc. Chem. Res.* **1995**, *28*, 2. (b) Qin, L.; Ren, X.; Lu, Y.; Li, Y.; Zhou, J. S. *Angew. Chem. Int. Ed.* **2012**, *51*, 5915. (c) Beller, M.; Riermeier, T. H. *Tetrahedron Lett.* **1996**, *37*, 6535. (d) Hallberg, A.; Westerlund, C. *Chem. Lett.* **1982**, 1993.

(24) (a) Schmidt, A. F.; Smirnov, V. V. *Kinet. Catal.* **2002**, *43*, 215. (b) Jutand, A.; Negri, S.; de Vries, J. G. *Eur. J. Inorg. Chem.* **2002**, 1711.

(25) Knowles, J. P.; Whiting, A. *Org. Biomol. Chem.* **2007**, *5*, 31.

(26) Santos, L. S. *Eur. J. Org. Chem.* **2008**, 235.

### 3.2 Rh-catalyzed C–H bond activation via N–C cleavage

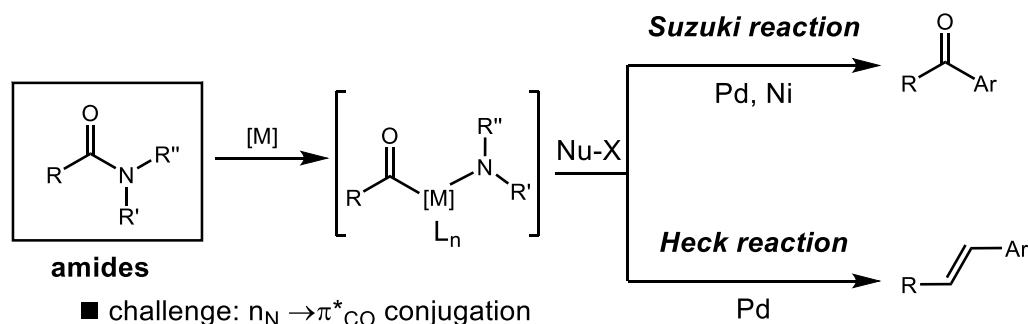
Parts of this section were adapted with permission from the article: “Rhodium-Catalyzed C–H Bond Functionalization with Amides by Double C–H/C–N Bond Activation” (*Org. Lett.* **2016**, *18*, 796). Copyright © 2016, American Chemical Society.

#### 3.2.1 Research background

In the last decade, tremendous advances have been made in the field of transition-metal-catalyzed direct C–H bond functionalization.<sup>1</sup> Site-selective functionalization of arene C–H bonds provides ready access to C–C,<sup>2</sup> C–O,<sup>3</sup> C–N,<sup>4</sup> and C–X<sup>5</sup> products with high atom economy.<sup>1–5</sup> In this context, the formation of C–C bonds constitutes the key bond forming event in organic synthesis.<sup>6</sup> The utility of the C–H activation technology to forge carbon-carbon bonds is ultimately limited by the availability of new coupling partners and the development of generic activation manifolds.<sup>7</sup> Chelation-assisted arene C–H functionalization with a number of coupling partners, including aryl halides,<sup>8a–d</sup> pseudohalides,<sup>8e–g</sup> organometallic reagents<sup>9</sup> and arenes<sup>10</sup> have been developed. However, the majority of these methods require the use of complex catalyst systems, oxidants, or have limited substrate scope. Recent progress was achieved by the use of acyl chlorides<sup>11</sup> and aldehydes<sup>12</sup> under Rh(I)/(III) catalysis to form C–C bonds after decarbonylation. Approaches to the development of chelation-assisted coupling of C–H bonds with imines,<sup>13a,b</sup> aldehydes<sup>13c</sup> and ketones<sup>13c</sup> via Rh(III) and Co(I)/(III)<sup>13d</sup> catalytic cycles have been reported. In contrast, at the start of this project, transition-metal-catalyzed C–H bond functionalization with significantly more challenging amides (amide bond

resonance of 15-20 kcal/mol)<sup>14</sup> has been elusive, despite the fundamental role of amide bonds as building blocks in chemistry and biology,<sup>14</sup> and the urgent need to develop new coupling partners for generic C–H activation methods under base-free, oxidant-free conditions, which would additionally show a wide substrate scope and be amenable to rational method development.<sup>15</sup>

■ Previous work: Suzuki and Heck coupling of amides (Pd, Ni catalysis)



■ This work: the first C–H functionalization by N–C amide activation (Rh catalysis)

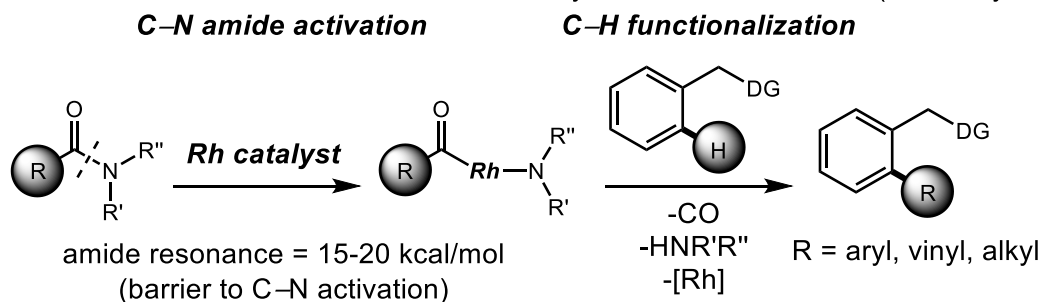


**Figure 3.2.1** Transformation of amides.

### 3.2.2 Reaction discovery

Based on our growing experience in N–C(O) bond activation of amides, we developed the first site-selective arene C–H bond functionalization with amides as the coupling partners via selective cleavage of the amide N–C bond, which proved possible with highly discriminating Rh(I) catalysis.<sup>16</sup> Our report constituted the first example of a



rhodium-catalyzed activation of the amide N–C bond.<sup>17</sup> The following features of our study were noteworthy: (1) The method provided important functionalized biaryls<sup>18</sup> from bench-stable, readily available amide precursors. (2) The reaction showed excellent functional group tolerance, including halides and aldehydes. (3) The Rh(I) catalyst showed very high specificity for the chelation-directed insertion into the amide N–C bond, overriding the inherent decarbonylation/dehalogenation. (4) The reaction was characterized by operational simplicity, and could be conducted in the presence of ambient air and moisture. This study demonstrated that typically inert, electronically-neutral amides could be utilized for C–C bond-forming reactions via C–H activation.<sup>19</sup> Given the utility of Rh(I) as highly useful C–H activation catalysts<sup>16</sup> and the importance of amides in organic synthesis,<sup>14</sup> this concept opened up new possibilities for using amides as coupling partners in C–H activation manifolds.

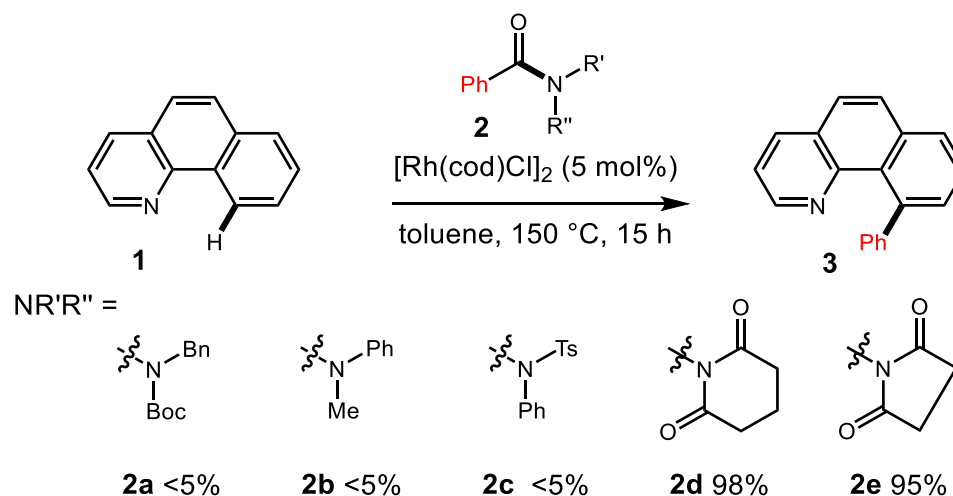


**Figure 3.2.2** Screening of amides.

As outlined in chapters 1-3, we reported the first Suzuki<sup>20a</sup> and Heck<sup>20b</sup> reactions of non-planar amides<sup>21</sup> under Pd(0)/(II) catalysis. Independently, Garg<sup>20c</sup> and Zou<sup>20d</sup> demonstrated the use of non-planar imides<sup>21</sup> in the Suzuki reaction using Ni<sup>20c,d</sup> and Pd catalysis (Figure 3.2.1).<sup>20d</sup> Altogether, these reactions represented the elusive class of transition-metal-catalyzed amide bond N–CO insertion/cross-coupling reactions for the formation of C–C bonds proceeding via selective N–C activation,<sup>22</sup> where the  $n_N \rightarrow \pi^*_{CO}$  amide bond resonance was disrupted by ligand coordination.<sup>23</sup> Ground-state distortion<sup>24a</sup> and electronic activation<sup>24b</sup> also contributed to the observed reactivity, and thus these transformations exploited selective transition-metal-catalyzed activation of the classically inert N–C amide bonds.<sup>14</sup> It is important to note that these methods employed bench-stable, readily available amide precursors<sup>25</sup> as acylating or even arylating reagents, thus enabling a new powerful transition-metal-catalyzed amide disconnection via acyl-metals.<sup>26</sup>

On the basis of our studies, we proposed that bench-stable amides could be employed as arylating C–H functionalization partners with arenes by identifying an appropriate amide precursor and catalyst system. A critical feature of this design is the capacity of a low-valent metal catalyst to insert into the inert amide N–C bond under mild conditions,<sup>17</sup> a step that would be compatible with the C–H activation cycle.<sup>11–13</sup> At the outset of this study, only two metals, Pd(0) and Ni(0), had been known to activate amide N–C bonds catalytically, operating under the conditions that are incompatible with C–H activation manifolds.<sup>1–5</sup> Thus, we realized from the start that the development of C–H functionalization with amides would require identifying anew catalyst system to insert

into the amide N–C bond and control the relative reactivity of the decarbonylation intermediates.

### 3.2.3 Reaction optimization

Our evaluation of the C–H bond functionalization strategy with amides was first examined by the coupling of benzo[*h*]quinoline **1** with amides **2** under various conditions (Figure 3.2.2). For our initial studies, we selected 2-phenylpyridine directing groups because of their well-known capacity to undergo cyclometalation under mild conditions,<sup>2a</sup> and the importance of pyridine-containing biaryls in medicinal chemistry.<sup>18</sup> Although the C–H functionalization products were not detected using Pd and Ni as catalysts, we found the proposed C–H functionalization was indeed possible using Rh(I)-catalysts and sterically-distorted amide **3.2.2d**. Importantly, less distorted anilides **3.2.2a**–**3.2.2c**<sup>21</sup> resulted only in trace quantities of the C–H activation product, consistent with the facility of metal insertion into the amide N–CO bond.<sup>17</sup> Interestingly, the coupling of **1** with a significantly less distorted amide **3.2.2e**<sup>21</sup> gave an excellent yield of the cross-coupling product, indicating very high activity of the Rh(I) catalyst for the N–CO insertion. Importantly, ketone products were not detected, consistent with the high capability of the Rh(I) catalyst to facilitate decarbonylation.<sup>16</sup> The arylation process occurred exclusively at the less electrophilic 10-position of benzo[*h*]quinoline, consistent with nitrogen-directed cyclometallation.<sup>2a</sup>

$\text{1} \xrightarrow[\text{toluene, 150 } ^\circ\text{C, 15 h}]{\text{[Rh(cod)Cl]}_2 \text{ (5 mol \%)}, \text{2}} \text{3}$

entry	catalyst	additive	solvent	yield (%)
1	[Rh(cod)Cl] <sub>2</sub>	-	toluene	>98
2	[Rh(CO) <sub>2</sub> Cl] <sub>2</sub>	-	toluene	30
3	[Rh(cod) <sub>2</sub> ]BF <sub>4</sub>	-	toluene	>98
4	RhCl(PPh <sub>3</sub> ) <sub>3</sub>	-	toluene	9
5	[Rh(C <sub>2</sub> H <sub>4</sub> ) <sub>2</sub> Cl] <sub>2</sub>	-	toluene	69
6	[RhCp <sup>*</sup> Cl <sub>2</sub> ] <sub>2</sub>	-	toluene	<5
7 <sup>b</sup>	[Rh(cod)Cl] <sub>2</sub>	CuI	toluene	39
8 <sup>c</sup>	[Rh(cod)Cl] <sub>2</sub>	O <sub>2</sub>	toluene	47
9 <sup>d</sup>	[Rh(cod)Cl] <sub>2</sub>	PPh <sub>3</sub>	toluene	30
10 <sup>d</sup>	[Rh(cod)Cl] <sub>2</sub>	DPPF	toluene	54
11 <sup>d</sup>	[Rh(cod)Cl] <sub>2</sub>	DPPP	toluene	<5
12	[Rh(cod)Cl] <sub>2</sub>	Na <sub>2</sub> CO <sub>3</sub>	toluene	75
13	[Rh(cod)Cl] <sub>2</sub>	KF	toluene	77
14	[Rh(cod)Cl] <sub>2</sub>	K <sub>2</sub> CO <sub>3</sub>	toluene	<5
15	[Rh(cod)Cl] <sub>2</sub>	-	dioxane	16
16	[Rh(cod)Cl] <sub>2</sub>	-	PhCl	<5
17	[Rh(cod)Cl] <sub>2</sub>	-	DCE	<5
18 <sup>e</sup>	[Rh(cod)Cl] <sub>2</sub>	-	toluene	30
19 <sup>f</sup>	[Rh(cod)Cl] <sub>2</sub>	H <sub>2</sub> O	toluene	>98

<sup>a</sup>Conditions: **1** (0.1 mmol), **3.2-2d** (1.5 equiv), catalyst (5 mol %), solvent (0.25 M), additive (1.5 equiv), 150 °C. <sup>b</sup>Additive (1.0 equiv). <sup>c</sup>1 atm. <sup>d</sup>Additive (0.1 equiv). <sup>e</sup>120 °C. <sup>f</sup>H<sub>2</sub>O (1.5 equiv).

**Table 3.2.1** General optimization.<sup>a</sup>

Our key optimization results with amide **3.2.2d** are shown in Table 3.2.1. Various catalysts were tested, and [Rh(cod)Cl]<sub>2</sub> showed the best catalytic activity (entries 1-6). Control experiments in the absence of metal catalyst resulted in full recovery of **3.2.2d**. The use of Rh(III) precatalysts resulted in recovery of **3.2.2d**. The use of oxidants resulted in low yields, consistent with a Rh(I)/(III) cycle (entries 7-8). Strongly coordinating ligands provided **3** in lower yields (entries 9-11). Bases had a deleterious

effect on the reaction efficiency (entries 12-14). Molecular sieves were not required for the reaction.<sup>11a</sup> The reaction could ensue at lower temperatures (entry 18); however, the process was less efficient. Finally, we noted that the reaction was highly practical; the reaction tolerated water and could be conducted in the presence of ambient air with no decrease in yields (entry 19). This was in sharp contrast to C–H arylation with more electrophilic acyl precursors, which required careful control of the reaction conditions and moisture.<sup>11a–d</sup> To our knowledge, this transformation represented the first example of both: (1) transition-metal catalyzed C–H arylation with amides; and (2) catalytic activation of an amide N–CO bond by a Rh catalyst.<sup>17</sup>

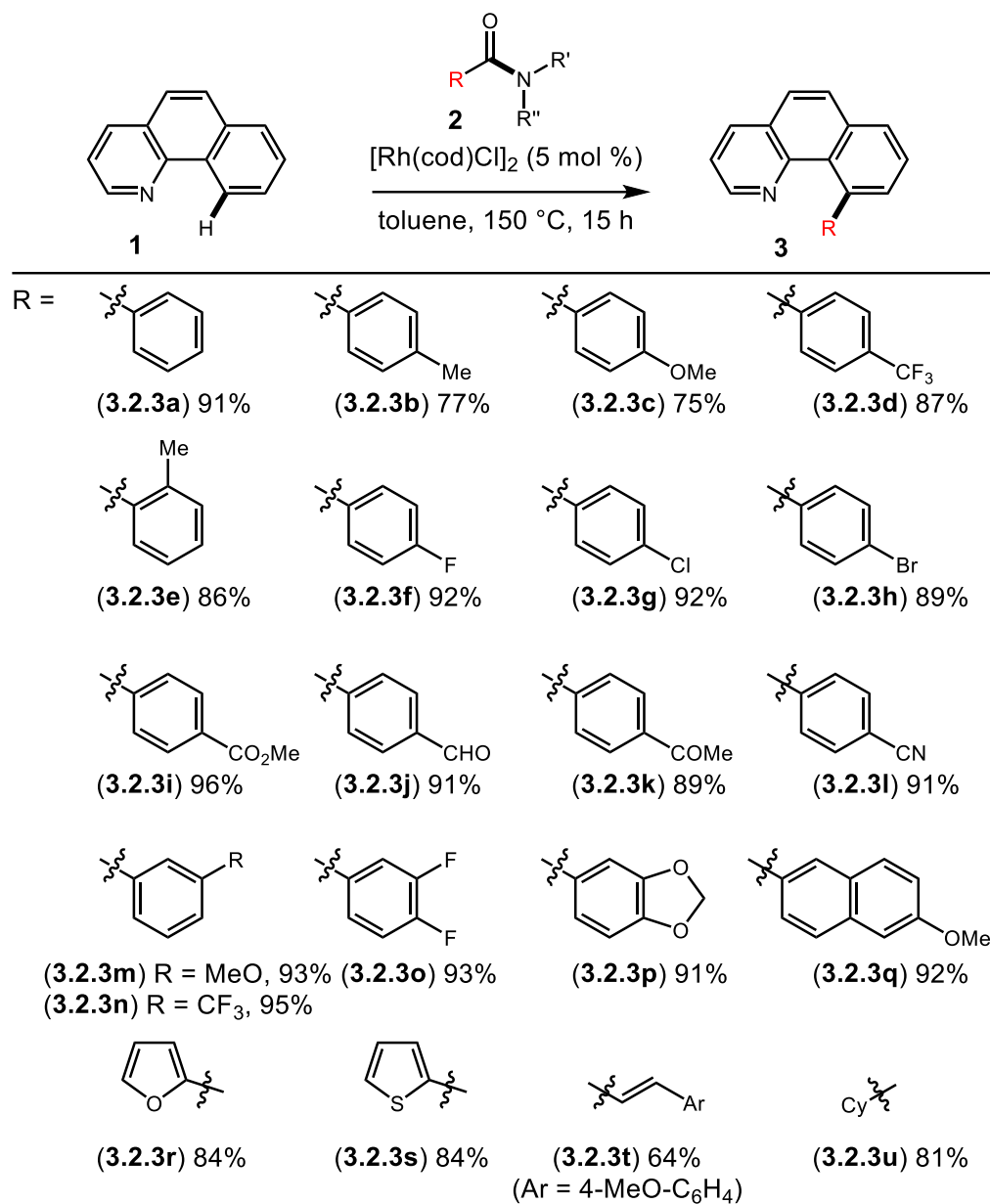


**Figure 3.2.3** Scope of amides.

### 3.2.4 Substrate scope

With optimal conditions in hand, we next explored the preparative scope of our Rh(I)-catalyzed C–H arylation with respect to the amide component (Figure 3.2.3). The

reaction tolerated a remarkably broad range of functional groups. Amides containing neutral, electron-donating and electron-withdrawing groups afforded the desired products in excellent yields (entries 1-4). Steric hindrance was well-tolerated (entry 5). 4-Fluoro, 4-chloro, and even 4-bromo groups gave the arylation product in high yields (entries 6-8), providing functional handles for further functionalization. Notably, the arylation with amide was accomplished in the presence of more reactive carbonyl functional groups such as esters and aldehydes (entries 9-10), which illustrated the strategic advantage of using typically inert amide bonds for transition metal catalyzed C–H activation. Other sensitive groups such as ketones and nitriles were also tolerated (entries 11-12). Meta-substitution (entries 13-14), and strongly electron-donating/ withdrawing functions were well-tolerated (entries 15-16). This protocol could be further applied to naphthalene rings (entry 17). Moreover, heterocycles were compatible with the reaction conditions (entries 18-19). Most importantly, the reaction was not limited to  $sp^2$ - $sp^2$  biaryl coupling as vinyl (entry 20) and even alkyl groups (entry 21) could be successfully coupled in high yields. The latter provided an alternative to Friedel-Crafts alkylation. Overall, this reaction showed the highest functional group tolerance of all previously reported transition-metal-catalyzed transformations of amides via C–N activation at the time of this project,<sup>17,20</sup> which highlighted the excellent selectivity of the developed Rh(I) catalyst system.

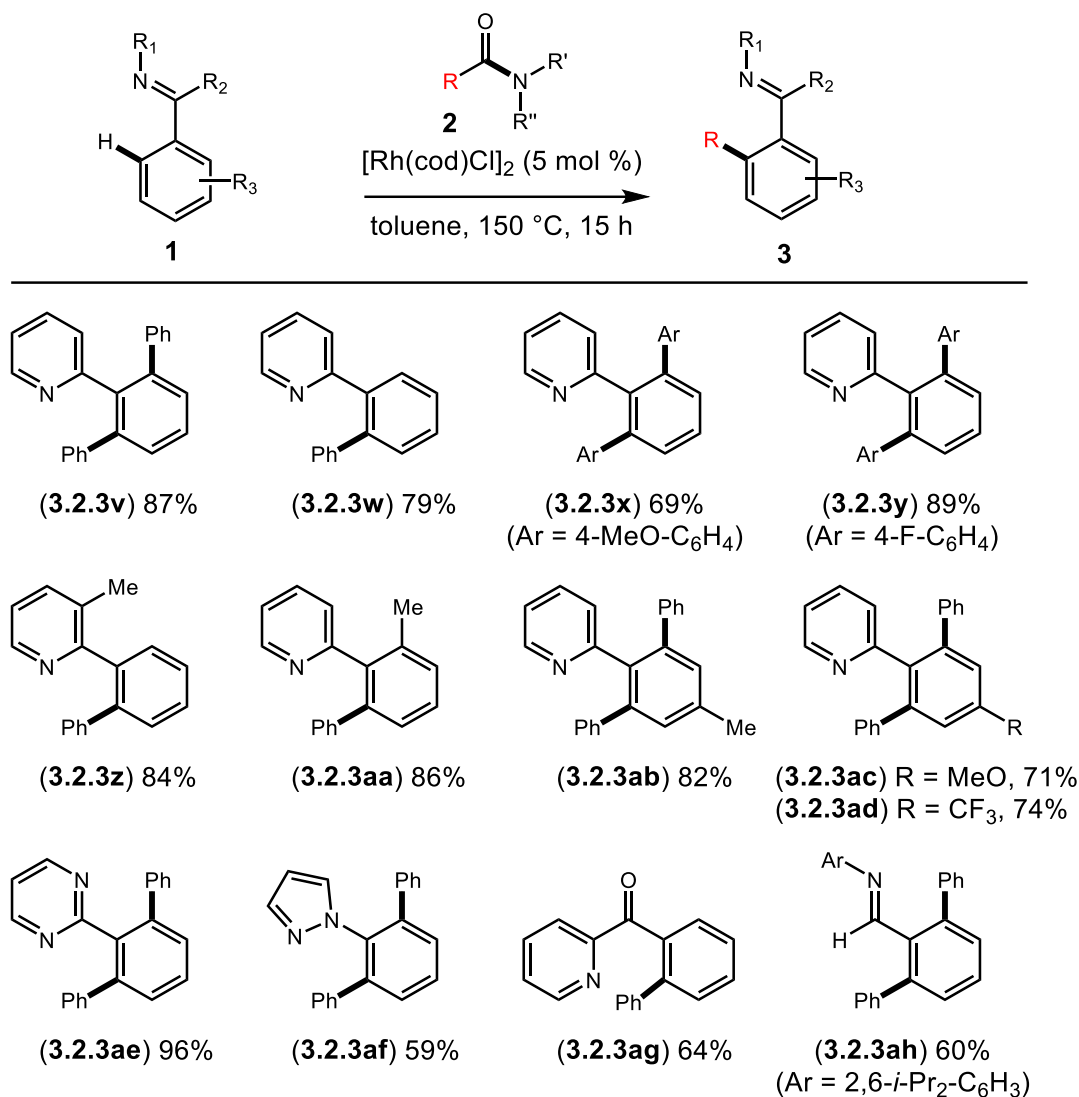


**Figure 3.2.4** Heterocycle scope.

Next, we investigated the effect of electronic and structural modifications of the directing group component (Figure 3.2.4). Typically, an excess of the amide precursor (3 equiv) was used for these reactions, resulting in double C–H activation.<sup>11</sup> However, the example with a stoichiometric amount (**3.2.3w**) illustrated that mono-arylation was possible with high selectivity. The reaction was successful for electron-withdrawing and donating



substrates (**3.2.3x-3.2.3y**). Moreover, mono-arylation was selectively achieved with substrates bearing ortho-substituents on the pyridine ring (**3.2.3z**). The sterically-demanding ortho-methyl substrate coupled in high yield (**3.2.3aa**). Substrates bearing electron withdrawing and electron donating groups at the para-position were well-tolerated (**3.2.3ab-3.2.3ad**). Furthermore, substrates bearing other directing groups such as pyrimidines (**3.2.3ae**), pyrazoles (**3.2.3af**), 2-acylpyridines (**3.2.3ag**) and imines (**3.2.3ah**) were successfully functionalized to furnish the biaryl products in good yields. Notably, the inherently difficult 6-membered metal acycles (**3.2.3ag**) could be accommodated.<sup>3d</sup> In this case, mono-arylation product was formed, consistent with slower cyclometallation. Importantly, the coupling of imines provided rapid access to synthetically valuable biaryl aldehydes after hydrolysis.

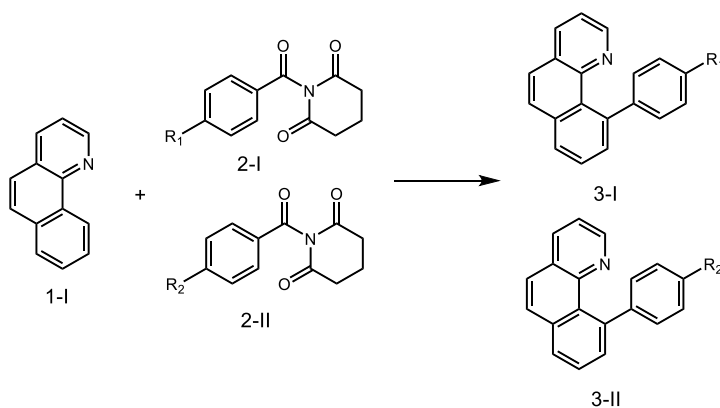
### 3.2.5 Mechanistic studies

entry	[Rh(cod)Cl] <sub>2</sub> (mol%)	yield (%)
1	5.0	>98
2	0.2	>98
3	0.1	98

**Table 3.2.2** Determination of TON.

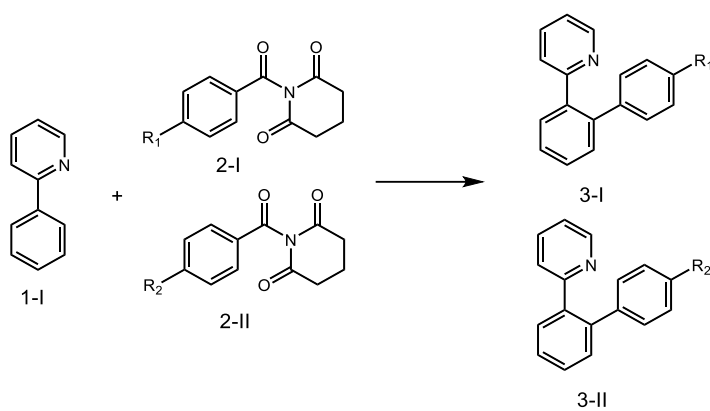
Considering the unique features of these Rh(I)-catalyzed C–H activation reactions, we conducted several studies to shed light on the mechanism (Table 3.2.2-3.2.6). (1) Intermolecular competition experiments between differently substituted amide substrates revealed that electron-deficient amides reacted preferentially irrespective of the directing

group, and that sterically-hindered amides were more reactive than unsubstituted aryl amides. (2) Further competition experiments between differently substituted 2-phenylpyridine substrates indicted that electron-poor arenes were more reactive. This observation was consistent with initial electrophilic deprotonation of the ortho-phenyl C–H bond. (3) A remarkably high TON for N–C bond activation of 1000 in the arylation of benzo[*h*]quinoline was achieved and demonstrated highly efficient catalysis (Table 3.2.2).



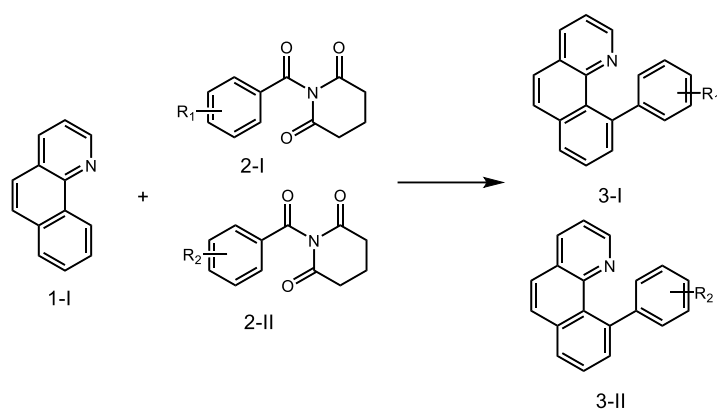
entry	<b>2-I</b> (R <sub>1</sub> )	<b>2-II</b> (R <sub>2</sub> )	amide (equiv)	<b>3-I:3-II</b> (R <sub>1</sub> :R <sub>2</sub> )
1	F-	MeO-	2.0	61:39
2	Me-	MeO-	2.0	58:42
3	Me-	F-	2.0	46:54
4	CF <sub>3</sub> -	MeO-	2.0	81:19

**Table 3.2.3** Selectivity studies: electronics.



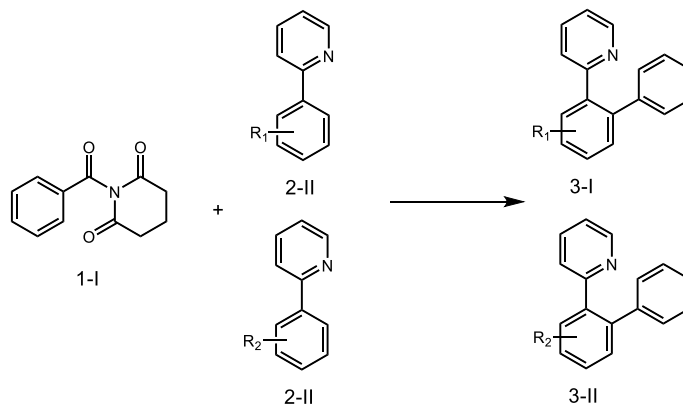
entry	<b>2-I</b> ( $R_1$ )	<b>2-II</b> ( $R_2$ )	amide (equiv)	<b>3-I:3-II</b> ( $R_1$ : $R_2$ )
1	F-	MeO-	2.0	75:25
2	Me-	MeO-	2.0	68:32
3	Me-	F-	2.0	46:54
4	CF <sub>3</sub> -	MeO-	2.0	74:26

**Table 3.2.4** Additional selectivity studies.



entry	<b>2-I</b> (R <sub>1</sub> )	<b>2-II</b> (R <sub>2</sub> )	<b>2</b> (equiv)	<b>3-I:3-II</b> (R <sub>1</sub> :R <sub>2</sub> )
1	4-Me-	2-Me-	2.0	24:76

**Table 3.2.5** Selectivity studies: sterics.



entry	<b>2-I</b> (R <sub>1</sub> )	<b>2-II</b> (R <sub>2</sub> )	<b>2</b> (equiv)	<b>3-I:3-II</b> (R <sub>1</sub> :R <sub>2</sub> )
1	benzo[ <i>h</i> ]quinoline	H	2.0	63:37
2	4-CF <sub>3</sub>	4-OMe	2.0	55:45

**Table 3.2.6** Selectivity studies: directing groups.

A possible mechanism consistent with the mechanistic studies is presented in Figure 3.2.5. The first step could involve initial Rh(I) insertion into the amide N–C bond to afford the acyl-Rh(III) intermediate. Step two of the proposed catalytic cycle could involve decarbonylation and chelation-assisted C–H activation to form a cyclometallated Ar-Rh(III) intermediate. The final step could involve base-mediated C–C bond formation by reductive elimination to afford the product and regeneration of the catalyst. While Rh(III) catalytic cycle could also be possible,<sup>22</sup> the product is formed with low efficiency in the presence of oxidants or Rh(III) precatalysts. An alternative mechanism involving chelation-assisted C–H activation by Rh(I), followed by amide insertion was also possible. Notably, the cleavage of the alternative N–C amide bond and the formation of ketone products were not observed under the reaction conditions, attesting to the high selectivity of the Rh(I) catalyst system.

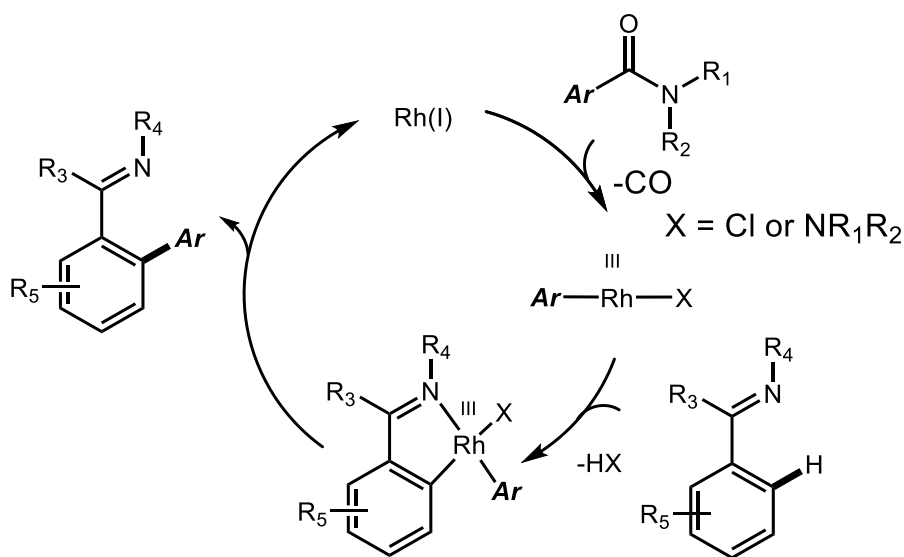


**Figure 3.2.5** Proposed mechanism.

### 3.2.6 Conclusion

In conclusion, we developed the first C–H arylation using amides by the N–C(O) activation of the amide bond. Given the importance of amides and advantages of C–H activation manifolds, the concept of using amides as arylating cross-coupling partners in C–H bond activation has provided new strategies for organic synthesis. Furthermore, our studies provided the first example of Rh(I)-catalysis for activation of inert N–C(O) amide bonds, and demonstrated that Rh(I) is significantly more efficient than Ni(0) in promoting the decarbonylative manifold of amides.

### 3.2.7 Experimental section

**General procedure for Rh-catalyzed C–H activation with amides.** An oven-dried vial (2 dram) equipped with a stir bar was charged with benzo[*h*]quinoline (neat, 1.0 equiv), amide substrate (typically, 1.5 equiv) and [Rh(cod)Cl]<sub>2</sub> (typically, 5 mol%). Toluene (typically, 0.25 M) was added with vigorous stirring at room temperature, the reaction mixture was placed in an oil bath and stirred for an indicated time at 150 °C. After the indicated time, the reaction mixture was diluted with CH<sub>2</sub>Cl<sub>2</sub> (10 mL), filtered, and concentrated. The sample was analyzed by GC-MS and <sup>1</sup>H NMR (CDCl<sub>3</sub>, 500 MHz) to obtain conversion, yield and selectivity using internal standard and comparison with authentic samples. Purification by chromatography on silica gel afforded the title product.

**3.2.1d.** <sup>1</sup>H NMR (500 MHz, CDCl<sub>3</sub>) δ 8.73 (d, *J* = 4.0 Hz, 1 H), 7.77 (t, *J* = 7.6 Hz, 1 H), 7.43 (d, *J* = 7.0 Hz, 2 H), 7.35-7.29 (m, 3 H), 7.28-7.24 (m, 1 H), 2.41 (s, 3 H). <sup>13</sup>C NMR (500 MHz, CDCl<sub>3</sub>) δ 160.06, 149.22, 140.46, 136.12, 135.75, 130.75, 129.64, 128.28,

125.89, 124.11, 121.63, 20.31. HRMS calcd for  $C_{12}H_{12}N$  ( $M^+ + H$ ) 170.0964, found 170.0953.

**3.2.1e.** Colorless oil.  $^1H$  NMR (500 MHz,  $CDCl_3$ )  $\delta$  8.71 (d,  $J = 4.7$  Hz, 1 H), 7.93 (d,  $J = 8.1$  Hz, 2 H), 7.77-7.70 (m, 2 H), 7.31 (d,  $J = 7.9$  Hz, 2 H), 7.24-7.20 (m, 1 H), 2.44 (s, 3 H).  $^{13}C$  NMR (500 MHz,  $CDCl_3$ )  $\delta$  157.48, 149.61, 138.94, 136.67, 136.64, 129.49, 126.78, 121.80, 120.25, 21.29. HRMS calcd for  $C_{24}H_{23}N_2$  ( $2 M^+ + H$ ) 339.1856, found 339.1851.

**3.2.1f.** Yellow solid.  $^1H$  NMR (500 MHz,  $CDCl_3$ )  $\delta$  8.68 (d,  $J = 4.3$  Hz, 1 H), 7.98 (d,  $J = 8.6$  Hz, 2 H), 7.76-7.66 (m, 2 H), 7.22-7.17 (m, 1 H), 7.02 (d,  $J = 8.6$  Hz, 2 H), 3.89 (s, 3 H).  $^{13}C$  NMR (500 MHz,  $CDCl_3$ )  $\delta$  160.46, 157.13, 149.55, 136.65, 132.05, 128.16, 121.41, 119.80, 114.13, 55.36. HRMS calcd for  $C_{24}H_{23}N_2O_2$  ( $2 M^+ + H$ ) 371.1754 found 371.1759.

**3.2.1g.** Yellow solid.  $^1H$  NMR (500 MHz,  $CDCl_3$ )  $\delta$  7.65 (d,  $J = 15.8$  Hz, 1 H), 7.53 (d,  $J = 8.4$  Hz, 2 H), 6.93 (d,  $J = 8.3$  Hz, 2 H), 6.58 (d,  $J = 15.7$  Hz, 1 H), 3.88 (s, 3 H), 2.76 (t,  $J = 6.6$  Hz, 4 H), 2.10 (m, 2 H).  $^{13}C$  NMR (500 MHz,  $CDCl_3$ )  $\delta$  155.90, 149.95, 142.69, 136.96, 130.81 ( $J^2 = 33.8$  Hz), 127.19, 125.69 ( $J^3 = 3.75$  Hz), 124.20 ( $J^I = 270.0$  Hz), 122.95, 120.85.  $^{19}F$  NMR (471 MHz,  $CDCl_3$ )  $\delta$  -62.58. HRMS calcd for  $C_{12}H_9F_3N$  ( $M^+ + H$ ) 224.0682 found 224.0670.

**3.2.1h.** Colorless oil.  $^1H$  NMR (500 MHz,  $CDCl_3$ )  $\delta$  8.84 (d,  $J = 4.8$  Hz, 2 H), 8.47 (dd,  $J = 6.8, 3.0$  Hz, 2 H), 7.52 (dd,  $J = 5.0, 1.7$  Hz, 3 H), 7.21 (t,  $J = 4.8$  Hz, 1 H).  $^{13}C$  NMR

(500 MHz,  $\text{CDCl}_3$ )  $\delta$  164.78, 157.26, 137.57, 130.79, 128.62, 128.14, 119.09. HRMS calcd for  $\text{C}_{20}\text{H}_{16}\text{N}_4\text{Na}$  ( $2\text{M}^+ + \text{Na}$ ) 335.1267 found 335.1273.

**3.2.1k.** Yellow solid.  $^1\text{H}$  NMR (500 MHz,  $\text{CDCl}_3$ )  $\delta$  8.24 (s, 1 H), 7.96 (d,  $J = 5.3$  Hz, 2 H), 7.55 (d,  $J = 5.8$  Hz, 3 H), 7.20 (d,  $J = 7.4$  Hz, 2 H), 7.17-7.11 (m, 1 H), 3.02 (m, 2 H), 1.21 (d,  $J = 6.9$  Hz, 12 H).  $^{13}\text{C}$  NMR (500 MHz,  $\text{CDCl}_3$ )  $\delta$  162.00, 149.26, 137.61, 136.05, 131.43, 128.84, 128.59, 124.12, 123.03, 27.96, 23.51. HRMS calcd for  $\text{C}_{19}\text{H}_{24}\text{N}$  ( $\text{M}^+ + \text{H}$ ) 266.1903 found 266.1931.

**3.2.3a.** Colorless oil.  $^1\text{H}$  NMR (500 MHz,  $\text{CDCl}_3$ )  $\delta$  8.49 (dd,  $J = 4.3, 1.9$  Hz, 1 H), 8.12 (dd,  $J = 8.0, 1.9$  Hz, 1 H), 7.98 (d,  $J = 7.9$  Hz, 1 H), 7.91 (d,  $J = 8.8$  Hz, 1 H), 7.74 (dd,  $J = 8.3, 6.6$  Hz, 2 H), 7.62 (d,  $J = 7.2$  Hz, 1 H), 7.51-7.42 (m, 5 H), 7.36 (dd,  $J = 7.9, 4.3$  Hz, 1 H).  $^{13}\text{C}$  NMR (125 MHz,  $\text{CDCl}_3$ )  $\delta$  146.90, 146.86, 146.47, 141.76, 135.23, 135.03, 131.54, 129.06, 128.78, 128.33, 127.99, 127.42, 127.26, 127.08, 125.97, 125.73, 121.10. HRMS calcd for  $\text{C}_{19}\text{H}_{14}\text{N}$  ( $\text{M}^+ + \text{H}$ ) 256.1121 found 256.1150.

**3.2.3b.** Colorless oil.  $^1\text{H}$  NMR (500 MHz,  $\text{CDCl}_3$ )  $\delta$  8.50 (dd,  $J = 4.3, 1.8$  Hz, 1 H), 8.11 (d,  $J = 8.0$  Hz, 1 H), 7.94 (d,  $J = 7.9$  Hz, 1 H), 7.88 (d,  $J = 8.7$  Hz, 1 H), 7.74-7.68 (m, 2 H), 7.58 (d,  $J = 7.3$  Hz, 1 H), 7.36 (dd,  $J = 8.0, 4.3$  Hz, 1 H), 7.31-7.28 (m, 2 H), 7.25 (d,  $J = 7.9$  Hz, 2 H), 2.50 (s, 3 H).  $^{13}\text{C}$  NMR (125 MHz,  $\text{CDCl}_3$ )  $\delta$  146.93, 146.83, 143.44, 141.73, 135.21, 135.10, 135.04, 131.67, 129.07, 128.64, 128.33, 128.11, 127.80, 127.22, 127.06, 125.88, 121.03, 21.34. HRMS calcd for  $\text{C}_{20}\text{H}_{16}\text{N}$  ( $\text{M}^+ + \text{H}$ ) 270.1277 found 270.1305.



**3.2.3c.** Yellow solid.  $^1\text{H}$  NMR (500 MHz,  $\text{CDCl}_3$ )  $\delta$  8.52 (dd,  $J = 4.3, 1.9$  Hz, 1 H), 8.11 (d,  $J = 8.0$  Hz, 1 H), 7.93 (d,  $J = 7.8$  Hz, 1 H), 7.88 (d,  $J = 8.8$  Hz, 1 H), 7.70 (t,  $J = 8.6$  Hz, 2 H), 7.58 (d,  $J = 7.2$  Hz, 1 H), 7.39-7.31 (m, 3 H), 7.02-6.97 (m, 2 H), 3.95 (s, 3 H).  $^{13}\text{C}$  NMR (125 MHz,  $\text{CDCl}_3$ )  $\delta$  157.96, 146.97, 146.87, 141.38, 138.90, 135.26, 135.10, 131.73, 129.82, 129.12, 128.36, 127.77, 127.23, 127.07, 125.89, 121.04, 112.84, 55.32. HRMS calcd for  $\text{C}_{20}\text{H}_{16}\text{NO}$  ( $\text{M}^+ + \text{H}$ ) 286.1226 found 286.1255.

**3.2.3d.** White solid.  $^1\text{H}$  NMR (500 MHz,  $\text{CDCl}_3$ )  $\delta$  8.44 (dd,  $J = 4.3, 1.8$  Hz, 1 H), 8.13 (dd,  $J = 8.0, 1.9$  Hz, 1 H), 8.00 (dd,  $J = 8.0, 1.3$  Hz, 1 H), 7.91 (d,  $J = 8.8$  Hz, 1 H), 7.78-7.72 (m, 2 H), 7.69 (d,  $J = 8.0$  Hz, 2 H), 7.53 (dd,  $J = 7.2, 1.3$  Hz, 1 H), 7.49 (d,  $J = 7.9$  Hz, 2 H), 7.37 (dd,  $J = 8.0, 4.3$  Hz, 1 H).  $^{13}\text{C}$  NMR (125 MHz,  $\text{CDCl}_3$ )  $\delta$  150.22, 146.92, 146.40, 140.21, 135.33, 134.95, 131.11, 128.99, 128.83, 128.55, 128.22, 127.79 ( $J^2 = 31.3$  Hz), 127.29, 127.08, 126.15, 124.81 ( $J^I = 270.0$  Hz), 124.29 ( $J^3 = 7.5$  Hz), 121.28.  $^{19}\text{F}$  NMR (471 MHz,  $\text{CDCl}_3$ )  $\delta$  -61.96. HRMS calcd for  $\text{C}_{20}\text{H}_{13}\text{NF}_3$  ( $\text{M}^+ + \text{H}$ ) 324.0995 found 324.1021.

**3.2.3e.** Colorless oil.  $^1\text{H}$  NMR (500 MHz,  $\text{CDCl}_3$ )  $\delta$  8.48 (dd,  $J = 4.3, 1.9$  Hz, 1 H), 8.11 (d,  $J = 8.0$  Hz, 1 H), 8.00 (d,  $J = 8.0$  Hz, 1 H), 7.92 (d,  $J = 8.8$  Hz, 1 H), 7.79-7.72 (m, 2 H), 7.54 (d,  $J = 7.2$  Hz, 1 H), 7.38-7.31 (m, 4 H), 7.25 (d,  $J = 7.1$  Hz, 1 H), 1.93 (s, 3 H).  $^{13}\text{C}$  NMR (125 MHz,  $\text{CDCl}_3$ )  $\delta$  147.49, 147.05, 146.48, 141.07, 135.91, 135.10, 134.68, 130.76, 129.48, 128.78, 127.94, 127.28, 126.98, 125.96, 125.86, 125.16, 121.00, 20.27. HRMS calcd for  $\text{C}_{20}\text{H}_{16}\text{N}$  ( $\text{M}^+ + \text{H}$ ) 270.1277 found 270.1304.

**3.2.3f.** White solid.  $^1\text{H}$  NMR (500 MHz,  $\text{CDCl}_3$ )  $\delta$  8.50 (d,  $J = 4.3$  Hz, 1 H), 8.12 (d,  $J = 8.0$  Hz, 1 H), 7.97 (dd,  $J = 7.8, 1.4$  Hz, 1 H), 7.89 (d,  $J = 8.8$  Hz, 1 H), 7.75-7.69 (m, 2 H), 7.56 (dd,  $J = 7.3, 1.4$  Hz, 1 H), 7.39-7.32 (m, 3 H), 7.17-7.11 (m, 2 H).  $^{13}\text{C}$  NMR (125 MHz,  $\text{CDCl}_3$ )  $\delta$  162.56, 160.62, 146.88, 146.75, 142.26 ( $J^d = 2.5$  Hz), 140.68, 135.31, 135.04, 131.52, 130.18 ( $J^3 = 7.5$  Hz), 129.06, 128.25 ( $J^l = 17.5$  Hz), 127.29, 127.05, 126.03, 121.17, 114.15 ( $J^2 = 21.3$  Hz).  $^{19}\text{F}$  NMR (471 MHz,  $\text{CDCl}_3$ )  $\delta$  -118.08. HRMS calcd for  $\text{C}_{19}\text{H}_{13}\text{NF}$  ( $\text{M}^+ + \text{H}$ ) 274.1027 found 274.1054.

**3.2.3g.** Colorless oil.  $^1\text{H}$  NMR (500 MHz,  $\text{CDCl}_3$ )  $\delta$  8.49 (dd,  $J = 4.3, 1.9$  Hz, 1 H), 8.12 (d,  $J = 8.0$  Hz, 1 H), 7.97 (d,  $J = 8.0$  Hz, 1 H), 7.89 (d,  $J = 8.7$  Hz, 1 H), 7.72 (dd,  $J = 14.8, 8.0$  Hz, 2 H), 7.53 (d,  $J = 7.2$  Hz, 1 H), 7.42-7.35 (m, 3 H), 7.32 (d,  $J = 8.4$  Hz, 2 H).  $^{13}\text{C}$  NMR (125 MHz,  $\text{CDCl}_3$ )  $\delta$  146.90, 146.63, 144.89, 140.40, 135.29, 134.99, 131.52, 131.34, 130.12, 128.92, 128.28, 128.26, 127.47, 127.27, 127.05, 126.06, 121.20. HRMS calcd for  $\text{C}_{19}\text{H}_{13}\text{NCl}$  ( $\text{M}^+ + \text{H}$ ) 290.0731 found 290.0756.

**3.2.3h.** Yellow solid.  $^1\text{H}$  NMR (500 MHz,  $\text{CDCl}_3$ )  $\delta$  8.49 (dd,  $J = 4.3, 1.9$  Hz, 1 H), 8.13 (d,  $J = 8.0$  Hz, 1 H), 7.97 (d,  $J = 8.0$  Hz, 1 H), 7.89 (d,  $J = 8.7$  Hz, 1 H), 7.76-7.68 (m, 2 H), 7.57-7.50 (m, 3 H), 7.37 (dd,  $J = 8.0, 4.3$  Hz, 1 H), 7.27-7.23 (m, 2 H).  $^{13}\text{C}$  NMR (125 MHz,  $\text{CDCl}_3$ )  $\delta$  146.91, 146.60, 145.38, 140.37, 135.29, 134.99, 131.27, 130.50, 130.40, 128.86, 128.30, 128.24, 127.26, 127.05, 126.06, 121.21, 119.65. HRMS calcd for  $\text{C}_{19}\text{H}_{13}\text{NBr}$  ( $\text{M}^+ + \text{H}$ ) 334.0226, 336.0206 found 334.0251, 336.0231.

**3.2.3i.** White solid.  $^1\text{H}$  NMR (500 MHz,  $\text{CDCl}_3$ )  $\delta$  8.41 (dd,  $J = 4.3, 1.8$  Hz, 1 H), 8.15-8.09 (m, 3 H), 7.98 (d,  $J = 7.9$  Hz, 1 H), 7.90 (d,  $J = 8.8$  Hz, 1 H), 7.76-7.70 (m, 2 H),

7.54 (d,  $J = 7.3$  Hz, 1 H), 7.47-7.43 (m, 2 H), 7.35 (dd,  $J = 8.0, 4.3$  Hz, 1 H), 4.01 (s, 3 H).  $^{13}\text{C}$  NMR (125 MHz,  $\text{CDCl}_3$ )  $\delta$  167.62, 151.62, 146.89, 146.44, 140.57, 135.26, 134.92, 130.98, 128.83, 128.81, 128.77, 128.44, 128.20, 127.40, 127.26, 127.04, 126.10, 121.25, 52.00. HRMS calcd for  $\text{C}_{21}\text{H}_{16}\text{NO}_2$  ( $\text{M}^+ + \text{H}$ ) 314.1176 found 314.1202.

**3.2.3j.** White solid.  $^1\text{H}$  NMR (500 MHz,  $\text{CDCl}_3$ )  $\delta$  10.15 (s, 1 H), 8.40 (d,  $J = 4.3$  Hz, 1 H), 8.14 (dd,  $J = 8.0, 1.9$  Hz, 1 H), 8.01 (d,  $J = 7.9$  Hz, 1 H), 7.95 (d,  $J = 7.8$  Hz, 2 H), 7.91 (d,  $J = 8.7$  Hz, 1 H), 7.79-7.70 (m, 2 H), 7.54 (d,  $J = 8.1$  Hz, 3 H), 7.37 (dd,  $J = 8.0, 4.3$  Hz, 1 H).  $^{13}\text{C}$  NMR (125 MHz,  $\text{CDCl}_3$ )  $\delta$  192.50, 153.42, 146.89, 146.29, 140.23, 135.36, 134.93, 134.15, 130.81, 129.43, 129.12, 128.75, 128.65, 128.21, 127.32, 127.09, 126.19, 121.34. HRMS calcd for  $\text{C}_{20}\text{H}_{14}\text{NO}$  ( $\text{M}^+ + \text{H}$ ) 284.1070 found 284.1099.

**3.2.3k.** White solid.  $^1\text{H}$  NMR (500 MHz,  $\text{CDCl}_3$ )  $\delta$  8.42 (dd,  $J = 4.3, 1.8$  Hz, 1 H), 8.13 (d,  $J = 7.9$  Hz, 1 H), 8.04 (d,  $J = 7.9$  Hz, 2 H), 7.99 (d,  $J = 7.9$  Hz, 1 H), 7.90 (d,  $J = 8.7$  Hz, 1 H), 7.77-7.71 (m, 2 H), 7.53 (d,  $J = 7.2$  Hz, 1 H), 7.47 (d,  $J = 7.9$  Hz, 2 H), 7.36 (dd,  $J = 8.0, 4.3$  Hz, 1 H), 2.72 (s, 3 H).  $^{13}\text{C}$  NMR (125 MHz,  $\text{CDCl}_3$ )  $\delta$  198.27, 151.91, 146.90, 146.40, 140.44, 135.32, 134.94, 134.67, 130.95, 128.94, 128.80, 128.51, 128.22, 127.69, 127.29, 127.07, 126.14, 121.28, 26.69. HRMS calcd for  $\text{C}_{21}\text{H}_{16}\text{NO}$  ( $\text{M}^+ + \text{H}$ ) 298.1226 found 298.1256.

**3.2.3l.** White solid.  $^1\text{H}$  NMR (500 MHz,  $\text{CDCl}_3$ )  $\delta$  8.42 (dd,  $J = 4.3, 1.9$  Hz, 1 H), 8.14 (d,  $J = 8.0$  Hz, 1 H), 8.01 (d,  $J = 7.9$  Hz, 1 H), 7.91 (d,  $J = 8.8$  Hz, 1 H), 7.79-7.72 (m, 2 H), 7.72-7.68 (m, 2 H), 7.50 (d,  $J = 7.2$  Hz, 1 H), 7.48-7.43 (m, 2 H), 7.38 (dd,  $J = 8.0, 4.3$  Hz, 1 H).  $^{13}\text{C}$  NMR (125 MHz,  $\text{CDCl}_3$ )  $\delta$  151.58, 146.89, 146.17, 139.65, 135.42,

134.93, 131.25, 130.76, 129.51, 128.84, 128.64, 128.19, 127.34, 127.10, 126.26, 121.41, 119.79, 109.24. HRMS calcd for  $C_{20}H_{13}N_2$  ( $M^+ + H$ ) 281.1073 found 281.1102.

**3.2.3m.** Colorless oil.  $^1H$  NMR (500 MHz,  $CDCl_3$ )  $\delta$  8.49 (s, 1 H), 8.11 (d,  $J = 7.9$  Hz, 1 H), 7.96 (d,  $J = 7.9$  Hz, 1 H), 7.89 (d,  $J = 8.7$  Hz, 1 H), 7.71 (td,  $J = 8.1, 7.6, 4.7$  Hz, 2 H), 7.61-7.57 (m, 1 H), 7.37-7.32 (m, 2 H), 6.99 (d,  $J = 7.6$  Hz, 1 H), 6.97-6.91 (m, 2 H), 3.83 (s, 3 H).  $^{13}C$  NMR (125 MHz,  $CDCl_3$ )  $\delta$  159.01, 147.83, 146.96, 146.73, 141.44, 135.15, 134.96, 131.30, 129.01, 128.30, 128.25, 128.01, 127.22, 127.01, 125.96, 121.44, 121.09, 114.34, 111.48, 55.26. HRMS calcd for  $C_{20}H_{16}NO$  ( $M^+ + H$ ) 282.1226 found 282.1255.

**3.2.3n.** Yellow oil.  $^1H$  NMR (500 MHz,  $CDCl_3$ )  $\delta$  8.41 (d,  $J = 4.3$  Hz, 1 H), 8.13 (d,  $J = 8.0$  Hz, 1 H), 8.00 (d,  $J = 8.0$  Hz, 1 H), 7.90 (d,  $J = 8.8$  Hz, 1 H), 7.77-7.71 (m, 2 H), 7.68-7.63 (m, 2 H), 7.59-7.53 (m, 3 H), 7.36 (dd,  $J = 8.1, 4.3$  Hz, 1 H).  $^{13}C$  NMR (125 MHz,  $CDCl_3$ )  $\delta$  146.92, 146.87, 146.42, 140.06, 135.34, 135.00, 131.87, 131.35, 129.44 ( $J^2 = 63.8$  Hz), 128.83, 128.59, 128.25, 127.73, 127.27, 127.09, 126.15, 126.11, 124.63 ( $J^1 = 270.0$  Hz), 122.42 ( $J^3 = 7.5$  Hz), 121.32.  $^{19}F$  NMR (471 MHz,  $CDCl_3$ )  $\delta$  -62.31. HRMS calcd for  $C_{20}H_{13}NF_3$  ( $M^+ + H$ ) 324.0995 found 324.1020.

**3.2.3o.** Yellow solid.  $^1H$  NMR (500 MHz,  $CDCl_3$ )  $\delta$  8.51 (dd,  $J = 4.3, 1.9$  Hz, 1 H), 8.13 (d,  $J = 8.0$  Hz, 1 H), 7.98 (d,  $J = 8.0$  Hz, 1 H), 7.89 (d,  $J = 8.8$  Hz, 1 H), 7.76-7.68 (m, 2 H), 7.53 (d,  $J = 7.2$  Hz, 1 H), 7.39 (dd,  $J = 7.9, 4.2$  Hz, 1 H), 7.24-7.14 (m, 2 H), 7.07 (m, 1 H).  $^{13}C$  NMR (125 MHz,  $CDCl_3$ )  $\delta$  150.33 ( $J^1 = 85.0$  Hz), 148.37 ( $J^1 = 85.0$  Hz), 147.00, 146.46, 143.23 ( $J^3 = 6.3$  Hz), 139.46, 135.35, 134.97, 131.22, 128.88, 128.53,

128.21, 127.32, 127.00, 126.16, 124.51 ( $J^3 = 6.3$  Hz), 121.28, 117.85 ( $J^2 = 17.5$  Hz), 115.99 ( $J^2 = 17.5$  Hz).  $^{19}\text{F}$  NMR (471 MHz,  $\text{CDCl}_3$ )  $\delta$  -140.48, -143.10. HRMS calcd for  $\text{C}_{19}\text{H}_{12}\text{NF}_2$  ( $\text{M}^+ + \text{H}$ ) 292.0932 found 292.0956.

**3.2.3p.** Colorless oil.  $^1\text{H}$  NMR (500 MHz,  $\text{CDCl}_3$ )  $\delta$  8.56 (dd,  $J = 4.3, 1.9$  Hz, 1 H), 8.12 (d,  $J = 8.0$  Hz, 1 H), 7.93 (d,  $J = 7.9$  Hz, 1 H), 7.87 (d,  $J = 8.8$  Hz, 1 H), 7.74-7.66 (m, 2 H), 7.57 (d,  $J = 7.2$  Hz, 1 H), 7.37 (dd,  $J = 7.9, 4.3$  Hz, 1 H), 6.93-6.89 (m, 1 H), 6.88-6.84 (m, 2 H), 6.05 (s, 2 H).  $^{13}\text{C}$  NMR (125 MHz,  $\text{CDCl}_3$ )  $\delta$  147.02, 146.79, 145.75, 141.20, 140.44, 135.24, 135.04, 131.52, 129.13, 128.27, 127.95, 127.27, 127.00, 125.96, 121.49, 121.08, 110.05, 107.58, 100.73. HRMS calcd for  $\text{C}_{20}\text{H}_{14}\text{NO}_2$  ( $\text{M}^+ + \text{H}$ ) 300.1019 found 300.1047.

**3.2.3q.** White solid.  $^1\text{H}$  NMR (500 MHz,  $\text{CDCl}_3$ )  $\delta$  8.37 (dd,  $J = 4.3, 1.9$  Hz, 1 H), 8.12 (d,  $J = 8.0$  Hz, 1 H), 7.98 (d,  $J = 7.9$  Hz, 1 H), 7.92 (d,  $J = 8.8$  Hz, 1 H), 7.85 (d,  $J = 1.8$  Hz, 1 H), 7.80 (d,  $J = 8.8$  Hz, 1 H), 7.77-7.72 (m, 2 H), 7.70 (d,  $J = 8.5$  Hz, 1 H), 7.67 (d,  $J = 7.2$  Hz, 1 H), 7.44 (d,  $J = 8.4$  Hz, 1H), 7.33 (dd,  $J = 8.0, 4.3$  Hz, 1H), 7.26 (d,  $J = 2.6$  Hz, 1 H), 7.20 (dd,  $J = 8.9, 2.6$  Hz, 1 H), 4.00 (s, 3 H).  $^{13}\text{C}$  NMR (125 MHz,  $\text{CDCl}_3$ )  $\delta$  157.30, 146.88, 146.79, 142.18, 141.58, 135.22, 135.07, 133.14, 132.01, 129.86, 129.58, 129.14, 129.05, 128.36, 128.00, 127.23, 127.20, 125.91, 125.38, 124.71, 121.07, 118.06, 105.92, 55.36. HRMS calcd for  $\text{C}_{24}\text{H}_{18}\text{NO}$  ( $\text{M}^+ + \text{H}$ ) 336.1383 found 336.1408.

**3.2.3r.** Colorless oil.  $^1\text{H}$  NMR (500 MHz,  $\text{CDCl}_3$ )  $\delta$  8.72 (dd,  $J = 4.3, 1.8$  Hz, 1 H), 8.14 (dd,  $J = 8.0, 1.8$  Hz, 1 H), 8.00 (d,  $J = 7.8$  Hz, 1 H), 7.86 (d,  $J = 8.8$  Hz, 1 H), 7.78 (dd,  $J = 7.3, 1.5$  Hz, 1 H), 7.76-7.69 (m, 2 H), 7.56 (s, 1 H), 7.42 (dd,  $J = 8.0, 4.3$  Hz, 1 H), 6.64

(t,  $J = 2.4$  Hz, 1 H), 6.52 (d,  $J = 3.1$  Hz, 1 H).  $^{13}\text{C}$  NMR (125 MHz,  $\text{CDCl}_3$ )  $\delta$  157.33, 148.05, 146.42, 140.99, 135.29, 134.95, 131.77, 130.31, 129.58, 127.95, 127.42, 127.07, 126.22, 121.33, 111.00, 105.66. HRMS calcd for  $\text{C}_{17}\text{H}_{12}\text{NO}$  ( $\text{M}^+ + \text{H}$ ) 246.0913 found 246.0943.

**3.2.3s.** Yellow solid.  $^1\text{H}$  NMR (500 MHz,  $\text{CDCl}_3$ )  $\delta$  8.62 (d,  $J = 4.3$  Hz, 1 H), 8.13 (d,  $J = 8.0$  Hz, 1 H), 7.98 (d,  $J = 7.8$  Hz, 1 H), 7.87 (d,  $J = 8.7$  Hz, 1 H), 7.77-7.67 (m, 3 H), 7.44-7.38 (m, 2 H), 7.15 (dd,  $J = 5.2, 3.5$  Hz, 1 H), 7.07 (dd,  $J = 3.4, 1.4$  Hz, 1 H).  $^{13}\text{C}$  NMR (125 MHz,  $\text{CDCl}_3$ )  $\delta$  148.10, 147.20, 146.61, 135.26, 134.95, 133.63, 132.75, 130.09, 129.04, 128.14, 127.38, 126.83, 126.22, 126.15, 124.73, 124.34, 121.29. HRMS calcd for  $\text{C}_{17}\text{H}_{12}\text{NS}$  ( $\text{M}^+ + \text{H}$ ) 262.0685 found 262.0712.

**3.2.3t.** Yellow oil.  $^1\text{H}$  NMR (500 MHz,  $\text{CDCl}_3$ )  $\delta$  9.08 (dd,  $J = 4.4, 1.9$  Hz, 1 H), 9.03 (d,  $J = 16.0$  Hz, 1 H), 8.20 (d,  $J = 8.0$  Hz, 1 H), 7.93 (d,  $J = 7.4$  Hz, 1 H), 7.89 (d,  $J = 7.8$  Hz, 1 H), 7.85 (d,  $J = 8.8$  Hz, 1 H), 7.74-7.64 (m, 4 H), 7.52 (dd,  $J = 8.0, 4.3$  Hz, 1 H), 7.04-6.89 (m, 3 H), 3.90 (s, 3 H).  $^{13}\text{C}$  NMR (125 MHz,  $\text{CDCl}_3$ )  $\delta$  158.88, 148.27, 147.79, 138.85, 135.56, 134.99, 132.68, 131.73, 128.72, 128.64, 127.92, 127.88, 127.70, 127.63, 127.24, 125.67, 120.80, 114.09, 55.36. HRMS calcd for  $\text{C}_{22}\text{H}_{18}\text{NO}$  ( $\text{M}^+ + \text{H}$ ) 312.1383 found 312.1405.

**3.2.3u.** Colorless oil.  $^1\text{H}$  NMR (500 MHz,  $\text{CDCl}_3$ )  $\delta$  9.05 (dd,  $J = 4.3, 2.0$  Hz, 1 H), 8.17 (dd,  $J = 8.0, 2.0$  Hz, 1 H), 7.86-7.73 (m, 3 H), 7.66 (dd,  $J = 8.2, 6.8$  Hz, 2 H), 7.50 (dd,  $J = 8.0, 4.2$  Hz, 1 H), 5.36 (m, 1 H), 2.24-2.10 (m, 2 H), 2.00-1.87 (m, 3 H), 1.73 (qt,  $J = 12.5, 3.3$  Hz, 2 H), 1.60 (td,  $J = 12.0, 3.1$  Hz, 2 H), 1.42 (qt,  $J = 13.1, 3.6$  Hz, 1 H).  $^{13}\text{C}$

NMR (125 MHz,  $\text{CDCl}_3$ )  $\delta$  148.90, 148.69, 147.00, 135.47, 135.42, 129.26, 128.70, 127.56, 127.48, 126.54, 125.87, 125.32, 120.52, 41.36, 35.05, 27.64, 26.92. HRMS calcd for  $\text{C}_{19}\text{H}_{20}\text{N}$  ( $\text{M}^+ + \text{H}$ ) 262.1590 found 262.1618.

**3.2.3v.** White solid.  $^1\text{H}$  NMR (500 MHz,  $\text{CDCl}_3$ )  $\delta$  8.34 (dt,  $J = 5.0, 1.2$  Hz, 1 H), 7.55 (dd,  $J = 8.5, 6.7$  Hz, 1 H), 7.51-7.46 (m, 2 H), 7.32 (td,  $J = 7.7, 1.9$  Hz, 1 H), 7.18 (qd,  $J = 5.0, 1.7$  Hz, 6 H), 7.13 (dt,  $J = 7.0, 2.7$  Hz, 4 H), 6.95-6.89 (m, 2 H).  $^{13}\text{C}$  NMR (125 MHz,  $\text{CDCl}_3$ )  $\delta$  158.94, 148.50, 141.85, 141.60, 138.52, 134.84, 129.64, 129.47, 128.16, 127.63, 126.79, 126.26, 120.86. HRMS calcd for  $\text{C}_{23}\text{H}_{18}\text{N}$  ( $\text{M}^+ + \text{H}$ ) 308.1434 found 308.1459.

**3.2.3w.** Colorless oil.  $^1\text{H}$  NMR (500 MHz,  $\text{CDCl}_3$ )  $\delta$  8.70 -8.62 (m, 1 H), 7.73 (dd,  $J = 5.7, 3.3$  Hz, 1 H), 7.49 (m, 3 H), 7.41 (td,  $J = 7.7, 1.8$  Hz, 1 H), 7.26 (qd,  $J = 4.7, 1.6$  Hz, 3 H), 7.15-7.12 (m, 1 H), 6.91 (d,  $J = 7.9$  Hz, 1 H).  $^{13}\text{C}$  NMR (125 MHz,  $\text{CDCl}_3$ )  $\delta$  159.27, 149.45, 141.37, 140.62, 139.51, 135.16, 130.49, 130.48, 129.72, 128.51, 128.05, 127.65, 126.69, 125.39, 121.33. HRMS calcd for  $\text{C}_{17}\text{H}_{14}\text{N}$  ( $\text{M}^+ + \text{H}$ ) 232.1121 found 232.1110.

**3.2.3x.** White solid.  $^1\text{H}$  NMR (500 MHz,  $\text{CDCl}_3$ )  $\delta$  8.39-8.37 (m, 1 H), 7.50 (dd,  $J = 8.4, 6.9$  Hz, 1 H), 7.42 (d,  $J = 7.3$  Hz, 2 H), 7.35 (t,  $J = 7.7$  Hz, 1 H), 7.05-7.01 (m, 4 H), 6.95 (ddd,  $J = 7.5, 4.9, 1.3$  Hz, 1 H), 6.90 (d,  $J = 7.9$  Hz, 1 H), 6.74-6.69 (m, 4 H), 3.77 (s, 6 H).  $^{13}\text{C}$  NMR (125 MHz,  $\text{CDCl}_3$ )  $\delta$  159.27, 158.05, 148.57, 141.41, 138.44, 135.00, 134.08, 130.67, 129.18, 128.11, 126.79, 120.80, 113.10, 55.13. HRMS calcd for  $\text{C}_{25}\text{H}_{22}\text{NO}_2$  ( $\text{M}^+ + \text{H}$ ) 368.1645 found 368.1668.

**3.2.3y.** White solid.  $^1\text{H}$  NMR (500 MHz,  $\text{CDCl}_3$ )  $\delta$  8.39-8.34 (m, 1 H), 7.54 (dd,  $J = 8.4$ , 7.0 Hz, 1 H), 7.45 (d,  $J = 7.7$  Hz, 2 H), 7.36 (t,  $J = 7.6$  Hz, 1 H), 7.07 (d,  $J = 12.9$  Hz, 4 H), 6.98 (dd,  $J = 7.5$ , 4.9 Hz, 1 H), 6.90-6.84 (m, 5 H).  $^{13}\text{C}$  NMR (125 MHz,  $\text{CDCl}_3$ )  $\delta$  162.56, 160.61, 158.63, 148.72, 140.89, 138.62, 137.39, 135.14, 131.10 ( $J^3 = 7.5$  Hz), 129.50, 127.47 ( $J^1 = 200$  Hz), 121.08, 114.60 ( $J^2 = 21.3$  Hz).  $^{19}\text{F}$  NMR (471 MHz,  $\text{CDCl}_3$ )  $\delta$  -116.37. HRMS calcd for  $\text{C}_{23}\text{H}_{16}\text{NF}_2$  ( $\text{M}^+ + \text{H}$ ) 344.1245 found 344.1270.

**3.2.3z.** Colorless oil.  $^1\text{H}$  NMR (500 MHz,  $\text{CDCl}_3$ )  $\delta$  8.52 (d,  $J = 5.1$  Hz, 1 H), 7.53-7.44 (m, 3 H), 7.45-7.41 (m, 1 H), 7.32 (d,  $J = 7.8$  Hz, 1 H), 7.19 (dd,  $J = 4.0$ , 2.5 Hz, 2 H), 7.17-7.10 (m, 3 H), 1.78 (s, 3 H).  $^{13}\text{C}$  NMR (125 MHz,  $\text{CDCl}_3$ )  $\delta$  159.49, 146.58, 141.12, 140.66, 137.44, 131.62, 129.89, 129.71, 129.27, 128.34, 127.82, 127.79, 127.43, 126.61, 122.09, 18.83. HRMS calcd for  $\text{C}_{18}\text{H}_{16}\text{N}$  ( $\text{M}^+ + \text{H}$ ) 246.1277 found 246.1307.

**3.2.3aa.** Colorless oil.  $^1\text{H}$  NMR (500 MHz,  $\text{CDCl}_3$ )  $\delta$  8.68-8.63 (m, 1 H), 7.47 (td,  $J = 6.8$ , 6.1, 1.6 Hz, 1 H), 7.38 (td,  $J = 7.5$ , 1.2 Hz, 1 H), 7.31 (dd,  $J = 10.3$ , 7.2 Hz, 2 H), 7.17-7.07 (m, 6 H), 6.90 (t,  $J = 7.9$  Hz, 1 H), 2.21 (s, 3 H).  $^{13}\text{C}$  NMR (125 MHz,  $\text{CDCl}_3$ )  $\delta$  159.60, 148.86, 141.67, 141.24, 139.34, 136.70, 135.67, 129.65, 129.41, 128.03, 127.59, 126.21, 125.61, 121.27, 20.49. HRMS calcd for  $\text{C}_{18}\text{H}_{16}\text{N}$  ( $\text{M}^+ + \text{H}$ ) 246.1277 found 246.1305.

**3.2.3ab.** White solid.  $^1\text{H}$  NMR (500 MHz,  $\text{CDCl}_3$ )  $\delta$  8.33 (d,  $J = 5.7$  Hz, 1 H), 7.31 (s, 3 H), 7.17 (d,  $J = 6.6$  Hz, 6 H), 7.15-7.11 (m, 4 H), 6.95-6.84 (m, 2 H), 2.51 (s, 3 H).  $^{13}\text{C}$  NMR (125 MHz,  $\text{CDCl}_3$ )  $\delta$  159.02, 148.47, 141.78, 141.73, 135.84, 134.80, 130.21,



129.62, 127.60, 126.92, 126.19, 120.72, 21.26. HRMS calcd for  $C_{24}H_{20}N$  ( $M^+ + H$ ) 322.1590 found 322.1619.

**3.2.3ac.** White solid.  $^1H$  NMR (500 MHz,  $CDCl_3$ )  $\delta$  8.35-8.29 (m, 1 H), 7.31 (d,  $J = 7.7$  Hz, 1 H), 7.18 (dt,  $J = 4.9, 2.2$  Hz, 6 H), 7.13 (dd,  $J = 6.8, 3.0$  Hz, 4 H), 7.02 (s, 2 H), 6.91 (dd,  $J = 7.5, 4.9$  Hz, 1 H), 6.86 (d,  $J = 7.8$  Hz, 1 H), 3.93 (s, 3 H).  $^{13}C$  NMR (125 MHz,  $CDCl_3$ )  $\delta$  158.88, 158.78, 148.43, 143.31, 141.62, 134.81, 131.57, 129.55, 127.64, 127.13, 126.39, 120.65, 114.88, 55.50. HRMS calcd for  $C_{24}H_{20}NO$  ( $M^+ + H$ ) 338.1539 found 338.1565.

**3.2.3ad.** Yellow solid.  $^1H$  NMR (500 MHz,  $CDCl_3$ )  $\delta$  8.37 (d,  $J = 5.0$  Hz, 1 H), 7.74 (s, 2 H), 7.36 (td,  $J = 7.7, 1.8$  Hz, 1 H), 7.24-7.18 (m, 6 H), 7.13 (dd,  $J = 6.6, 3.1$  Hz, 4 H), 6.98 (dd,  $J = 7.6, 4.9$  Hz, 1 H), 6.90 (d,  $J = 7.8$  Hz, 1 H).  $^{13}C$  NMR (125 MHz,  $CDCl_3$ )  $\delta$  157.65, 148.71, 142.77, 141.70, 140.23, 135.18, 130.37 ( $J^2 = 63.8$  Hz), 129.48, 127.89, 126.96, 126.50, 126.09 ( $J^3 = 7.5$  Hz), 124.04 ( $J^I = 271.3$  Hz), 121.44.  $^{19}F$  NMR (471 MHz,  $CDCl_3$ )  $\delta$  -62.53. HRMS calcd for  $C_{24}H_{17}NF_3$  ( $M^+ + H$ ) 376.1308 found 376.1330.

**3.2.3ae.** White solid.  $^1H$  NMR (500 MHz,  $CDCl_3$ )  $\delta$  8.48 (d,  $J = 4.9$  Hz, 2 H), 7.58 (dd,  $J = 8.3, 7.0$  Hz, 1 H), 7.50 (d,  $J = 7.5$  Hz, 2H), 7.21-7.14 (m, 10 H), 6.94 (t,  $J = 4.9$  Hz, 1 H).  $^{13}C$  NMR (125 MHz,  $CDCl_3$ )  $\delta$  168.10, 156.02, 141.48, 141.34, 137.64, 129.30, 129.18, 128.72, 127.82, 126.44, 118.05. HRMS calcd for  $C_{22}H_{16}N_2Na$  ( $M^+ + Na$ ) 331.1206 found 331.1216.

**3.2.3af.** Colorless oil.  $^1H$  NMR (500 MHz,  $CDCl_3$ )  $\delta$  7.60 (dd,  $J = 8.5, 6.7$  Hz, 1 H), 7.52 (d,  $J = 7.5$  Hz, 2 H), 7.40 (d,  $J = 1.8$  Hz, 1 H), 7.26 (p,  $J = 3.9$  Hz, 6 H), 7.15 (dt,  $J = 7.1,$

3.9 Hz, 4 H), 7.10 (d,  $J = 2.4$  Hz, 1 H), 6.08 (t,  $J = 2.2$  Hz, 1 H).  $^{13}\text{C}$  NMR (125 MHz,  $\text{CDCl}_3$ )  $\delta$  140.42, 139.36, 138.76, 132.39, 130.09, 129.08, 128.44, 128.26, 128.04, 127.19, 106.03. HRMS calcd for  $\text{C}_{21}\text{H}_{17}\text{N}_2$  ( $\text{M}^+ + \text{H}$ ) 297.1386 found 297.1411.

**3.2.3ag.** White solid.  $^1\text{H}$  NMR (500 MHz,  $\text{CDCl}_3$ )  $\delta$  8.45 (dt,  $J = 4.7, 1.3$  Hz, 1 H), 7.83 (d,  $J = 7.8$ , 1 H), 7.70-7.60 (m, 3 H), 7.54-7.48 (m, 2 H), 7.28-7.21 (m, 3 H), 7.20-7.15 (m, 2 H), 7.14-7.10 (m, 1 H).  $^{13}\text{C}$  NMR (125 MHz,  $\text{CDCl}_3$ )  $\delta$  198.49, 154.65, 148.78, 141.93, 140.73, 138.38, 136.33, 130.91, 129.83, 129.35, 129.11, 128.03, 127.15, 127.08, 125.95, 123.73. HRMS calcd for  $\text{C}_{18}\text{H}_{14}\text{NO}$  ( $\text{M}^+ + \text{H}$ ) 260.1070 found 260.1099.

**3.2.3ah.** Colorless oil.  $^1\text{H}$  NMR (500 MHz,  $\text{CDCl}_3$ )  $\delta$  9.99 (s, 1 H), 7.63 (t,  $J = 7.6$  Hz, 1 H), 7.48-7.41 (m, 9 H), 7.40-7.37 (m, 4 H).  $^{13}\text{C}$  NMR (125 MHz,  $\text{CDCl}_3$ )  $\delta$  193.59, 144.30, 139.66, 133.16, 131.53, 130.40, 129.59, 128.18, 127.66. HRMS calcd for  $\text{C}_{19}\text{H}_{14}\text{ONa}$  ( $\text{M}^+ + \text{Na}$ ) 281.0937 found 281.0965.

## References

- (1) (a) Lyons, T.; Sanford, M. *Chem. Rev.* **2010**, *110*, 1147. (b) *Topics in Current Chemistry: C–H Activation*, Yu, J. Q.; Shi, Z. J., Eds.; Springer: Berlin, 2010. (c) Wencel-Delord, J.; Glorius, F. *Nat. Chem.* **2013**, *5*, 369. (d) Yeung, C. S.; Dong, V. M. *Chem. Rev.* **2011**, *111*, 1215. (e) Yamaguchi, J.; Yamaguchi, A. D.; Itami, K. *Angew. Chem. Int. Ed.* **2012**, *51*, 8960. (f) McMurray, L.; O'Hara, F.; Gaunt, M. J. *Chem. Soc. Rev.* **2011**, *40*, 1885. (g) Ackermann, L.; Vicente, R.; Kapdi, A. R. *Angew. Chem. Int. Ed.* **2009**, *48*, 9792. (h) Alberico, D.; Scott, M. E.; Lautens, M. *Chem. Rev.* **2007**, *107*, 174. (i) Godula, K.; Sames, D. *Science* **2006**, *312*, 67. (j) Bergman, R. G. *Nature* **2007**, *446*, 391. (k) Baudoin, O. *Chem. Soc. Rev.* **2011**, *40*, 4902.
- (2) (a) Kalyani, D.; Deprez, N. R.; Desai, L. V.; Sanford, M. S. *J. Am. Chem. Soc.* **2005**, *127*, 7330. (b) Chiong, H. A.; Pham, Q. N.; Daugulis, O. *J. Am. Chem. Soc.* **2007**, *129*, 9879. (c) Campeau, L. C.; Schipper, D. J.; Fagnou, K. C. *J. Am. Chem. Soc.* **2008**, *130*, 3266. (d) Engle, K. M.; Mei, T. S.; Wasa, M.; Yu, J. Q. *Acc. Chem. Res.* **2012**, *45*, 788. (e) Colby, D. A.; Tsai, A. S.; Bergman, R. G.; Ellman, J. A. *Acc. Chem. Res.* **2012**, *45*, 814. (f) Fang, P.; Li, M.; Ge, H. *J. Am. Chem. Soc.* **2010**, *132*, 11898. (g) Wu, X.; Zhao, Y.; Ge, H. *J. Am. Chem. Soc.* **2014**, *136*, 1789. (h) Ahira, Y.; Chatani, N. *J. Am. Chem. Soc.* **2013**, *135*, 5308. (i) Ahira, Y.; Chatani, N. *J. Am. Chem. Soc.* **2014**, *136*, 898. (j) Norinder, J.; Matsumoto, A.; Yoshikai, N.; Nakamura, E. *J. Am. Chem. Soc.* **2008**, *130*, 5858.

- (3) (a) Dick, A. R.; Hull, K. R.; Sanford, M. S. *J. Am. Chem. Soc.* **2004**, *126*, 2300. (b) Mo, F.; Trzepakowski, L. J.; Dong, G. *Angew. Chem. Int. Ed.* **2012**, *51*, 13075. (c) Shan, G.; Yang, X.; Ma, L.; Rao, Y. *Angew. Chem. Int. Ed.* **2012**, *51*, 13070.
- (4) Shin, K.; Kim, H.; Chang, S. *Acc. Chem. Res.* **2015**, *48*, 1040.
- (5) Engle, K. M.; Mei, T. S.; Wang, X.; Yu, J. Q. *Angew. Chem. Int. Ed.* **2011**, *50*, 1478.
- (6) Johansson-Seechurn, C. C. C.; Kitching, M. O.; Colacot, T. J. Snieckus, V. *Angew. Chem. Int. Ed.* **2012**, *51*, 5062.
- (7) (a) Jia, C.; Kitamura, T.; Fujiwara, Y. *Acc. Chem. Res.* **2001**, *34*, 633. (b) Kakiuchi, F.; Chatani, N. *Adv. Synth. Catal.* **2003**, *345*, 1077. (c) Kakiuchi, F.; Kochi, T. *Synthesis* **2008**, 3013.
- (8) (a) Kametani, Y.; Satoh, T.; Miura, M.; Nomura, M. *Tetrahedron Lett.* **2000**, *41*, 2655. (b) Daugulis, O.; Zaitsev, V. G.; *Angew. Chem. Int. Ed.* **2005**, *44*, 4046. (c) Berman, A. M.; Lewis, J. C.; Bergman, R. G.; Ellman, J. A. *J. Am. Chem. Soc.* **2008**, *130*, 14926. (d) Kim, M.; Kwak, J.; Chang, S. *Angew. Chem. Int. Ed.* **2009**, *48*, 8935. (e) Ackermann, L.; Althammer, A.; Born, R. *Angew. Chem. Int. Ed.* **2006**, *45*, 2619. (f) Roger, J.; Doucet, H. *Org. Biomol. Chem.* **2008**, *6*, 169. (g) Ackermann, L.; Althammer, A.; Fenner, S. *Angew. Chem. Int. Ed.* **2009**, *121*, 207.
- (9) Sun, C. L.; Li, B. J.; Shi, Z. *J. Chem. Commun.* **2010**, 46, 677.
- (10) Zhao, X.; Yeung, C. S.; Dong, V. M. *J. Am. Chem. Soc.* **2010**, *132*, 5837.

- (11) (a) Zhao, X.; Yu, Z. *J. Am. Chem. Soc.* **2008**, *130*, 8136. (b) Ye, W.; Luo, N.; Yu, Z. *Organometallics* **2010**, *29*, 1049. (c) Jin, W.; Yu, Z.; He, W.; Ye, W.; Xiao, W. J. *Org. Lett.* **2009**, *11*, 1317. (d) Pan, F.; Lei, Z. Q.; Wang, H.; Li, H.; Sun, J.; Shi, Z. J. *Angew. Chem. Int. Ed.* **2013**, *52*, 2063.
- (12) Shuai, Q.; Yang, L.; Guo, X.; Basle, O.; Li, C. J. *J. Am. Chem. Soc.* **2010**, *132*, 12212.
- (13) (a) Tsai, A. S.; Tauchert, M. E.; Bergman, R. G.; Ellman, J. A. *J. Am. Chem. Soc.* **2011**, *133*, 1248. (b) Li, Y.; Li, B. J.; Wang, W. H.; Huang, W. P.; Zhang, X. S.; Chen, K.; Shi, Z. J. *Angew. Chem. Int. Ed.* **2011**, *50*, 2115. (c) Zhang, X. S.; Chen, K.; Shi, Z. J. *Chem. Sci.* **2014**, *5*, 2146. (d) Gao, K.; Yoshikai, N. *Chem. Commun.* **2012**, *48*, 4305.
- (14) Greenberg, A.; Breneman, C. M.; Liebman, J. F. *The Amide Linkage: Structural Significance in Chemistry, Biochemistry and Materials Science*; Wiley-VCH: New York, 2003.
- (15) Wencel-Delord, J.; Dröge, T.; Liu, F.; Glorius, F. *Chem. Soc. Rev.* **2011**, *40*, 4740.
- (16) Colby, D. A.; Bergman, R. G.; Ellman, J. A. *Chem. Rev.* **2010**, *110*, 624.
- (17) Ouyang, K.; Hao, W.; Zhang, W. X.; Xi, Z. *Chem. Rev.* **2015**, *115*, 12045.
- (18) Hassan, J.; Sevignon, M.; Gozzi, C.; Schulz, E.; Lemaire, M. *Chem. Rev.* **2002**, *102*, 1359.
- (19) *Metal-Catalyzed Cross-Coupling Reactions and More*, de Meijere, A.; Bräse, S.; Oestreich, M., Eds.; Wiley: New York, 2014.

(20) (a) Meng, G.; Szostak, M. *Org. Lett.* **2015**, *17*, 5144. (b) Meng, G.; Szostak, M. *Angew. Chem. Int. Ed.* **2015**, *54*, 14518. (c) Weires, N. A.; Baker, E. L.; Garg, N. K. *Nat. Chem.* **2016**, *8*, 75. (d) Li, X.; Zou, G. *Chem. Commun.* **2015**, *51*, 5089. (e) Hie, L.; Nathel, N. F. F.; Shah, T. K.; Baker, E. L.; Hong, X.; Yang, Y. F.; Liu, P.; Houk, K. N.; Garg, N. K. *Nature* **2015**, *524*, 79.

(21) Szostak, M.; Aubé, J. *Chem. Rev.* **2013**, *113*, 5701.

(22) (a) Lei, Y.; Wroblewski, A. D.; Golden, J. E.; Powell, D. R.; Aubé, J. *J. Am. Chem. Soc.* **2005**, *127*, 4552. (b) Tobisu, M.; Nakamura, K.; Chatani, N. *J. Am. Chem. Soc.* **2014**, *136*, 5587.

(23) (a) Greenberg, A.; Venanzi, C. A. *J. Am. Chem. Soc.* **1993**, *115*, 6951. (b) Greenberg, A.; Moore, D. T.; DuBois, T. D. *J. Am. Chem. Soc.* **1996**, *118*, 8658. (c) Szostak, R.; Aubé, J.; Szostak, M. *Chem. Commun.* **2015**, *51*, 6395. (d) Szostak, R.; Aubé, J.; Szostak, M. *J. Org. Chem.* **2015**, *80*, 7905. (e) Cox, C.; Lectka, T. *Acc. Chem. Res.* **2000**, *33*, 849.

(24) (a) Hutchby, M.; Houlden, C. E.; Haddow, M. F.; Tyler, S. N.; Lloyd-Jones, G. C.; Booker-Milburn, K. I. *Angew. Chem. Int. Ed.* **2012**, *51*, 548. (b) Glover, S. A. *Tetrahedron* **1998**, *54*, 7229.

(25) (a) Trost, B. M.; Fleming, I. *Comprehensive Organic Synthesis*; Pergamon Press: 1991. (b) Lundberg, H.; Tinnis, F.; Selander, N.; Adolfsson, H. *Chem. Soc. Rev.* **2014**, *43*, 2714. (c) Prabhu, G.; Basavaprabhu; Narendra, N.; Vishwanatha, T. M.; Sureshbabu, V. *Tetrahedron* **2015**, *71*, 2785.

- (26) (a) Brennführer, A.; Neumann, H.; Beller, M. *Angew. Chem. Int. Ed.* **2009**, 48, 4114.
- (b) *Handbook of Organopalladium Chemistry for Organic Synthesis*, Negishi, E., Ed.; Wiley: New York, 2002.

### 3.3 Cooperative strategy for double amide N–C(O) activation/aryl C–H activation

Parts of this section were adapted with permission from the article: “Site-Selective C – H/C–N Activation by Cooperative Catalysis: Primary Amides as Arylating Reagents in Directed C–H Arylation” (*ACS Catal.* **2017**, 7, 7251). Copyright ©2016, American Chemical Society.

#### 3.3.1 Research background

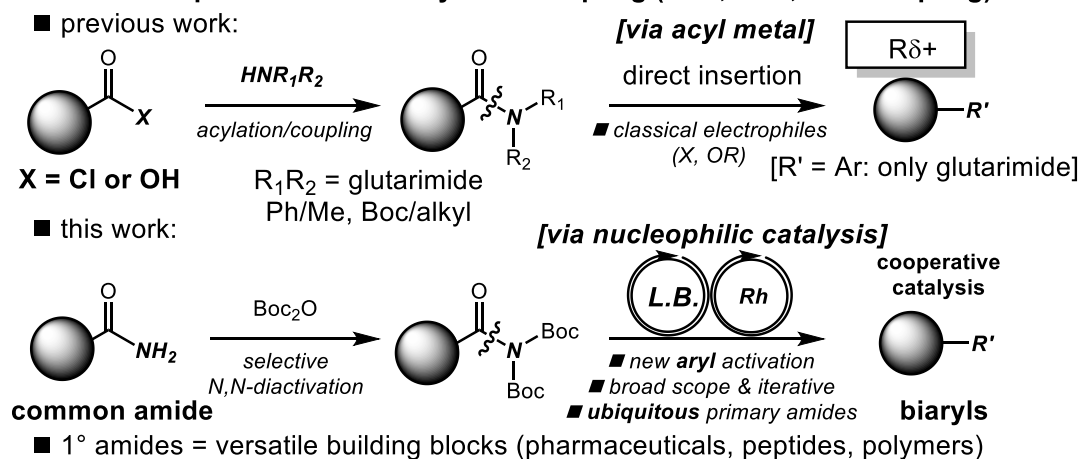
As outlined in Chapters 1-3, amides are among the most important and prevalent functional groups in drug discovery, polymers and chemical industry.<sup>1</sup> At the start of this project, we realized that while numerous methods for the functionalization of amide bonds by selective N–C cleavage<sup>2–6</sup> had been developed utilizing amide Nlp to C=O ground-state destabilization<sup>7,8</sup> (barrier to rotation, amide bond resonance in primary amides of 15-20 kcal/mol), cross-coupling of generic primary amides remained a challenging undertaking. In particular, despite the prevalence of primary amides as fundamental building blocks in pharmaceuticals, agrochemicals and electronic materials,<sup>9,10</sup> chemical methods that induce site-selective N–C insertion/decarbonylation and catalytically generate aryl electrophiles had remained elusive to direct catalytic decarbonylative pathways.<sup>4–6</sup>

At the same time, transition-metal-catalyzed C–H activation has been established as a very attractive method for the preparation of biaryl motifs.<sup>11</sup> Invention of new methods and arylating reagents for the site-selective construction of biaryls utilizing non-acidic C(sp<sup>2</sup>)–H bonds had a wide-ranging impact on the field of chemical synthesis.<sup>12–14</sup>



Recently, a number of processes for the selective activation/C–H cross-coupling of C(sp<sup>2</sup>)–O bonds has been developed.<sup>15</sup> Significant advances have been made in the development of biaryl synthesis, involving C–X and C–C cleavage that enable a range of functional groups to selectively participate in the assembly of biaryls.<sup>16,17</sup>

### Amide electrophiles in decarbonylative coupling (C–C, C–N, C–H coupling)



### *N,N*-Boc<sub>2</sub>-activated 1° amides in direct acyl Negishi cross-coupling

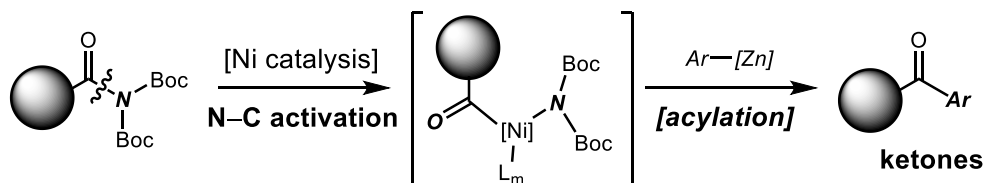


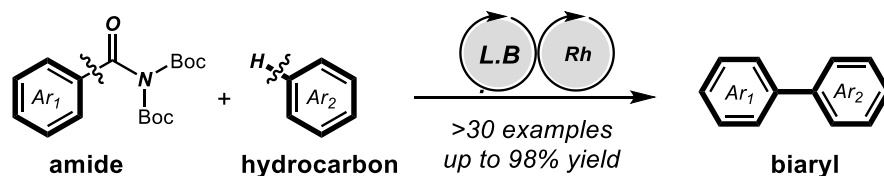
**Figure 3.3.1** Decarbonylative cross-coupling of amides by N–C bond activation: current state-of-the-art and our study.

### 3.3.2 Reaction discovery

Advancing the study on direct functionalization of primary amide bonds (Chapter 2.3) and decarbonylative cross-coupling of amides (Chapter 3.2), we developed a new concept for aryl–aryl coupling that utilizes primary amides as arylating reagents via highly

chemoselective C–N/C–C/C–H cleavages in the absence of oxidants, enabled by the union of cooperative rhodium(I) and Lewis base catalysis.<sup>18</sup> Notably, at the time of this project the method represented the first biaryl synthesis using common primary amides by N–C(O) bond activation (Figure 3.3.1).<sup>4–6</sup> This reaction manifold is very different from the direct acyl cross-coupling of primary amides using Ni catalysis, wherein metal insertion proceeded directly into the amide N–C bond.<sup>8c</sup> This catalytic cooperative strategy enlisting decarbonylation overrides the inherent reactivity of amides<sup>18c</sup> and provided a way for the generic application of common acyclic amides<sup>9,10</sup> as aryl donor components in the synthesis of aryl–aryl motifs.<sup>12</sup>

**A. Decarbonylative cross-coupling of common 1° amides by cooperative catalysis**



**B. Proposed catalytic cycle**

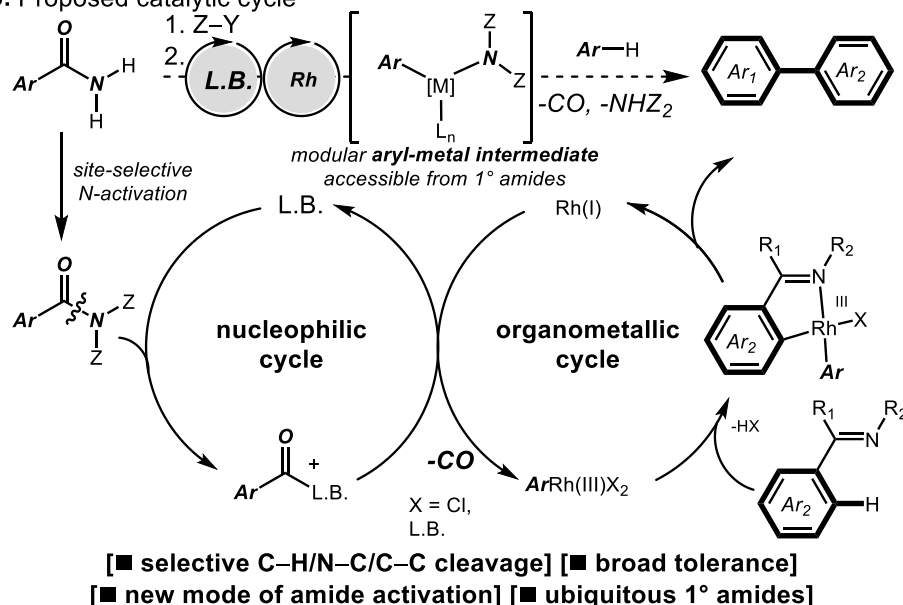
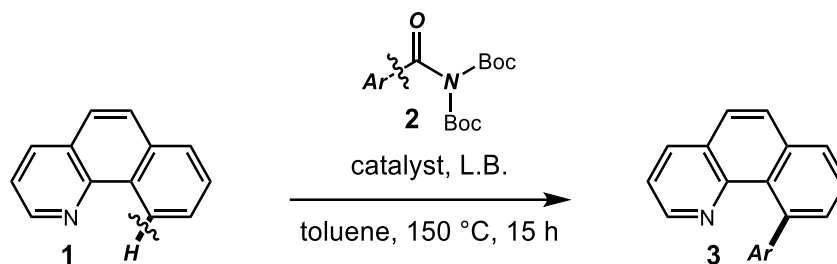


**Figure 3.3.2** Proposed mechanism.

Notable features of our study included: (1) the first use of common primary amides as arylating reagents via redox-neutral decarbonylation; (2) cooperative catalytic system to selectively access aryl metal intermediates from amides by N–C(O)/C–C activation.

Based on our previous work in electrophilic activation of amides and metal-catalysis as outlined in Chapter 2, we proposed the mechanism shown in Figure 3.3.2. In particular, initial amide transacylation enabled by N,N-diacylation of the amide bond<sup>19</sup> ( $E_R = 7.6$  kcal/mol) with an appropriate Lewis base would produced acylammonium intermediate (nucleophilic cycle). In a simultaneous organometallic cycle, Rh(I), would undergo selective oxidative addition into weak acylammonium bond<sup>20,21</sup> to generate a highly reactive acyl-Rh(III) intermediate. The feasibility of our proposal heavily relied on the propensity of the acyl-Rh(III) intermediate to undergo controlled decarbonylation.<sup>22</sup> The subsequent chelation-directed ortho-C–H arylation by aryl–Rh(III)<sup>23</sup> would give diaryl rhodium(III), releasing the Lewis base catalyst. The diarylrhodium(III) would undergo reductive elimination to generate the biaryl C–H activation product and release the Rh(I) catalyst to complete the cycle. Given the marked increase in electrophilicity of the N–C(O) bond following selective N-*tert*-butoxycarbonyl activation,<sup>19</sup> we proposed that the nucleophilic capture of the amide bond would be facile. Protonating the carbonyl group of the N–carbamate would further increase the propensity of the amide bond for metal insertion.<sup>24</sup> Finally, the mild conditions associated with Rh(I)-catalysis<sup>23</sup> would obviate the undesired cleavage of the N–carbamate, which is a common side reaction with nucleophilic Ni(0) and Pd(0)-catalytic systems,<sup>2–6</sup> thus resulting in a broadly applicable process.

### 3.3.3 Reaction optimization



εντρψ	χαταλυστ	νυχλεοπηλε	αδδιτισε	ψιελδ (%) <sup>β</sup>
1	[Pη(χοδ)Xλ] <sub>2</sub>	Bu <sub>3</sub> N	H <sub>2</sub> O	>98
2	[Pη(χοδ) <sub>2</sub> ]BΦ <sub>4</sub>	Bu <sub>3</sub> N	H <sub>2</sub> O	70
3	[Pη(X <sub>2</sub> H <sub>4</sub> ) <sub>2</sub> Xλ] <sub>2</sub>	Bu <sub>3</sub> N	H <sub>2</sub> O	53
4	[Pη(XO) <sub>2</sub> Xλ] <sub>2</sub>	Bu <sub>3</sub> N	H <sub>2</sub> O	35
5	PηXλ(ΠΠη <sub>3</sub> ) <sub>3</sub>	Bu <sub>3</sub> N	H <sub>2</sub> O	<5
6	[Pη(χοδ)Xλ] <sub>2</sub>	Et <sub>3</sub> N	H <sub>2</sub> O	97
7	[Pη(χοδ)Xλ] <sub>2</sub>	ΔIEA	H <sub>2</sub> O	29
8	[Pη(χοδ)Xλ] <sub>2</sub>	ισοθυνολινε	H <sub>2</sub> O	<5
9	[Pη(χοδ)Xλ] <sub>2</sub>	πψριδινε	H <sub>2</sub> O	18
10	[Pη(χοδ)Xλ] <sub>2</sub>	θυνολινε	H <sub>2</sub> O	73
11	[Pη(χοδ)Xλ] <sub>2</sub>	ΔΜΑΠ	H <sub>2</sub> O	<5
12	[Pη(χοδ)Xλ] <sub>2</sub>	Bu <sub>3</sub> N	–	59
13	[Pη(χοδ)Xλ] <sub>2</sub>	–	H <sub>2</sub> O	20
14	[Pη(χοδ)Xλ] <sub>2</sub>	–	–	19
15	[Pη(χοδ)Xλ] <sub>2</sub>	K <sub>2</sub> XO <sub>3</sub>	–	<5
16 <sup>ζ</sup>	[Pη(χοδ)Xλ] <sub>2</sub>	Bu <sub>3</sub> N	H <sub>2</sub> O	20
17 <sup>δ</sup>	[Pη(χοδ)Xλ] <sub>2</sub>	Bu <sub>3</sub> N	H <sub>2</sub> O	79
18	[Pη(χοδ)Xλ] <sub>2</sub>	Bu <sub>3</sub> N	H <sub>3</sub> BO <sub>3</sub>	98

<sup>α</sup>Conditions: **1** (1.0 equiv), amide (1.5 equiv), catalyst (5 mol%), L.B. (30 mol%), additive (1.5 equiv), toluene (0.25 M), 150 °C, 15 h.  
<sup>β</sup><sup>γ</sup>GC/<sup>1</sup>H NMR yields. <sup>δ</sup>Bu<sub>3</sub>N (1.0 equiv). <sup>ε</sup>H<sub>2</sub>O (3.0 equiv). L.B. = Lewis base.

**Table 3.3.1** Optimization of the reaction conditions.<sup>a</sup>

We first optimized the reaction conditions for the cross-coupling of N,N-di-Boc-activated amide (**1**) with benzo[*h*]quinoline as the model substrate for investigation (Table 3.3.1, entry 1). The optimized conditions utilized [Rh(cod)Cl]<sub>2</sub> (5 mol%), *n*-Bu<sub>3</sub>N (30 mol%), H<sub>2</sub>O (1.5 equiv) in toluene at 150 °C, affording the desired product in quantitative yield.

Several key points were noted: (1) all N,N-di-Boc activated amides were prepared directly in one-step from the corresponding benzamides, including substrates with Lewis basic sites.<sup>25</sup> This represented a major difference to the cross-coupling of other types of amides, which at the time of the project had been limited to the coupling of less common tertiary amides that were ultimately from carboxylic acids or aroyl chlorides<sup>2-6</sup> (cf. from ubiquitous primary amides).<sup>9,10</sup> (2) The cooperative catalytic cycle by-passed the direct metal insertion into the amide bond, thus providing a novel catalytic approach that is triggered by complementary reactivity to the conventional organometallic insertion.<sup>18</sup> (3) The high chemoselectivity of the process toward decarbonylation would permit the development of direct arylation reactions with other amide electrophiles,<sup>26</sup> and hinged upon high capability of Rh(I) to facilitate decarbonylation.

Our key optimization results are presented in Table 3.3.1. Various catalysts were tested, and [Rh(cod)Cl]<sub>2</sub> showed the best activity (entries 1-5). Wilkinson's catalyst showed poor reactivity in the coupling. Other Lewis bases could also be used; however, *n*-Bu<sub>3</sub>N provided consistently the best results (entries 6-11). Water was an essential additive in this coupling (entries 12-14). Water could be substituted with H<sub>3</sub>BO<sub>3</sub> without a significant decrease in the reaction efficiency (entries 18). We hypothesized that the amide bond is activated by switchable O-/O-coordination of the N-carbamate.<sup>24</sup> The inclusion of an inorganic base, K<sub>2</sub>CO<sub>3</sub>, inhibited the reaction (entry 15 cf. 14).<sup>16i</sup> As expected, no product formation was observed in the absence of rhodium catalyst and minimal product formation is 14). The optimized stoichiometry was critical to match the

efficiency of both cycles (entries 16-17). Finally, we noted that the process was highly practical; the reaction could be conducted in the presence of air in excellent yields.

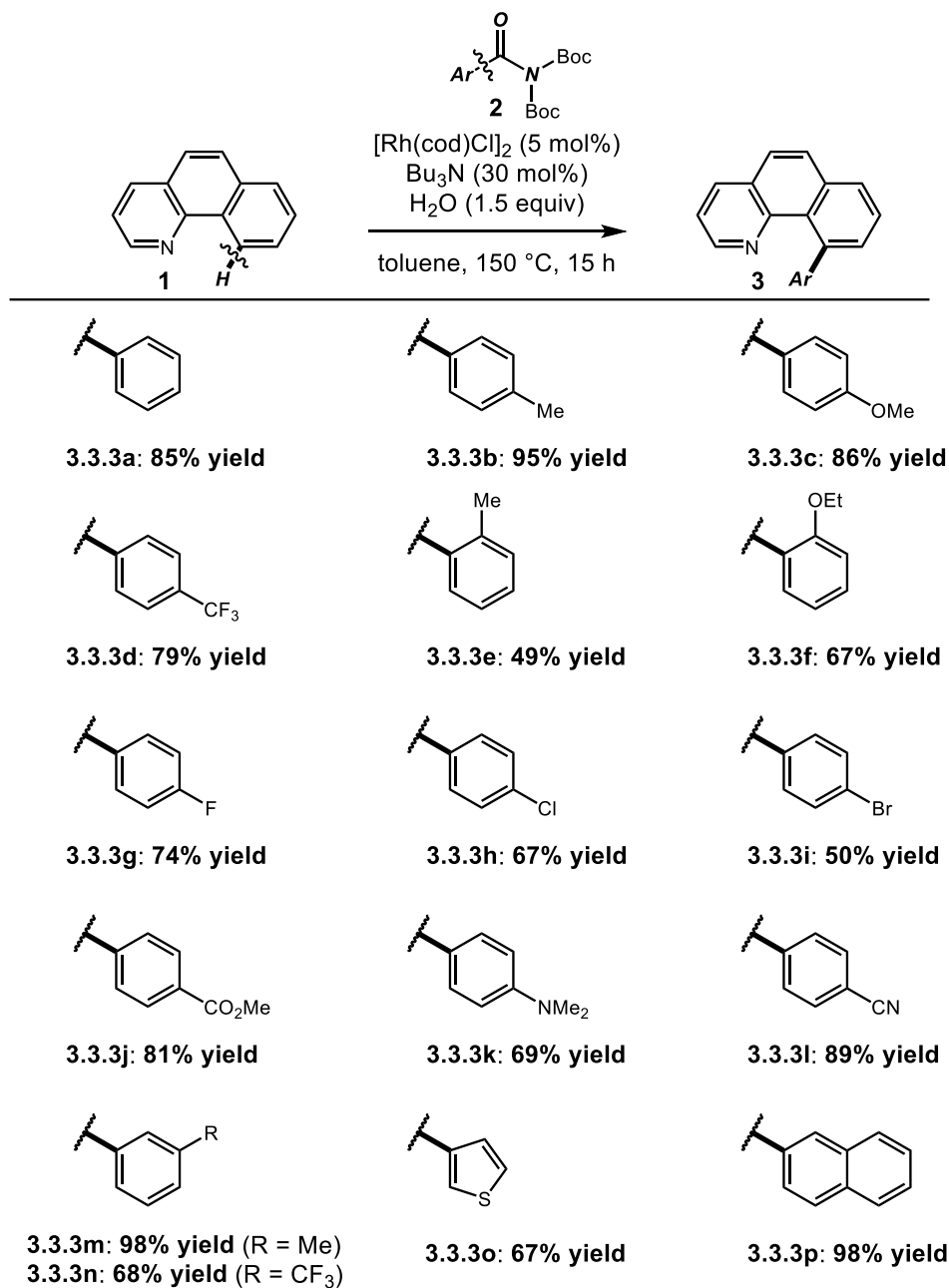


**Figure 3.3.3** Scope of amides.

### 3.3.4 Substrate scope

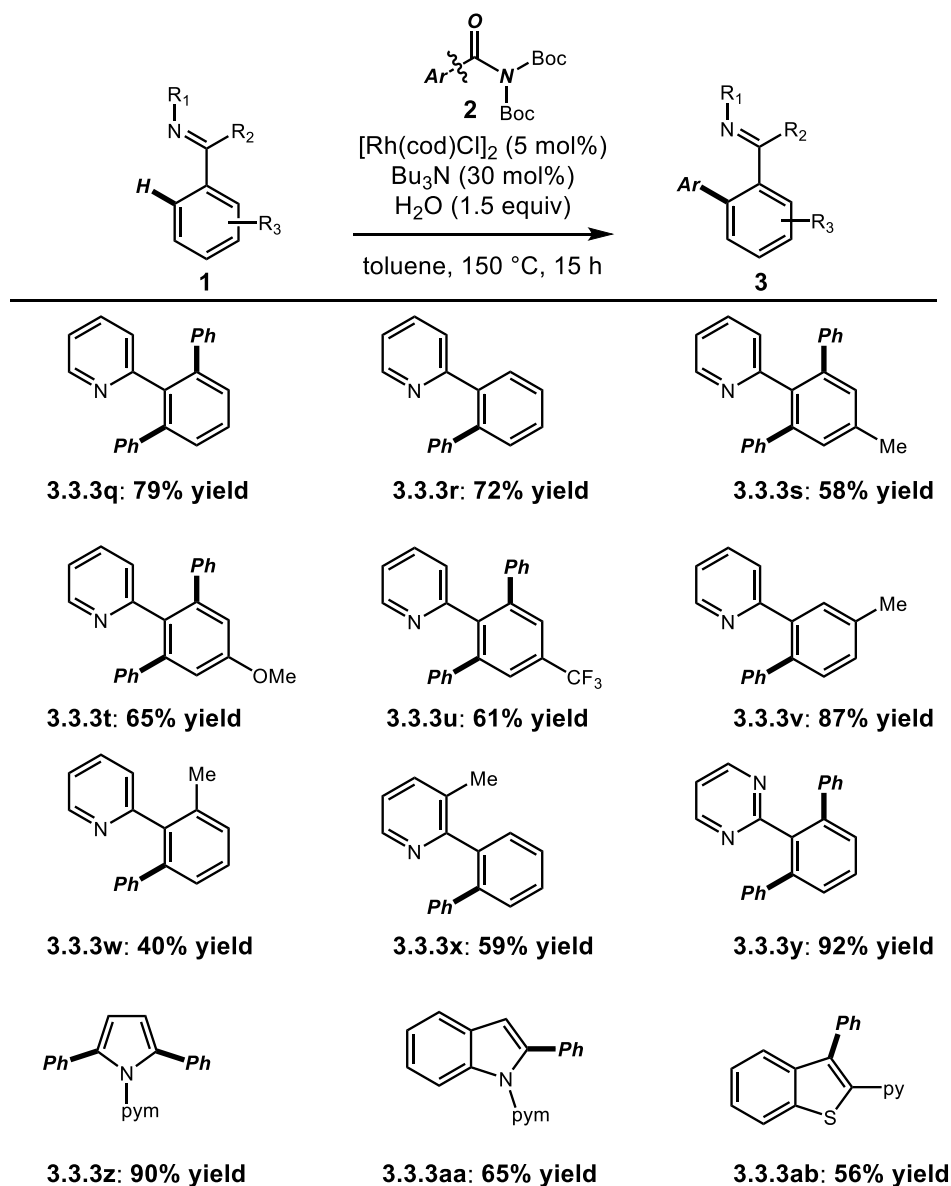


**Figure 3.3.4** Heterocycle scope.

With our newly developed conditions in hand the substrate scope of this novel C–C/C–H coupling was next investigated. As shown in Figure 3.3.3, a wide range of electronically-diverse amides could be employed in this transformation (**3.3.3a-3.3.3d**). Notably, bulky

ortho-substituted amides could be tolerated, albeit in slightly diminished yields (**3.3.3e-3.3.3f**). The latter substrate directly utilized 2-ethoxybenzamide (anti-inflammatory drug),<sup>27</sup> thus highlighting the capacity of the method to engage common substrates bearing primary amide bond. Particularly noteworthy was the functional group tolerance of this method, including fluorides (**3.3.3g**), chlorides (**3.3.3h**), bromides (**3.3.3i**), esters (**3.3.3j**), anilines (**3.3.3k**), and nitriles (**3.3.3l**) that would be problematic with Grignard reagents. Meta-substitution was well-tolerated (**3.3.3m-3.3.3n**). Furthermore, heterocycles (**3.3.3o**) and polyarenes (**3.3.3p**) were compatible with the reaction conditions, despite their capacity to undergo deamidative decomposition. The scope with respect to the directing group component was also evaluated (Figure 3.3.4). Typically, excess of the amide was used, resulting in double C–H arylation (**3.3.3q**). This highly efficient process resulted in selective breaking of 6 different bonds (96.1% efficiency per bond). The example with stoichiometric amount (**3.3.3r**) illustrated that monoarylation was possible with high selectivity. Substrates bearing para- (**3.3.3s-3.3.3u**) and meta-substituents (**3.3.3v**) on the 2-phenylpyridine component were successfully coupled in good yields. The more sterically-demanding ortho-methyl substrate successfully coupled, albeit in lower yield (**3.3.3w**). Ortho-substitution on the pyridine was well-tolerated, resulting in high selectivity for monoarylation (**3.3.3x**). Furthermore, substrates bearing other heterocycles, such as pyrimidine (**3.3.3y**), pyrrole (**3.3.3z**), indole (**3.3.3aa**) and benzothiophene (**3.3.3ab**) were successfully coupled with amides to afford the biaryl products in good to excellent yields.



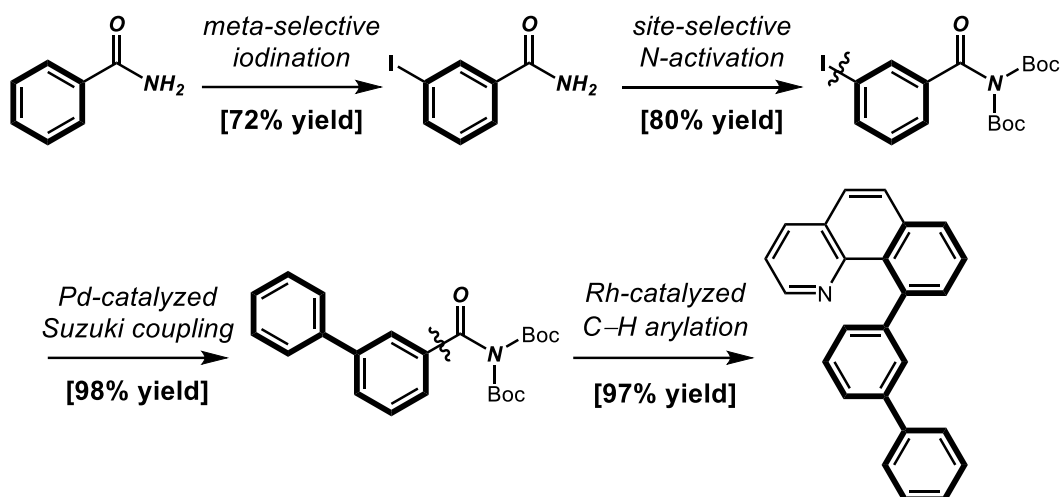


**Figure 3.3.5** Sequential cross-coupling/C–H activation.

The potential of primary benzamides to serve as a directing group was demonstrated in the sequential meta-iodination, Suzuki cross-coupling/C–H arylation (Figure 3.3.5). Importantly, Suzuki cross-coupling was readily performed in the presence of the electrophilic N,N-di-Boc moiety, allowing for a strategically valuable disconnection similar to Weinreb amides,<sup>28</sup> but via a decarbonylative catalytic mechanism.

Importantly, although these reactions conditions were optimized for N,N-di-Boc-benzamides, we found that acyclic N,N-Ph/Boc and N,N-Ph/Ts amides that were readily prepared from common secondary<sup>2,4c</sup> amides underwent arylation in 49–76% yields (Figure 3.3.6). Importantly, this observation showed the potential of cooperative catalytic strategy to engage common secondary acyclic amides as arylating reagents for directed C–H arylation.

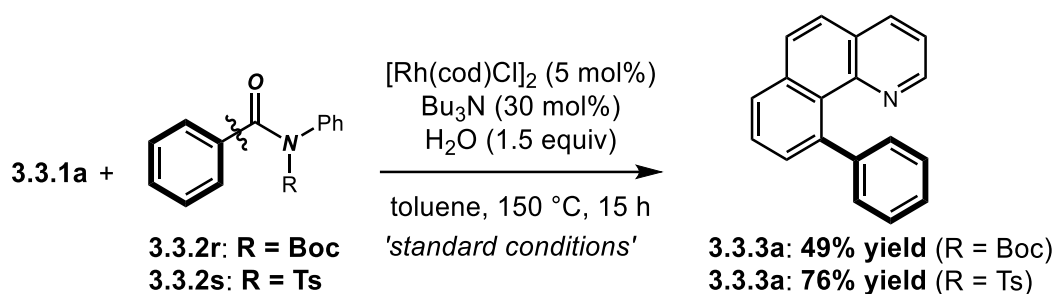


**Figure 3.3.6** C–H activation with acyclic secondary amides.

### 3.3.5 Mechanistic studies

We performed several studies to gain insight into the mechanism (Figure 3.3.7). (1) Intermolecular competition experiments between differently substituted amides (R = 4-MeO/4-CF<sub>3</sub>) revealed that the coupling was relatively insensitive to the electronics of electrophile (1:1). (2) Further competition experiments with differently substituted 2-phenylpyridines revealed the electron-rich arenes were inherently more reactive (R = 4-MeO/4-CF<sub>3</sub>, 4:1). (3) The following order of reactivity of amide electrophiles was established: N,N-Boc<sub>2</sub> ≈ N,N-Ts/Ph >> N,N-Boc/Ph. In addition, anilides (N,N-alkyl/Ph) and N,N-dialkyl amides were recovered unchanged from these conditions, attesting to the potential of the method in chemoselective synthesis and consistent with the electrophilicity of the amide bond undergoing N–C cleavage.<sup>19</sup> (4) Deuterium incorporation experiments revealed reversibility of the C–H activation step at the ortho-position of **3.3.1a**. (5) TON of 480 in Rh in the arylation of **3.3.1a** with **3.3.2a** was determined, showing highly efficient catalysis. Overall, these mechanistic findings strongly supported reversible C–H functionalization by electrophilic substitution pathway.<sup>15e</sup>

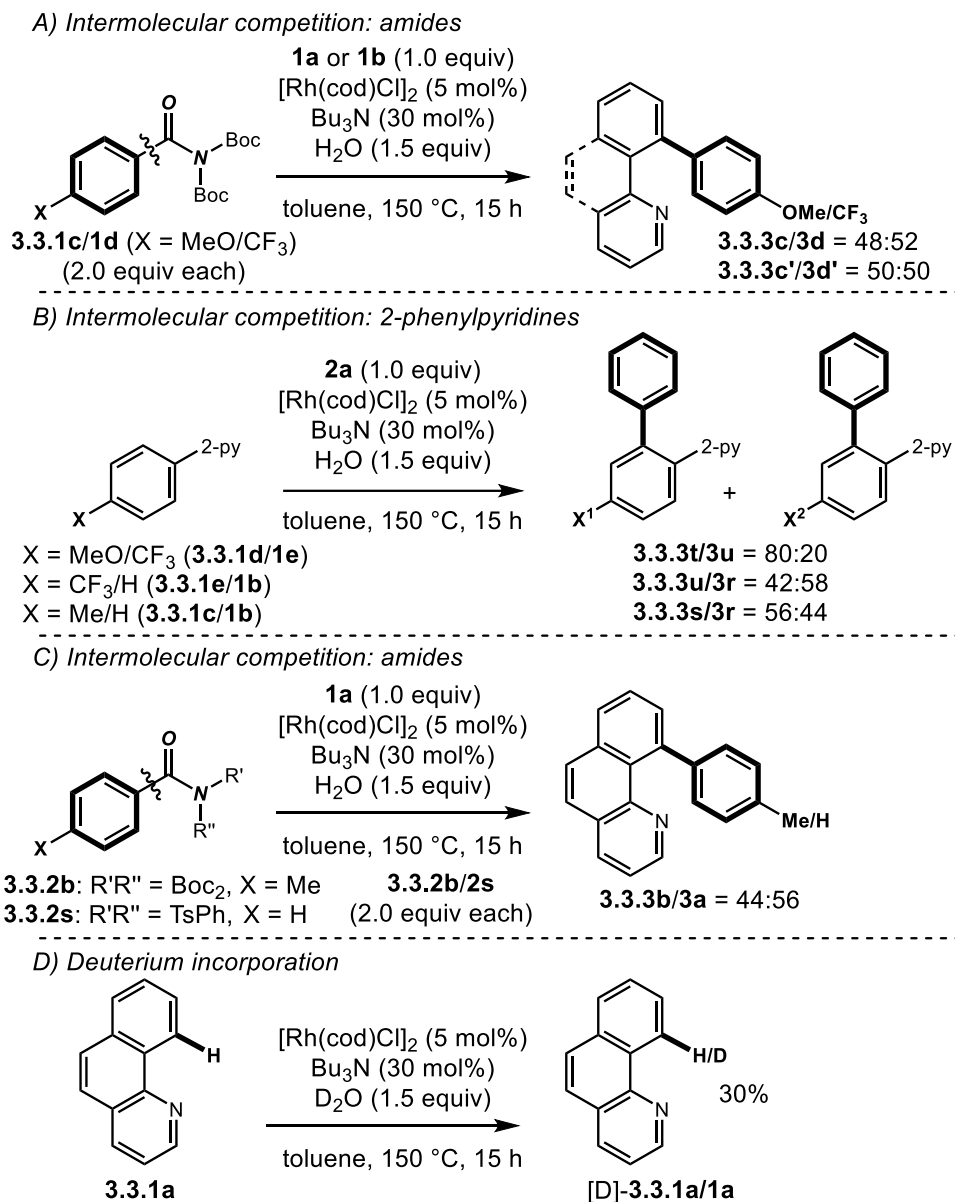


**Figure 3.3.7.** Mechanistic studies.

### 3.3.6 Conclusion

In summary, we developed the first example of arylation of non-acidic C(sp<sup>2</sup>)-H bonds with primary amides as arylating reagents. The most important finding in the successful development of this strategy was the use of cooperative rhodium(I) catalysis and Lewis

base catalysis, which promoted activation of inert C–N bonds in ubiquitous primary amides after selective *N*-*tert*-butoxycarbonyl activation in a highly efficient manner by a sequence of C–N, C–C and C–H bond cleavages. Considering that primary amides are among the most important amide derivatives in small organic molecules and prevalent intermediates in pharmaceuticals and biologically active materials, this concept provided a novel method for generating aryl electrophiles from amides for a potentially broad range of arylations by synergistic catalysis mechanisms.

### 3.3.7 Experimental section

**General procedure for Rh-catalyzed C–H arylation with primary amides.** An oven-dried vial equipped with a stir bar was charged with a C–H activation substrate (neat, 1.0 equiv), an amide substrate (typically, 1.5–3.0 equiv), [Rh(cod)Cl]<sub>2</sub> (typically, 5 mol%), water (typically, 1.5 equiv), Bu<sub>3</sub>N (typically, 30 mol%). Toluene (typically, 0.25 M) was added with vigorous stirring at room temperature, the reaction mixture was placed in a preheated oil bath at 150 °C, and stirred for an indicated time at 150 °C. After the indicated time, the reaction mixture was diluted with CH<sub>2</sub>Cl<sub>2</sub> (10 mL), filtered, and concentrated. The sample was analyzed by GC-MS and <sup>1</sup>H NMR (CDCl<sub>3</sub>, 500 MHz) to obtain conversion, yield and selectivity using internal standard and comparison with authentic samples. Purification by chromatography on silica gel (hexanes/ethyl acetate) afforded the title product.

**3.3.3a.** Colorless oil. <sup>1</sup>H NMR (500 MHz, CDCl<sub>3</sub>) δ 8.49 (dd, *J* = 4.3, 1.9 Hz, 1 H), 8.12 (dd, *J* = 8.0, 1.9 Hz, 1 H), 7.98 (d, *J* = 7.9 Hz, 1 H), 7.91 (d, *J* = 8.8 Hz, 1 H), 7.74 (dd, *J*

= 8.3, 6.6 Hz, 2 H), 7.62 (d,  $J = 7.2$  Hz, 1 H), 7.51-7.42 (m, 5 H), 7.36 (dd,  $J = 7.9$ , 4.3 Hz, 1 H).  $^{13}\text{C}$  NMR (125 MHz,  $\text{CDCl}_3$ )  $\delta$  146.90, 146.86, 146.47, 141.76, 135.23, 135.03, 131.54, 129.06, 128.78, 128.33, 127.99, 127.42, 127.26, 127.08, 125.97, 125.73, 121.10.

**3.3.3b.** Colorless oil.  $^1\text{H}$  NMR (500 MHz,  $\text{CDCl}_3$ )  $\delta$  8.50 (dd,  $J = 4.3$ , 1.8 Hz, 1 H), 8.11 (d,  $J = 8.0$  Hz, 1 H), 7.94 (d,  $J = 7.9$  Hz, 1 H), 7.88 (d,  $J = 8.7$  Hz, 1 H), 7.74-7.68 (m, 2 H), 7.58 (d,  $J = 7.3$  Hz, 1 H), 7.36 (dd,  $J = 8.0$ , 4.3 Hz, 1 H), 7.31-7.28 (m, 2 H), 7.25 (d,  $J = 7.9$  Hz, 2 H), 2.50 (s, 3 H).  $^{13}\text{C}$  NMR (125 MHz,  $\text{CDCl}_3$ )  $\delta$  146.93, 146.83, 143.44, 141.73, 135.21, 135.10, 135.04, 131.67, 129.07, 128.64, 128.33, 128.11, 127.80, 127.22, 127.06, 125.88, 121.03, 21.34.

**3.3.3c.** White solid.  $^1\text{H}$  NMR (500 MHz,  $\text{CDCl}_3$ )  $\delta$  8.52 (d,  $J = 5.7$  Hz, 1 H), 8.13-8.09 (m, 1 H), 7.93 (d,  $J = 7.7$  Hz, 1 H), 7.88 (d,  $J = 8.7$  Hz, 1 H), 7.70 (t,  $J = 8.5$  Hz, 2 H), 7.58 (d,  $J = 7.1$  Hz, 1 H), 7.35 (dd,  $J = 12.4$ , 6.2 Hz, 3 H), 7.00 (d,  $J = 8.5$  Hz, 2 H), 3.95 (s, 3 H).  $^{13}\text{C}$  NMR (125 MHz,  $\text{CDCl}_3$ )  $\delta$  157.96, 146.97, 146.87, 141.38, 138.90, 135.26, 135.10, 131.73, 129.82, 129.12, 128.36, 127.77, 127.23, 127.07, 125.89, 121.04, 112.84, 55.32.

**3.3.3d.** White solid.  $^1\text{H}$  NMR (500 MHz,  $\text{CDCl}_3$ )  $\delta$  8.44 (dd,  $J = 4.3$ , 1.8 Hz, 1 H), 8.13 (dd,  $J = 8.0$ , 1.9 Hz, 1 H), 8.00 (dd,  $J = 8.0$ , 1.3 Hz, 1 H), 7.91 (d,  $J = 8.8$  Hz, 1 H), 7.78-7.72 (m, 2 H), 7.69 (d,  $J = 8.0$  Hz, 2 H), 7.53 (dd,  $J = 7.2$ , 1.3 Hz, 1 H), 7.49 (d,  $J = 7.9$  Hz, 2 H), 7.37 (dd,  $J = 8.0$ , 4.3 Hz, 1 H).  $^{13}\text{C}$  NMR (125 MHz,  $\text{CDCl}_3$ )  $\delta$  150.22, 146.92, 146.40, 140.21, 135.33, 134.95, 131.11, 128.99, 128.83, 128.55, 128.22, 127.79 ( $J^2 =$

31.3 Hz), 127.29, 127.08, 126.15, 124.81 ( $J^I = 270.0$  Hz), 124.29 ( $J^3 = 7.5$  Hz), 121.28.

$^{19}\text{F}$  NMR (471 MHz,  $\text{CDCl}_3$ )  $\delta$  -61.96.

**3.3.3e.** Colorless oil.  $^1\text{H}$  NMR (500 MHz,  $\text{CDCl}_3$ )  $\delta$  8.48 (dd,  $J = 4.3, 1.9$  Hz, 1 H), 8.11 (d,  $J = 8.0$  Hz, 1 H), 8.00 (d,  $J = 8.0$  Hz, 1 H), 7.92 (d,  $J = 8.8$  Hz, 1 H), 7.79-7.72 (m, 2 H), 7.54 (d,  $J = 7.2$  Hz, 1 H), 7.38-7.31 (m, 4 H), 7.25 (d,  $J = 7.1$  Hz, 1 H), 1.93 (s, 3 H).

$^{13}\text{C}$  NMR (125 MHz,  $\text{CDCl}_3$ )  $\delta$  147.49, 147.05, 146.48, 141.07, 135.91, 135.10, 134.68, 130.76, 129.48, 128.78, 127.94, 127.28, 126.98, 125.96, 125.86, 125.16, 121.00, 20.27.

**3.3.3f.** Colorless oil.  $^1\text{H}$  NMR (500 MHz,  $\text{CDCl}_3$ )  $\delta$  8.47 (dd,  $J = 4.2, 1.7$  Hz, 1 H), 8.10 (d,  $J = 9.6$  Hz, 1 H), 7.97-7.92 (m, 1 H), 7.88 (d,  $J = 8.7$  Hz, 1 H), 7.76-7.67 (m, 2 H), 7.58 (d,  $J = 7.2$  Hz, 1 H), 7.41-7.32 (m, 3 H), 7.11 (t,  $J = 7.7$  Hz, 1 H), 6.89 (d,  $J = 8.0$  Hz, 1 H), 3.91-3.79 (m, 1 H), 3.60-3.47 (m, 1 H), 0.55 (t,  $J = 7.0$  Hz, 3 H).  $^{13}\text{C}$  NMR (125 MHz,  $\text{CDCl}_3$ )  $\delta$  156.78, 147.50, 146.87, 138.00, 136.23, 134.93, 134.41, 131.43, 129.87, 129.15, 128.42, 127.94, 127.36, 127.29, 126.59, 125.54, 120.86, 120.26, 111.03, 63.65, 14.16. HRMS calcd for  $\text{C}_{21}\text{H}_{16}\text{NO}$  ( $\text{M}^+ - \text{H}$ ) 298.1226, found 298.1244.

**3.3.3g.** White solid.  $^1\text{H}$  NMR (500 MHz,  $\text{CDCl}_3$ )  $\delta$  8.50 (d,  $J = 4.3$  Hz, 1 H), 8.12 (d,  $J = 8.0$  Hz, 1 H), 7.97 (dd,  $J = 7.8, 1.4$  Hz, 1 H), 7.89 (d,  $J = 8.8$  Hz, 1 H), 7.75-7.69 (m, 2 H), 7.56 (dd,  $J = 7.3, 1.4$  Hz, 1 H), 7.39-7.32 (m, 3 H), 7.17-7.11 (m, 2 H).  $^{13}\text{C}$  NMR (125 MHz,  $\text{CDCl}_3$ )  $\delta$  161.59 ( $J^I = 242.5$  Hz), 146.88, 146.75, 142.26 ( $J^d = 2.5$  Hz), 140.68, 135.31, 135.04, 131.52, 130.18 ( $J^3 = 7.5$  Hz), 129.06, 128.32, 128.18, 127.29, 127.05, 126.03, 121.17, 114.15 ( $J^2 = 21.3$  Hz).  $^{19}\text{F}$  NMR (471 MHz,  $\text{CDCl}_3$ )  $\delta$  -118.08.

**3.3.3h.** Colorless oil.  $^1\text{H}$  NMR (500 MHz,  $\text{CDCl}_3$ )  $\delta$  8.49 (dd,  $J = 4.2, 1.7$  Hz, 1 H), 8.12 (d,  $J = 8.0$  Hz, 1 H), 7.97 (d,  $J = 7.7$  Hz, 1 H), 7.89 (d,  $J = 8.8$  Hz, 1 H), 7.72 (dd,  $J = 14.8, 8.1$  Hz, 2 H), 7.53 (d,  $J = 6.7$  Hz, 1 H), 7.42-7.35 (m, 3 H), 7.32 (d,  $J = 8.4$  Hz, 2 H).  $^{13}\text{C}$  NMR (125 MHz,  $\text{CDCl}_3$ )  $\delta$  146.90, 146.63, 144.89, 140.40, 135.29, 134.99, 131.52, 131.34, 130.12, 128.92, 128.28, 128.26, 127.47, 127.27, 127.05, 126.06, 121.20.

**3.3.3i.** White solid.  $^1\text{H}$  NMR (500 MHz,  $\text{CDCl}_3$ )  $\delta$  8.49 (dd,  $J = 4.2, 1.7$  Hz, 1 H), 8.13 (dd,  $J = 8.0, 1.7$  Hz, 1 H), 7.97 (d,  $J = 7.8$  Hz, 1 H), 7.89 (d,  $J = 8.8$  Hz, 1 H), 7.76-7.68 (m, 2 H), 7.53 (t,  $J = 7.7$  Hz, 3 H), 7.37 (dd,  $J = 8.0, 4.3$  Hz, 1 H), 7.26 (d,  $J = 8.3$  Hz, 2 H).  $^{13}\text{C}$  NMR (125 MHz,  $\text{CDCl}_3$ )  $\delta$  146.91, 146.60, 145.38, 140.37, 135.29, 134.99, 131.27, 130.50, 130.40, 128.86, 128.30, 128.24, 127.26, 127.05, 126.06, 121.21, 119.65.

**3.3.3j.** White solid.  $^1\text{H}$  NMR (500 MHz,  $\text{CDCl}_3$ )  $\delta$  8.41 (dd,  $J = 4.3, 1.8$  Hz, 1 H), 8.15-8.09 (m, 3 H), 7.98 (d,  $J = 7.9$  Hz, 1 H), 7.90 (d,  $J = 8.8$  Hz, 1 H), 7.76-7.70 (m, 2 H), 7.54 (d,  $J = 7.3$  Hz, 1 H), 7.47-7.43 (m, 2 H), 7.35 (dd,  $J = 8.0, 4.3$  Hz, 1 H), 4.01 (s, 3 H).  $^{13}\text{C}$  NMR (125 MHz,  $\text{CDCl}_3$ )  $\delta$  167.62, 151.62, 146.89, 146.44, 140.57, 135.26, 134.92, 130.98, 128.83, 128.81, 128.77, 128.44, 128.20, 127.40, 127.26, 127.04, 126.10, 121.25, 52.00.

**3.3.3k.** White solid.  $^1\text{H}$  NMR (500 MHz,  $\text{CDCl}_3$ )  $\delta$  8.54 (d,  $J = 5.9$  Hz, 1 H), 8.10 (d,  $J = 9.7$  Hz, 1 H), 7.87 (dd,  $J = 14.5, 8.2$  Hz, 2 H), 7.71-7.65 (m, 2 H), 7.59 (d,  $J = 7.3$  Hz, 1 H), 7.35 (dd,  $J = 7.9, 4.3$  Hz, 1 H), 7.30 (d,  $J = 8.9$  Hz, 2 H), 6.84 (d,  $J = 8.6$  Hz, 2 H), 3.05 (s, 6 H).  $^{13}\text{C}$  NMR (125 MHz,  $\text{CDCl}_3$ )  $\delta$  149.08, 147.22, 146.87, 141.92, 135.17,

135.16, 135.00, 131.80, 129.56, 128.37, 127.31, 127.14, 127.07, 125.76, 120.92, 112.05, 40.97.

**3.3.3l.** White solid.  $^1\text{H}$  NMR (500 MHz,  $\text{CDCl}_3$ )  $\delta$  8.41 (d,  $J = 3.5$  Hz, 1 H), 8.14 (d,  $J = 7.9$  Hz, 1 H), 8.01 (d,  $J = 7.9$  Hz, 1 H), 7.91 (d,  $J = 8.8$  Hz, 1 H), 7.78-7.72 (m, 2 H), 7.70 (d,  $J = 8.0$  Hz, 2 H), 7.49 (d,  $J = 7.2$  Hz, 1 H), 7.46 (d,  $J = 8.0$  Hz, 2 H), 7.38 (dd,  $J = 7.9$ , 4.3 Hz, 1 H).  $^{13}\text{C}$  NMR (125 MHz,  $\text{CDCl}_3$ )  $\delta$  151.58, 146.89, 146.16, 139.64, 135.43, 134.92, 131.26, 130.76, 129.50, 128.84, 128.62, 128.19, 127.33, 127.10, 126.27, 121.42, 119.80, 109.23.

**3.3.3m.** Colorless oil.  $^1\text{H}$  NMR (500 MHz,  $\text{CDCl}_3$ )  $\delta$  8.47 (s, 1 H), 8.11 (d,  $J = 7.9$  Hz, 1 H), 7.94 (d,  $J = 7.8$  Hz, 1 H), 7.88 (d,  $J = 8.7$  Hz, 1 H), 7.71 (t,  $J = 9.4$  Hz, 2 H), 7.58 (d,  $J = 7.2$  Hz, 1 H), 7.35 (dd,  $J = 7.4$ , 3.9 Hz, 1 H), 7.31 (t,  $J = 7.6$  Hz, 1 H), 7.24 (s, 1 H), 7.19 (t,  $J = 8.9$  Hz, 2 H), 2.43 (s, 3 H).  $^{13}\text{C}$  NMR (125 MHz,  $\text{CDCl}_3$ )  $\delta$  146.86, 146.25, 141.80, 136.83, 135.17, 135.00, 131.52, 129.30, 129.01, 128.30, 127.84, 127.20, 127.17, 127.02, 126.41, 125.99, 125.88, 121.05, 21.62.

**3.3.3n.** Colorless oil.  $^1\text{H}$  NMR (500 MHz,  $\text{CDCl}_3$ )  $\delta$  8.41 (d,  $J = 4.3$  Hz, 1 H), 8.13 (d,  $J = 8.0$  Hz, 1 H), 8.00 (d,  $J = 8.0$  Hz, 1 H), 7.90 (d,  $J = 8.8$  Hz, 1 H), 7.77-7.71 (m, 2 H), 7.68-7.63 (m, 2 H), 7.59-7.53 (m, 3 H), 7.36 (dd,  $J = 8.1$ , 4.3 Hz, 1 H).  $^{13}\text{C}$  NMR (125 MHz,  $\text{CDCl}_3$ )  $\delta$  146.92, 146.87, 146.42, 140.06, 135.34, 135.00, 131.87, 131.35, 129.44 ( $J^2 = 63.8$  Hz), 128.83, 128.59, 128.25, 127.73, 127.27, 127.09, 126.15, 126.11, 124.63 ( $J^1 = 270.0$  Hz), 122.42 ( $J^3 = 7.5$  Hz), 121.32.  $^{19}\text{F}$  NMR (471 MHz,  $\text{CDCl}_3$ )  $\delta$  -62.34.



**3.3.3o.** Colorless oil.  $^1\text{H}$  NMR (500 MHz,  $\text{CDCl}_3$ )  $\delta$  8.62 (s, 1 H), 8.13 (d,  $J = 7.9$  Hz, 1 H), 7.98 (d,  $J = 7.7$  Hz, 1 H), 7.87 (d,  $J = 8.7$  Hz, 1 H), 7.71 (dt,  $J = 21.7, 7.6$  Hz, 3 H), 7.44-7.37 (m, 2 H), 7.18-7.12 (m, 1 H), 7.07 (s, 1 H).  $^{13}\text{C}$  NMR (125 MHz,  $\text{CDCl}_3$ )  $\delta$  148.09, 147.19, 146.60, 135.27, 134.95, 133.62, 132.75, 130.07, 129.04, 128.14, 127.38, 126.84, 126.22, 126.15, 124.73, 124.34, 121.29. HRMS calcd for  $\text{C}_{17}\text{H}_{12}\text{NS}$  ( $\text{M}^+ + \text{H}$ ) 262.0685, found 262.0702.

**3.3.3p.** White solid.  $^1\text{H}$  NMR (500 MHz,  $\text{CDCl}_3$ )  $\delta$  8.36-8.32 (m, 1 H), 8.12 (d,  $J = 7.8$  Hz, 1 H), 7.99 (d,  $J = 7.8$  Hz, 1 H), 7.92 (d,  $J = 7.1$  Hz, 4 H), 7.80 (d,  $J = 8.4$  Hz, 1 H), 7.78-7.72 (m, 2 H), 7.67 (d,  $J = 7.0$  Hz, 1 H), 7.55-7.49 (m, 2 H), 7.47 (d,  $J = 8.4$  Hz, 1 H), 7.32 (dd,  $J = 7.3, 4.4$  Hz, 1 H).  $^{13}\text{C}$  NMR (125 MHz,  $\text{CDCl}_3$ )  $\delta$  146.93, 146.67, 144.48, 141.46, 135.20, 135.03, 133.77, 132.14, 131.95, 129.44, 129.04, 128.33, 128.15, 128.08, 127.59, 127.23, 127.20, 125.97, 125.66, 125.52, 125.37, 125.16, 121.12.

**3.3.3q.** White solid.  $^1\text{H}$  NMR (500 MHz,  $\text{CDCl}_3$ )  $\delta$  8.34 (dt,  $J = 5.0, 1.2$  Hz, 1 H), 7.55 (dd,  $J = 8.5, 6.7$  Hz, 1 H), 7.51-7.46 (m, 2 H), 7.32 (td,  $J = 7.7, 1.9$  Hz, 1 H), 7.18 (qd,  $J = 5.0, 1.7$  Hz, 6 H), 7.13 (dt,  $J = 7.0, 2.7$  Hz, 4 H), 6.95-6.89 (m, 2 H).  $^{13}\text{C}$  NMR (125 MHz,  $\text{CDCl}_3$ )  $\delta$  158.94, 148.50, 141.85, 141.60, 138.52, 134.84, 129.64, 129.47, 128.16, 127.63, 126.79, 126.26, 120.86.

**3.3.3r.** Colorless oil.  $^1\text{H}$  NMR (500 MHz,  $\text{CDCl}_3$ )  $\delta$  8.70-8.62 (m, 1 H), 7.73 (dd,  $J = 5.7, 3.3$  Hz, 1 H), 7.49 (m, 3 H), 7.41 (td,  $J = 7.7, 1.8$  Hz, 1 H), 7.26 (qd,  $J = 4.7, 1.6$  Hz, 3 H), 7.15-7.12 (m, 1 H), 6.91 (d,  $J = 7.9$  Hz, 1 H).  $^{13}\text{C}$  NMR (125 MHz,  $\text{CDCl}_3$ )  $\delta$  159.27,

149.45, 141.37, 140.62, 139.51, 135.16, 130.49, 130.48, 129.72, 128.51, 128.05, 127.65, 126.69, 125.39, 121.33.

**3.3.3s.** Colorless oil.  $^1\text{H}$  NMR (500 MHz,  $\text{CDCl}_3$ )  $\delta$  8.33 (s, 1 H), 7.30 (s, 3 H), 7.14 (d,  $J$  = 16.5 Hz, 10 H), 6.95-6.86 (m, 2 H), 2.51 (s, 3 H).  $^{13}\text{C}$  NMR (125 MHz,  $\text{CDCl}_3$ )  $\delta$  159.00, 148.46, 141.77, 141.71, 137.81, 135.82, 134.82, 130.20, 129.61, 127.60, 126.92, 126.19, 120.73, 21.25.

**3.3.3t.** White solid.  $^1\text{H}$  NMR (500 MHz,  $\text{CDCl}_3$ )  $\delta$  8.32 (d,  $J$  = 4.4 Hz, 1H), 7.32-7.27 (m, 2 H), 7.18 (dd,  $J$  = 5.3, 1.9 Hz, 6 H), 7.13 (dd,  $J$  = 6.8, 3.0 Hz, 4 H), 7.02 (s, 2 H), 6.93-6.89 (m, 1 H), 6.86 (d,  $J$  = 7.8 Hz, 1 H), 3.93 (s, 3 H).  $^{13}\text{C}$  NMR (125 MHz,  $\text{CDCl}_3$ )  $\delta$  158.88, 158.78, 148.43, 143.31, 141.62, 134.81, 131.57, 129.55, 127.64, 127.13, 126.39, 120.65, 114.88, 55.50.

**3.3.3u.** White solid.  $^1\text{H}$  NMR (500 MHz,  $\text{CDCl}_3$ )  $\delta$  8.37 (d,  $J$  = 5.0 Hz, 1 H), 7.74 (s, 2 H), 7.36 (td,  $J$  = 7.7, 1.8 Hz, 1 H), 7.24-7.18 (m, 6 H), 7.13 (dd,  $J$  = 6.6, 3.1 Hz, 4 H), 6.98 (dd,  $J$  = 7.6, 4.9 Hz, 1 H), 6.90 (d,  $J$  = 7.8 Hz, 1 H).  $^{13}\text{C}$  NMR (125 MHz,  $\text{CDCl}_3$ )  $\delta$  157.65, 148.71, 142.77, 141.70, 140.23, 135.18, 130.37 ( $J^2$  = 63.8 Hz), 129.48, 127.89, 126.96, 126.50, 126.09 ( $J^3$  = 7.5 Hz), 124.04 ( $J^I$  = 271.3 Hz), 121.44.  $^{19}\text{F}$  NMR (471 MHz,  $\text{CDCl}_3$ )  $\delta$  -62.53.

**3.3.3v.** White solid.  $^1\text{H}$  NMR (500 MHz,  $\text{CDCl}_3$ )  $\delta$  8.66 (d,  $J$  = 4.8 Hz, 1 H), 7.55 (s, 1 H), 7.38 (dd,  $J$  = 17.7, 8.0 Hz, 2 H), 7.30 (d,  $J$  = 7.8 Hz, 1 H), 7.23 (s, 3 H), 7.18-7.14 (m, 2H), 7.14-7.09 (m, 1 H), 6.88 (d,  $J$  = 7.9 Hz, 1 H), 2.47 (s, 3 H).  $^{13}\text{C}$  NMR (125 MHz,

CDCl<sub>3</sub>)  $\delta$  159.34, 149.38, 141.30, 139.20, 137.81, 137.43, 135.15, 131.07, 130.46, 129.74, 129.29, 128.01, 126.50, 125.49, 121.29, 21.09.

**3.3.3w.** White solid. <sup>1</sup>H NMR (500 MHz, CDCl<sub>3</sub>)  $\delta$  8.65 (d,  $J$  = 4.8 Hz, 1 H), 7.47 (t,  $J$  = 8.3 Hz, 1 H), 7.38 (t,  $J$  = 7.6 Hz, 1 H), 7.31 (d,  $J$  = 10.2 Hz, 2 H), 7.17-7.07 (m, 6 H), 6.90 (d,  $J$  = 7.8 Hz, 1 H), 2.21 (s, 3 H). <sup>13</sup>C NMR (125 MHz, CDCl<sub>3</sub>)  $\delta$  159.60, 148.85, 141.67, 141.24, 139.34, 136.70, 135.67, 129.65, 129.41, 128.02, 127.58, 126.21, 125.61, 121.27, 20.49.

**3.3.3x.** Colorless oil. <sup>1</sup>H NMR (500 MHz, CDCl<sub>3</sub>)  $\delta$  8.52 (d,  $J$  = 4.5 Hz, 1 H), 7.53-7.45 (m, 3 H), 7.43 (d,  $J$  = 6.6 Hz, 1 H), 7.32 (d,  $J$  = 7.6 Hz, 1 H), 7.22-7.16 (m, 3 H), 7.16-7.11 (m, 3 H), 1.78 (s, 3 H). <sup>13</sup>C NMR (125 MHz, CDCl<sub>3</sub>)  $\delta$  159.49, 146.58, 141.12, 140.66, 139.47, 137.44, 131.62, 129.89, 129.71, 129.27, 128.34, 127.79, 127.43, 126.84, 126.61, 122.09, 18.83.

**3.3.3y.** White solid. <sup>1</sup>H NMR (500 MHz, CDCl<sub>3</sub>)  $\delta$  8.48 (d,  $J$  = 3.8 Hz, 2 H), 7.58 (t,  $J$  = 7.2 Hz, 1 H), 7.50 (d,  $J$  = 7.5 Hz, 2 H), 7.17 (d,  $J$  = 11.0 Hz, 10 H), 6.94 (t,  $J$  = 3.7 Hz, 1 H). <sup>13</sup>C NMR (125 MHz, CDCl<sub>3</sub>)  $\delta$  168.10, 156.02, 141.48, 141.34, 137.63, 129.30, 129.18, 128.72, 127.82, 126.45, 118.05.

**3.3.3z.** White solid. <sup>1</sup>H NMR (500 MHz, CDCl<sub>3</sub>)  $\delta$  8.64 (d,  $J$  = 4.8 Hz, 2 H), 7.21 (m, 7 H), 7.14 (d,  $J$  = 7.1 Hz, 4 H), 6.51 (s, 2 H). <sup>13</sup>C NMR (125 MHz, CDCl<sub>3</sub>)  $\delta$  158.62, 158.39, 136.44, 133.34, 128.17, 128.09, 126.50, 119.34, 111.05.

**3.3.3aa.** White solid. <sup>1</sup>H NMR (500 MHz, CDCl<sub>3</sub>)  $\delta$  8.70 (d,  $J$  = 4.8 Hz, 2 H), 8.17 (d,  $J$  = 8.2 Hz, 1 H), 7.68 (d,  $J$  = 7.6 Hz, 1 H), 7.34-7.29 (m, 6 H), 7.26 (d,  $J$  = 7.0 Hz, 1 H), 7.15

(t,  $J = 4.8$  Hz, 1 H), 6.84 (s, 1 H).  $^{13}\text{C}$  NMR (125 MHz,  $\text{CDCl}_3$ )  $\delta$  158.22, 158.15, 140.49, 138.11, 133.97, 129.35, 128.17, 128.13, 127.12, 123.56, 122.14, 120.69, 117.61, 112.79, 108.23.

**3.3.3ab.** Colorless oil.  $^1\text{H}$  NMR (500 MHz,  $\text{CDCl}_3$ )  $\delta$  8.65 (d,  $J = 2.7$  Hz, 1 H), 7.93 (d,  $J = 7.9$  Hz, 1 H), 7.51 (dq,  $J = 20.5, 7.8, 7.3$  Hz, 4 H), 7.44 (d,  $J = 7.4$  Hz, 2 H), 7.40 (t,  $J = 7.7$  Hz, 2 H), 7.33 (t,  $J = 7.4$  Hz, 1H), 7.15-7.10 (m, 1 H), 6.98 (d,  $J = 8.0$  Hz, 1 H).  $^{13}\text{C}$  NMR (125 MHz,  $\text{CDCl}_3$ )  $\delta$  152.81, 149.53, 141.58, 140.55, 139.66, 135.81, 134.90, 130.05, 129.16, 128.05, 125.23, 124.31, 123.68, 122.38, 122.29, 122.18.

**3.3.2qb.** Yellow solid. Mp= 68-70 °C.  $^1\text{H}$  NMR (500 MHz,  $\text{CDCl}_3$ )  $\delta$  8.13 (s, 1H), 7.93 (d,  $J = 7.9$  Hz, 1 H), 7.79 (d,  $J = 7.8$  Hz, 1 H), 7.23 (t,  $J = 7.8$  Hz, 1 H), 1.42 (s, 18 H).  $^{13}\text{C}$  NMR (125 MHz,  $\text{CDCl}_3$ )  $\delta$  167.88, 149.62, 142.02, 137.61, 136.10, 130.31, 128.06, 93.87, 84.75, 27.60. HRMS calcd for  $\text{C}_{17}\text{H}_{22}\text{NO}_5\text{INa}$  ( $\text{M}^+ + \text{Na}$ ) 470.0435, found 470.0464.

**3.3.3ac.** Colorless oil.  $^1\text{H}$  NMR (500 MHz,  $\text{CDCl}_3$ )  $\delta$  8.47 (s, 1 H), 8.12 (d,  $J = 7.8$  Hz, 1 H), 7.98 (d,  $J = 7.7$  Hz, 1 H), 7.91 (d,  $J = 8.6$  Hz, 1 H), 7.77-7.71 (m, 2 H), 7.65 (d,  $J = 6.8$  Hz, 5 H), 7.52 (t,  $J = 7.1$  Hz, 1 H), 7.42 (t,  $J = 7.4$  Hz, 3 H), 7.38-7.30 (m, 2 H).  $^{13}\text{C}$  NMR (125 MHz,  $\text{CDCl}_3$ )  $\delta$  146.93, 146.79, 146.72, 141.75, 141.54, 139.97, 135.22, 135.03, 131.55, 129.03, 128.60, 128.32, 128.08, 127.95, 127.87, 127.59, 127.25, 127.19, 127.08, 126.92, 125.98, 124.53, 121.15. HRMS calcd for  $\text{C}_{25}\text{H}_{18}\text{N}$  ( $\text{M}^+ + \text{H}$ ) 332.1434, found 332.1455. Note: the iterative arylation sequence can also be conducted in the following order: 1. Iodination. 2. Pd-catalyzed Suzuki coupling (yield 89%). 3. Site-

selective N-activation (yield 57%). 4. Rh-catalyzed C–H arylation. The capacity to select the order of cross-coupling/N-activation events allows for synthetically appealing flexibility in the synthesis of biaryls/terphenyls exploiting the electrophilicity of *N,N*-di-Boc-benzamides.

## References

- (1) (a) Greenberg, A.; Breneman, C. M.; Liebman, J. F. *The Amide Linkage: Structural Significance in Chemistry, Biochemistry and Materials Science*; Wiley-VCH: New York, 2003. (b) Pattabiraman, V. R.; Bode, J. W. *Nature* **2011**, *480*, 471. (c) Ruider, S.; Maulide, N. *Angew. Chem. Int. Ed.* **2015**, *54*, 13856.
- (2) (a) Takise, R.; Muto, K.; Yamaguchi, J. *Chem. Soc. Rev.* **2017**, *46*, 5864. (b) Meng, G.; Shi, S.; Szostak, M. *Synlett* **2016**, *27*, 2530. (c) Liu, C.; Szostak, M. *Chem. Eur. J.* **2017**, *23*, 7157.
- (3) (a) *Science of Synthesis: Cross-Coupling and Heck-Type Reactions*, Molander, G. A.; Wolfe, J. P.; Larhed, M., Eds.; Thieme: Stuttgart, 2013. (b) *Metal-Catalyzed Cross-Coupling Reactions and More*, de Meijere, A.; Bräse, S.; Oestreich, M., Eds.; Wiley: New York, 2014. (c) *New Trends in Cross-Coupling*; Colacot, T. J., Ed.; The Royal Society of Chemistry: Cambridge, 2015.
- (4) (a) Hie, L.; Nathel, N. F. F.; Shah, T. K.; Baker, E. L.; Hong, X.; Yang, Y. F.; Liu, P.; Houk, K. N.; Garg, N. K. *Nature* **2015**, *524*, 79. (b) Meng, G.; Szostak, M. *Org. Lett.* **2015**, *17*, 4364. (c) Lei, P.; Meng, G.; Szostak, M. *ACS Catal.* **2017**, *7*, 1960. (d) Meng, G.; Lei, P.; Szostak, M. *Org. Lett.* **2017**, *19*, 2158. (e) Amani, J.; Alam, R.; Badir, S.; Molander, G. A. *Org. Lett.* **2017**, *19*, 2426. (f) Ni, S.; Zhang, W.; Mei, H.; Han, J.; Pan, Y. *Org. Lett.* **2017**, *19*, 2536. (g) Lei, P.; Meng, G.; Shi, S.; Ling, Y.; An, J.; Szostak, R.; Szostak, M. *Chem. Sci.* **2017**, *8*, 6525.

- (5) (a) Meng, G.; Szostak, M. *Angew. Chem. Int. Ed.* **2015**, *54*, 14518. (b) Shi, S.; Meng, G.; Szostak, M. *Angew. Chem. Int. Ed.* **2016**, *55*, 6959. (c) Meng, G.; Szostak, M. *Org. Lett.* **2016**, *18*, 796. (d) Dey, A.; Sasmai, S.; Seth, K.; Lahiri, G. K.; Maiti, D. *ACS Catal.* **2017**, *7*, 433. (e) Yue, H.; Guo, L.; Liao, H. H.; Cai, Y.; Zhu, C.; Rueping, M. *Angew. Chem. Int. Ed.* **2017**, *56*, 4282. (f) Yue, H.; Guo, L.; Lee, S. C.; Liu, X.; Rueping, M. *Angew. Chem. Int. Ed.* **2017**, *56*, 3972. (g) Srimontree, W.; Chatupheeraphat, A.; Liao, H. H.; Rueping, M. *Org. Lett.* **2017**, *19*, 3091. (h) Shi, S.; Szostak, M. *Org. Lett.* **2017**, *19*, 3095.
- (6) Walker, J. A.; Vickerman, K. L.; Humke, J. N.; Stanley, L. M. *J. Am. Chem. Soc.* **2017**, *139*, 10228.
- (7) (a) Tani, K.; Stoltz, B. M. *Nature* **2006**, *441*, 731. (b) Greenberg, A.; Venanzi, C. A. *J. Am. Chem. Soc.* **1993**, *115*, 6951. (c) Aubé, J. *Angew. Chem. Int. Ed.* **2012**, *51*, 3063.
- (8) (a) Szostak, R.; Shi, S.; Meng, G.; Lalancette, R.; Szostak, M. *J. Org. Chem.* **2016**, *81*, 8091. (b) Pace, V.; Holzer, W.; Meng, G.; Shi, S.; Lalancette, R.; Szostak, R.; Szostak, M. *Chem. Eur. J.* **2016**, *22*, 14494. (c) Szostak, R.; Meng, G.; Szostak, M. *J. Org. Chem.* **2017**, *82*, 6373. (d) See, ref. 1c. (e) Shi, S.; Szostak, M. *Org. Lett.* **2016**, *18*, 5872.
- (9) (a) Roughley, S. D.; Jordan, A. M. *J. Med. Chem.* **2011**, *54*, 3451. (b) Kaspar, A. A.; Reichert, J. M. *Drug Discov. Today* **2013**, *18*, 807. (c) Marchildon, K. *Macromol. React. Eng.* **2011**, *5*, 22 (d) Chen, Y.; Turlik, A.; Newhouse, T. *J. Am. Chem. Soc.* **2016**, *138*, 1166.

- (10) (a) Larock, R. C. *Comprehensive Organic Transformations*; Wiley: New York, 1999.  
(b) Zabicky, J. *The Chemistry of Amides*; Interscience: New York, 1970.
- (11) (a) Yu, J. Q. *Science of Synthesis: Catalytic Transformations via C–H Activation*; Thieme: Stuttgart, 2015. (b) Chen, Z.; Wang, B.; Zhang, J.; Yu, W.; Liu, Z.; Zhang, Y. *Org. Chem. Front.* **2015**, 2, 1107. (c) Daugulis, O.; Roane, J.; Tran, L. D. *Acc. Chem. Res.* **2015**, 48, 1053. (d) Miao, J.; Ge, H. *Eur. J. Org. Chem.* **2015**, 7859. (e) Rossi, R.; Bellina, F.; Lessi, M.; Manzini, C. *Adv. Synth. Catal.* **2014**, 356, 17. (f) Engle, K. M.; Mei, T. S.; Wasa, M.; Yu, J. Q. *Acc. Chem. Res.* **2012**, 45, 788. (g) Yamaguchi, J.; Yamaguchi, A. D.; Itami, K. *Angew. Chem. Int. Ed.* **2012**, 51, 8960. (h) Yeung, C. S.; Dong, V. M. *Chem. Rev.* **2011**, 111, 1215. (i) Lyons, T.; Sanford, M. *Chem. Rev.* **2010**, 110, 1147.
- (12) (a) Hussain, I.; Singh, T. *Adv. Synth. Catal.* **2014**, 356, 1661. (b) *Modern Arylation Methods*, Burke, A. J.; Marques, C. S., Eds.; Wiley-VCH: Weinheim, 2015.
- (13) Giri, R.; Thapa, S.; Kafle, A. *Adv. Synth. Catal.* **2014**, 356, 1395.
- (14) Liu, Y.; Ge, H. *Nat. Chem.* **2017**, 9, 26.
- (15) (a) Amaike, K.; Muto, K.; Yamaguchi, J.; Itami, K. *J. Am. Chem. Soc.* **2012**, 134, 13573. (b) Muto, K.; Yamaguchi, J.; Lei, A.; Itami, K. *J. Am. Chem. Soc.* **2013**, 135, 16384. (c) Muto, K.; Hatakeyama, T.; Yamaguchi, J.; Itami, K. *Chem. Sci.* **2015**, 6, 6792. (d) Song, W.; Ackermann, L. *Angew. Chem. Int. Ed.* **2012**, 51, 8251. (e) Tobisu, M.; Yasui, K.; Aihara, Y.; Chatani, N. *Angew. Chem. Int. Ed.* **2017**, 56, 1877.



- (16) (a) Kametani, Y.; Satoh, T.; Miura, M.; Nomura, M. *Tetrahedron Lett.* **2000**, *41*, 2655. (b) Daugulis, O.; Zaitsev, V. G.; *Angew. Chem. Int. Ed.* **2005**, *44*, 4046. (c) Berman, A. M.; Lewis, J. C.; Bergman, R. G.; Ellman, J. A. *J. Am. Chem. Soc.* **2008**, *130*, 14926. (d) Kim, M.; Kwak, J.; Chang, S. *Angew. Chem. Int. Ed.* **2009**, *48*, 8935. (e) Ackermann, L.; Althammer, A.; Born, R. *Angew. Chem. Int. Ed.* **2006**, *45*, 2619. (f) Roger, J.; Doucet, H. *Org. Biomol. Chem.* **2008**, *6*, 169. (g) Sun, C. L.; Li, B. J.; Shi, Z. J. *Chem. Commun.* **2010**, *46*, 677. (h) Zhao, X.; Yeung, C. S.; Dong, V. M. *J. Am. Chem. Soc.* **2010**, *132*, 5837. (i) Zhao, X.; Yu, Z. *J. Am. Chem. Soc.* **2008**, *130*, 8136. (j) Jin, W.; Yu, Z.; He, W.; Ye, W.; Xiao, W. J. *Org. Lett.* **2009**, *11*, 1317. (k) Pan, F.; Lei, Z. Q.; Wang, H.; Li, H.; Sun, J.; Shi, Z. J. *Angew. Chem. Int. Ed.* **2013**, *52*, 2063. (l) Shuai, Q.; Yang, L.; Guo, X.; Basle, O.; Li, C. J. *J. Am. Chem. Soc.* **2010**, *132*, 12212.
- (17) (a) Gooßen, L. J.; Deng, G.; Levy, L. M. *Science* **2006**, *313*, 662. (b) Gooßen, L. J.; Rodriguez, N.; Melzer, B.; Linder, C.; Deng, G.; Levy, L. M. *J. Am. Chem. Soc.* **2007**, *129*, 4824. (c) Wei, Y.; Hu, P.; Zhang, M.; Su, W. *Chem. Rev.* **2017**, *117*, 8864.
- (18) (a) Peters, R. *Cooperative Catalysis: Designing Efficient Catalysts for Synthesis*; Wiley-VCH: 2015. (b) Du, Z.; Shao, Z. *Chem. Soc. Rev.* **2013**, *42*, 1337. (c) Allen, A. E.; MacMillan, D. W. C. *Chem. Sci.* **2012**, *3*, 633.
- (19) Davidsen, S. K.; May, P. D.; Summers, J. B. *J. Org. Chem.* **1991**, *56*, 5482.
- (20) (a) Blakey, S. B.; MacMillan, D. W. C. *J. Am. Chem. Soc.* **2003**, *125*, 6046. (b) Buszek, K. R.; Brown, N. *Org. Lett.* **2007**, *9*, 707.

- (21) (a) Gooßen, L. J.; Rodriguez, N.; Gooßen, K. *Angew. Chem. Int. Ed.* **2008**, *47*, 3100.  
(b) Dzik, W. I.; Lange, P. P.; Gooßen, L. J. *Chem. Sci.* **2012**, *3*, 2671.
- (22) Johnson, J. B.; Rovis, T. *Acc. Chem. Res.* **2008**, *41*, 327.
- (23) Colby, D. A.; Bergman, R. G.; Ellman, J. A. *Chem. Rev.* **2010**, *110*, 624.
- (24) Cox, C.; Lectka, T. *Acc. Chem. Res.* **2000**, *33*, 849.
- (25) See the Experimental section.
- (26) Bera, M.; Agasti, S.; Chowdhury, R.; Mondal, R.; Pal, D.; Maiti, D. *Angew. Chem. Int. Ed.* **2017**, *56*, 5272.
- (27) Lemke, T. L.; Williams, D. A. *Foye's Principles of Medicinal Chemistry*, Lippincott: Philadelphia, 2013.
- (28) Nahm, S.; Weinreb, S. M. *Tetrahedron Lett.* **1981**, *22*, 3815.

## Chapter 4

### Amides as New Acyl Precursors Enabled by NHC Catalyst Systems

#### 4.1 N-Acylpyrroles and pyrazoles: planar electronically-activated amides

Parts of this section were adapted with permission from the article: “Suzuki–Miyaura Cross-Coupling of N-Acylpyrroles and Pyrazoles: Planar, Electronically Activated Amides in Catalytic N–C Cleavage” (*Org. Lett.* **2017**, *19*, 3596). Copyright ©2017, American Chemical Society.

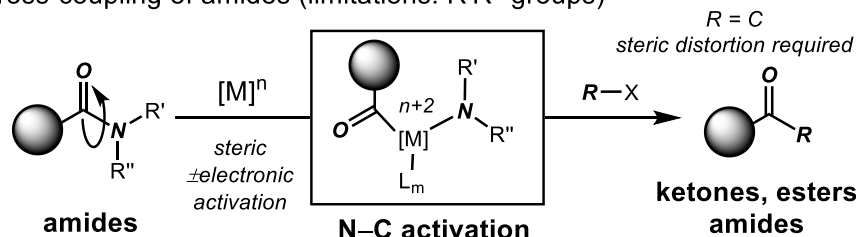
##### 4.1.1 Research background

Our previous research has shown that the development of efficient methods for coupling of amides by transition-metal-catalyzed N–C bond cleavage has become an important goal in organic synthesis.<sup>1,2</sup> Using this bond forming manifold, typically-considered inert amide bonds can be harnessed into generic acyl-metal reactivity mechanism.<sup>3</sup> Given that amides represent ubiquitous linkages in biologically-active compounds and common intermediates in organic synthesis,<sup>4</sup> the discovery of new catalytic reactivity by amide N–C cleavage has a significant potential in various fields of chemistry.<sup>5,6</sup>

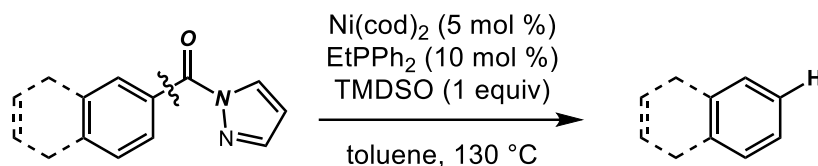
At the start of this project we realized that while methods that induce N–C bond activation<sup>7</sup> in sterically-distorted amides<sup>8</sup> had been well-established,<sup>9</sup> catalytic processes that enable carbon–carbon bond formation from planar amides were absent from the literature altogether (Figure 4.1.1A). As a rate example proceeding via a directing group mechanism, Maiti and co-workers reported a method for nickel-catalyzed reduction of

amides to aromatic hydrocarbons using N-acylpyrazoles as the reaction partners (Figure 4.1.1B).<sup>10</sup> It was shown that N–Ni-coordination at the 2-position of the pyrazole ring was critical for high reactivity; unfortunately, synthetically valuable *N*-acylpyrroles<sup>11</sup> were found unreactive in this process.<sup>12</sup>

■ A. Cross-coupling of amides (limitations: R'R'' groups)



■ B. Previous study: Ni-catalyzed deamidative step-down reduction



■ Ni catalysis ■ N–Ni coordination required

■ conjugated aromatics ■ decarbonylative cleavage

■ C. This study: Pd-catalyzed Suzuki cross-coupling of N-acylpyrroles/pyrazoles

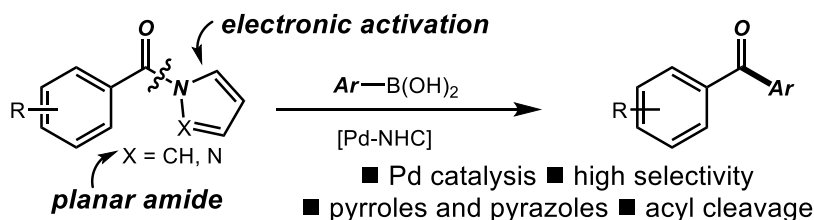


**Figure 4.1.1** Studies on activation of planar amide bonds.

## 4.1.2 Reaction discovery

We developed a palladium-catalyzed activation of N–C amide bonds in planar amides enabled by electronic-activation of the amide nitrogen atom (Figure 4.1.1C). We realized that cross-coupling of planar amides is significantly more challenging than that of

distorted amides as distortion disrupts amidic resonance more effectively than electronic destabilization;<sup>1b</sup> However the activation concept of electronically activated planar amides would offer new attractive directions in amide N–C(O) activation. Specially, our study (1) demonstrated high reactivity of both N-acylpyrroles and N-acylpyrazoles, resulting in an operationally-simple, catalytic synthesis of biaryl ketones from N-acylpyrroles as Weinreb amide equivalents, without resorting to a two-step protocol via tetrahedral intermediates;<sup>11</sup> (2) provided a method to activate NH<sub>2</sub> bonds from primary amides; since N-acylpyrroles can be readily prepared from primary benzamides (the Paal-Knorr pyrrole synthesis),<sup>13</sup> this method offered a rapid entry to metal-catalyzed coupling of unactivated primary amides; (3) demonstrated another example of the beneficial effect of Pd-NHC (NHC = N-heterocyclic carbene) catalysis<sup>14</sup> over Pd-phosphines in the activation of inert amide N–C bonds,<sup>9</sup> which could have implications for the design and optimization of amide cross-coupling manifolds. Mechanistic studies provided insight into the origin and selectivity of forming acylmetals from *N*-acylpyrroles,<sup>1–3</sup> moving from the twist to reagent control in the general activation manifold of the amide bond. In this way, the study opened up new avenues for generating acyl-metal intermediates from planar, electronically-activated amides catalytic coupling reactions via acyl- and decarbonylative pathways.

As outlined in chapter 1 – 3, we introduced new methods for cross-coupling of sterically-activated amides by ground-state resonance destabilization.<sup>9h–m</sup> In this context, in our initial study, we examined the reactivity of sterically-distorted N-acyl-2,5-dimethylpyrrole (<5% yield,<sup>9h</sup>  $\tau = 39.7^\circ$ ;  $\chi_N = 8.4^\circ$ ,<sup>15</sup> Winkler-Dunitz distortion

parameters). Having gained considerable experience in amide bond cross-coupling we questioned whether electronic-activation of nitrogen through delocalization of  $N_{lp}$  into the  $\pi$ -electron system of the pyrrole ring<sup>16</sup> might be sufficient to selectively insert palladium into the amide N–C bond in the absence of coordination or steric distortion, resulting in a much more general process.

### 4.1.3 Reaction optimization

entry	catalyst	ligand	base	solvent	yield (%) <sup>b</sup>
1	Pd(OAc) <sub>2</sub>	PCy <sub>3</sub> HBF <sub>4</sub>	K <sub>2</sub> CO <sub>3</sub>	THF	<2
2	Pd <sub>2</sub> (dba) <sub>3</sub>	PCy <sub>3</sub> HBF <sub>4</sub>	Na <sub>2</sub> CO <sub>3</sub>	dioxane	<2
3	Pd(OAc) <sub>2</sub>	PPh <sub>3</sub>	K <sub>2</sub> CO <sub>3</sub>	THF	<2
4	Pd(OAc) <sub>2</sub>	PPh <sub>3</sub>	K <sub>2</sub> CO <sub>3</sub>	DMF	<2
5	Pd(OAc) <sub>2</sub>	PPh <sub>3</sub>	K <sub>2</sub> CO <sub>3</sub>	NMP	<2
6	Pd(OAc) <sub>2</sub>	<i>Pn</i> Bu <sub>3</sub>	K <sub>2</sub> CO <sub>3</sub>	THF	<2
7	Pd(OAc) <sub>2</sub>	IPrHCl	K <sub>2</sub> CO <sub>3</sub>	THF	<2
8	(IPr)Pd(allyl)Cl		K <sub>2</sub> CO <sub>3</sub>	THF	82
9	(SIPr)Pd(cinnamyl)Cl		K <sub>2</sub> CO <sub>3</sub>	THF	57
10	(IPr)Pd(cinnamyl)Cl		K <sub>2</sub> CO <sub>3</sub>	THF	92
11	(IPr)Pd(cinnamyl)Cl		K <sub>2</sub> CO <sub>3</sub>	dioxane	<2
12	(IPr)Pd(cinnamyl)Cl		K <sub>2</sub> CO <sub>3</sub>	toluene	<2
13	(IPr)Pd(cinnamyl)Cl		K <sub>3</sub> PO <sub>4</sub>	THF	<2
14	(IPr)Pd(cinnamyl)Cl		KF	THF	<2
15	(IPr)Pd(cinnamyl)Cl		KOH	THF	<2
16	(IPr)Pd(cinnamyl)Cl		NaOtBu	THF	<2
17 <sup>c</sup>	(IPr)Pd(cinnamyl)Cl		K <sub>2</sub> CO <sub>3</sub>	THF	56

<sup>a</sup>Conditions: amide (1.0 equiv), R-B(OH)<sub>2</sub> (2.0 equiv), catalyst (6 mol %), base (3.0 equiv), solvent (0.50 M), 110 °C, 15 h. Entries 1-6: [Pd] (3 mol %), ligand (6 mol %). <sup>b</sup>GC/<sup>1</sup>H NMR yields. <sup>c</sup>[Pd] (3 mol %).

**Table 4.1.1** General optimization.<sup>a</sup>

After very extensive optimization, we found that Pd-NHC catalysis was indeed capable of promoting the desired reaction [(IPr)Pd(cinnamyl)Cl, 6 mol %, 4-Tol-B(OH)<sub>2</sub>, 2.0 equiv, K<sub>2</sub>CO<sub>3</sub>, 3.0 equiv, THF, 110 °C]. Selected optimization results are summarized in Table 4.1.1. Of particular note, Pd-PR<sub>3</sub> systems were found ineffective as catalysts for

amide N–C cross-coupling, resulting in a full recovery of the starting material (entries 1–6). We hypothesized that strong  $\sigma$ -donation of the NHC ligand in facilitating oxidative addition was critical for the N–C coupling reactivity. Evaluation of different Pd–NHC catalysts revealed (IPr)Pd(cinnamyl)Cl to be optimal (entries 7–10). The choice of base and solvent had a dramatic effect on the reaction efficiency (entries 10–16). Other bases ( $\text{K}_3\text{PO}_4$ , KF, KOH, NaO-*t*Bu) and solvents (dioxane, toluene) provided inferior results to  $\text{K}_2\text{CO}_3/\text{THF}$ .<sup>14</sup>

#### 4.1.4 Substrate scope

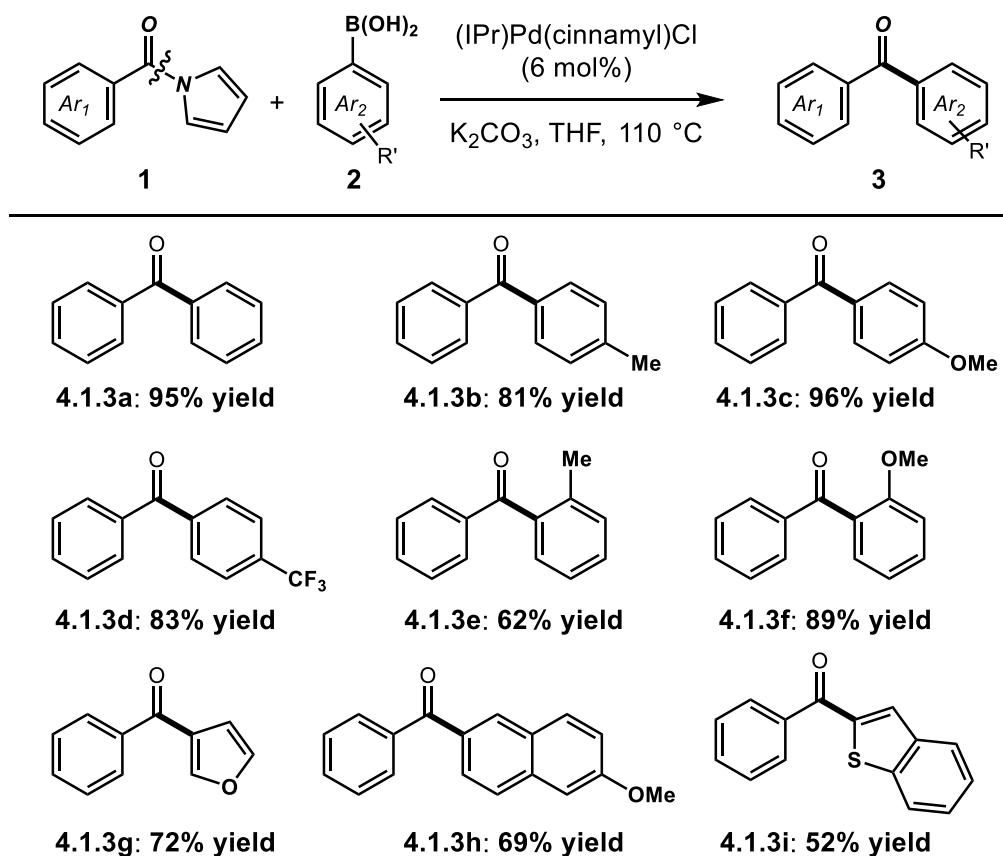


**Figure 4.1.2** Boronic acid scope.

Having identified the optimal conditions, we next evaluated the scope of the reaction with respect to the boronic acid component (Figure 4.1.2). As shown, these conditions were compatible with diverse boronic acids, including neutral (**4.1.3a**), electron-rich (**4.1.3b-4.1.3c**), electron-withdrawing (**4.1.3d**), sterically-hindered (**4.1.3e-4.1.3f**), and heterocyclic boronic acids (**4.1.3g**). At the present stage, nitrophenyl has not been tested. Moreover, conjugated aromatic (**4.1.3h**), and challenging 2-substituted heteroaromatic boronic acids (**4.1.3i**) were well-tolerated, delivering the desired biaryl ketones in good to excellent yields.

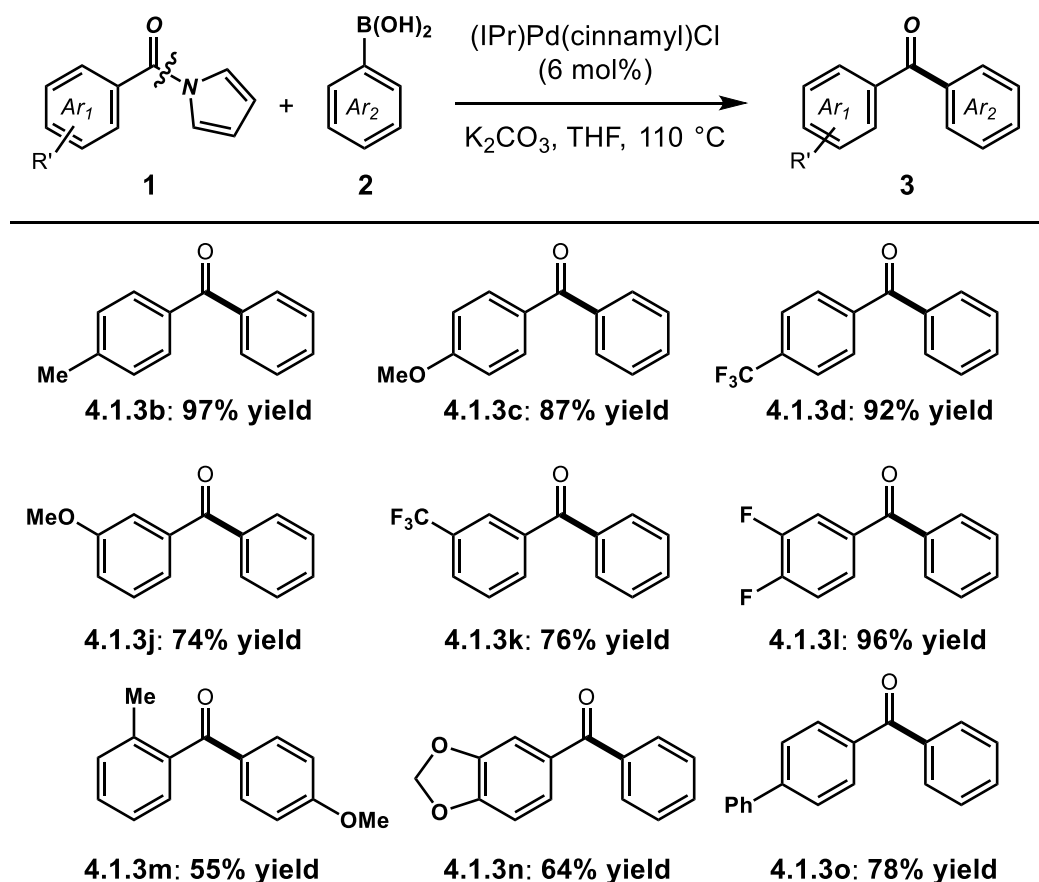


**Figure 4.1.3** Scope of amides.



Importantly, amides containing both electron rich (**4.1.3b-4.1.3c**) and electron-withdrawing (**4.1.3d**) substituents at the conjugating 4-position of the aromatic ring were compatible with the reaction conditions (Figure 4.1.3). Meta-substitution with electronically-diverse functional groups was well-tolerated (**4.1.3j-4.1.3k**). The scope of the reaction could be further extended to medicinally-relevant fluorine-containing (**4.1.3l**), sterically-hindered (**4.1.3m**), heterocyclic (**4.1.3n**) and conjugated 4-biphenyl amides (**4.1.3o**). Interestingly, in the latter case the deamidative reduction was not observed, even though the process is facilitated by conjugated aromatics,<sup>10</sup> demonstrating complementary scope of the reaction protocol.

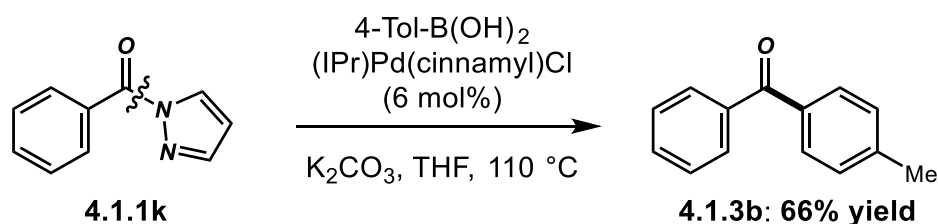


**Figure 4.1.4** Cross-coupling of N-acylpyrazole.

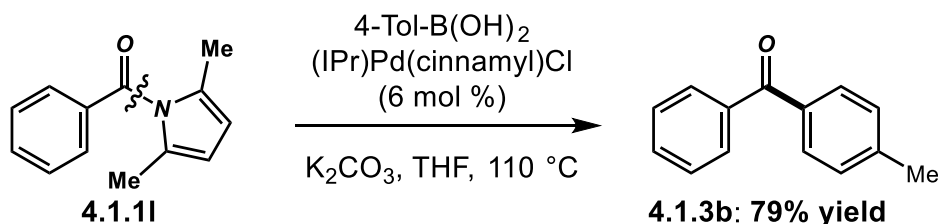


**Figure 4.1.5** Cross-coupling of a twisted N-acyl-2,5-dimethylpyrrole.

Furthermore, we found that the coupling of N-acylpyrazole proceeded uneventfully without modification of the reaction conditions (Figure 4.1.4), despite different electronic properties of the amide bond,<sup>16</sup> highlighting the versatility of Pd-NHC catalysts.

Intriguingly, our catalytic system could be applied to couple the twisted N-acyl-2,5-Me<sub>2</sub>-pyrrole (Figure 4.1.5).<sup>15</sup> The successful coupling of sterically-distorted **4.1.1l** under the same conditions as planar **4.1.1a** suggested that amide twist might not be required for N–C(O) activation.

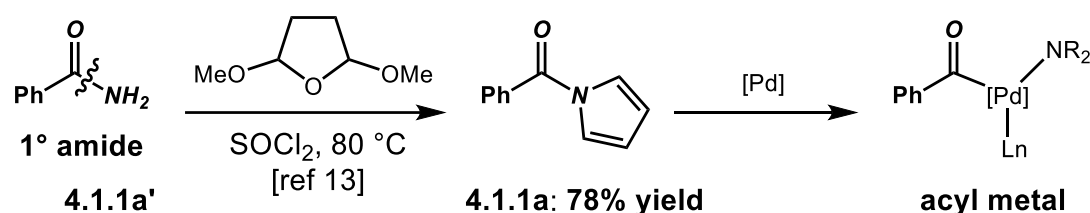


**Figure 4.1.6** Access to acyl-metals directly from primary amides.

Importantly, since N-acylpyrroles can be readily prepared from primary benzamides,<sup>13</sup> our method offered a rapid entry to acyl-metal intermediates from unactivated primary amides (Figure 4.1.6). Primary amides are ubiquitous intermediates and target compounds in pharmaceutical and organic materials applications.<sup>5,6</sup> Catalytic methods for direct coupling of unactivated primary amides using Pd were at the time of the study absent from the literature altogether.<sup>1,9n</sup>

#### 4.1.5 Mechanistic studies

We performed competition studies to establish the relative reactivity of amides (Figure 4.1.7). Similar relative reactivity of **4.1.1b** and **4.1.1k** under thermodynamic conditions of the experiment was found. The intermolecular competition between planar N-acylpyrrole (**4.1.1b**) and twisted N-acyl-2,5-Me<sub>2</sub>-pyrrole (**4.1.1l**) gave mixture of products, some resulting from background nucleophilic transamidation of the twisted amide bond.<sup>17</sup>

Undoubtedly, the use of planar amides was advantageous due to higher stability to nucleophilic capture.

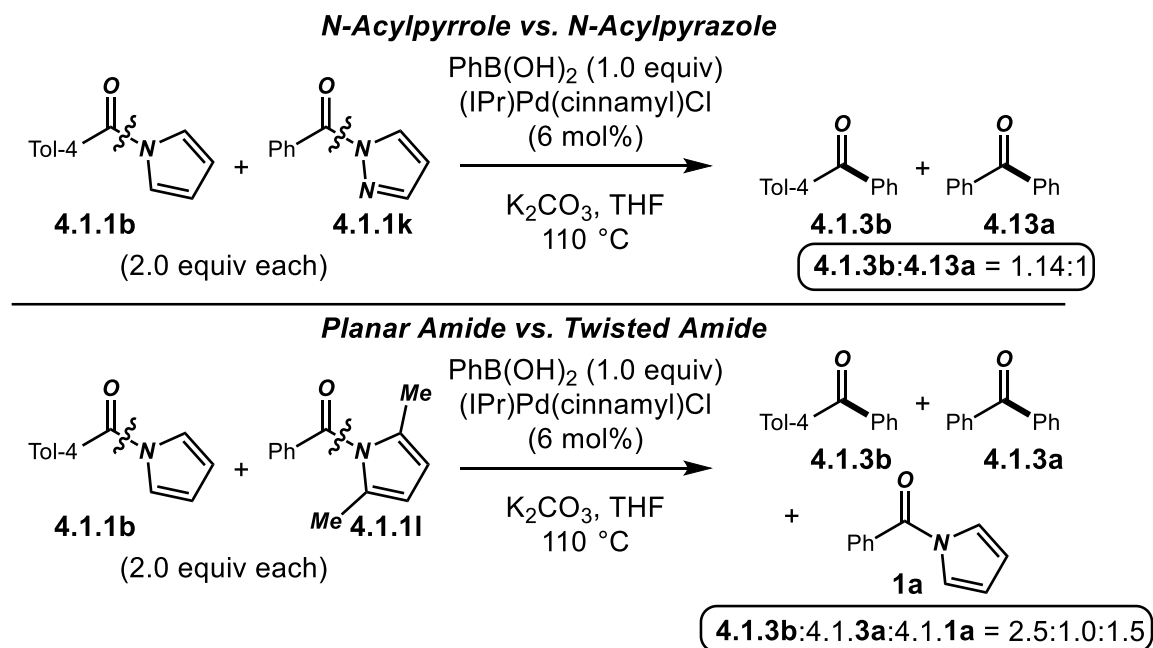


**Figure 4.1.7** Competition reactions.

Kinetic studies were performed to further evaluate the relative reactivity of amides **4.1.1a**, **4.1.1k**, **4.1.1l** undergoing the coupling. Initial rates revealed the following order of reactivity: (**4.1.1a**) ( $v_{\text{initial}} = 2.1 \times 10^{-1} \text{ mM s}^{-1}$ )  $\approx$  (**4.1.1k**) ( $v_{\text{initial}} = 2.2 \times 10^{-1} \text{ mM s}^{-1}$ )  $\approx$  (**4.1.1l**) ( $v_{\text{initial}} = 3.6 \times 10^{-1} \text{ mM s}^{-1}$ ). (1) The rates paralleled relative reactivity under the thermodynamic conditions. (2) All three amides reacted at similar rates, irrespective of electronic properties and amide twist. Collectively, the studies suggested that the rate determining step might not involve N–C activation under these reaction conditions. Transmetallation has been generally considered as the rate determining step in Suzuki-Miyaura couplings of aryl electrophiles.<sup>18</sup>

#### 4.1.6 Conclusion

In conclusion, we have demonstrated the first catalytic C–C bond formation from planar amides enabled by electronic activation of the amide nitrogen atom in N-acylpyrroles and pyrazoles. The method was operationally-convenient and exploited N-acylpyrroles as Weinreb amide equivalents. The present findings highlighted the utility of Pd-NHC catalysis<sup>14</sup> in selective activation of inert amide N–C bonds. The direct synthesis of N-acylpyrroles from primary amides opened the door for catalytic coupling of unactivated primary amides by metal catalysis. Most importantly, the study provided an avenue for catalytic cross-coupling reactions via acyl-metal intermediates from planar, electronically-activated amides.

#### 4.1.7 Experimental section

**General procedure for amide synthesis.** An oven-dried flask (100 mL) equipped with a stir bar was charged with amine (typically, 8.84 mmol, 1.0 equiv), triethylamine (typically, 2.0 equiv), 4-dimethylaminopyridine (typically, 0.25 equiv) and dichloromethane (typically, 0.20 M), placed under a positive pressure of argon, and subjected to three evacuation/backfilling cycles under high vacuum. Benzoyl chloride (typically, 1.1 equiv) was added dropwise to the reaction mixture with vigorous stirring at 0 °C, and the reaction mixture was stirred for 15 h at room temperature. After the indicated time, the reaction mixture was diluted with Et<sub>2</sub>O (30 mL), filtered, the organic layer was washed with HCl (1.0 N, 30 mL), brine (30 mL), dried over Na<sub>2</sub>SO<sub>4</sub>, filtered,

and concentrated. The crude product was purified by chromatography on silica gel (EtOAc/hexanes) to afford the title product

**General procedure for N-acylpyrrole synthesis from primary amides.** An oven-dried flask (100 mL) equipped with a stir bar was charged with benzamide (typically, 2.0 mmol), 2,5-dimethoxytetrahydrofuran (typically, 5 mL), and thionyl chloride (typically, 1.0 equiv) was added dropwise to the reaction mixture with vigorous stirring at room temperature. The reaction mixture was heated at 80 °C for 20 minutes. After the indicated time, the reaction mixture was cooled down to room temperature, poured onto iced water (10 mL), and extracted with dichloromethane (20 mL). The organic layer was washed with water (10 mL), brine (10 mL), dried over Na<sub>2</sub>SO<sub>4</sub>, filtered, and concentrated. The crude product was purified by chromatography on silica gel (EtOAc/hexanes) to afford the title product. This method can be used to synthesize *N*-acylpyrroles in 60-85% yields.

**General procedure for synthesis of (2,5-dimethyl-1*H*-pyrrol-1-yl)(phenyl)methanone: twisted N-acylpyrrole.** An oven-dried flask (100 mL) equipped with a stir bar was charged with benzamide (typically, 8.84 mmol), 2,5-hexanedione (typically, 1.1 equiv), *p*-toluenesulfonic acid (typically, 2.0 mol%) and toluene (0.35 M), placed under a positive pressure of argon, subjected to three evacuation/backfilling cycles under high vacuum, and the resulting reaction mixture was heated for 4 hours at 120 °C. After the indicated time, the reaction was cooled down to room temperature and concentrated. The crude product was purified by chromatography on silica gel (EtOAc/hexanes) to afford the title product.

**General procedure for Suzuki-Miyaura cross-coupling of N-acylpyrroles.** An oven-dried vial equipped with a stir bar was charged with an amide substrate (neat, 1.0 equiv), potassium carbonate (typically, 3.0 equiv), boronic acid (typically, 2.0 equiv), Pd-NHC catalyst (typically, 6 mol%), placed under a positive pressure of argon, and subjected to three evacuation/backfilling cycles under high vacuum. THF (typically, 0.50 M) was added with vigorous stirring at room temperature, the reaction mixture was placed in a preheated oil bath at 110 °C and stirred for an indicated time. After the indicated time, the reaction mixture was cooled down to room temperature, diluted with CH<sub>2</sub>Cl<sub>2</sub> (10 mL), filtered, and concentrated. The sample was analyzed by <sup>1</sup>H NMR (CDCl<sub>3</sub>, 500 MHz) and GC-MS to obtain conversion, selectivity and yield using internal standard and comparison with authentic samples. Purification by chromatography on silica gel (EtOAc/hexanes) afforded the title product. Caution: Reactions involving high pressure must be carried out in a hood with appropriate pressure vessels, pressure relief equipment and/or blast shields.

**4.1.1a.** Yield 83%. Colorless oil. <sup>1</sup>H NMR (500 MHz, CDCl<sub>3</sub>) δ 7.77 (d, *J* = 7.4 Hz, 2 H), 7.63 (t, *J* = 7.4 Hz, 1 H), 7.53 (t, *J* = 7.4 Hz, 2 H), 7.32 (s, 2 H), 6.38 (s, 2 H). <sup>13</sup>C NMR (125 MHz, CDCl<sub>3</sub>) δ 167.71, 133.27, 132.28, 129.50, 128.49, 121.31, 113.16.

**4.1.1b.** Yield 71%. White solid. <sup>1</sup>H NMR (500 MHz, CDCl<sub>3</sub>) δ 7.69 (d, *J* = 7.4 Hz, 2 H), 7.33 (d, *J* = 10.1 Hz, 4 H), 6.37 (s, 2 H), 2.48 (s, 3 H). <sup>13</sup>C NMR (125 MHz, CDCl<sub>3</sub>) δ 167.72, 143.07, 130.35, 129.75, 129.14, 121.32, 112.91, 21.64.

**4.1.1c.** Yield 71%. White solid.  $^1\text{H}$  NMR (500 MHz,  $\text{CDCl}_3$ )  $\delta$  7.78 (d,  $J = 7.6$  Hz, 2 H), 7.32 (s, 2 H), 7.02 (d,  $J = 7.6$  Hz, 2 H), 6.36 (s, 2 H), 3.91 (s, 3 H).  $^{13}\text{C}$  NMR (125 MHz,  $\text{CDCl}_3$ )  $\delta$  167.17, 163.00, 132.03, 125.26, 121.37, 113.81, 112.74, 55.54.

**4.1.1d.** Yield 62%. Colorless oil.  $^1\text{H}$  NMR (500 MHz,  $\text{CDCl}_3$ )  $\delta$  7.88 (d,  $J = 7.8$  Hz, 2 H), 7.81 (d,  $J = 7.8$  Hz, 2 H), 7.27 (s, 2 H), 6.41 (s, 2 H).  $^{13}\text{C}$  NMR (125 MHz,  $\text{CDCl}_3$ )  $\delta$  166.38, 136.64, 133.85 ( $J^2 = 32.5$  Hz), 129.70, 125.58 ( $J^3 = 3.8$  Hz), 123.48 ( $J^1 = 271.3$  Hz), 121.11, 113.82.  $^{19}\text{F}$  NMR (471 MHz,  $\text{CDCl}_3$ )  $\delta$  -63.12.

**4.1.1e.** Yield 61%. Colorless oil,  $^1\text{H}$  NMR (500 MHz,  $\text{CDCl}_3$ )  $\delta$  7.43 (t,  $J = 7.9$  Hz, 1 H), 7.32 (dd,  $J = 5.0, 2.6$  Hz, 3 H), 7.29 (d,  $J = 3.6$  Hz, 1 H), 7.16 (d,  $J = 8.3$  Hz, 1 H), 6.37 (p,  $J = 3.1$  Hz, 2 H), 3.88 (s, 3 H).  $^{13}\text{C}$  NMR (125 MHz,  $\text{CDCl}_3$ )  $\delta$  167.51, 159.54, 134.46, 129.52, 121.75, 121.31, 118.48, 114.37, 113.16, 55.52.

**4.1.1f.** Yield 84%. Colorless oil.  $^1\text{H}$  NMR (500 MHz,  $\text{CDCl}_3$ )  $\delta$  8.04 (s, 1 H), 7.96 (d,  $J = 7.7$  Hz, 1 H), 7.90 (d,  $J = 7.8$  Hz, 1 H), 7.69 (t,  $J = 7.7$  Hz, 1 H), 7.27 (s, 2 H), 6.42 (s, 2 H).  $^{13}\text{C}$  NMR (125 MHz,  $\text{CDCl}_3$ )  $\delta$  166.22, 134.11, 132.56, 131.27 ( $J^2 = 33.8$  Hz), 129.20, 128.84 ( $J^3 = 2.5$  Hz), 126.35 ( $J^3 = 3.8$  Hz), 123.46 ( $J^1 = 271.3$  Hz), 121.14, 113.84.  $^{19}\text{F}$  NMR (471 MHz,  $\text{CDCl}_3$ )  $\delta$  -62.85. HRMS calcd for  $\text{C}_{12}\text{H}_8\text{F}_3\text{NONa}$  ( $\text{M}^+ + \text{Na}$ ) 262.0450, found 262.0459.

**4.1.1g.** Yield 72%. Colorless oil.  $^1\text{H}$  NMR (500 MHz,  $\text{CDCl}_3$ )  $\delta$  7.65 (t,  $J = 8.8$  Hz, 1 H), 7.57 (d,  $J = 7.9$  Hz, 1 H), 7.34 (q,  $J = 8.5, 8.1$  Hz, 1 H), 7.29-7.26 (m, 2 H), 6.40 (s, 2 H).  $^{13}\text{C}$  NMR (125 MHz,  $\text{CDCl}_3$ )  $\delta$  165.33, 153.08 ( $J^1 = 253.8$  Hz), 150.13 ( $J^1 = 251.3$  Hz),

130.01 ( $J^3 = 5.0$  Hz), 126.51 ( $J^3 = 6.3$  Hz), 121.17, 119.26 ( $J^2 = 18.8$  Hz), 117.69 ( $J^2 = 17.5$  Hz), 113.71.  $^{19}\text{F}$  NMR (471 MHz,  $\text{CDCl}_3$ )  $\delta$  -130.25, -135.37. HRMS calcd for  $\text{C}_{11}\text{H}_7\text{F}_2\text{NONa}$  ( $\text{M}^+ + \text{Na}$ ) 230.0388, found 230.0397.

**4.1.1h.** Yield 78%. Colorless oil.  $^1\text{H}$  NMR (500 MHz,  $\text{CDCl}_3$ )  $\delta$  7.45 (t,  $J = 7.5$  Hz, 1 H), 7.40 (d,  $J = 7.5$  Hz, 1 H), 7.34-7.29 (m, 2 H), 7.17 (s, 2 H), 6.34 (s, 2 H), 2.37 (s, 3 H).  $^{13}\text{C}$  NMR (125 MHz,  $\text{CDCl}_3$ )  $\delta$  168.19, 136.45, 133.68, 130.83, 127.81, 125.51, 120.65, 113.41, 19.37. HRMS calcd for  $\text{C}_{12}\text{H}_{11}\text{NONa}$  ( $\text{M}^+ + \text{Na}$ ) 208.0733, found 208.0741.

**4.1.1i.** Yield 77%. White solid. Mp = 67-68 °C.  $^1\text{H}$  NMR (500 MHz,  $\text{CDCl}_3$ )  $\delta$  7.35 (dt,  $J = 40.7, 18.4$  Hz, 4 H), 7.03-6.87 (m, 1 H), 6.40 (d,  $J = 41.0$  Hz, 2 H), 6.13 (d,  $J = 40.9$  Hz, 2 H).  $^{13}\text{C}$  NMR (125 MHz,  $\text{CDCl}_3$ )  $\delta$  166.82, 151.38, 147.92, 126.82, 125.58, 121.38, 112.97, 110.11, 108.15, 102.08. HRMS calcd for  $\text{C}_{12}\text{H}_9\text{NO}_3\text{Na}$  ( $\text{M}^+ + \text{Na}$ ) 238.0475, found 238.0482.

**4.1.1j.** Yield 82%. White solid. Mp = 97-99 °C.  $^1\text{H}$  NMR (500 MHz,  $\text{CDCl}_3$ )  $\delta$  7.87 (d,  $J = 7.3$  Hz, 2 H), 7.76 (d,  $J = 7.5$  Hz, 2 H), 7.67 (d,  $J = 7.7$  Hz, 2 H), 7.52 (t,  $J = 7.1$  Hz, 2 H), 7.45 (t,  $J = 7.2$  Hz, 1 H), 7.37 (s, 2 H), 6.40 (s, 2 H).  $^{13}\text{C}$  NMR (125 MHz,  $\text{CDCl}_3$ )  $\delta$  167.50, 145.34, 139.73, 131.84, 130.20, 129.03, 128.32, 127.30, 127.14, 121.33, 113.15. HRMS calcd for  $\text{C}_{17}\text{H}_{13}\text{NONa}$  ( $\text{M}^+ + \text{Na}$ ) 270.0889, found 270.0900.

**4.1.1k.** Yield 81%. Colorless oil.  $^1\text{H}$  NMR (500 MHz,  $\text{CDCl}_3$ )  $\delta$  8.47 (s, 1 H), 8.15 (d,  $J = 7.4$  Hz, 2 H), 7.83 (s, 1 H), 7.64 (t,  $J = 7.3$  Hz, 1 H), 7.53 (t,  $J = 7.3$  Hz, 2 H), 6.55 (s, 1



H).  $^{13}\text{C}$  NMR (125 MHz,  $\text{CDCl}_3$ )  $\delta$  166.41, 144.51, 133.02, 131.50, 130.43, 128.12, 109.46.

**4.1.11.** Yield 26%. Colorless oil.  $^1\text{H}$  NMR (500 MHz,  $\text{CDCl}_3$ )  $\delta$  7.72 (d,  $J = 9.5$  Hz, 2 H), 7.62 (t,  $J = 8.1$  Hz, 1 H), 7.50 (t,  $J = 7.0$  Hz, 2 H), 5.90 (s, 2 H), 2.09 (s, 6 H).  $^{13}\text{C}$  NMR (125 MHz,  $\text{CDCl}_3$ )  $\delta$  171.17, 135.67, 133.18, 130.34, 130.12, 128.67, 110.14, 14.70.

**4.1.3a.** White solid.  $^1\text{H}$  NMR (500 MHz,  $\text{CDCl}_3$ )  $\delta$  7.86-7.81 (m, 2 H), 7.64-7.59 (m, 1 H), 7.51 (t,  $J = 7.7$  Hz, 2 H).  $^{13}\text{C}$  NMR (125 MHz,  $\text{CDCl}_3$ )  $\delta$  196.74, 137.62, 132.41, 130.06, 128.31.

**4.1.3b.** White solid.  $^1\text{H}$  NMR (500 MHz,  $\text{CDCl}_3$ )  $\delta$  7.81 (d,  $J = 7.7$  Hz, 2 H), 7.75 (d,  $J = 7.5$  Hz, 2 H), 7.60 (t,  $J = 7.4$  Hz, 1 H), 7.50 (t,  $J = 7.2$  Hz, 2 H), 7.31 (d,  $J = 7.7$  Hz, 2 H), 2.47 (s, 3 H).  $^{13}\text{C}$  NMR (125 MHz,  $\text{CDCl}_3$ )  $\delta$  196.49, 143.22, 137.98, 134.90, 132.14, 130.31, 129.93, 128.97, 128.20, 21.66.

**4.1.3c.** White solid.  $^1\text{H}$  NMR (500 MHz,  $\text{CDCl}_3$ )  $\delta$  7.86 (d,  $J = 8.5$  Hz, 2 H), 7.78 (d,  $J = 7.8$  Hz, 2 H), 7.59 (t,  $J = 7.0$  Hz, 1 H), 7.50 (t,  $J = 7.5$  Hz, 2 H), 6.99 (d,  $J = 8.5$  Hz, 2 H), 3.92 (s, 3 H).  $^{13}\text{C}$  NMR (125 MHz,  $\text{CDCl}_3$ )  $\delta$  195.56, 163.22, 138.30, 132.57, 131.89, 130.17, 129.73, 128.19, 113.56, 55.51.

**4.1.3d.** White solid.  $^1\text{H}$  NMR (500 MHz,  $\text{CDCl}_3$ )  $\delta$  7.92 (d,  $J = 7.9$  Hz, 2 H), 7.83 (d,  $J = 7.8$  Hz, 2 H), 7.78 (d,  $J = 7.9$  Hz, 2 H), 7.66 (t,  $J = 7.3$  Hz, 1 H), 7.54 (t,  $J = 7.5$  Hz, 2 H).  $^{13}\text{C}$  NMR (125 MHz,  $\text{CDCl}_3$ )  $\delta$  195.53, 140.73, 136.74, 133.73 ( $J^2 = 32.5$  Hz), 133.09,

130.13 ( $J^4 = 3.8$  Hz), 128.53, 125.36 ( $J^3 = 7.5$  Hz), 123.68 ( $J^1 = 271.3$  Hz).  $^{19}\text{F}$  NMR (471 MHz,  $\text{CDCl}_3$ )  $\delta$  -63.01.

**4.1.3e.** Colorless oil.  $^1\text{H}$  NMR (500 MHz,  $\text{CDCl}_3$ )  $\delta$  7.84 (d,  $J = 8.5$  Hz, 2 H), 7.61 (t,  $J = 6.5$  Hz, 1 H), 7.49 (t,  $J = 7.0$  Hz, 2 H), 7.42 (t,  $J = 7.5$  Hz, 1 H), 7.33 (m, 2 H), 7.29 (m, 1 H), 2.35 (s, 3 H).  $^{13}\text{C}$  NMR (125 MHz,  $\text{CDCl}_3$ )  $\delta$  198.64, 138.63, 137.75, 136.75, 133.14, 131.00, 130.24, 130.14, 128.52, 128.46, 125.20, 20.00.

**4.1.3f.** White solid.  $^1\text{H}$  NMR (500 MHz,  $\text{CDCl}_3$ )  $\delta$  7.84 (d,  $J = 7.5$  Hz, 2 H), 7.58 (t,  $J = 7.1$  Hz, 1 H), 7.47 (dt,  $J = 14.9, 7.5$  Hz, 3 H), 7.39 (d,  $J = 7.2$  Hz, 1 H), 7.07 (t,  $J = 7.3$  Hz, 1 H), 7.02 (d,  $J = 8.3$  Hz, 1 H).  $^{13}\text{C}$  NMR (125 MHz,  $\text{CDCl}_3$ )  $\delta$  196.46, 157.36, 137.82, 132.92, 131.87, 129.83, 129.59, 128.22, 120.49, 111.46, 55.61.

**4.1.3g.** Colorless oil.  $^1\text{H}$  NMR (500 MHz,  $\text{CDCl}_3$ )  $\delta$  7.95 (d,  $J = 1.3$  Hz, 1 H), 7.88 (d,  $J = 7.0$  Hz, 2 H), 7.62 (t,  $J = 7.0$  Hz, 1 H), 7.56-7.49 (m, 3 H), 6.94 (d,  $J = 1.8$  Hz, 1 H).  $^{13}\text{C}$  NMR (125 MHz,  $\text{CDCl}_3$ )  $\delta$  189.44, 148.57, 143.96, 138.83, 132.48, 128.83, 128.56, 126.53, 110.23.

**4.1.3h.** White solid.  $^1\text{H}$  NMR (500 MHz,  $\text{CDCl}_3$ )  $\delta$  8.24 (d,  $J = 1.7$  Hz, 1 H), 7.97 (dd,  $J = 8.6, 1.7$  Hz, 1 H), 7.90-7.82 (m, 4 H), 7.67-7.61 (m, 1 H), 7.54 (dd,  $J = 8.4, 7.0$  Hz, 2 H), 7.26-7.20 (m, 2 H), 3.99 (s, 3 H).  $^{13}\text{C}$  NMR (125 MHz,  $\text{CDCl}_3$ )  $\delta$  196.59, 159.70, 138.22, 137.02, 132.70, 132.13, 132.00, 131.04, 129.99, 128.30, 127.61, 127.02, 126.57, 119.74, 105.77, 55.46.

**4.1.3i.** Colorless oil.  $^1\text{H}$  NMR (500 MHz,  $\text{CDCl}_3$ )  $\delta$  7.95 (dd,  $J = 7.5, 1.0$  Hz, 3 H), 7.90 (d,  $J = 7.5$  Hz, 1 H), 7.89 (s, 1 H), 7.66 (t,  $J = 7.0$  Hz, 1 H), 7.57 (t,  $J = 7.6$  Hz, 2 H), 7.52 (ddd,  $J = 8.1, 7.1, 1.2$  Hz, 1 H), 7.45 (ddd,  $J = 8.1, 7.1, 1.1$  Hz, 1 H).  $^{13}\text{C}$  NMR (125 MHz,  $\text{CDCl}_3$ )  $\delta$  189.66, 143.14, 142.73, 139.07, 137.88, 132.49, 132.23, 129.28, 128.53, 127.46, 126.06, 125.05, 122.93.

**4.1.3j.** White solid.  $^1\text{H}$  NMR (500 MHz,  $\text{CDCl}_3$ )  $\delta$  7.83 (d,  $J = 7.2$  Hz, 2 H), 7.61 (t,  $J = 7.4$  Hz, 1 H), 7.50 (t,  $J = 7.7$  Hz, 2 H), 7.42-7.34 (m, 3 H), 7.16 (dd,  $J = 8.0, 2.6$  Hz, 1 H), 3.88 (s, 3 H).  $^{13}\text{C}$  NMR (125 MHz,  $\text{CDCl}_3$ )  $\delta$  196.51, 159.58, 138.91, 137.63, 132.43, 130.04, 129.22, 128.26, 122.87, 118.86, 114.33, 55.48.

**4.1.3k.** White solid.  $^1\text{H}$  NMR (500 MHz,  $\text{CDCl}_3$ )  $\delta$  8.07 (s, 1 H), 7.98 (d,  $J = 7.7$  Hz, 1 H), 7.85 (d,  $J = 7.8$  Hz, 1 H), 7.80 (d,  $J = 7.8$  Hz, 2 H), 7.63 (t,  $J = 7.5$  Hz, 2 H), 7.52 (t,  $J = 7.5$  Hz, 2 H).  $^{13}\text{C}$  NMR (125 MHz,  $\text{CDCl}_3$ )  $\delta$  195.32, 138.45, 136.92, 133.25, 133.14, 133.17 ( $J^2 = 32.5$  Hz), 130.16, 129.09, 128.97 ( $J^3 = 3.8$  Hz), 128.71, 126.84 ( $J^3 = 3.8$  Hz), 123.82 ( $J^1 = 271.3$  Hz).  $^{19}\text{F}$  NMR (471 MHz,  $\text{CDCl}_3$ )  $\delta$  -62.77.

**4.1.3l.** White solid.  $^1\text{H}$  NMR (500 MHz,  $\text{CDCl}_3$ )  $\delta$  7.81-7.77 (m, 2 H), 7.71 (dd,  $J = 10.2, 7.7$  Hz, 1 H), 7.66-7.59 (m, 2 H), 7.53 (t,  $J = 7.7$  Hz, 2 H), 7.32-7.27 (m, 1 H).  $^{13}\text{C}$  NMR (125 MHz,  $\text{CDCl}_3$ )  $\delta$  194.07, 153.19 ( $J^1 = 255.0$  Hz,  $J^3 = 12.5$  Hz), 150.10 ( $J^1 = 250.0$  Hz,  $J^3 = 12.5$  Hz), 136.88, 134.45 ( $J^3 = 8.8$  Hz), 132.80, 129.85, 128.50, 127.10 ( $J^3 = 5.6$  Hz), 119.33 ( $J^2 = 18.8$  Hz), 117.27 ( $J^2 = 18.8$  Hz).  $^{19}\text{F}$  NMR (471 MHz,  $\text{CDCl}_3$ )  $\delta$  -130.57, -136.19.

**4.1.3m.** White solid.  $^1\text{H}$  NMR (500 MHz,  $\text{CDCl}_3$ )  $\delta$  7.82 (d,  $J = 8.7$  Hz, 2 H), 7.39 (t,  $J = 7.4$  Hz, 1 H), 7.29 (dt,  $J = 13.3, 6.7$  Hz, 3 H), 6.95 (d,  $J = 8.7$  Hz, 2 H), 3.90 (s, 3 H), 2.33 (s, 3 H).  $^{13}\text{C}$  NMR (125 MHz,  $\text{CDCl}_3$ ).  $^{13}\text{C}$  NMR (126 MHz,  $\text{CDCl}_3$ )  $\delta$  197.38, 163.71, 139.22, 136.17, 132.52, 130.82, 130.55, 129.79, 127.93, 125.18, 113.71, 55.52, 19.80.

**4.1.3n.** White solid.  $^1\text{H}$  NMR (500 MHz,  $\text{CDCl}_3$ )  $\delta$  7.77 (d,  $J = 8.4$  Hz, 2 H), 7.59 (t,  $J = 7.4$  Hz, 1 H), 7.49 (t,  $J = 7.6$  Hz, 2 H), 7.42-7.37 (m, 2 H), 6.89 (d,  $J = 7.9$  Hz, 1 H), 6.09 (s, 2 H).  $^{13}\text{C}$  NMR (125 MHz,  $\text{CDCl}_3$ )  $\delta$  195.14, 151.51, 147.94, 138.14, 131.99, 131.92, 129.71, 128.21, 126.86, 109.93, 107.70, 101.85.

**4.1.3o.** White solid.  $^1\text{H}$  NMR (500 MHz,  $\text{CDCl}_3$ )  $\delta$  7.93 (d,  $J = 7.5$  Hz, 2 H), 7.87 (d,  $J = 7.6$  Hz, 2 H), 7.74 (d,  $J = 7.7$  Hz, 2 H), 7.68 (d,  $J = 7.5$  Hz, 2 H), 7.63 (t,  $J = 7.3$  Hz, 1 H), 7.52 (q,  $J = 8.0$  Hz, 4 H), 7.44 (t,  $J = 7.2$  Hz, 1 H).  $^{13}\text{C}$  NMR (125 MHz,  $\text{CDCl}_3$ )  $\delta$  196.33, 145.24, 140.00, 137.78, 136.26, 132.36, 130.73, 130.00, 128.97, 128.31, 128.18, 127.31, 126.97.

## References

- (1) (a) Meng, G.; Shi, S.; Szostak, M. *Synlett* **2016**, 27, 2530. (b) Liu, C.; Szostak, M. *Chem. Eur. J.* **2017**, 23, 7157. (c) Dander, J. E.; Garg, N. K. *ACS Catal.* **2017**, 7, 1413.
- (2) (a) *Metal-Catalyzed Cross-Coupling Reactions and More*, de Meijere, A.; Bräse, S.; Oestreich, M., Eds.; Wiley: New York, 2014. (b) *Science of Synthesis: Cross-Coupling and Heck-Type Reactions*, Molander, G. A.; Wolfe, J. P.; Larhed, M., Eds.; Thieme: Stuttgart, 2013.
- (3) Dzik, W. I.; Lange, P. P.; Gooßen, L. J. *Chem. Sci.* **2012**, 3, 2671.
- (4) (a) Greenberg, A.; Breneman, C. M.; Liebman, J. F., Eds. *The Amide Linkage: Structural Significance in Chemistry, Biochemistry, and Materials Science*; Wiley: New York, 2000. Pharmaceuticals: (b) Roughley, S. D.; Jordan, A. M. *J. Med. Chem.* **2011**, 54, 3451. Polymers: (c) Marchildon, K. *Macromol. React. Eng.* **2011**, 5, 22. Peptides: (d) Pattabiraman, V. R.; Bode, J. W. *Nature* **2011**, 480, 471.
- (5) Johansson-Seechurn, C. C. C.; Kitching, M. O.; Colacot, T. J.; Snieckus, V. *Angew. Chem. Int. Ed.* **2012**, 51, 5062.
- (6) (a) Kaiser, D.; Maulide, N. *J. Org. Chem.* **2016**, 81, 4421. (b) Ruider, S. A.; Maulide, N. *Angew. Chem. Int. Ed.* **2015**, 54, 13856.
- (7) (a) Blakey, S. B.; MacMillan, D. W. C. *J. Am. Chem. Soc.* **2003**, 125, 6046. (b) Buszek, K. R.; Brown, N. *Org. Lett.* **2007**, 9, 707. (c) Maity, P.; Shacklady-McAtee, D. M.; Yap, G. P. A.; Sirianni, E. R.; Watson, M. P. *J. Am. Chem. Soc.* **2013**, 135, 280. (d)

Tobisu, M.; Nakamura, K.; Chatani, N. *J. Am. Chem. Soc.* **2014**, *136*, 5587. (e) Zhang, H.; Hagihara, S.; Itami, K. *Chem. Eur. J.* **2015**, *21*, 16796. (f) Basch, C. H.; Liao, J.; Xu, J.; Piane, J. J.; Watson, M. P. *J. Am. Chem. Soc.* **2017**, *139*, 5313.

(8) (a) Szostak, R.; Shi, S.; Meng, G.; Lalancette, R.; Szostak, M. *J. Org. Chem.* **2016**, *81*, 8091. (b) Pace, V.; Holzer, W.; Meng, G.; Shi, S.; Lalancette, R.; Szostak, R.; Szostak, M. *Chem. Eur. J.* **2016**, *22*, 14494.

(9) (a) Hie, L.; Nathel, N. F. F.; Shah, T. K.; Baker, E. L.; Hong, X.; Yang, Y. F.; Liu, P.; Houk, K. N.; Garg, N. K. *Nature* **2015**, *524*, 79. (b) Weires, N. A.; Baker, E. L.; Garg, N. K. *Nat. Chem.* **2016**, *8*, 75. (c) Simmons, B. J.; Weires, N. A.; Dander, J. E.; Garg, N. K. *ACS Catal.* **2016**, *6*, 3176. (d) Baker, E. L.; Yamano, M. M.; Zhou, Y.; Anthony, S. M.; Garg, N. K. *Nat. Commun.* **2016**, *7*, 11554. (e) Dander, J. E.; Weires, N. A.; Garg, N. K. *Org. Lett.* **2016**, *18*, 3934. (f) Hie, L.; Baker, E. L.; Anthony, S. M.; Desrosiers, J. N.; Senanayake, C.; Garg, N. K. *Angew. Chem. Int. Ed.* **2016**, *55*, 15129. (g) Li, X.; Zou, G. *Chem. Commun.* **2015**, *51*, 5089. (h) Meng, G.; Szostak, M. *Org. Lett.* **2015**, *17*, 4364. (i) Meng, G.; Szostak, M. *Org. Biomol. Chem.* **2016**, *14*, 5690. (j) Shi, S.; Szostak, M. *Chem. Eur. J.* **2016**, *22*, 10420. (k) Meng, G.; Szostak, M. *Angew. Chem. Int. Ed.* **2015**, *54*, 14518. (l) Shi, S.; Meng, G.; Szostak, M. *Angew. Chem. Int. Ed.* **2016**, *55*, 6959. (m) Meng, G.; Szostak, M. *Org. Lett.* **2016**, *18*, 796. (n) Meng, G.; Shi, S.; Szostak, M. *ACS Catal.* **2016**, *6*, 7335. (o) Shi, S.; Szostak, M. *Org. Lett.* **2016**, *18*, 5872. (p) Liu, C.; Meng, G.; Liu, Y.; Liu, R.; Lalancette, R.; Szostak, R.; Szostak, M. *Org. Lett.* **2016**, *18*, 4194. (q) Liu, C.; Meng, G.; Szostak, M. *J. Org. Chem.* **2016**, *81*, 12023. (r) Lei, P.; Meng, G.; Szostak, M. *ACS Catal.* **2017**, *7*, 1960. (s) Liu, C.; Liu, Y.; Liu, R.; Lalancette,

R.; Szostak, R.; Szostak, M. *Org. Lett.* **2017**, *19*, 1434. (t) Meng, G.; Lei, P.; Szostak, M. *Org. Lett.* **2017**, *19*, 2158. (u) Shi, S.; Szostak, M. *Org. Lett.* **2017**, *19*, 3095. (v) Hu, J.; Zhao, Y.; Liu, J.; Zhang, Y.; Shi, Z. *Angew. Chem. Int. Ed.* **2016**, *55*, 8718. (w) Cui, M.; Wu, H.; Jian, J.; Wang, H.; Liu, C.; Daniel, S.; Zeng, Z. *Chem. Commun.* **2016**, *52*, 12076. (x) Wu, H.; Liu, T.; Cui, M.; Li, Y.; Jian, J.; Wang, H.; Zeng, Z. *Org. Biomol. Chem.* **2017**, *15*, 536. (y) Liu, L.; Chen, P.; Sun, Y.; Wu, Y.; Chen, S.; Zhu, J.; Zhao, Y. *J. Org. Chem.* **2016**, *81*, 11686. (z) Yue, H.; Guo, L.; Liao, H. H.; Cai, Y.; Zhu, C.; Rueping, M. *Angew. Chem. Int. Ed.* **2017**, *56*, 4282. (aa) Yue, H.; Guo, L.; Lee, S. C.; Liu, X.; Rueping, M. *Angew. Chem. Int. Ed.* **2017**, *56*, 3972. (ab) Amani, J.; Alam, R.; Badir, S.; Molander, G. A. *Org. Lett.* **2017**, *19*, 2426. (ac) Hu, J.; Wang, M.; Pu, X.; Shi, Z. *Nat. Commun.* **2017**, *8*, 14993. (ad) Ni, S.; Zhang, W.; Mei, H.; han, J.; Pan, Y. *Org. Lett.* **2017**, *19*, 2536.

(10) Dey, A.; Sasmai, S.; Seth, K.; Lahiri, G. K.; Maiti, D. *ACS Catal.* **2017**, *7*, 433.

(11) Evans, D. A.; Borg, G.; Scheidt, K. A. *Angew. Chem. Int. Ed.* **2002**, *41*, 3188.

(12) Tasker, S. Z.; Standley, E. A.; Jamison, T. F. *Nature* **2014**, *509*, 299.

(13) (a) Ekkati, A. R.; Bates, D. K. *Synthesis* **2003**, 1959. (b) Goldys, A. M.; McErlean, C. S. P. *Eur. J. Org. Chem.* **2012**, 1877.

(14) (a) Fortman, G. C.; Nolan, S. P. *Chem. Soc. Rev.* **2011**, *40*, 5151. (b) Marion, N.; Navarro, O.; Mei, J.; Stevens, E. D.; Scott, N. M.; Nolan, S. P. *J. Am. Chem. Soc.* **2006**, *128*, 4101.

- (15) Bennet, A. J.; Somayaji, V.; Brown, R. S.; Santarsiero, B. D. *J. Am. Chem. Soc.* **1991**, *113*, 7563.
- (16) Staab, H. A. *Angew. Chem. Int. Ed.* **1962**, *7*, 351.
- (17) Liu, Y.; Shi, S.; Achtenhagen, M.; Liu, R.; Szostak, M. *Org. Lett.* **2017**, *19*, 1614.
- (18) Nishihara, Y. *Applied Cross-Coupling Reactions*; Springer: Heidelberg, 2013.
- (19) Greenberg, A.; Venanzi, C. A. *J. Am. Chem. Soc.* **1993**, *115*, 6951.
- (20) Unproductive reactivity of **4.1.1m** was consistent with rapid dissociation of imidazole upon N-coordination.



## 4.2 N-Methylamino pyrimidyl amides (MAPA): planar electronically-activated amides

Parts of this section were adapted with permission from the article “N-Methylamino Pyrimidyl Amides (MAPA): Highly Reactive, Electronically-Activated Amides in Catalytic N–C(O) Cleavage” (*Org. Lett.* **2017**, *19*, 4656). Copyright ©2017, American Chemical Society.

### 4.2.1 Research background

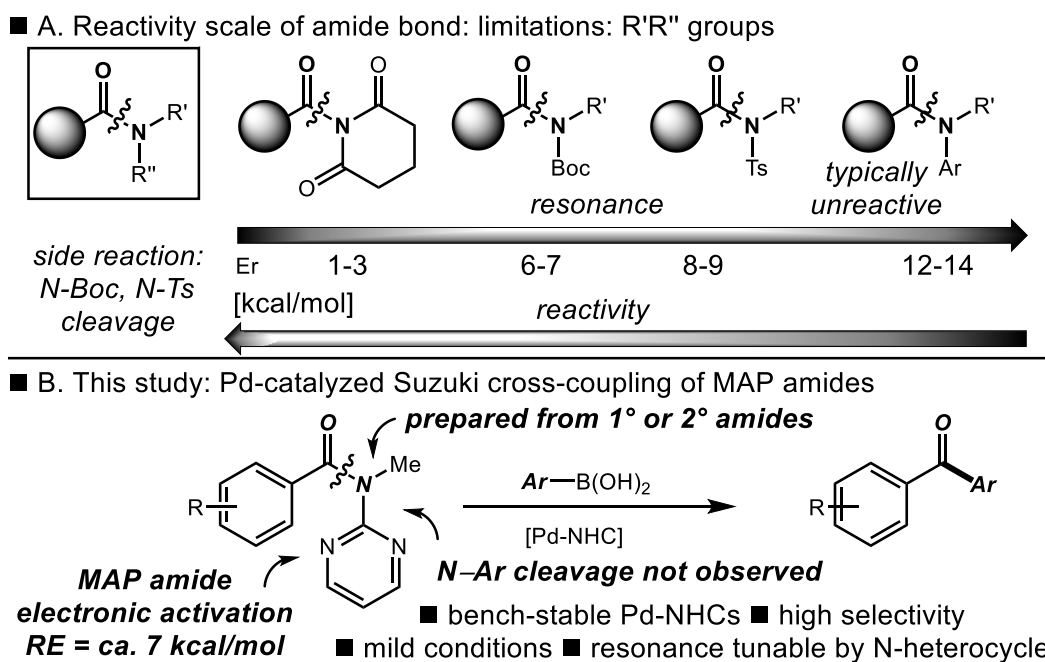


**Figure 4.2.1** (a) Activation of amides and derivatives. (b) Coupling of MAPA amides enabled by selective  $n_N \rightarrow \pi_{Ar}$  delocalization.

As our research has shown, direct activation of N–C amide bonds has been receiving increasing attention in organic synthesis.<sup>1–5</sup> This mode of reactivity induced traditionally

difficult to achieve insertion of a low-valent metal catalyst into the inert N–C(O) moiety ( $n_N \rightarrow \pi^*_{C=O}$  conjugation, barrier to rotation in planar amides of 15-20 kcal/mol),<sup>6</sup> thus enabling amides to participate in acyl- and decarbonylative cross-coupling reactions of high synthetic value. In a broader context, the amide bond activation methods were a subset of a more general strategy to catalytically activate bench-stable carboxylic acid derivatives under redox neutral conditions,<sup>7</sup> including esters,<sup>1a</sup> wherein the amide bond offered the major advantage of selective tuning of the amide bond geometry by tricoordinate nitrogen that was unavailable in other acyl-precursors.<sup>8</sup> Considering that the amide bond is a preeminent motif in various bioactive and pharmaceutically-relevant compounds,<sup>9</sup> as well as, historically, an irreplaceable intermediate in organic synthesis,<sup>10</sup> new methods for selective manipulation of amides are of great importance of within the field.

We realized that while recent developments have provided many examples for constructing carbon–heteroatom and carbon–carbon bonds through direct N–C amide bond activation, whereby the amide bond is engineered by specifically-designed N-substituents that result in the amide bond ground-state steric destabilization by steric distortion (amide bond twist),<sup>1-5,8</sup> direct methods to activate the amide bond in electronically-biased amides were noticeably lacking. In particular, the direct activation of N-alkyl-N-aryl amides has been a challenging transformation because of the high resonance energy of the amide bond in these precursors (RE, resonance energy, 13.5 kcal/mol).<sup>11</sup> These anilides already feature significantly decreased amidic resonance (cf. planar amides, 15-20 kcal/mol) as a consequence of electronic activation; however, the

resonance values were still prohibitive for synthetically useful Pd insertion under mild conditions. In consideration of these limitations, we developed N-methylamino pyrimidyl amides (MAPA) as highly-reactive, electronically-activated amides for catalytic N–C(O) cleavage (Figure 4.1.1). The following features of our research made the study noteworthy: (1) we demonstrated unusually high reactivity of MAPA amides under versatile Pd-catalysis<sup>12</sup> using user-friendly, operationally simple protocols, providing rapid entry to biaryl ketones; (2) since MAPA amides could be readily prepared from unactivated primary or secondary amides, our method offered a rapid entry to metal-catalyzed coupling of common amides; (3) we demonstrated yet another example of the advantageous effect of Pd-NHC catalysis<sup>13</sup> over Pd-phosphines in the amide bond cross-coupling manifold. From a user perspective, the use of bench-stable, commercially-available, well-defined Pd-NHC precatalysts offered a major practical advantage;<sup>14</sup> (4) Our mechanistic studies strongly supported external N–C(O) amide bond  $n_N \rightarrow \pi_{Ar}$  conjugation pathway. Collectively, the discovery that MAPA amides are highly reactive, electronically-activated amides opened the door for using N-alkyl-N-hetaryl amide electrophiles in a wide range of cross-coupling manifolds via acyl- and decarbonylative pathways in a rational and predictable manner.

In this study, we were inspired by our development of the reactivity scale of the amide bond, wherein the amide bond resonance of approx. 10 kcal/mol represented a guideline for synthetically useful Pd-insertion into the amide bond.<sup>3c</sup> In this respect, the use of anilides was synthetically limited because of the low reactivity of the amide bond (RE of 13.5 kcal/mol, N-Me-N-Ph-benzamide). The key electronic interaction<sup>15</sup> in our MAPA

design was the  $n_N \rightarrow \pi_{Ar}$  delocalization into the pyrimidine ring, which, could be translated into other heterocycles, resulting in a gradually-varying resonance and, thus, a generic activation mode of the amide bond. Importantly, this new gradual  $n_N \rightarrow \pi_{Ar}$  delocalization mechanism is not readily available by other destabilization methods of the amide bond, including steric distortion and Nlp to C=O delocalization.<sup>8</sup>

#### 4.2.2 Reaction optimization

entry	catalyst	ligand	additive	solvent	Yield (%) <sup>b</sup>
1 <sup>c</sup>	Pd(OAc) <sub>2</sub>	PCy <sub>3</sub> HBF <sub>4</sub>	H <sub>3</sub> BO <sub>3</sub>	THF	12
2 <sup>d</sup>	Pd(OAc) <sub>2</sub>	PCy <sub>3</sub> HBF <sub>4</sub>	H <sub>3</sub> BO <sub>3</sub>	THF	20
3 <sup>c</sup>	Pd(OAc) <sub>2</sub>	PCy <sub>3</sub> HBF <sub>4</sub>	TFA	THF	<2
4 <sup>c</sup>	Pd(OAc) <sub>2</sub>	PCy <sub>3</sub> HBF <sub>4</sub>	HBF <sub>4</sub>	THF	21
5	Pd(OAc) <sub>2</sub>	PCy <sub>3</sub> HBF <sub>4</sub>	-	THF	<2
6 <sup>c</sup>	Pd(OAc) <sub>2</sub>	PCy <sub>3</sub> HBF <sub>4</sub>	H <sub>2</sub> O	THF	<2
7 <sup>d,f</sup>	Pd(OAc) <sub>2</sub>	PCy <sub>3</sub> HBF <sub>4</sub>	H <sub>3</sub> BO <sub>3</sub>	THF	50
8 <sup>g</sup>	Pd <sub>2</sub> (dba) <sub>3</sub>	PCy <sub>3</sub> HBF <sub>4</sub>	-	dioxane	<2
9 <sup>d</sup>	Pd(OAc) <sub>2</sub>	PCy <sub>3</sub> HBF <sub>4</sub>	H <sub>3</sub> BO <sub>3</sub>	CH <sub>3</sub> CN	17
10 <sup>d</sup>	Pd(OAc) <sub>2</sub>	PCy <sub>3</sub> HBF <sub>4</sub>	H <sub>3</sub> BO <sub>3</sub>	THF	5
11	(IPr)Pd(cinnamyl)Cl	-	-	THF	82
12	(IPr)Pd(cinnamyl)Cl	-	-	THF	85
13	Pd(OAc) <sub>2</sub>	IPrHCl	-	THF	<2
14 <sup>e</sup>	(IPr)Pd(cinnamyl)Cl	-	H <sub>2</sub> O	THF	89
15 <sup>e</sup>	(SIPr)Pd(cinnamyl)Cl	-	H <sub>2</sub> O	THF	76
16 <sup>e</sup>	(IPr)Pd(allyl)Cl	-	H <sub>2</sub> O	THF	70
17 <sup>d</sup>	(IPr)Pd(cinnamyl)Cl	-	H <sub>3</sub> BO <sub>3</sub>	THF	<2

<sup>a</sup>Conditions: amide (1.0 equiv), R-B(OH)<sub>2</sub> (2.0 equiv), catalyst (6 mol %), K<sub>2</sub>CO<sub>3</sub> (3.0 equiv), additive (2.0-10.0 equiv), solvent (0.25 M), 65-110 °C, 15 h. Entries 1-11: [Pd] (3 mol %), ligand (12 mol %). <sup>b</sup>GC/<sup>1</sup>H NMR yields. <sup>c</sup>Additive (2.0 equiv). <sup>d</sup>Additive (4.0 equiv). <sup>e</sup>Additive (10 equiv). <sup>f</sup>(0.50 M). <sup>g</sup>Na<sub>2</sub>CO<sub>3</sub> (3.0 equiv). Entries 1-11: 110 °C. Entries 12-17: 65 °C.

**Table 4.2.1** General optimization.<sup>a</sup>

After extensive optimization, we identified N-methylamino pyrimidyl amides<sup>16</sup> as suitable electrophiles for this process. Selected optimization results are presented in Table 4.2.1. We observed the desired cross-coupling product in our proof-of-concept reaction using Pd(OAc)<sub>2</sub>/PCy<sub>3</sub> catalyst system and H<sub>3</sub>BO<sub>3</sub> as the promoter (entry 1). The acid

could protonate N-heterocycle, resulting in cis-trans isomer switch and selective metal-insertion along the isomerization pathway.<sup>17</sup> From an early stage we indentified the use of acid as essential for the formation of the desired product using Pd/phosphine catalysis (entries 1-10). After extensive screening of various conditions, the yield was increased to 50% (entry 7). At this point, we examined Pd-NHC-based catalysts systems.<sup>3c,d</sup> After experimentation, we found that (IPr)Pd(cinnamyl)Cl promoted the desired reaction with significantly improved efficiency (entry 11). As expected, strong  $\sigma$ -donation of the NHC ligand facilitated oxidative addition, while flexible steric bulk stabilized the active catalyst and promoted reductive elimination.<sup>13</sup> Importantly, the reaction temperature could be decreased to 65 °C without a deleterious effect (entry 12). A further improvement was realized by using water as an additive, presumably to enhance solubility (entry 14). As expected, the transformation was found to be strongly dependent on the Pd-NHC catalyst used, with (IPr)Pd(cinnamyl)Cl providing the optimal results (entries 14-16). Interestingly, the use of acid with Pd-NHC catalysis was ineffective (entry 17), indicating that N-protonation was not required for this catalysis to occur. The finding that Pd-NHC act as superior catalysts to Pd-PR<sub>3</sub> systems further underscores the potential of well-defined Pd(II)-NHCs as privileged catalysts for amide N–C cleavage cross-coupling.

## 4.2.3. Substrate scope

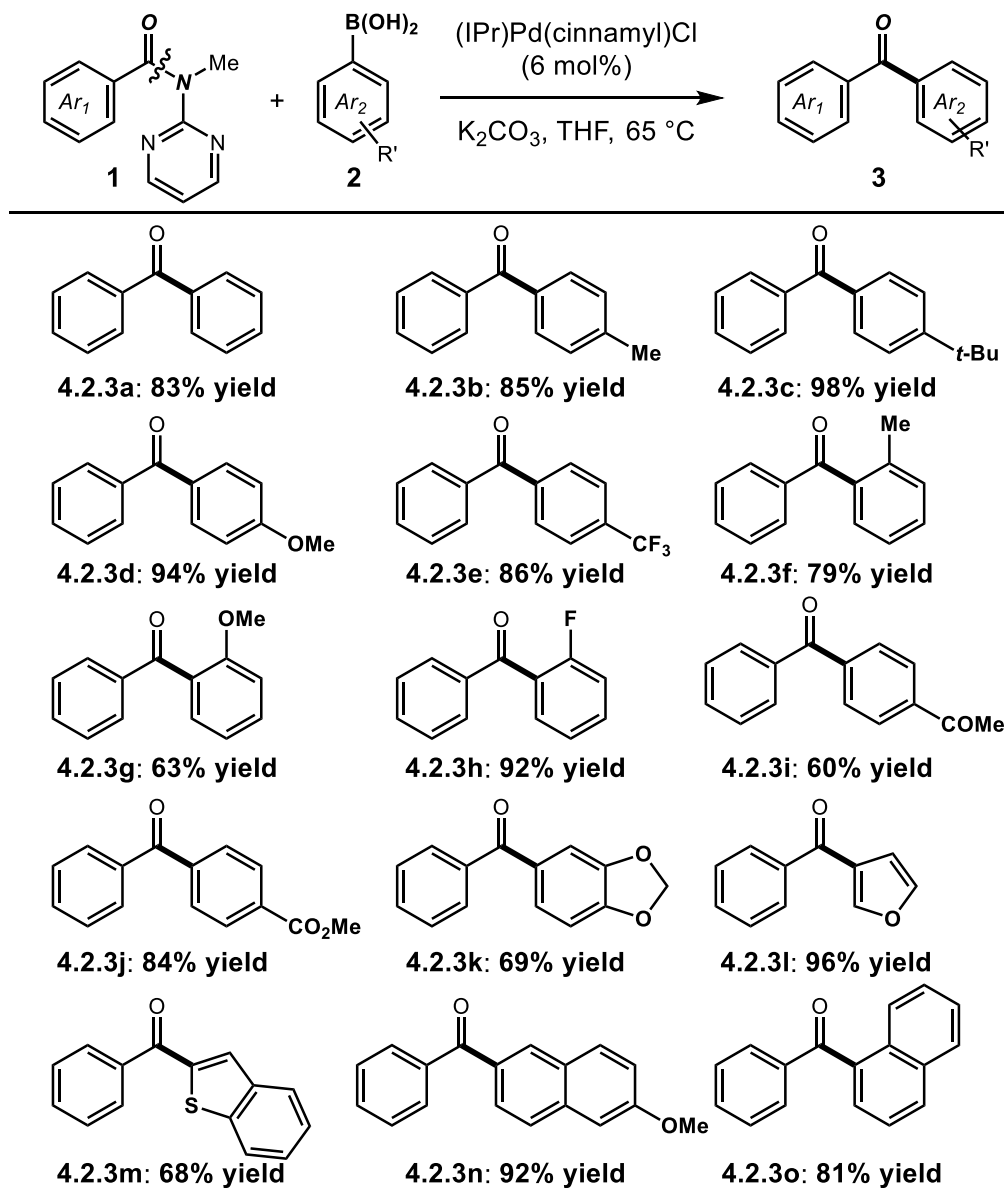
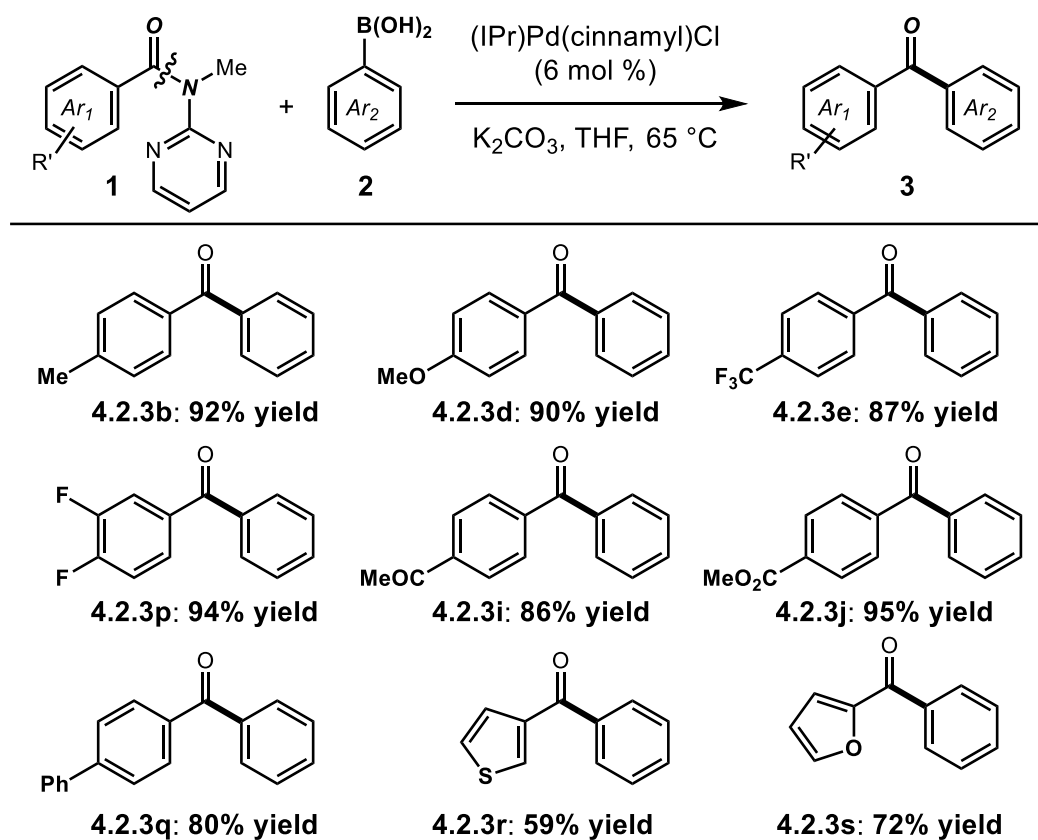


Figure 4.2.2 Boronic acid scope.

With the optimal conditions in hand, next we evaluated the scope of the reaction with respect to the boronic acid component (Figure 4.2.2). The protocol exhibited broad tolerance, including neutral (4.2.3a-4.2.3c), electron-rich (4.2.3d), electron-deficient

(**4.2.3e**) and ortho-substituted (**4.2.3f-4.2.3h**) substrates. Importantly, electrophilic functional groups, such as ketones (**4.2.3i**) and esters (**4.2.3j**) were readily accommodated. Moreover, heterocycles such as benzodioxole (**4.2.3k**), furan (**4.2.3l**), and benzothiophene (**4.2.3m**) were tolerated. Interestingly, high efficiency was observed for polyaromatic substrates (**4.2.3n-4.2.3o**), including sterically-demanding arenes (**4.2.3o**).



**Figure 4.2.3** Scope of amides

We next focused on the scope of the amide cross-coupling partner (Figure 4.2.3). MAPA amides afforded high efficiency in the cross-coupling, regardless of electronic substitution (**4.2.3b-4.2.3e**), including deactivated amides such as **4.2.3d**. Furthermore, polyfluorinated amides (**4.2.3p**) relevant from the medicinal chemistry point of view

were compatible. Importantly, electrophilic functional groups such as ketones (**4.2.3j**) and esters (**4.2.3j**) were well-tolerated. Moreover, conjugated biaryl amides (**4.2.3q**) that are prone to decarbonylation<sup>4d</sup> and heterocyclic amides (**4.2.3r-4.2.3s**), including those substituted at the electron-rich 2-position (**4.2.3s**) coupled with good levels of reactivity.

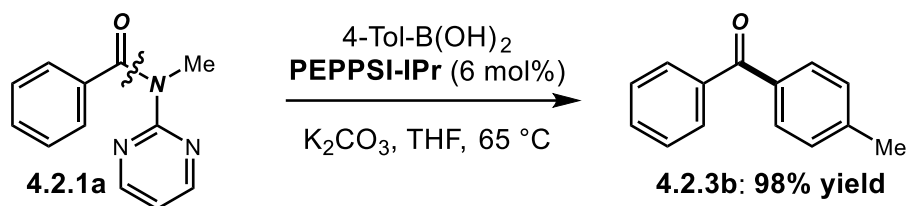


**Figure 4.2.4** Cross-coupling of MAPA amides using Pd-PEPPSI-IPr.

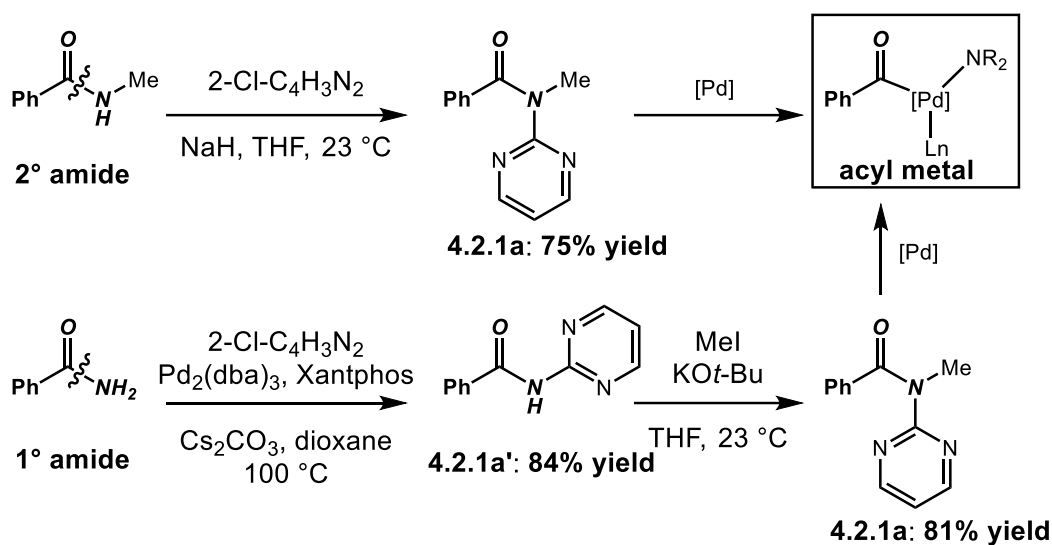


**Figure 4.2.5** Synthesis of MAPA amides from 1° or 2° amides.

Moreover, we demonstrated that the coupling could be performed using the synthetically attractive, well-defined Pd-PEPPSI-IPr type of precatalysts<sup>18</sup> without modification of the reaction conditions (Figure 4.2.4), highlighting the versatility of our protocol.



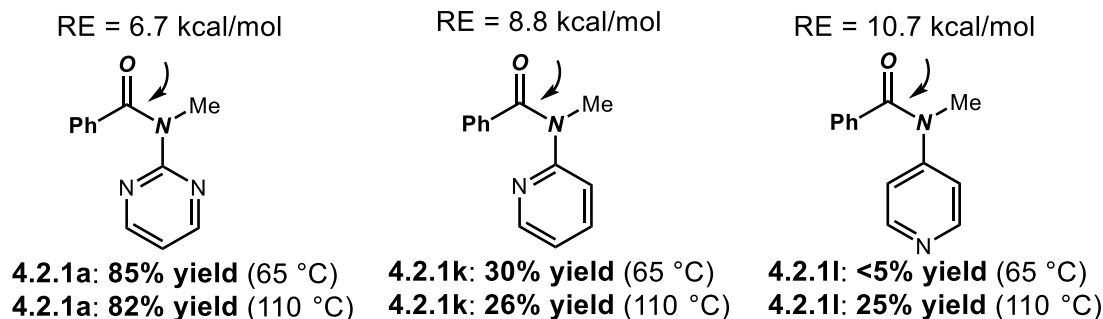


**Figure 4.2.6** Effect of the activating group.

Importantly, since MAPA amides could be readily prepared from unactivated primary or secondary amides (Figure 4.2.5),<sup>16</sup> our method offered a rapid entry to acyl-metal intermediates from generic unactivated amides. Primary and secondary amides are among of the most common intermediates in organic synthesis, which underscores the importance of developing amide cross-coupling reactions of these common substrates.<sup>9,10</sup>

#### 4.2.4. Mechanistic studies

We conducted several studies to gain insight into the mechanism. Initial rates revealed the following reactivity: (**4.2.1a**) ( $v_{\text{initial}} = 6.9 \times 10^{-2} \text{ mM s}^{-1}$ , which could be compared with the coupling of N,N-Ph,Boc benzamide under the same reaction conditions ( $v_{\text{initial}} = 7.5 \times 10^{-2} \text{ mM s}^{-1}$ ). The high reactivity of N-alkyl MAPA amide was unprecedented and suggested that these amides should be widely utilized in amide bond cross-coupling.

We performed studies to evaluate the capacity for N-directed Pd insertion into the N–C(O) bond. Towards this end, we prepared N-Me-N-2-pyridyl (**4.2.1k**) and N-Me-N-4-pyridyl (**4.2.1l**) amides and subjected these amides to the reaction (Figure 4.2.6). These substrates

underwent the coupling in 25-26% yield, consistent with electronic  $n_N \rightarrow \pi_{Ar}$  activation (cf. directed Pd-insertion).

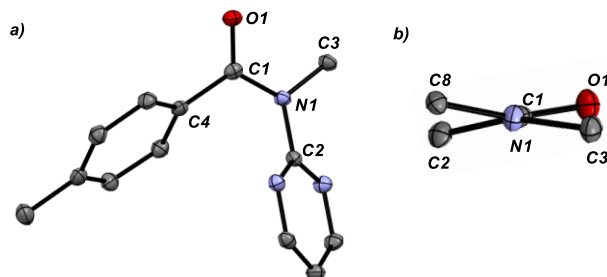


**Figure 4.2.7** X-ray structure of MAPA amide **4.2.1b**.

We further demonstrated the X-ray structure of **4.2.1b** (Figure 4.2.7). The amide showed relatively planar amide bond ( $\tau = 20.9^\circ$ ,  $\chi_N = 5.2^\circ$ ,  $\chi_C = 3.9^\circ$ ). The N–C(O), C=O and N–Ar bond lengths were 1.378 Å, 1.225 Å, and 1.407 Å. Compared with the corresponding N-Me-N-2-pyridyl ( $\tau = 15.0^\circ$ ,  $\chi_N = 8.4^\circ$ ,  $\chi_X = 4.0^\circ$ ; N–C(O) = 1.366 Å; C=O = 1.226 Å, N–Ar = 1.428 Å),<sup>17</sup> and N-Me-N-Ph benzamide ( $\tau = 9.1^\circ$ ,  $\chi_N = 6.6^\circ$ ,  $\chi_X = 2.1^\circ$ ; N–C(O) = 1.355 Å; C=O = 1.232 Å, N–Ar = 1.437 Å),<sup>11</sup> these values indicate a gradual increase in  $n_N \rightarrow \pi_{Ar}$  conjugation.

#### 4.2.5. Conclusion

In summary, we developed the first method for the direct activation of N-methylamino pyrimidinyl amides (MAPA) by selective N–C amide bond cleavage. The reaction used commercially-available and bench-stable Pd-NHC precatalysts, occurred with high N–C activation chemoselectivity and was operationally simple. Most importantly, this method introduced MAPA amides as resonance-controlled, practical alternatives to anilides for a

range of catalytic coupling reactions via acyl- and decarbonylative pathways. In these amides, the N–X cleavage reaction, the most common side process in the amide bond activation was not observed. Furthermore, MAPA amides provided rapid entry to acyl metal intermediates from common unactivated primary and secondary amides. Mechanistic studies strongly supported  $n_N \rightarrow \pi_{Ar}$  delocalization as an efficient concept for activating the amide bond.

#### 4.2.6 Experimental section

**General procedure for amide synthesis.** An oven-dried flask (100 mL) equipped with a stir bar was charged with *N*-methylpyrimidin-2-amine (typically, 5.0 mmol, 1.0 equiv), triethylamine (typically, 2.0 equiv), 4-dimethylaminopyridine (typically, 0.25 equiv) and dichloromethane (typically, 0.20 M), placed under a positive pressure of argon, and subjected to three evacuation/backfilling cycles under high vacuum. Benzoyl chloride (typically, 1.1 equiv) was added dropwise to the reaction mixture with vigorous stirring at 0 °C, and the reaction mixture was stirred for 15 h at room temperature. After the indicated time, the reaction mixture was diluted with Et<sub>2</sub>O (30 mL), filtered, the organic layer was washed with HCl (1.0 *N*, 30 mL), brine (30 mL), dried over Na<sub>2</sub>SO<sub>4</sub>, filtered, and concentrated. The crude product was purified by chromatography on silica gel (EtOAc/hexanes) to afford the title product.

**General procedure for MAPA amide synthesis from secondary amides.** An oven-dried flask (100 mL) equipped with a stir bar was charged with *N*-methylbenzamide (5.5 mmol, typically, 1.1 equiv) and THF (0.50 M), and cooled to 0 °C. Sodium hydride

(typically, 1.1 equiv) was added under a positive pressure of argon with vigorous stirring at 0 °C. After stirring for 10 min at 0 °C, 2-chloropyrimidine (5.0 mmol, 1.0 equiv) in THF (0.50 M) was added dropwise to the reaction mixture with vigorous stirring at 0 °C, and the reaction mixture was stirred for 48 h at room temperature. After the indicated time, the reaction mixture was diluted with water (20 mL), extracted with CH<sub>2</sub>Cl<sub>2</sub> (2 x 10 mL), the organic layers were combined, washed with brine (30 mL), dried over Na<sub>2</sub>SO<sub>4</sub>, filtered, and concentrated. The crude product was purified by chromatography on silica gel (EtOAc/hexanes) to afford the title product. Yield: 75%.

**General procedure for MAPA amide synthesis from primary amides.** *Step 1:* An oven-dried flask (25 mL) equipped with a stir bar was charged with benzamide (typically, 1.0 mmol, 1.0 equiv), 2-chloropyrimidine (typically, 1.2 equiv), Pd<sub>2</sub>(dba)<sub>3</sub> (typically, 5.0 mol%), Xantphos (typically, 15.0 mol%), and Cs<sub>2</sub>CO<sub>3</sub> (typically, 1.4 equiv), placed under a positive pressure of argon, and subjected to three evacuation/backfilling cycles under high vacuum. Dioxane (0.50 M) was added under a positive pressure of argon, and the reaction mixture was stirred for 15 h at 100 °C. After the indicated time, the reaction mixture was concentrated and purified directly by chromatography on silica gel (EtOAc/hexanes) to afford the title product. Yield 84% (167.2 mg). White solid. *Step 2:* An oven-dried flask (25 mL) was charged with *N*-(pyrimidin-2-yl)benzamide (1.0 mmol, 1.0 equiv) KO<sup>*t*</sup>-Bu (typically, 2.0 mmol, 2.0 equiv) and THF (0.125 M) ), and cooled to 0 °C. Methyl iodide (typically, 4.0 mmol, 4.0 equiv) in THF (2 mL) was added dropwise to the reaction mixture with vigorous stirring at 0 °C, and the reaction mixture was stirred for 48 h at room temperature. After the indicated time, the reaction mixture was diluted

with water (5 mL), extracted with CH<sub>2</sub>Cl<sub>2</sub> (2 x 5 mL), the organic layers were combined, washed with brine (30 mL), dried over Na<sub>2</sub>SO<sub>4</sub>, filtered, and concentrated. The crude product was purified by chromatography on silica gel (EtOAc/hexanes) to afford the title product. Yield: 81% (172.7 mg). White solid.

**General procedure for Suzuki-Miyaura cross-coupling of MAPA amides.** An oven-dried vial equipped with a stir bar was charged with an amide substrate (neat, 1.0 equiv), potassium carbonate (typically, 3.0 equiv), boronic acid (typically, 2.0 equiv), Pd-NHC catalyst (typically, 6 mol%), water (typically, 10.0 equiv), placed under a positive pressure of argon, and subjected to three evacuation/backfilling cycles under high vacuum. THF (typically, 0.25 M) was added with vigorous stirring at room temperature, the reaction mixture was placed in a preheated oil bath at 65 °C and stirred for an indicated time. After the indicated time, the reaction mixture was cooled down to room temperature, diluted with CH<sub>2</sub>Cl<sub>2</sub> (10 mL), filtered, and concentrated. The sample was analyzed by <sup>1</sup>H NMR (CDCl<sub>3</sub>, 500 MHz) and GC-MS to obtain conversion, selectivity and yield using internal standard and comparison with authentic samples. Purification by chromatography on silica gel (EtOAc/hexanes) afforded the title product.

**4.2.1a.** Yield 83%. White solid. <sup>1</sup>H NMR (500 MHz, CDCl<sub>3</sub>) δ 8.47-8.41 (m, 2 H), 7.38 (d, *J* = 7.3 Hz, 2 H), 7.34 (d, *J* = 7.0 Hz, 1 H), 7.25 (t, *J* = 7.1 Hz, 2 H), 6.96-6.91 (m, 1 H), 3.69 (s, 3 H). <sup>13</sup>C NMR (125 MHz, CDCl<sub>3</sub>) δ 172.31, 162.58, 157.65, 137.06, 130.21, 128.07, 127.99, 116.74, 34.88.

**4.2.1b.** Yield 79%. White solid. Mp = 111-114 °C.  $^1\text{H}$  NMR (500 MHz,  $\text{CDCl}_3$ )  $\delta$  8.46 (d,  $J$  = 4.8 Hz, 2 H), 7.29 (d,  $J$  = 8.1 Hz, 2 H), 7.06 (d,  $J$  = 7.9 Hz, 2 H), 6.94 (t,  $J$  = 4.8 Hz, 1 H), 3.68 (s, 3 H), 2.33 (s, 3 H).  $^{13}\text{C}$  NMR (125 MHz,  $\text{CDCl}_3$ )  $\delta$  172.31, 162.79, 157.66, 140.62, 134.05, 128.68, 128.27, 116.59, 34.98, 21.44. HRMS calcd for  $\text{C}_{13}\text{H}_{13}\text{N}_3\text{ONa}$  ( $\text{M}^+ + \text{Na}$ ) 250.0951, found 250.0960.

**4.2.1c.** Yield 75%. White solid. Mp = 79-80 °C.  $^1\text{H}$  NMR (500 MHz,  $\text{CDCl}_3$ )  $\delta$  8.46 (d,  $J$  = 4.8 Hz, 2 H), 7.36 (d,  $J$  = 8.7 Hz, 2 H), 6.93 (t,  $J$  = 4.8 Hz, 1 H), 6.76 (d,  $J$  = 8.7 Hz, 2 H), 3.80 (s, 3 H), 3.66 (s, 3 H).  $^{13}\text{C}$  NMR (125 MHz,  $\text{CDCl}_3$ )  $\delta$  171.92, 162.95, 161.32, 157.70, 130.28, 129.12, 116.45, 113.30, 55.28, 35.08. HRMS calcd for  $\text{C}_{13}\text{H}_{13}\text{N}_3\text{O}_2\text{Na}$  ( $\text{M}^+ + \text{Na}$ ) 266.0900, found 266.0910.

**4.2.1d.** Yield 77%. White solid. Mp = 50-53 °C.  $^1\text{H}$  NMR (500 MHz,  $\text{CDCl}_3$ )  $\delta$  8.43 (d,  $J$  = 4.8 Hz, 2 H), 7.52 (d,  $J$  = 8.3 Hz, 2 H), 7.47 (d,  $J$  = 8.2 Hz, 2 H), 6.96 (t,  $J$  = 4.8 Hz, 1 H), 3.69 (s, 3 H).  $^{13}\text{C}$  NMR (125 MHz,  $\text{CDCl}_3$ )  $\delta$  170.92, 161.96, 157.69, 140.79, 131.68 ( $J^2$  = 32.5 Hz), 128.14, 125.02, 123.73 ( $J^1$  = 271.3 Hz), 117.07, 34.68.  $^{19}\text{F}$  NMR (471 MHz,  $\text{CDCl}_3$ )  $\delta$  -62.88. HRMS calcd for  $\text{C}_{13}\text{H}_{10}\text{N}_3\text{F}_3\text{ONa}$  ( $\text{M}^+ + \text{Na}$ ) 304.0668, found 304.0675.

**4.2.1e.** Yield 89%. Colourless oil.  $^1\text{H}$  NMR (500 MHz,  $\text{CDCl}_3$ )  $\delta$  8.48 (d,  $J$  = 4.8 Hz, 2 H), 7.27 (d,  $J$  = 10.4 Hz, 1 H), 7.11-7.06 (m, 1 H), 7.06-7.01 (m, 1 H), 6.99 (t,  $J$  = 4.8 Hz, 1 H), 3.67 (s, 3 H).  $^{13}\text{C}$  NMR (125 MHz,  $\text{CDCl}_3$ )  $\delta$  170.10, 162.17, 157.81, 151.69 ( $J^1$  = 207.5 Hz), 149.69 ( $J^1$  = 205.0 Hz), 134.10 ( $J^3$  = 4.4 Hz), 124.53 ( $J^3$  = 4.4 Hz), 117.62 ( $J^2$

= 17.5 Hz), 117.04, 116.89 ( $J^2 = 17.5$  Hz), 34.93.  $^{19}\text{F}$  NMR (471 MHz,  $\text{CDCl}_3$ )  $\delta$  -134.17, -137.19. HRMS calcd for  $\text{C}_{12}\text{H}_9\text{N}_3\text{F}_2\text{ONa}$  ( $\text{M}^+ + \text{Na}$ ) 272.0606, found 272.0617.

**4.2.1f.** Yield 79%. White solid. Mp = 79-81 °C.  $^1\text{H}$  NMR (500 MHz,  $\text{CDCl}_3$ )  $\delta$  8.45-8.41 (m, 2 H), 7.85 (d,  $J = 11.6$  Hz, 2 H), 7.45 (d,  $J = 11.7$  Hz, 2 H), 6.98-6.94 (m, 1 H), 3.70 (s, 3 H), 2.60 (s, 3 H).  $^{13}\text{C}$  NMR (125 MHz,  $\text{CDCl}_3$ )  $\delta$  197.53, 171.29, 162.03, 157.71, 141.59, 137.84, 128.04, 128.00, 117.02, 34.65, 26.73. HRMS calcd for  $\text{C}_{14}\text{H}_{13}\text{N}_3\text{O}_2\text{Na}$  ( $\text{M}^+ + \text{Na}$ ) 278.0900, found 278.0909.

**4.2.1g.** Yield 72%. White solid. Mp = 105-107 °C.  $^1\text{H}$  NMR (500 MHz,  $\text{CDCl}_3$ )  $\delta$  8.42 (d,  $J = 4.8$  Hz, 2 H), 7.93 (d,  $J = 8.2$  Hz, 2 H), 7.43 (d,  $J = 8.2$  Hz, 2 H), 6.95 (t,  $J = 4.8$  Hz, 1 H), 3.92 (s, 3 H), 3.70 (s, 3 H).  $^{13}\text{C}$  NMR (125 MHz,  $\text{CDCl}_3$ )  $\delta$  171.40, 166.45, 162.06, 157.68, 141.52, 131.24, 129.28, 127.80, 116.99, 52.27, 34.64. HRMS calcd for  $\text{C}_{14}\text{H}_{13}\text{N}_3\text{O}_3\text{Na}$  ( $\text{M}^+ + \text{Na}$ ) 294.0849, found 294.0856.

**4.2.1h.** Yield 83%. White solid. Mp = 168-170 °C.  $^1\text{H}$  NMR (500 MHz,  $\text{CDCl}_3$ )  $\delta$  8.48 (d,  $J = 5.8$  Hz, 2 H), 7.59 (d,  $J = 8.1$  Hz, 2 H), 7.51 (d,  $J = 7.6$  Hz, 2 H), 7.47-7.42 (m, 4 H), 7.37 (t,  $J = 7.3$  Hz, 1 H), 6.95 (t,  $J = 5.3$  Hz, 1 H).  $^{13}\text{C}$  NMR (125 MHz,  $\text{CDCl}_3$ )  $\delta$  172.04, 162.65, 157.68, 143.09, 140.12, 135.78, 128.83, 128.69, 127.80, 127.10, 126.67, 116.73, 34.95. HRMS calcd for  $\text{C}_{18}\text{H}_{15}\text{N}_3\text{ONa}$  ( $\text{M}^+ + \text{Na}$ ) 312.1107, found 312.1117.

**4.2.1i.** Yield 67%. White solid. Mp = 71-73 °C.  $^1\text{H}$  NMR (500 MHz,  $\text{CDCl}_3$ )  $\delta$  8.52 (brs, 2 H), 7.51 (brs, 1 H), 7.14 (brs, 1 H), 7.02 (s, 1 H), 6.90 (brs, 1 H), 3.64 (s, 3 H).  $^{13}\text{C}$

NMR (125 MHz, CDCl<sub>3</sub>)  $\delta$  166.79, 162.60, 157.80, 138.34, 129.10, 127.30, 125.06, 116.99, 34.84. HRMS calcd for C<sub>10</sub>H<sub>9</sub>N<sub>3</sub>OSNa (M<sup>+</sup> + Na) 242.0359, found 242.0367.

**4.2.1j.** Yield 62%. White solid. Mp = 51-52 °C. <sup>1</sup>H NMR (500 MHz, CDCl<sub>3</sub>)  $\delta$  8.56 (d, *J* = 4.8 Hz, 2 H), 7.18 (s, 1 H), 7.04 (t, *J* = 4.8 Hz, 1 H), 7.00 (d, *J* = 3.4 Hz, 1 H), 6.44-6.40 (m, 1 H), 3.63 (s, 3 H). <sup>13</sup>C NMR (125 MHz, CDCl<sub>3</sub>)  $\delta$  162.17, 161.38, 157.78, 148.83, 143.62, 116.91, 116.17, 111.66, 34.55. HRMS calcd for C<sub>10</sub>H<sub>9</sub>N<sub>3</sub>O<sub>2</sub>Na (M<sup>+</sup> + Na) 226.0587, found 226.0596.



## References

(1) (a) Takise, R.; Muto, K.; Yamaguchi, J. *Chem. Soc. Rev.* **2017**, DOI: 10.1039/c7cs00182g. (b) Meng, G.; Shi, S.; Szostak, M. *Synlett* **2016**, 27, 2530. (c) Liu, C.; Szostak, M. *Chem. Eur. J.* **2017**, 23, 7157. (d) Dander, J. E.; Garg, N. K. *ACS Catal.* **2017**, 7, 1413.

(2) (a) *Metal-Catalyzed Cross-Coupling Reactions and More*, de Meijere, A.; Bräse, S.; Oestreich, M., Eds.; Wiley: New York, 2014. (b) *Science of Synthesis: Cross-Coupling and Heck-Type Reactions*, Molander, G. A.; Wolfe, J. P.; Larhed, M., Eds.; Thieme: Stuttgart, 2013.

(3) (a) Hie, L.; Nathel, N. F. F.; Shah, T. K.; Baker, E. L.; Hong, X.; Yang, Y. F.; Liu, P.; Houk, K. N.; Garg, N. K. *Nature* **2015**, 524, 79. (b) Meng, G.; Szostak, M. *Org. Lett.* **2015**, 17, 4364. (c) Lei, P.; Meng, G.; Szostak, M. *ACS Catal.* **2017**, 7, 1960. (d) Meng, G.; Lei, P.; Szostak, M. *Org. Lett.* **2017**, 19, 2158. (e) Amani, J.; Alam, R.; Badir, S.; Molander, G. A. *Org. Lett.* **2017**, 19, 2426. (f) Ni, S.; Zhang, W.; Mei, H.; Han, J.; Pan, Y. *Org. Lett.* **2017**, 19, 2536. (g) Lei, P.; Meng, G.; Shi, S.; Ling, Y.; An, J.; Szostak, R.; Szostak, M. *Chem. Sci.* **2017**, 8, 6525. (h) Tatamidani, H.; Kakiuchi, F.; Chatani, N. *Org. Lett.* **2004**, 6, 3597. (i) Li, X.; Zou, G. *Chem. Commun.* **2015**, 51, 5089. (j) Meng, G.; Szostak, M. *Org. Biomol. Chem.* **2016**, 14, 5690.

(4) (a) Meng, G.; Szostak, M. *Angew. Chem. Int. Ed.* **2015**, 54, 14518. (b) Shi, S.; Meng, G.; Szostak, M. *Angew. Chem. Int. Ed.* **2016**, 55, 6959. (c) Meng, G.; Szostak, M. *Org. Lett.* **2016**, 18, 796. (d) Dey, A.; Sasmai, S.; Seth, K.; Lahiri, G. K.; Maiti, D. *ACS Catal.*

- 2017**, 7, 433. (e) Yue, H.; Guo, L.; Liao, H. H.; Cai, Y.; Zhu, C.; Rueping, M. *Angew. Chem. Int. Ed.* **2017**, 56, 4282. (f) Yue, H.; Guo, L.; Lee, S. C.; Liu, X.; Rueping, M. *Angew. Chem. Int. Ed.* **2017**, 56, 3972. (g) Shi, S.; Szostak, M. *Org. Lett.* **2017**, 19, 3095.
- (5) Walker, J. A.; Vickerman, K. L.; Humke, J. N.; Stanley, L. M. *J. Am. Chem. Soc.* **2017**, 139, 10228.
- (6) (a) Kaiser, D.; Maulide, N. *J. Org. Chem.* **2016**, 81, 4421. (b) Ruider, S. A.; Maulide, N. *Angew. Chem. Int. Ed.* **2015**, 54, 13856. (c) Valerio, V.; Petkova, D.; Madelaine, C.; Maulide, N. *Chem. Eur. J.* **2013**, 19, 2606.
- (7) (a) Dzik, W. I.; Lange, P. P.; Gooßen, L. J. *Chem. Sci.* **2012**, 3, 2671. (b) Amaike, K.; Muto, K.; Yamaguchi, J.; Itami, K. *J. Am. Chem. Soc.* **2012**, 134, 13573.
- (8) (a) Szostak, R.; Shi, S.; Meng, G.; Lalancette, R.; Szostak, M. *J. Org. Chem.* **2016**, 81, 8091. (b) Pace, V.; Holzer, W.; Meng, G.; Shi, S.; Lalancette, R.; Szostak, R.; Szostak, M. *Chem. Eur. J.* **2016**, 22, 14494.
- (9) (a) Greenberg, A.; Breneman, C. M.; Liebman, J. F., Eds. *The Amide Linkage: Structural Significance in Chemistry, Biochemistry, and Materials Science*; Wiley: New York, 2000. (b) Roughley, S. D.; Jordan, A. M. *J. Med. Chem.* **2011**, 54, 3451. (c) Marchildon, K. *Macromol. React. Eng.* **2011**, 5, 22. (d) Pattabiraman, V. R.; Bode, J. W. *Nature* **2011**, 480, 471.
- (10) Trost, B. M.; Fleming, I. *Comprehensive Organic Synthesis*; Pergamon Press: Oxford, 1991.

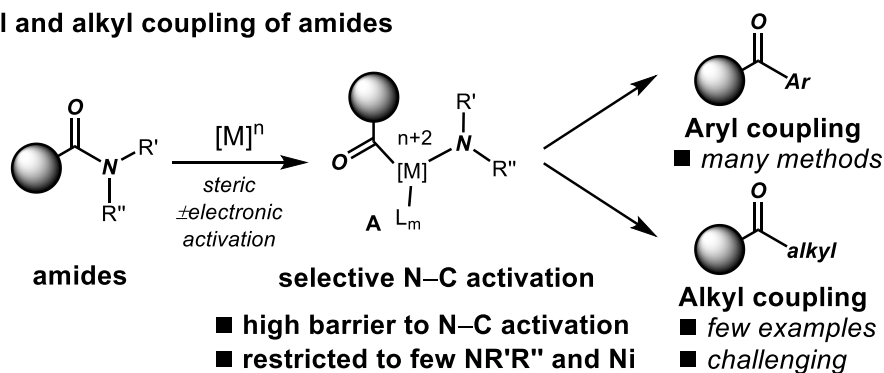
- (11) Szostak, R.; Meng, G.; Szostak, M. *J. Org. Chem.* **2017**, *82*, 6373.
- (12) Johansson-Seechurn, C. C. C.; Kitching, M. O.; Colacot, T. J.; Snieckus, V. *Angew. Chem. Int. Ed.* **2012**, *51*, 5062.
- (13) (a) Fortman, G. C.; Nolan, S. P. *Chem. Soc. Rev.* **2011**, *40*, 5151. (b) Marion, N.; Navarro, O.; Mei, J.; Stevens, E. D.; Scott, N. M.; Nolan, S. P. *J. Am. Chem. Soc.* **2006**, *128*, 4101.
- (14) (a) *Science of Synthesis: N-Heterocyclic Carbenes in Catalytic Organic Synthesis*, Nolan, S. P.; Cazin, C. S. J., Eds.; Thieme: Stuttgart, 2017. (b) Hazari, N.; Melvin, P. R.; Beromi, M. M. *Nat. Rev. Chem.* **2017**, *1*, 25.
- (15) Vatsadze, S. Z.; Loginova, Y. D.; dos Passos Gomes, G.; Alabugin, I. V. *Chem. Eur. J.* **2017**, *23*, 1521.
- (16) (a) Meyers, A. I.; Comins, D. L. *Tetrahedron Lett.* **1978**, *19*, 5179. (b) Bennet, A. J.; Somayaji, V.; Brown, R. S.; Santarsiero, B. D. *J. Am. Chem. Soc.* **1991**, *113*, 7563.
- (17) Okamoto, I.; Nabeta, M.; Yamamoto, M.; Mikami, M.; Takeya, T.; Tamura, O. *Tetrahedron Lett.* **2006**, *47*, 7143.
- (18) (a) Lei, P.; Meng, G.; Ling, Y.; An, J.; Szostak, M. *J. Org. Chem.* **2017**, *82*, 6638. (b) Valente, C.; Calimsiz, S.; Hoi, K. H.; Mallik, D.; Sayah, M.; Organ, M. G. *Angew. Chem. Int. Ed.* **2012**, *51*, 3314.

### 4.3 B-Alkyl cross-coupling of amides

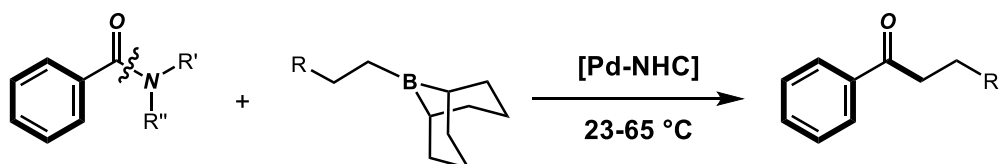
Parts of this section were adapted with permission from the article “Palladium/NHC (NHC = N-Heterocyclic Carbene)-Catalyzed B-Alkyl Suzuki Cross-Coupling of Amides by Selective N–C Bond Cleavage” (*Org. Lett.* **2017**, *20*, 6789). Copyright ©2017, American Chemical Society.

#### 4.3.1 Research background

##### A. Aryl and alkyl coupling of amides



##### B. B-Alkyl Suzuki Cross-Coupling of 1° Amides via N–C Activation



- challenging catalytic alkylation of amides by N–C cleavage
- modular, air-stable Pd-NHC precatalysts
- orthogonal cross-coupling
- high selectivity for N–C acyl scission
- common primary amides

**Figure 4.3.1** Palladium/NHC-catalyzed B-alkyl Suzuki-Miyaura cross-coupling of amides by selective N–C cleavage.

As outlined in chapters 1-3 of this thesis, the cross-coupling of amides has emerged as a powerful route to carbon–carbon and carbon–heteroatom bond formation by engaging

traditionally inert amide bonds (amidic resonance, 15-20 kcal/mol,  $n_N \rightarrow \pi^*_{C=O}$  conjugation).<sup>1-3</sup> Direct functionalization of amides is an important goal in organic synthesis<sup>4-8</sup> especially due to the potential to unlock Weinreb amide-type reactivity of amides<sup>9</sup> by catalytic metal insertion with much improved functional group tolerance, chemoselectivity<sup>10</sup> and operational convenience by avoiding strong organometallic reagents. Furthermore, the direct activation of amides by N-Boc or N-Ts protection offers significant advantages to manipulate common primary and secondary amide bonds,<sup>11</sup> providing a new synthetic disconnection for the construction of functionalized molecules from ubiquitous amides.<sup>12</sup> We realized that despite recent progress in C(acyl)-aryl cross-couplings of amides,<sup>3,4,6-8</sup> alkylation of amide bonds by transition-metal-catalysis has remained a significant challenge due to competing  $\beta$ -hydride elimination/protodemetalation decomposing the organometallic and slower transmetalation.<sup>13</sup> In previous work, Ni-catalyzed alkylation of N-Ts activated amides using alkylzinc reagents and Ni-catalyzed alkylation of N-Ph/Me activated amides using alkylborane reagents has been reported.<sup>14</sup> Furthermore, a Ni-catalyzed reductive C(acyl)-alkyl cross-coupling of N-acyl-succinimide amides has been reported.<sup>4e</sup> We turned our attention to the B-alkyl Suzuki cross-coupling<sup>15</sup> of amides using Pd-catalysis to promote selective formation of acyl-metal from more challenging N-Boc and N-cyclic amides that are inaccessible by Ni-catalysis.

entry	catalyst	base	solvent	T (°C)	yield (%)
1	(IPr)Pd(cin)Cl	K <sub>2</sub> CO <sub>3</sub>	THF	23	56
2	(IPr)Pd(cin)Cl	K <sub>2</sub> CO <sub>3</sub>	THF	65	67
3 <sup>b</sup>	(IPr)Pd(cin)Cl	K <sub>2</sub> CO <sub>3</sub>	THF	65	48
4 <sup>c</sup>	(IPr)Pd(cin)Cl	K <sub>2</sub> CO <sub>3</sub>	THF	23	70
5 <sup>d</sup>	(IPr)Pd(cin)Cl	K <sub>2</sub> CO <sub>3</sub>	THF	23	53
6	(IPr)Pd(cin)Cl	K <sub>2</sub> CO <sub>3</sub>	THF	23	84
7	(IPr)Pd(cin)Cl	K <sub>2</sub> CO <sub>3</sub>	THF	65	91
8	(IPr)Pd(cin)Cl	Cs <sub>2</sub> CO <sub>3</sub>	THF	23	<5
9	(IPr)Pd(cin)Cl	K <sub>3</sub> PO <sub>4</sub>	THF	23	27
10	(IPr)Pd(cin)Cl	K <sub>2</sub> CO <sub>3</sub>	toluene	23	28
11	(IPr)Pd(cin)Cl	K <sub>2</sub> CO <sub>3</sub>	Et <sub>2</sub> O	23	21
12	(IPr)Pd(allyl)Cl	K <sub>3</sub> PO <sub>4</sub>	THF	23	5
13	(IMes)Pd(cin)Cl	K <sub>2</sub> CO <sub>3</sub>	THF	23	7
14	(SIPr)Pd(cin)Cl	K <sub>2</sub> CO <sub>3</sub>	THF	23	21
15	Pd-PEPPSI-IPr	K <sub>2</sub> CO <sub>3</sub>	THF	23	15
16	(IPr)Pd(1- <i>t</i> -Bu-ind)Cl	K <sub>2</sub> CO <sub>3</sub>	THF	23	57
17	-	K <sub>2</sub> CO <sub>3</sub>	THF	23	<5
18 <sup>e</sup>	Pd(PPh <sub>3</sub> ) <sub>4</sub>	Cs <sub>2</sub> CO <sub>3</sub>	THF	110	<5

<sup>a</sup>Conditions: **1** (1.0 equiv), *n*-C<sub>10</sub>H<sub>21</sub>-9-BBN (2.0 equiv), catalyst (3-6 mol %), base (3.0 equiv), solvent (0.25 M), 23-110 °C, 15 h. Entries 1-5: [Pd] (3 mol %), entries 6-17: [Pd] (6 mol %). <sup>b</sup>K<sub>2</sub>CO<sub>3</sub> (4.5 equiv). <sup>c</sup>H<sub>2</sub>O (10 equiv). <sup>d</sup>Et<sub>3</sub>N (30 mol %). <sup>e</sup>[Pd] (5 mol %). See SI for experimental details.

**Table 4.3.1** General optimization.<sup>a</sup>

We developed a highly chemoselective, palladium-NHC (NHC = N-heterocyclic carbene)-catalyzed, direct cross-coupling between B-sp<sup>3</sup>-alkyl reagents and activated amides by N–C(O) cleavage (Figure 4.3.1). Importantly, various amides, including challenging primary amides after direct and site-selective N,N-di-Boc activation and sensitive N-glutarimide amides,<sup>3a,b</sup> were compatible with this method. The synthetic potential of this mild protocol was demonstrated in sequential C(sp<sup>2</sup>)–C(sp<sup>2</sup>)/C(sp<sup>2</sup>)–C(sp<sup>3</sup>) cross-couplings using a common primary amide bond. Most importantly, the method expanded the well-developed manifold of Pd-catalyzed Suzuki-Miyaura aryl cross-coupling of amides to the B-alkyl cross-coupling using versatile organoboron reagents.<sup>15</sup> Furthermore, the method provided a rare example of air- and moisture-stable,

well-defined and highly reactive Pd-NHC precatalysts in B-alkyl-Suzuki cross-couplings.<sup>16</sup>

### 4.3.2 Optimization studies

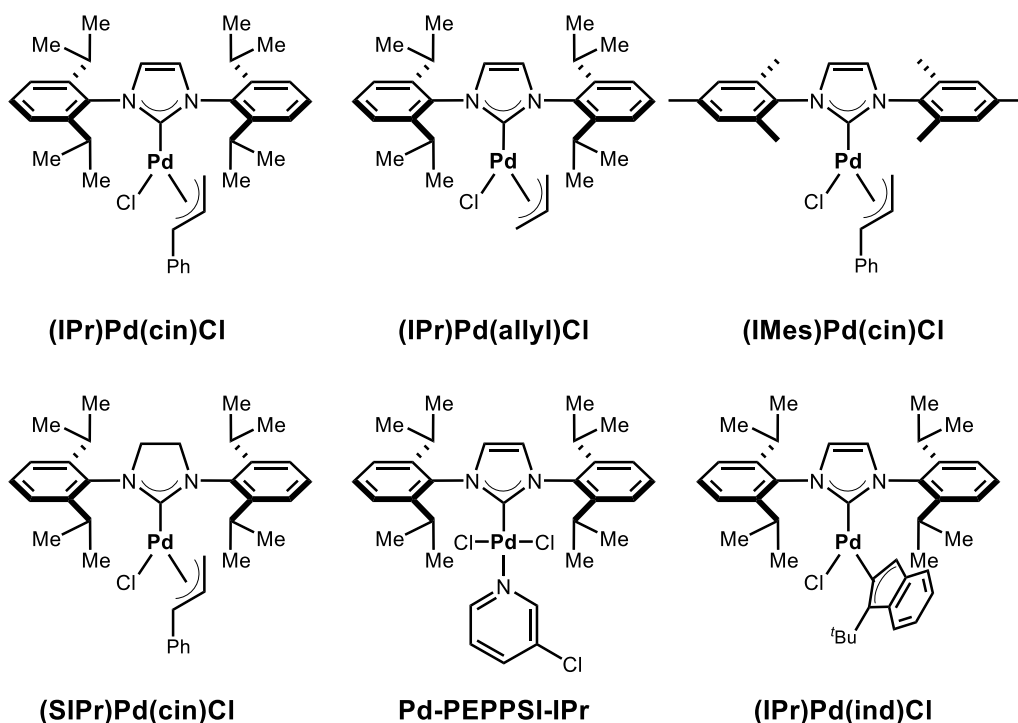


**Figure 4.3.2** Structures of palladium-NHC precatalysts.

Table 4.3.1 presents our key results obtained during the optimization of the reaction conditions. To test the B-alkyl-Suzuki cross-coupling, we selected N,N-di-Boc activated benzamide. The site-selective N,N-diacylation of the 1° amide bond permits a significant decrease in amidic resonance ( $E_R = 7.6$  kcal/mol) to engage common benzamides in general cross-coupling manifolds.<sup>11</sup> However, the major challenge in the cross-coupling of N,N-di-Boc amides is the propensity of the N-Boc group to undergo scission, deactivating the acyl amide bond towards metal insertion. We found that the desired B-

alkyl Suzuki alkylation product was formed using [(IPr)Pd(cin)Cl] precatalyst<sup>17</sup> (3 mol%) in a promising 56% yield at room temperature (Table 1, entry 1) using *n*-C<sub>10</sub>H<sub>21</sub>-9-BBN (2.0 equiv) in the presence of K<sub>2</sub>CO<sub>3</sub> as a base. Improvement in the reaction efficiency was realized by increasing the reaction temperature to 65 °C (entry 2); however, the reaction was less efficient using an excess of base (entry 3), consistent with facile decomposition of the alkyl- organometallic.<sup>13</sup> The addition of water had a minor, but positive effect on the reaction efficiency (entry 4); however, our attempts to generate the more reactive acylammonium species in situ by using Lewis bases<sup>4c</sup> did not result in noticeable improvements of the reaction efficiency (entry 5). Further optimization revealed that yields could be dramatically improved by employing 6 mol% of the Pd-NHC precatalyst (entries 6-7), consistent with the difficulty of the cross-coupling. Tuning of different bases and solvents further demonstrated that a combination of K<sub>2</sub>CO<sub>3</sub> and THF was preferred for this coupling (entries 8-11). An extensive screen of various Pd-NHC precatalysts (Figure 4.3.2) identified [(IPr)Pd(cin)Cl] as essential for this coupling (Table 2, entries 12-16). Changes in the throw-away ligand ([IPr)Pd(allyl)Cl], [Pd-PEPPSI-IPr]) and in the NHC scaffold ([IMes)Pd(cin)Cl], [(SIPr)Pd(cin)Cl]) resulted in significantly diminished yields.<sup>18</sup> However, we identified the [(IPr)Pd(1-*t*-Bu-ind)Cl] precatalyst as a promising Pd(II)-NHC precatalyst<sup>19</sup> for the B-alkyl-Suzuki cross-coupling of amides. In line with previous studies and the high reactivity of the preformed Pd(II)-NHC precatalysts, control experiments in the absence of the catalyst and using representative Pd-PR<sub>3</sub> conditions,<sup>14e</sup> revealed the requirement for a strong σ-donating Pd-NHC in this cross-coupling protocol.



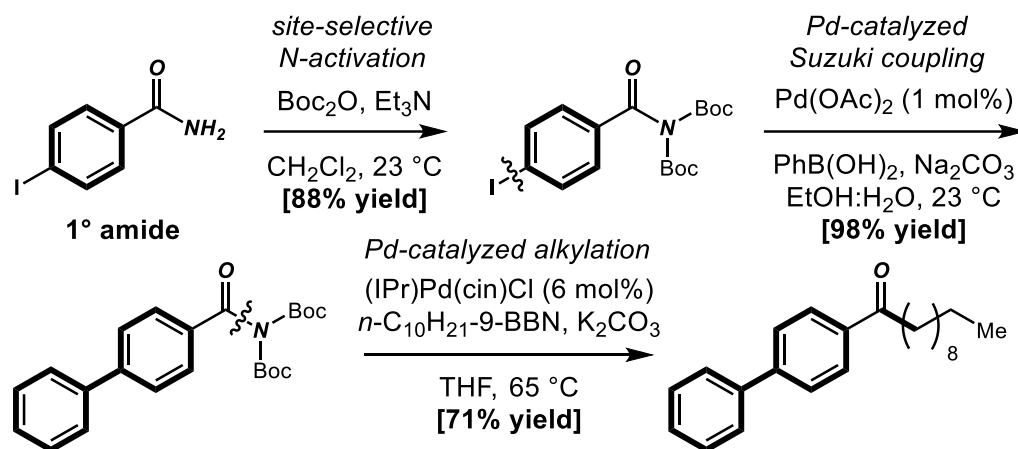


**Figure 4.3.3.** Sequential alkyl/aryl cross-coupling of primary amides.

### 4.3.3 Substrate scope

With the optimized conditions in hand, we next tested the preparative scope of the reaction using N,N-di-Boc amide as a standard electrophile (Table 4.3.2). This challenging alkylation reaction tolerated a range of B-alkyl-9-BBN reagents, including those with simple (entries 1-2) and sensitive functional groups such as ether (entry 3), imide (entry 4), indole (entry 5) and ester (entry 6). While in some cases the yield was modest, the reaction provided a proof-of-concept and a simple method for selectively installing functionalized alkyl groups from amides derived from common primary benzamides in a catalytic manner. Furthermore, we were pleased to find that a variety of amides was tolerated in this B-alkyl-Suzuki cross-coupling. Most interestingly, N-acyl-glutarimides that featured two activated carbonyl groups<sup>20</sup> were selectively cross-coupled at the exo-cyclic N-acyl bond, attesting that this catalytic system is selective for cleavage of N–C(O) bonds (entries 7-12). Furthermore, N-Ph/Boc and atom-economical N-Ph/Ms amides that could be prepared directly from common secondary amides readily

participated in this coupling (entries 13-14).<sup>3a,b</sup> Finally, we found that even sensitive N-benzoyl-saccharin that typically undergoes CO addition to the saccharine ring and SO<sub>2</sub> cleavage with strong organometallics,<sup>3a,b</sup> delivered the desired coupling product, albeit in a modest yield (entry 15).

We speculated that the potential of this mild alkylation protocol could be demonstrated in sequential C(sp<sup>2</sup>)–C(sp<sup>2</sup>)/C(sp<sup>2</sup>)–C(sp<sup>3</sup>) cross-couplings employing amides derived from common primary amide bonds. To this end, site-selective N,N-di-Boc activation of 4-iodobenzamide, followed by aryl Suzuki cross-coupling and C(acyl)–B-alkyl Suzuki cross-coupling could be accomplished with a high degree of efficiency and excellent chemoselectivity (Figure 4.3.3). Of note, aryl Suzuki cross-coupling could be readily performed in the presence of the electrophilic N,N-di-Boc amide, which together with the B-alkyl alkylation method allows for a strategically valuable disconnection typical to Weinreb amides, but in a catalytic manner.

entry	amide	product	4.3.3	conditions	yield(%) <sup>b</sup>
1			<b>4.3.3a</b>	A	73
2			<b>4.3.3b</b>	B	48
3			<b>4.3.3c</b>	C	75
4			<b>4.3.3d</b>	B	46
5			<b>4.3.3e</b>	B	32
6			<b>4.3.3f</b>	C	71
7			<b>4.3.3a</b>	A	85
8			<b>4.3.3g</b>	A	79
9			<b>4.3.3h</b>	B	61
10			<b>4.3.3i</b>	A	74
11			<b>4.3.3b</b>	B	72
12			<b>4.3.3e</b>	B	81
13			<b>4.3.3a</b>	B	72
14			<b>4.3.3a</b>	B	84
15			<b>4.3.3a</b>	A	34

<sup>a</sup>Conditions: A: **1** (1.0 equiv), **2** (2.0 equiv), (IPr)Pd(cin)Cl (6 mol %), K<sub>2</sub>CO<sub>3</sub> (3.0 equiv), THF (0.25 M), 23 °C, 15 h. B: 65 °C. C: (IPr)Pd(1-*t*-Bu-ind)Cl (6 mol %), 65 °C. <sup>b</sup>Isolated yields.

**Table 4.3.2** Substrate scope.<sup>a</sup>

#### 4.3.4 Conclusion

In conclusion, we developed a new method for highly chemoselective, palladium-NHC-catalyzed, direct cross-coupling between B- $\text{sp}^3$ -alkyl reagents and activated amides by N–C acyl cleavage. This protocol was compatible with various amides, including challenging primary amides after direct and site-selective N,N-di-Boc activation and sensitive N-cyclic amides. The method delivered chemoselective alkylation products of amides that are inaccessible by applying strong organometallic reagents. We have further demonstrated the utility of the method in sequential  $\text{C}(\text{sp}^2)\text{--C}(\text{sp}^2)/\text{C}(\text{sp}^2)\text{--C}(\text{sp}^3)$  cross-couplings employing amides derived from common primary amide bonds. We anticipated that further studies on optimization of the catalyst system and reaction parameters will expand the substrate scope to facilitate further reaction development.

#### 4.3.5 Experimental section

**General procedure for preparation of alkyl-9-BBNs.** All alkyl-9-BBNs were prepared in situ from the corresponding alkenes using 9-BBN dimer (0.50 M, THF). An oven-dried vial equipped with a stir bar was charged with the corresponding alkene (neat, 1.20 mmol) and 9-BBN dimer (1.0 mmol, THF solution) and the resulting reaction mixture was stirred for 15 h at room temperature. The solutions of alkyl-9-BBNs were used directly in cross-coupling reactions.

**General procedure for B-alkyl Suzuki-Miyaura cross-coupling of amides.** An oven-dried vial equipped with a stir bar was charged with amide substrate (neat, 1.0 equiv), Pd-NHC (typically, 6.0 mol%),  $\text{K}_2\text{CO}_3$  (typically, 3.0 equiv) and alkyl-9-BBN (typically, 2.0

equiv), placed under a positive pressure of argon, and subjected to three evacuation/backfilling cycles under high vacuum. The reaction mixture was stirred at 23 °C or placed in a preheated oil bath at 65 °C, and stirred for the indicated time at 65 °C. After the indicated time, the reaction mixture was diluted with CH<sub>2</sub>Cl<sub>2</sub> (10 mL), filtered, and concentrated. The sample was analyzed by <sup>1</sup>H NMR (CDCl<sub>3</sub>, 500 MHz) and GC-MS to obtain conversion, yield and selectivity using internal standard and comparison with authentic samples. Purification by chromatography on silica gel (hexanes/ethyl acetate) afforded the title product.

**4.3.3a.** Colorless oil. <sup>1</sup>H NMR (500 MHz, CDCl<sub>3</sub>) δ 7.98 (d, *J* = 7.6 Hz, 2 H), 7.57 (t, *J* = 7.4 Hz, 1 H), 7.48 (t, *J* = 7.6 Hz, 2 H), 2.98 (t, *J* = 7.5 Hz, 2 H), 1.75 (q, *J* = 7.4 Hz, 2 H), 1.40-1.26 (m, 14 H), 0.90 (t, *J* = 6.8 Hz, 3 H). <sup>13</sup>C NMR (125 MHz, CDCl<sub>3</sub>) δ 200.65, 137.11, 132.85, 128.54, 128.06, 38.66, 31.91, 29.59, 29.52, 29.49, 29.40, 29.33, 24.41, 22.69, 14.13.

**4.3.3b.** White solid. <sup>1</sup>H NMR (500 MHz, CDCl<sub>3</sub>) δ 7.95 (d, *J* = 7.2 Hz, 2 H), 7.57 (t, *J* = 7.4 Hz, 1 H), 7.47 (t, *J* = 7.7 Hz, 2 H), 7.32 (t, *J* = 7.5 Hz, 2 H), 7.23 (dd, *J* = 9.7, 7.7 Hz, 3 H), 3.01 (t, *J* = 7.3 Hz, 2 H), 2.75 (t, *J* = 7.6 Hz, 2 H), 2.11 (q, *J* = 7.4 Hz, 2 H). <sup>13</sup>C NMR (125 MHz, CDCl<sub>3</sub>) δ 200.13, 141.69, 137.01, 132.95, 128.56, 128.52, 128.40, 128.02, 125.96, 37.70, 35.21, 25.71.

**4.3.3c.** White solid. <sup>1</sup>H NMR (500 MHz, CDCl<sub>3</sub>) δ 7.99 (d, *J* = 7.2 Hz, 2 H), 7.58 (t, *J* = 7.4 Hz, 1 H), 7.49 (t, *J* = 7.6 Hz, 2 H), 7.33-7.28 (m, 2 H), 6.95 (t, *J* = 7.4 Hz, 1 H), 6.92 (d, *J* = 7.9 Hz, 2 H), 3.98 (t, *J* = 6.5 Hz, 2 H), 3.00 (t, *J* = 7.4 Hz, 2 H), 1.80 (dt, *J* = 13.7,

7.0 Hz, 4 H), 1.51 (dd,  $J = 13.6, 6.5$  Hz, 2 H), 1.47-1.41 (m, 4 H).  $^{13}\text{C}$ -NMR (125 MHz,  $\text{CDCl}_3$ )  $\delta$  200.51, 159.09, 137.08, 132.90, 129.41, 128.57, 128.06, 120.47, 114.49, 67.79, 38.57, 29.30, 29.26, 25.96, 24.28.

**4.3.3d.** White solid.  $^1\text{H}$  NMR (500 MHz,  $\text{CDCl}_3$ )  $\delta$  7.97 (d,  $J = 7.3$  Hz, 2 H), 7.86 (dd,  $J = 5.5, 3.0$  Hz, 2 H), 7.72 (dd,  $J = 5.4, 3.0$  Hz, 2 H), 7.57 (t,  $J = 7.4$  Hz, 1 H), 7.47 (t,  $J = 7.6$  Hz, 2 H), 3.70 (t,  $J = 7.3$  Hz, 2 H), 2.97 (t,  $J = 7.4$  Hz, 2 H), 1.73 (dt,  $J = 22.4, 7.0$  Hz, 4 H), 1.40 (brs, 6 H).  $^{13}\text{C}$  NMR (125 MHz,  $\text{CDCl}_3$ )  $\delta$  200.48, 168.47, 137.06, 133.85, 132.87, 132.17, 128.54, 128.04, 123.16, 38.52, 38.00, 29.19, 29.01, 28.55, 26.71, 24.22.

**4.3.3e.** White solid.  $^1\text{H}$  NMR (500 MHz,  $\text{CDCl}_3$ )  $\delta$  7.89 (d,  $J = 7.2$  Hz, 2 H), 7.66 (d,  $J = 8.0$  Hz, 1 H), 7.57 (t,  $J = 7.4$  Hz, 1 H), 7.45 (t,  $J = 7.7$  Hz, 2 H), 7.41 (d,  $J = 8.3$  Hz, 1H), 7.22 (d,  $J = 7.2$  Hz, 1H), 7.15 – 7.10 (m, 2H), 6.52 (d,  $J = 3.1$  Hz, 1H), 4.30 (t,  $J = 6.8$  Hz, 2 H), 2.95 (t,  $J = 6.8$  Hz, 2 H), 2.33 (p,  $J = 6.8$  Hz, 2 H).  $^{13}\text{C}$  NMR (125 MHz,  $\text{CDCl}_3$ )  $\delta$  199.22, 136.69, 136.00, 133.19, 128.62, 127.96, 127.83, 121.56, 120.99, 119.35, 109.46, 101.29, 45.41, 34.98, 24.46.

**4.3.3f.** White solid.  $^1\text{H}$  NMR (500 MHz,  $\text{CDCl}_3$ )  $\delta$  7.98 (d,  $J = 7.6$  Hz, 2 H), 7.57 (t,  $J = 7.4$  Hz, 1 H), 7.48 (t,  $J = 7.6$  Hz, 2 H), 3.69 (s, 3 H), 2.98 (t,  $J = 7.4$  Hz, 2 H), 2.32 (t,  $J = 7.5$  Hz, 2 H), 1.79-1.72 (m, 2 H), 1.64 (d,  $J = 7.3$  Hz, 2 H), 1.39-1.28 (m, 12 H).  $^{13}\text{C}$  NMR (125 MHz,  $\text{CDCl}_3$ )  $\delta$  200.60, 174.33, 137.11, 132.85, 128.54, 128.05, 51.44, 38.63, 34.12, 29.44, 29.41, 29.38, 29.36, 29.22, 29.13, 24.95, 24.38.

**4.3.3g.** White solid.  $^1\text{H}$  NMR (500 MHz,  $\text{CDCl}_3$ )  $\delta$  8.08 (d,  $J = 8.0$  Hz, 2 H), 7.75 (d,  $J = 8.1$  Hz, 2 H), 3.00 (t,  $J = 7.4$  Hz, 2 H), 1.77 (t,  $J = 7.3$  Hz, 2 H), 1.41-1.25 (m, 14 H), 0.90 (t,  $J = 6.7$  Hz, 3 H).  $^{13}\text{C}$  NMR (125 MHz,  $\text{CDCl}_3$ )  $\delta$  199.51, 139.74, 134.21 ( $J_2 = 32.71$  Hz), 128.36, 125.64 ( $J_3 = 6.92$  Hz), 123.64 ( $J_1 = 272.96$  Hz), 38.93, 31.89, 29.56, 29.48, 29.44, 29.31, 29.29, 24.16, 22.67, 14.10.  $^{19}\text{F}$  NMR (471 MHz,  $\text{CDCl}_3$ )  $\delta$  -63.11.

**4.3.3h.** White solid.  $^1\text{H}$  NMR (500 MHz,  $\text{CDCl}_3$ )  $\delta$  7.97 (d,  $J = 8.4$  Hz, 2 H), 6.95 (d,  $J = 8.4$  Hz, 2 H), 3.89 (s, 3 H), 2.93 (t,  $J = 7.4$  Hz, 2 H), 1.74 (p,  $J = 7.4$  Hz, 2 H), 1.39-1.27 (m, 14 H), 0.90 (t,  $J = 6.8$  Hz, 3 H).  $^{13}\text{C}$  NMR (125 MHz,  $\text{CDCl}_3$ )  $\delta$  199.28, 163.29, 130.31, 130.23, 113.66, 55.45, 38.34, 31.90, 29.59, 29.53, 29.50, 29.46, 29.32, 24.67, 22.68, 14.11.

**4.3.3i.** White solid.  $^1\text{H}$  NMR (500 MHz,  $\text{CDCl}_3$ )  $\delta$  8.14 (d,  $J = 8.1$  Hz, 2 H), 8.02 (d,  $J = 8.0$  Hz, 2 H), 3.97 (s, 3 H), 3.00 (t,  $J = 7.4$  Hz, 2 H), 1.81-1.71 (m, 2 H), 1.41-1.25 (m, 14 H), 0.90 (t,  $J = 6.8$  Hz, 3 H).  $^{13}\text{C}$  NMR (125 MHz,  $\text{CDCl}_3$ )  $\delta$  200.05, 166.28, 140.32, 133.68, 129.81, 127.94, 99.99, 52.44, 39.01, 31.89, 29.57, 29.49, 29.46, 29.31, 24.20, 22.68, 14.11.

**4.3.1bc.** White solid.  $^1\text{H}$  NMR (500 MHz,  $\text{CDCl}_3$ )  $\delta$  7.94 (d,  $J = 8.3$  Hz, 2 H), 7.72 (d,  $J = 8.3$  Hz, 2 H), 7.66 (d,  $J = 7.5$  Hz, 2 H), 7.51 (t,  $J = 7.5$  Hz, 2 H), 7.44 (t,  $J = 7.3$  Hz, 1 H), 1.43 (s, 18 H).  $^{13}\text{C}$  NMR (125 MHz,  $\text{CDCl}_3$ )  $\delta$  169.03, 149.83, 146.27, 139.56, 132.80, 129.79, 129.02, 128.46, 127.29, 115.33, 84.32, 27.66.

**4.3.3j.** White solid.  $^1\text{H}$  NMR (500 MHz,  $\text{CDCl}_3$ )  $\delta$  8.06 (d,  $J = 8.0$  Hz, 2 H), 7.71 (d,  $J = 8.1$  Hz, 2 H), 7.65 (d,  $J = 7.6$  Hz, 2 H), 7.50 (t,  $J = 7.6$  Hz, 2 H), 7.43 (d,  $J = 7.3$  Hz, 1 H), 3.01 (t,  $J = 7.4$  Hz, 2 H), 1.79 (t,  $J = 7.4$  Hz, 2 H), 1.42-1.28 (m, 14 H), 0.91 (t,  $J = 6.7$  Hz, 3 H).  $^{13}\text{C}$  NMR (125 MHz,  $\text{CDCl}_3$ )  $\delta$  200.24, 145.54, 139.97, 135.82, 128.94, 128.66, 128.17, 127.26, 127.21, 38.72, 31.91, 29.60, 29.53, 29.51, 29.43, 29.33, 24.51, 22.69, 14.12.



## References

- (1) (a) Greenberg, A.; Breneman, C. M.; Liebman, J. F. *The Amide Linkage: Structural Significance in Chemistry, Biochemistry and Materials Science*; Wiley: New York, 2003. For a highlight, see: (b) Ruider, S.; Maulide, N. *Angew. Chem. Int. Ed.* **2015**, *54*, 13856.
- (2) (a) *Metal-Catalyzed Cross-Coupling Reactions and More*, de Meijere, A.; Bräse, S.; Oestreich, M., Eds.; Wiley: New York, 2014. (b) *Science of Synthesis: Cross-Coupling and Heck-Type Reactions*, Molader, G.; Wolfe, J. P.; Larhed, M., Eds.; Thieme: Stuttgart, 2013. (c) *New Trends in Cross-Coupling*; Colacot, T. J., Ed.; RSC: Cambridge, 2015.
- (3) (a) Kaiser, D.; Bauer, A.; Lemmerer, M.; Maulide, N. *Chem. Soc. Rev.* **2018**, *47*, 7899. (b) Liu, C.; Szostak, M. *Chem. Eur. J.* **2017**, *23*, 7157. (c) Takise, R.; Muto, K.; Yamaguchi, J. *Chem. Soc. Rev.* **2017**, *46*, 5864. (d) Meng, G.; Shi, S.; Szostak, M. *Synlett* **2016**, *27*, 2530. (e) Dander, J. E.; Garg, N. K. *ACS Catal.* **2017**, *7*, 1413.
- (4) (a) Hie, L.; Nathel, N. F. F.; Shah, T. K.; Baker, E. L.; Hong, X.; Yang, Y. F.; Liu, P.; Houk, K. N.; Garg, N. K. *Nature* **2015**, *524*, 79. (b) Meng, G.; Szostak, M. *Org. Lett.* **2015**, *17*, 4364. (c) Meng, G.; Shi, S.; Szostak, M. *ACS Catal.* **2016**, *6*, 7335. (d) Meng, G.; Lei, P.; Szostak, M. *Org. Lett.* **2017**, *19*, 2158. (e) Amani, J.; Alam, R.; Badir, S.; Molander, G. A. *Org. Lett.* **2017**, *19*, 2426. (f) Ni, S.; Zhang, W.; Mei, H.; Han, J.; Pan, Y. *Org. Lett.* **2017**, *19*, 2536. (g) Lei, P.; Meng, G.; Shi, S.; Ling, Y.; An, J.; Szostak, R.; Szostak, M. *Chem. Sci.* **2017**, *8*, 6525.
- (5) (a) Meng, G.; Szostak, M. *Angew. Chem. Int. Ed.* **2015**, *54*, 14518. (b) Shi, S.; Meng, G.; Szostak, M. *Angew. Chem. Int. Ed.* **2016**, *55*, 6959. (c) Meng, G.; Szostak, M. *Org.*

*Lett.* **2016**, *18*, 796. (d) Dey, A.; Sasmai, S.; Seth, K.; Lahiri, G. K.; Maiti, D. *ACS Catal.* **2017**, *7*, 433. (e) Yue, H.; Guo, L.; Liao, H. H.; Cai, Y.; Zhu, C.; Rueping, M. *Angew. Chem. Int. Ed.* **2017**, *56*, 4282. (f) Yue, H.; Guo, L.; Lee, S. C.; Liu, X.; Rueping, M. *Angew. Chem. Int. Ed.* **2017**, *56*, 3972. (g) Srimontree, W.; Chatupheeraphat, A.; Liao, H. H.; Rueping, M. *Org. Lett.* **2017**, *19*, 3091. (h) Shi, S.; Szostak, M. *Org. Lett.* **2017**, *19*, 3095.

(6) Walker, J. A.; Vickerman, K. L.; Humke, J. N.; Stanley, L. M. *J. Am. Chem. Soc.* **2017**, *139*, 10228.

(7) (a) Wybon, C. C. D.; Mensch, C.; Hollanders, K.; Gadals, C.; Herrebout, W. A.; Ballet, S.; Maes, B. U. W. *ACS Catal.* **2018**, *8*, 203. (b) Bourne-Branchu, Y.; Gosmini, C.; Danoun, G. *Chem. Eur. J.* **2017**, *23*, 10043. (c) Chen, C.; Liu, P.; Luo, M.; Zeng, X. *ACS Catal.* **2018**, *8*, 5864. (d) Liu, L.; Zhou, D.; Liu, M.; Zhou, Y.; Chen, T. *Org. Lett.* **2018**, *20*, 2741. (e) Liu, C.; Szostak, M. *Angew. Chem. Int. Ed.* **2017**, *56*, 12718. (f) Liu, C.; Meng, G. J. *Org. Chem.* **2016**, *81*, 12023. (g) Chatupheeraphat, A.; Liao, H. H.; Lee, S. C.; Rueping, M. *Org. Lett.* **2017**, *19*, 4255. (h) Lee, S. C.; Guo, L.; Yue, H.; Liao, H. H.; Rueping, M. *Synlett* **2017**, *28*, 2594. (i) Lee, S. C.; Liao, H. H.; Chatupheeraphat, A.; Rueping, M. *Chem. Eur. J.* **2018**, *24*, 3608.

(8) (a) Liu, Y.; Shi, S.; Achtenhagen, M.; Liu, R.; Szostak, M. *Org. Lett.* **2017**, *19*, 1614. (b) Verho, O.; Lati, M. P.; Oschmann, M. *J. Org. Chem.* **2018**, *83*, 4464. (c) Wu, H.; Guo, W.; Stelck, D.; Li, Y.; Liu, C.; Zeng, Z. *Chem. Eur. J.* **2018**, *24*, 3444.

(9) Nahm, S.; Weinreb, S. M. *Tetrahedron Lett.* **1981**, *22*, 3815.

- (10) Afagh, N. A.; Yudin, A. K. *Angew. Chem. Int. Ed.* **2010**, *49*, 262.
- (11) Meng, G.; Shi, S.; Lalancette, R.; Szostak, R.; Szostak, M. *J. Am. Chem. Soc.* **2018**, *140*, 727.
- (12) Trost, B. M.; Fleming, I. *Comprehensive Organic Synthesis*; Pergamon Press: Oxford, 1991.
- (13) (a) Jana, R.; Pathak, T. P.; Sigman, M. S. *Chem. Rev.* **2011**, *111*, 1417. (b) Giri, R.; Thapa, S.; Kafle, A. *Adv. Synth. Catal.* **2014**, *356*, 1395.
- (14) (a) Simmons, B. J.; Weires, N. A.; Dander, J. E.; Garg, N. K. *ACS Catal.* **2016**, *6*, 3176. (b) Liu, X.; Hsiao, C. C.; Guo, L.; Rueping, M. *Org. Lett.* **2018**, *20*, 2976. (c) Masson-Makdissi, Vandavasi, J. K.; Newman, S. G. *Org. Lett.* **2018**, *20*, 4094. (d) Kabalka, G. W.; Malladi, R. R.; Tejedor, D.; Kelley, S. *Tetrahedron Lett.* **2000**, *41*, 999. (e) Yasui, Y.; Tsuchida, S.; Miyabe, H.; Takemoto, Y. *J. Org. Chem.* **2007**, *72*, 5898. (f) Miyaura, N.; Ishiyama, T.; Sasaki, H.; Ishikawa, M.; Satoh, M.; Suzuki, A. *J. Am. Chem. Soc.* **1989**, *111*, 314. (g) Lee, N. R.; Linstadt, R. T. H.; Gloisten, D. J.; Gallou, F.; Lipshutz, B. H. *Org. Lett.* **2018**, *20*, 2902.
- (15) (a) Chemler, S. R.; Trauner, D.; Danishefsky, S. J. *Angew. Chem. Int. Ed.* **2001**, *40*, 4544. (b) Seidel, G.; Fürstner, A. *Chem. Commun.* **2012**, *48*, 2055; (c) Lennox, A. J. J.; Lloyd-Jones, G. C. *Chem. Soc. Rev.* **2014**, *43*, 412.

- (16) (a) *Science of Synthesis: N-Heterocyclic Carbenes in Catalytic Organic Synthesis*, Nolan, S. P.; Cazin, C. S. J., Eds.; Thieme: Stuttgart, 2017. (b) Peh, G. R.; Kantchev, E. A. B.; Er, J. C.; Ying, J. Y. *Chem. Eur. J.* **2010**, *16*, 4010.
- (17) (a) Marion, N.; Navarro, O.; Mei, J.; Stevens, E. D.; Scott, N. M.; Nolan, S. P. *J. Am. Chem. Soc.* **2006**, *128*, 4101. (b) Navarro, O.; Marion, N.; Mei, J.; Nolan, S. P. *Chem. Eur. J.* **2006**, *12*, 5142.
- (18) (a) Marion, N.; Nolan, S. P. *Acc. Chem. Res.* **2008**, *41*, 1440. (b) Fortman, G. C.; Nolan, S. P. *Chem. Soc. Rev.* **2011**, *40*, 5151.
- (19) Melvin, P. R.; Nova, A.; Balcells, D.; Dai, W.; Hazari, N.; Hruszkewycz, D. P.; Shah, H. P.; Tudge, M. T. *ACS Catal.* **2015**, *5*, 3680.
- (20) Meng, G.; Szostak, M. *Eur. J. Org. Chem.* **2018**, 2352.

## Chapter 5

### Conclusion

The research outlined in this thesis aimed to employ amides as electrophiles in metal-catalyzed acyl and decarbonylative cross-coupling reactions, and also to find more efficient ways for the transformation of generic amides by manipulation of ubiquitous amide bonds by selective N–C(O) activation. The main achievements of this work are summarized below:

(1) Acyl coupling reactions: we developed the first example of palladium-catalyzed Suzuki cross-coupling reactions with N-acylglutarimides, and demonstrated that these compounds represented the most reactive amides to be developed in amide bond cross-coupling. We developed the now broadly utilized hypothesis of ground-state-destabilization in amide bond cross-coupling. Subsequently, we successfully developed primary amides as electrophilic substrates in palladium-catalyzed Suzuki cross-coupling by a cooperative strategy.

(2) Decarbonylative coupling reactions: we developed the first example of a decarbonylative Heck reaction of amides. This reaction represented the first catalytic decarbonylative cross-coupling of amides of any type, and opened the door for using amides as electrophilic arylating reagents by many research groups. Subsequently, we developed the first methods for C–H bond activation using N-acylglutarimides and primary amides as electrophilic coupling partners enabled by Rh catalysis.

(3) New Pd-NHC catalyst systems: considering the advantages of NHC ligands over phosphine ligands, we developed the first example of Pd-NHC catalysts in amide N–C(O) bond activation. We further developed the first example of planar amides, in which activation proceeds by electronic factors rather than steric-distortion. Furthermore, we developed the first general manifold to construct C(sp<sup>2</sup>)-C(sp<sup>3</sup>) bonds in a B-alkyl type Suzuki cross-coupling of amides.

We expect that our research results will guide the design of new types of reactions and the development of new strategies for amide bond activation.